Universidade do Minho
Escola de Engenharia

Fernando Eduardo Freitas de Oliveira

The role of iron uptake in *Staphylococcus epidermidis* biofilm formation and virulence

dezembro de 2019

The role of iron uptake in *Staphylococcus epidermidis* biofilm formation and virulence
Fernando Eduardo Freitas de Oliveira
UMinho | 2019

FCT Fundação para a Ciência e a Tecnologia

UNIÃO EUROPEIA
Fundo Europeu de Desenvolvimento Regional

NORTE 2020
PROGRAMA OPERACIONAL REGIONAL DO NORTE

PORTUGAL 2020

DFG Deutsche Forschungsgemeinschaft

Damp Stiftung

Universidade do Minho
Escola de Engenharia

Fernando Eduardo Freitas de Oliveira

The role of iron uptake in *Staphylococcus epidermidis* biofilm formation and virulence

Tese de Doutoramento em Bioengenharia

Trabalho efetuado sob a orientação do
Doutor Nuno Cerca
do
Prof. Dr. med. Holger Rohde
e do
Professor Doutor Manuel Vilanova

dezembro de 2019

Acknowledgements

A realização desta longa e desafiante jornada foi apenas possível devido ao contributo de um conjunto de pessoas a quem importa agora transmitir os meus mais sinceros agradecimentos.

Em primeiro lugar agradeço à fantástica equipa de orientadores com a qual tive o prazer de trabalhar: ao **Doutor Nuno Cerca** agradeço o desafio proposto, o acompanhamento regular dos trabalhos, com partilha de conhecimentos e sugestões construtivas, a exigência e o pragmatismo que tanto o caracterizam, e todas as oportunidades que me tem concedido. To **Professor Holger Rohde** I want to thank him for giving me the opportunity to work in his research group and sharing with me his knowledge on Molecular Microbiology. During the most difficult period of this journey, his expertise, suggestions and contagious good mood were fundamental for the successful achievement of my goals in Hamburg. Vielen Dank! Ao **Professor Manuel Vilanova** agradeço o facto de me ter recebido e integrado na sua equipa, todas as suas sugestões e partilha de conhecimentos na área da Imunologia.

A todos os membros, atuais e passados, da "**Equipa NC**" agradeço o companheirismo, boa disposição, e espírito de entreajuda. Agradeço especialmente à **Ângela** pela sua contribuição em parte do trabalho aqui apresentado, e às minhas companheiras de jornada **Andreia**, **Daniela**, **Joana** e **Susana**. I would like to thank all my labmates from **AG Rohde** (**Anna**, **Ben**, **Christian**, **Gesche**, **Henning**, **Joon,** and **Samira** in particular). Aos membros da **Imunobiologia do I3S**, em particular à **Alexandra**, **Filipa**, **Mariana**, **Ricardo**, **Rita** e **Tânia**, agradeço o companheirismo e sugestões científicas. À **Ana** agradeço o auxílio que me prestou durante o seu período de estágio no grupo.

Um agradecimento especial às **Professoras Simone Morais** e **Cristina Soares** (DEQ-ISEP), à **Rute Oliveira** (I3S-MicroBioSyn) e ao staff do I3S: **Rui Fernandes** e **Rita Malheiro** (HEMS); **Paula Sampaio** e **Maria Azevedo** (ALM); **André Maia** (BSS).

A todas as pessoas que, de forma menos direta, mas não menos importante, tiveram um contributo importante ao longo desta caminhada deixo aqui o meu profundo agradecimento (devido a restrições impostas ao nível da extensão dos agradecimentos, não serão tão elaborados quanto gostaria): ao **Professor Eugénio Ferreira** (CEB), às **Professoras Cristina Prudêncio** e **Mónica Vieira** (ESS); a todos os meus **colegas do Programa Doutoral em Bioengenharia**; to my **flatmates in Hamburg** (**Fadi** in particular); aos meus **amigos**; aos meus parceiros dos **Living Stone Desert**; aos meus **familiares** (especialmente à **Améli** e aos meus priminhos **Miguel** e **Nonô**); aos meus futuros sogros, **António** e **Eduarda**, e à **Bruna**.

Por fim agradeço às pessoas mais importantes da minha vida e a quem dedico este trabalho:

Aos meus **pais:** agradeço-vos todo o amor, carinho e apoio incondicional. Tomarei para sempre como exemplo de vida a forma como me educaram e que levou à construção de uma atitude otimista que me tem permitido enfrentar e ultrapassar os mais diversos obstáculos, nomeadamente os que surgiram ao longo desta caminhada.

À **Liliana**: por mais belas que possam ser as palavras que aqui te endereço, jamais expressarão na totalidade o enorme sentimento de amor, admiração e gratidão que tenho por ti. Sinto-me absolutamente abençoado por fazeres parte da minha vida há já longos anos. Em ti encontrei o verdadeiro sentimento de amor incondicional, de dar sem esperar nada em troca. Esta jornada foi sem dúvida o maior teste à nossa relação e, apesar dos momentos difíceis, da minha ausência prolongada, chegamos a este ponto com a certeza de que a nossa relação está mais forte do que nunca. AMO-TE <3

This study was supported by the Portuguese Foundation for Science and Technology (FCT) through an individual PhD scholarship (SFRH/BD/101399/2014), the funded project PTDC/BIA-MOL/29553/2017, under the scope of COMPETE2020 (POCI-01-0145-FEDER-029553), and the strategic funding of UID/BIO/04469/2019 unit. This study was also supported through funds from the German Research Council (DFG) and the Damp Foundation.

STATEMENT OF INTEGRITY

I hereby declare having conducted this academic work with integrity. I confirm that I have not used plagiarism or any form of undue use of information or falsification of results along the process leading to its elaboration.

I further declare that I have fully acknowledged the Code of Ethical Conduct of the University of Minho.

O papel da aquisição de ferro na formação de biofilme e virulência de *Staphylococcus epidermidis*

Resumo

Staphylococcus epidermidis é um importante microrganismo comensal da pele e mucosas em humanos, sendo também uma causa frequente de infeções potencialmente fatais em pacientes imunocomprometidos. A sua capacidade assinalável de formar biofilmes é amplamente apontada como o seu principal determinante patogénico. Apesar de se terem alcançado significativos avanços no entendimento dos seus mecanismos de formação de biofilme, esta espécie bacteriana continua a ser responsável por uma proporção significativa de infeções associadas aos cuidados de saúde, particularmente aquelas relacionadas com o uso de dispositivos médicos implantáveis. Este facto enfatiza a importância de um melhor entendimento do processo de formação de biofilme em *S. epidermidis* e dos fatores que o modulam. Tendo em conta que *S. epidermidis* enfrenta uma severa privação de ferro assim que entra na corrente sanguínea, testou-se a hipótese de que a aquisição de ferro desempenha um papel importante na formação de biofilme por *S. epidermidis* e na sua evasão ao sistema imune inato do hospedeiro.

Os primeiros dados experimentais revelaram uma capacidade comprometida de *S. epidermidis* em formar biofilmes sob condições de restrição de ferro, principalmente atribuíveis a uma redução da taxa de crescimento, da viabilidade celular e da produção de adesina polissacarídica intercelular (PIA/PNAG). No entanto, e não obstante as condições desfavoráveis, *S. epidermidis* apresenta capacidade de proliferar neste cenário, implicando que esta espécie tem mecanismos dedicados à aquisição de ferro. Uma inspeção dos genomas de *S. epidermidis* disponíveis, juntamente com experiências de transcrição, levou à identificação de um grupo de genes putativamente envolvidos na aquisição de ferro. Seguindo uma abordagem mutagénica, foi demonstrado que uma dessas regiões genéticas (subsequentemente denominada *sfaABCD*) codifica a única via biossintética de sideróforos em *S. epidermidis*. Surpreendentemente, a eliminação de *sfaABCD* ou de dois outros loci que codificam um putativo transportador ABC de complexos ferro-sideróforo (*htsABC* e *fhuA*) resultou em estirpes mutantes seriamente incapacitadas de formar biofilme em condições de restrição de ferro. A eliminação de *sfaABCD* foi igualmente associada a uma replicação bacteriana mais baixa ou nula em macrófagos humanos e de ratinho, a uma inibição da produção de espécies reativas de oxigénio por neutrófilos e uma maior suscetibilidade à morte mediada por peróxido de hidrogénio.

Os dados deste estudo mostram que a aquisição de ferro mediada por sideróforo é um importante processo para a formação de biofilmes por *S. epidermidis* sob condições de deficiência de ferro, mas também para a modulação da interação desta bactéria com o sistema imune inato do hospedeiro. Em última instância, estes resultados sugerem que a inibição deste processo de aquisição de ferro pode ser eficaz no tratamento de infeções por *S. epidermidis* associadas à formação de biofilme.

Palavras chave: biofilmes, ferro, macrófagos, sideróforos, *Staphylococcus epidermidis*

The role of iron uptake in *Staphylococcus epidermidis* biofilm formation and virulence

Abstract

Staphylococcus epidermidis is one of the most important commensal microorganisms of human skin and mucosae, but additionally it is often the cause of potential life-threatening infections in immunocompromised patients. A remarkable ability to form biofilms is widely regarded as its major known pathogenic determinant. Although a significant amount of knowledge on its biofilm formation mechanisms has been achieved, this bacterial species still accounts for a significant proportion of hospital-acquired infections, particularly those related with the use of implantable biomedical devices. This emphasizes the importance of a better understanding of biofilm formation in *S. epidermidis* and of the factors that modulate this process. Given that *S. epidermidis* faces severe deprivation of iron after entering the bloodstream, it was tested the hypothesis that iron acquisition plays an important role in *S. epidermidis* biofilm development and escape from the host innate immune system.

The first experimental data revealed a compromised ability of *S. epidermidis* to form biofilms under iron-restricted conditions, mainly attributable to a reduced growth rate, cell viability, and production of polysaccharide intercellular adhesin (PIA/PNAG). However, and despite the unfavorable conditions, *S. epidermidis* is still able to proliferate in this scenario, implying that this species has dedicated mechanisms to acquire iron. An inspection of available *S. epidermidis* genomes along with transcriptional experiments has led to the identification of a group of genes putatively involved in iron acquisition, such as siderophore biosynthesis and uptake of iron-siderophore complexes. By following a mutagenesis approach, it was demonstrated that one of those genetic regions (subsequently termed *sfaABCD*) encodes the sole siderophore biosynthetic pathway in *S. epidermidis*. Strikingly, deletion of *sfaABCD* or two other loci putatively encoding an iron-siderophore ABC transporter (*htsABC* and *fhuA*) resulted in mutant strains severely incapacitated for biofilm formation in iron-restricted conditions. Deletion of *sfaABCD* was also associated with lower to null bacterial replication within murine and human macrophages, inhibition of reactive oxygen species generation by neutrophils, and higher susceptibility to hydrogen peroxide-mediated killing.

The data collected in this study show that siderophore-mediated iron acquisition is an important process for *S. epidermidis* to form biofilms under conditions of iron starvation, but also for the modulation of the interaction of this bacterium with the host innate immune system. Ultimately, these results suggest that inhibiting this iron acquisition process may be effective in the treatment of biofilm-associated *S. epidermidis* infections.

Keywords: biofilms, iron, macrophages, siderophores, *Staphylococcus epidermidis*

Table of contents

List of abbreviations

Aap	Accumulation-associated protein
ABC	ATP-binding cassette
Agr	Accessory gene regulator
APC	Antigen-presenting cell
ATCC	American Type Culture Collection
Bip	2,2′-bipyridine
bp	Base pair
CAS	Chrome azurol S
CDM	Chemically defined medium
CDM_{Fe-}	Iron-restricted chemically defined medium
CDM_{Fe+}	Iron-enriched chemically defined medium
cDNA	Complementary deoxyribonucleic acid
CFU	Colony-forming unit
CLSM	Confocal laser scanning microscopy
CoNS	Coagulase-negative staphylococci
DAPI	4',6-diamidine-2'-phenylindole dihydrochloride
DNA	Deoxyribonucleic acid
DPBS	Dulbecco's phosphate buffered saline
ECDC	European Centre for Disease Prevention and Control
Embp	Extracellular matrix-binding protein
FBS	Fetal bovine serum
Fhu	Ferric hydroxamate uptake
Fur	Ferric uptake regulator
GlcNAc	N-acetylglucosamine
GM-CSF	Granulocyte-macrophage colony-stimulating factor
HAIs	Health care-associated infections
hMDMs	Human monocyte-derived macrophages
ica	Intercellular adhesion operon
IFN-γ	Interferon gamma
IL	Interleukin

Isd	Iron-regulated surface determinant
Iuc	Iron uptake chelate
LB	Lysogeny Broth
LTA	Lipoteichoic acid
M-CSF	Macrophage colony-stimulating factor
MACS	Magnetic-activated cell sorting
MFI	Mean fluorescence intensity
MFS	Major facilitator superfamily
MHC	Major histocompatibility complex
MOI	Multiplicity of infection
mRNA	Messenger ribonucleic acid
NCBI	National Center for Biotechnology Information
NETs	Neutrophil extracellular traps
NIS	NRPS-independent synthetase pathway
NRPS	Non-ribosomal peptide synthetase pathway
OD	Optical density
PAMP	Pathogen-associated molecular pattern
PBMC	Peripheral blood mononuclear cell
PBS	Phosphate buffered saline
PCR	Polymerase chain reaction
PI	Propidium iodide
PIA/PNAG	Polysaccharide intercellular adhesin/ poly-N-acetylglucosamine
PMNs	Polymorphonuclear leukocytes
PSM	Phenol-soluble modulin
qPCR	Quantitative PCR
RNA	Ribonucleic acid
ROS	Reactive oxygen species
RT	Room temperature
Sbp	Small basic protein
TAE	Tris–acetate–EDTA
TCR	T-cell receptor
TEM	Transmission electron microscopy

TfR	Transferrin receptor
TLR	Toll-like receptor
TNF-α	Tumor necrosis factor-alpha
TSA	Tryptic soy agar
TSB	Tryptic soy broth
TSB_G	TSB supplemented with 0.4% (w/v) glucose
WGA	Wheat germ agglutinin
WT	Wild-type

List of figures

CHAPTER 1

CHAPTER 2

CHAPTER 3

CHAPTER 4

CHAPTER 5

List of tables

CHAPTER 3

CHAPTER 4

CHAPTER 5

List of publications

A significant proportion of the work described in this thesis has been published elsewhere.

Papers in peer-reviewed journals

Oliveira F, França A, Cerca N. *Staphylococcus epidermidis* is largely dependent on iron availability to form biofilms. Int J Med Microbiol. 2017; 307(8): 552-63. doi: 10.1016/j.ijmm.2017.08.009.

Poster communication at international scientific conferences

Oliveira F, Rohde H, Cerca N. *Staphylococcus epidermidis* heavily relies on its iron acquisition systems to form biofilms, ISSSI2018 - 18th International Symposium on Staphylococci and Staphylococcal Infections, August 23-26, 2018, Copenhagen, Denmark.

Oliveira F, Cerca N. Biological validation of putative iron-related genes in *Staphylococcus epidermidis*: how iron induces physiologic and transcriptomic changes on biofilm cells. FEMS 2017 - 7th Congress of European Microbiologists, July 9-13, 2017, Valencia, Spain.

Oliveira F, Soares P, Cerca N. Iron availability modulates biofilm formation by *Staphylococcus epidermidis*. Biofilms 7, June 26-28, 2016, Porto, Portugal.

Aos meus pais.

À Liliana.

CHAPTER 1

Introduction

Summary

This chapter introduces the reader to the research questions and hypothesis that led to the development of this thesis. A brief background is provided, as well as the significance and outline of the thesis.

1.1 Background

Health care-associated infections (HAIs) have been recognized as an increasing public health issue, raising serious concerns worldwide. Among the microorganisms that significantly account for such infections are staphylococci, particularly *Staphylococcus epidermidis* (1). Despite being a major colonizer of the human skin and mucous membranes, where it develops a benign relationship with its host, *S. epidermidis* is often the cause of potential life-threatening infections in immunocompromised patients (2). *S. epidermidis* takes advantage of its striking ability to establish complex, multilayered biofilms, which allows persistence in the host and evasion of the innate immune system (3). Hence, biofilm-associated infections are considered a major problem in modern medicine, affecting millions of people over the world (4).

Notwithstanding important discoveries that have been made concerning *S. epidermidis* pathogenesis, there is still much to uncover about the infective nature of this species, especially when it comes to its interaction with the host immune system. Over the past few years, iron acquisition in pathogenic bacteria and its role in their infectiveness has been the target of intense research (5–9). Iron has long been recognized as a pivotal nutrient in bacterial replication and pathogenesis and a fairly good comprehension of the iron acquisition mechanisms employed by different bacterial species has been achieved (10,11). Conversely, research about iron acquisition mechanisms in *S. epidermidis* is almost absent and confined to a couple of studies dating back to the 90s and early 2000s (12–14). A study published some years ago by França et al. (15) demonstrated that *S. epidermidis* biofilm cells exhibit an increased transcription of genes putatively involved in iron acquisition when in contact with human blood. This led to the hypothesis that iron may play a significant role during *S. epidermidis* infections.

In this study, the general role of iron in *S. epidermidis* biofilm formation was first studied in detail. Afterwards, a set of mutant strains were constructed to study (i) the different mechanisms employed by *S. epidermidis* to acquire iron; (ii) the importance of such mechanisms for biofilm formation; and (iii) how they modulate the host-pathogen interaction. The elucidation of these points is expected to pave the way for the development of innovative preventive and/ or treatment strategies of *S. epidermidis* biofilm-associated infections.

1.2 Research questions

The following questions will be addressed throughout this thesis:

1. Does iron availability modulate the ability of *S. epidermidis* to form a biofilm?

2. What are the molecular mechanisms employed by *S. epidermidis* to acquire iron and regulate its homeostasis?

3. Do iron acquisition mechanisms have an impact on *S. epidermidis* virulence and its recognition by the host innate immune system?

Answers to these questions are expected to improve the current knowledge on *S. epidermidis* pathogenesis, which ultimately may point out iron uptake as an appealing target for the treatment of staphylococcal infections.

1.3 Hypothesis and aims

1.3.1 Hypothesis

The importance of iron for bacterial replication is well established for different bacterial species. In this study the hypothesis was tested if iron acquisition plays a role in *S. epidermidis* biofilm development and escape from the host innate immune system.

1.3.2 Aims

The major aim of this study was to shed light into the importance of iron availability for *S. epidermidis* biofilm formation and host interactions. To achieve this, the following specific aims were addressed.

Aim 1: To evaluate the effect of iron on *S. epidermidis* biofilm formation and gene transcription.

- **a)** To analyze the biofilm formation ability (biomass, structure and matrix composition) of different *S. epidermidis* strains under iron-deficient and iron-enriched conditions.
- **b)** To study the influence of iron availability on the transcription of putative iron acquisition-related genes.

Aim 2: To characterize *S. epidermidis* strains defective in iron uptake.

- **a)** To generate specific deletion mutant strains for putative iron acquisition-related genes.

b) To perform a phenotypic characterization of the mutant strains at the level of their ultrastructure, iron content, siderophore production, growth rate and biofilm formation.

Aim 3: To study the interactions between *S. epidermidis* strains and the host innate immune system.

a) To assess the survival of *S. epidermidis* in different populations of macrophages.

b) To evaluate the susceptibility of *S. epidermidis* to the bactericidal mechanisms employed by the host phagocytic cells.

c) To analyze the role of iron acquisition in the survival/ persistence of *S. epidermidis* in the host.

1.4 Significance

While iron acquisition is a well-studied process in Gram-negative bacteria, the same does not hold true for Gram-positive species. Regarding staphylococci, most of the knowledge on their iron acquisition mechanisms comes from *Staphylococcus aureus*, whereas studies on *S. epidermidis* are still very scarce. While both species share similar features, there are key differences regarding their molecular mechanisms of pathogenicity (16–18) that justifies the need to assess iron acquisition specifically in *S. epidermidis*. Iron is recognized as a key element in several biological processes, including cell proliferation. Nevertheless, several studies have also implicated iron in more specific processes, namely biofilm formation (19–21). Taking this into account, along with the fact that biofilm formation is of paramount importance in *S. epidermidis* infections, it is reasonable to hypothesize that iron may be an essential element throughout the lifecycle of this species.

Furthermore, and over the years, a significant proportion of research on pathogenic bacteria has been based on experiments performed with planktonic cultures that are grown under nutrient-rich conditions. Despite their importance, such experimental conditions do not appropriately represent conditions that a pathogen faces in an infection scenario. In this investigation, we attempted to overcome these limitations by giving a special focus on biofilm formation and iron-deprived growth conditions. By following this approach, it is anticipated that the results generated by this work, along with important findings from other research groups elsewhere, may be an important contribution for the development of novel strategies in the treatment of staphylococcal infections.

1.5 Thesis outline

After this introductory chapter, this thesis presents a literature review (**Chapter 2**) that provides the reader with important information on *S. epidermidis* virulence factors. A particular emphasis is given to biofilm formation and iron acquisition processes.

All experimental data obtained are shown throughout **Chapters 3** to **5**. Each of these chapters can be read independently, as a summary, introduction, materials and methods, results, discussion, and conclusions are provided for each one.

In **Chapter 3** the effect of iron on *S. epidermidis* biofilm formation and transcription of a selected panel of genes is addressed. Biofilms of three *S. epidermidis* strains were grown under high- and low-iron conditions and several physiologic and transcriptomic changes were assessed.

Chapter 4 describes a thorough study of different *S. epidermidis* strains defective in iron uptake that were constructed for the purpose of this study. Assessment of several parameters, such as ultrastructure, iron content, siderophore production, growth rate and biofilm formation, is covered in this chapter.

The interaction of *S. epidermidis* strains defective in iron uptake with different host immune effectors is described in **Chapter 5**. A special attention is given to macrophages and their bactericidal mechanisms.

This thesis is concluded with **Chapter 6** that summarizes the major findings and limitations of the study and points out future directions in this field of research.

Figure 1.1 depicts an outline of this thesis and shows the relationship among different chapters.

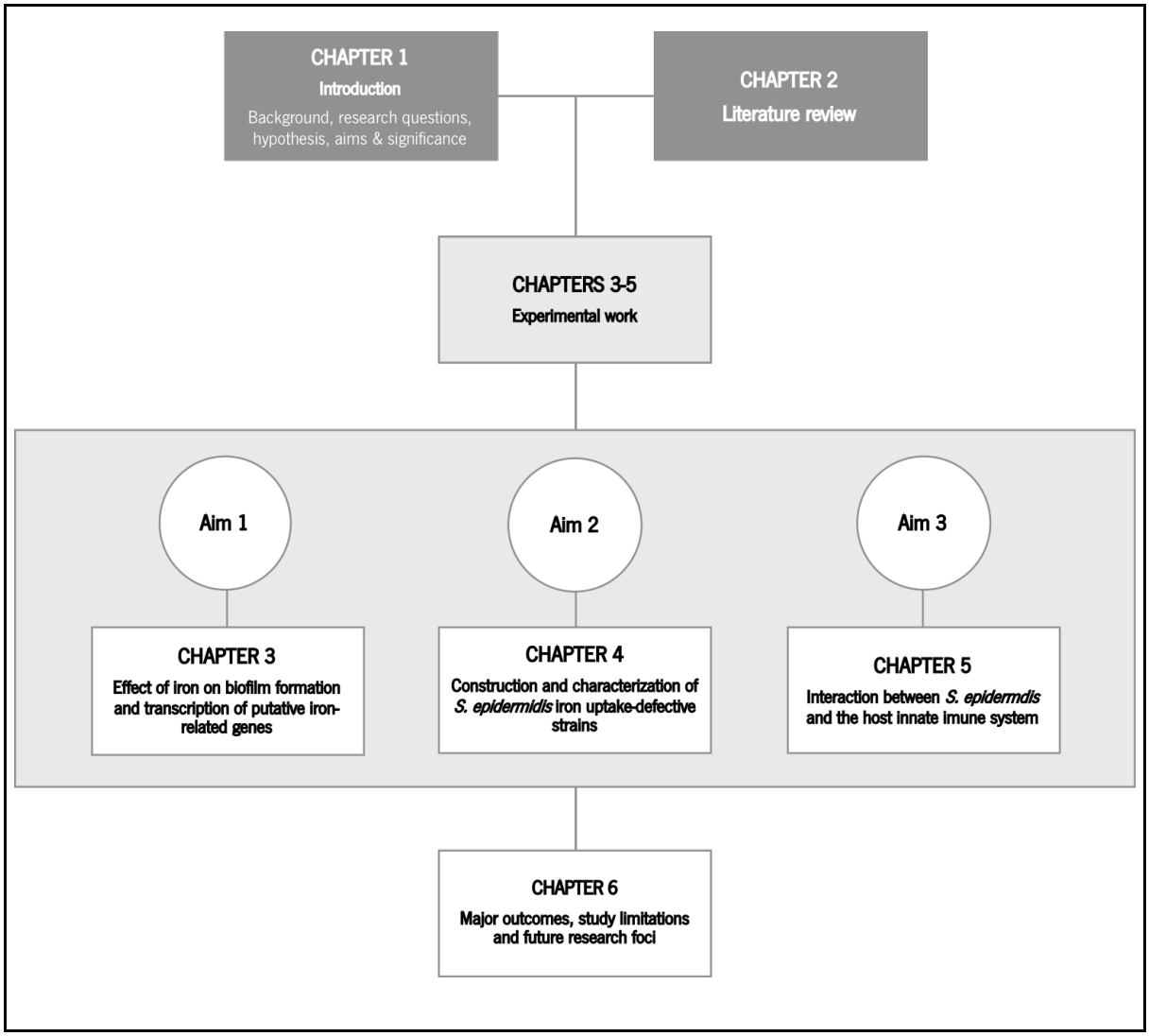

Figure 1.1. Thesis outline.

1.6 References

1. Ziebuhr W, Hennig S, Eckart M, Kränzler H, Batzilla C, Kozitskaya S. Nosocomial infections by *Staphylococcus epidermidis*: how a commensal bacterium turns into a pathogen. Int J Antimicrob Agents. 2006;28(Supplement 1):14–20.
2. Otto M. *Staphylococcus epidermidis* - the 'accidental' pathogen. Nat Rev Microbiol. 2009;7(8):555–67.
3. Otto M. *Staphylococcus epidermidis* pathogenesis. In: Fey PD, (ed.) *Staphylococcus epidermidis* Methods in Molecular Biology (Methods and Protocols). Totowa: Humana Press; 2014. p.17–31.
4. Del Pozo JL. Biofilm-related disease. Expert Rev Anti Infect Ther. 2018;16(1):51–65.
5. Minandri F, Imperi F, Frangipani E, Bonchi C, Visaggio D, Facchini M, et al. Role of iron uptake systems in *Pseudomonas aeruginosa* virulence and airway infection. Infect Immun. 2016;84(8):2324–35.
6. Torres VJ, Attia AS, Mason WJ, Hood MI, Corbin BD, Beasley FC, et al. *Staphylococcus aureus fur* regulates the expression of virulence factors that contribute to the pathogenesis of pneumonia. Infect Immun. 2010;78(4):1618–28.
7. Gao Q, Wang X, Xu H, Xu Y, Ling J, Zhang D, et al. Roles of iron acquisition systems in virulence of extraintestinal pathogenic *Escherichia coli*: Salmochelin and aerobactin contribute more to virulence than heme in a chicken infection model. BMC Microbiol. 2012;12:143.
8. Miao X, He J, Zhang L, Zhao X, Ge R, He QY, et al. A novel iron transporter SPD_1590 in *Streptococcus pneumoniae* contributing to bacterial virulence properties. Front Microbiol. 2018;9:1624.
9. Pandey R, Rodriguez GM. IdeR is required for iron homeostasis and virulence in *Mycobacterium tuberculosis*. Mol Microbiol. 2014;91(1):98–109.
10. Sheldon JR, Heinrichs DE. Recent developments in understanding the iron acquisition strategies of gram positive pathogens. FEMS Microbiol Rev. 2015;39(4):592–630.
11. Runyen-Janecky LJ. Role and regulation of heme iron acquisition in gram-negative pathogens. Front Cell Infect Microbiol. 2013;3:55.
12. Lindsay JA, Riley T V. Staphylococcal iron requirements, siderophore production, and iron-regulated protein expression. Infect Immun. 1994;62(6):2309–14.
13. Lindsay JA, Riley T V., Mee BJ. Production of siderophore by coagulase-negative staphylococci and its relation to virulence. Eur J Clin Microbiol Infect Dis. 1994;13(12):1063–6.
14. Modun B, Morrissey J, Williams P. The staphylococcal transferrin receptor: a glycolytic enzyme with novel functions. Trends Microbiol. 2000;8(5):231–7.
15. França A, Carvalhais V, Maira-Litrán T, Vilanova M, Cerca N, Pier G. Alterations in the *Staphylococcus epidermidis* biofilm transcriptome following interaction with whole human blood. Pathog Dis. 2014;70(3):444–8.
16. Knobloch JKM, Jäger S, Horstkotte MA, Rohde H, Mack D. RsbU-dependent regulation of *Staphylococcus epidermidis* biofilm formation is mediated via the alternative sigma factor σB by repression of the negative regulator gene *icaR*. Infect Immun. 2004;72(7):3838–48.
17. O'Gara JP. *ica* and beyond: Biofilm mechanisms and regulation in *Staphylococcus epidermidis* and *Staphylococcus aureus*. FEMS Microbiol Lett. 2007;270(2):179–88.

18. Cerca N, Brooks JL, Jefferson KK. Regulation of the intercellular adhesin locus regulator (*icaR*) by SarA, σB, and IcaR in *Staphylococcus aureus*. J Bacteriol. 2008;190(19):6530–3.

19. Lin MH, Shu JC, Huang HY, Cheng YC. Involvement of iron in biofilm formation by *Staphylococcus aureus*. PLoS One. 2012;7(3):e34388.

20. Oglesby-Sherrouse AG, Djapgne L, Nguyen AT, Vasil AI, Vasil ML. The complex interplay of iron, biofilm formation, and mucoidy affecting antimicrobial resistance of *Pseudomonas aeruginosa*. Pathog Dis. 2014;70(3):307–20.

21. Lin CS, Tsai YH, Chang CJ, Tseng SF, Wu TR, Lu CC, et al. An iron detection system determines bacterial swarming initiation and biofilm formation. Sci Rep. 2016;15(6):36747.

CHAPTER 2

Literature review

Summary

This chapter provides the reader with important information on the clinical relevance of *S. epidermidis* and its main virulence factors. A special attention is given to biofilm formation and iron acquisition processes.

2.1 *S. epidermidis:* a life between commensalism and pathogenicity

The genus *Staphylococcus* represents a large group of Gram-positive cocci, comprising nowadays more than 50 different bacterial species (1). A typical cell arrangement in irregular grape-like clusters, along with an extreme ability to thrive in high-salt environments are the main distinctive features of staphylococci. They are also well known as non-motile, non-spore forming, facultative anaerobic bacteria (2). Staphylococci have long been classified according to their ability to produce the enzyme coagulase: *S. aureus* is the major member of the coagulase-positive group; from the coagulase-negative staphylococci (CoNS) group, *S. epidermidis* is one of the most significant species. Regarding the latter, it is frequently found as part of the normal microflora of humans and other mammalians, colonizing specific niches such as skin, nares or mucosal membranes (3). *S. epidermidis* colonization does not usually pose a threat for the host, as it plays an important role not only in maintaining the normal commensal microflora, but also in inhibiting the colonization by other pathogenic microorganisms (4,5). Despite its commensal nature, *S. epidermidis* has been acknowledged as an opportunistic pathogen, being the etiological agent of a wide range of HAIs in patients with predisposing factors (6). Among these factors are premature birth (7), primary and secondary immunodeficiencies (8,9), transplant-related (10) or chemotherapy-induced immunosuppression (11), and most importantly, implantable medical devices (12). In fact, when it comes to medical device-associated infections (e.g., those originated by the use of catheter systems, prosthetic joints, and a range of other polymer and metal implants), *S. epidermidis* has consistently been found to be one of the most frequently isolated microorganisms (12–14). For this reason, this bacterial species is regarded as a paradigm of how harmless commensal bacteria can become pathogenic.

2.1.1. Clinical relevance

The detection of *S. epidermidis* in a clinical specimen is not always indicative of infection. In this context, it is extremely important to take into account that *S. epidermidis* makes up a significant proportion of the human skin microbiota (15), hence it is a common cause of contamination in clinical specimens (16–18). Therefore, its detection usually poses a challenge in clinical practice, as distinguishing whether it represents infection or simply colonization/ contamination is usually a difficult task (14). Considering the increasing importance of *S. epidermidis* in the context of HAIs[†], it is fundamental that its detection in a clinical specimen is correctly interpreted (19).

[†] According to the Centers for Disease Control and Prevention (CDC), a HAI is a localized or systemic condition (i) that results from an adverse reaction to the presence of an infectious agent(s) or its toxin(s), (ii) that occurs during a hospital admission, (iii) for which there is no evidence that the infection was present or incubating at the time of admission (231).

It is also important to emphasize that HAIs are a significant cause of morbidity and mortality around the world and represent an increasing problem in modern medicine (20). According to published studies, the estimated HAIs incidence rate in the United States was 4.5% in 2002, corresponding to nearly 1.7 million affected patients, with more than 98 000 deaths (~6%) due to HAIs (21). The European Centre for Disease Prevention and Control (ECDC) estimated that more than 4 million patients are affected by HAIs every year in Europe, with an average prevalence rate of 7.1%, which accounts for an annual cost of approximately 7 billion, including direct costs only (22,23). In developing countries, the estimated prevalence rates of HAIs are even higher, ranging from 5.7% to 19.1% (pooled prevalence rate of 10.1%) (23,24). In Portugal, the estimated prevalence rate of HAIs is 7.8% (25).

As stated above, *S. epidermidis* is a leading pathogen in the context of HAIs, particularly those associated with temporarily or permanently implanted medical devices (12,14). These infections can be confined to implant location, presenting local inflammation signs such as pain, swelling, tenderness, erythema, and purulent drainage, or disseminated systemically via hematogenous route, leading to a variety of systemic infections, particularly sepsis (14,26,27). Several studies have demonstrated that *S. epidermidis* is a major cause of a wide range of HAIs, such as catheter-related bloodstream infections (22,28), prosthetic (29) and native valve endocarditis (30), and prosthetic joint infections (31,32).

2.1.2. Pathogenic mechanisms

Despite significant advances in the field of *S. epidermidis* pathogenesis, it is still debatable whether this microorganism presents a clear pathogenic profile that surpasses its colonizing abilities, or it is only an "accidental" pathogen that uses the determinants that support its commensal lifestyle as virulence factors (6,33,34).

The switch from a commensal to a pathogenic lifestyle in *S. epidermidis* is often associated with the damage of superficial protective barriers (e.g. skin) (6). This phenomenon has been potentiated by the increasing use of indwelling medical devices over the last decades, particularly in immunocompromised patients (35) (**Figure 2.1**). The fact that *S. epidermidis* makes up a significant proportion of the normal human skin microflora makes the risk of contamination of medical devices with the patient's own flora extremely high (36). Additionally, evidence is available that a significant amount of *S. epidermidis* infections are due to specific strains that are able to somehow persist in hospital settings (37,38).

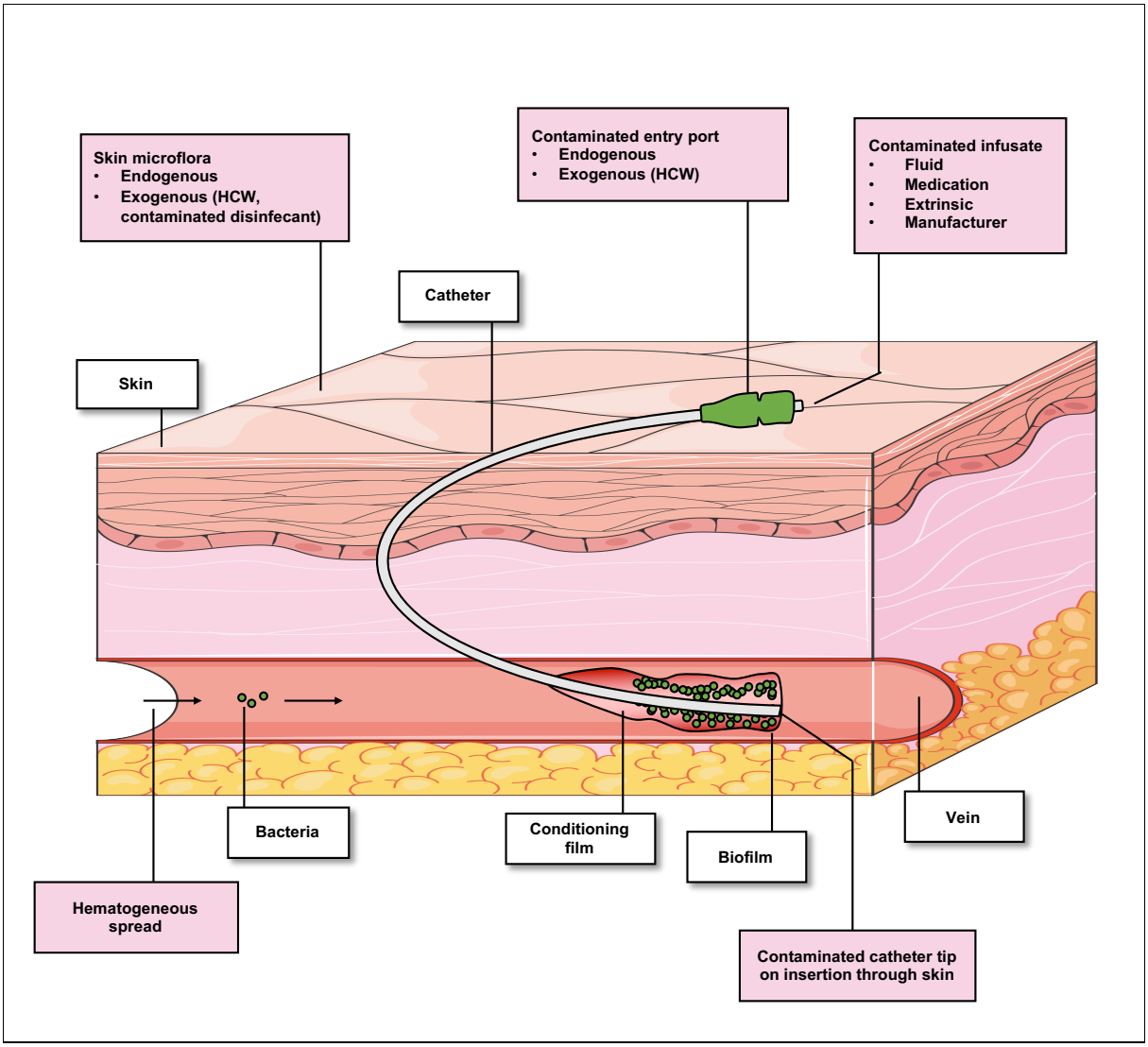

Figure 2.1. Diagram of a biofilm formed on the surface of an intravenous catheter and potential sources of contamination. HCW, healthcare worker. Adapted from James H, et al. (39).

Unlike *S. aureus*, *S. epidermidis* is equipped with few virulence factors and the mechanisms it employs to survive during infection are generally of a passive nature. Rather than aggressively attacking the host, *S. epidermidis* uses a strategy that allows persistence, which explains why most infections caused by this species are seldom life-threatening and progress towards a chronic nature (40). Its success as a pathogen is mostly attributable to its remarkable ability to adhere to different kinds of surfaces and to form complex bacterial agglomerations called biofilms (discussed in detail in section **2.1.3**). It is well established that the formation of biofilms renders *S. epidermidis* more tolerant to antibiotic therapy and to the host's immune system (41,42). Therefore, the molecular mechanisms governing bacterial adhesion and biofilm formation in *S. epidermidis* have received significant attention.

Additionally, *S. epidermidis* is able to produce factors that (i) confers resistance to antimicrobial peptides (AMPs), such is the case of SepA protease (43), and (ii) induce inflammatory responses or damage of host tissues. Although not recognized as a classical toxin producer, the production of phenol-soluble modulins (PSMs) is thought to be widespread across the majority of *S. epidermidis* strains (44). PSMs are peptide complexes with strong ability to activate the human innate immune response (45). *S. epidermidis* PSMγ (also known as δ-toxin) has been suggested to have cytolytic properties, while other PSMs share homology to *S. aureus* PSMs that have a strong ability to lyse human neutrophils (46). Interestingly, PSM production is also apparently involved in the modulation of the biofilm formation process in *S. epidermidis* by triggering the dispersion of bacteria from mature biofilms, and contributing for the dissemination of the infection (47).

In a review article about the molecular basis of the commensal and infectious lifestyles of *S. epidermidis* (6), staphyloferrins (a type of iron-binding molecules collectively known as siderophores) were also included in a list of *S. epidermidis* virulence factors. Although siderophores have been implicated in the pathogenesis of other species (48–50), there is currently not a single study on the genetic and molecular mechanisms behind siderophore production in *S. epidermidis,* let alone about its role on pathogenesis[‡].

2.1.3. Biofilm formation

A biofilm is defined as a structured community of microorganisms adhered to each other and/ or to a surface that is frequently embedded in a self-produced matrix of extracellular polymeric substance (51). Despite its frequent association with infectious diseases, it is important to bear in mind that this mode of growth is also adopted by non-pathogenic bacteria in different locations of the human body, such as skin (52) or gastrointestinal tract (53). For instance, it is widely accepted that *S. epidermidis* also adopts a biofilm mode of growth while inhabiting the human skin (6,40). Therefore, the ability to grow as a biofilm can be generally regarded as a way bacteria employ to cope with harsh environments (54). *S. epidermidis* follows a basic stepwise process that can be defined into four distinct stages (**Figure 2.2**): (1) primary attachment of cells to a surface, (2) accumulation of cells in multiple layers, (3) maturation of the biofilm structure, and (4) detachment (also referred to as dispersal) (55).

[‡] Iron acquisition in staphylococci is covered in detail in section **2.2.4. Chapters 4** and **5** include a wide range of experimental data that shed light into the genetic/ molecular mechanisms behind iron acquisition in *S. epidermidis,* as well as their role in virulence.

2.1.3.1. Attachment

Primary attachment of planktonic cells may occur in two distinct ways: (i) direct adhesion to a surface, or (ii) adhesion to a layer of host matrix proteins covering the surface (commonly referred as "conditioning film" and mostly associated with medical device-related infections). Despite the huge contribution of non-specific forces (e.g. van der Waals forces, hydrophobic and electrostatic interactions) (56), bacteria also produce cell surface proteins that play an important role in this step. *S. epidermidis* produces several molecules, such as the autolysins/ adhesins AtlE and Aae (57,58) and cell wall-associated adhesins, that interact with host extracellular matrix components and have been implicated in this step (59–61). These adhesins, also called Microbial Surface Components Recognizing Adhesive Matrix Molecules play a special role in the initiation of a medical device-associated infection, since devices become covered by extracellular matrix proteins (e.g. collagen, fibronectin, fibrinogen, vitronectin) once they cross the epithelial layer (34).

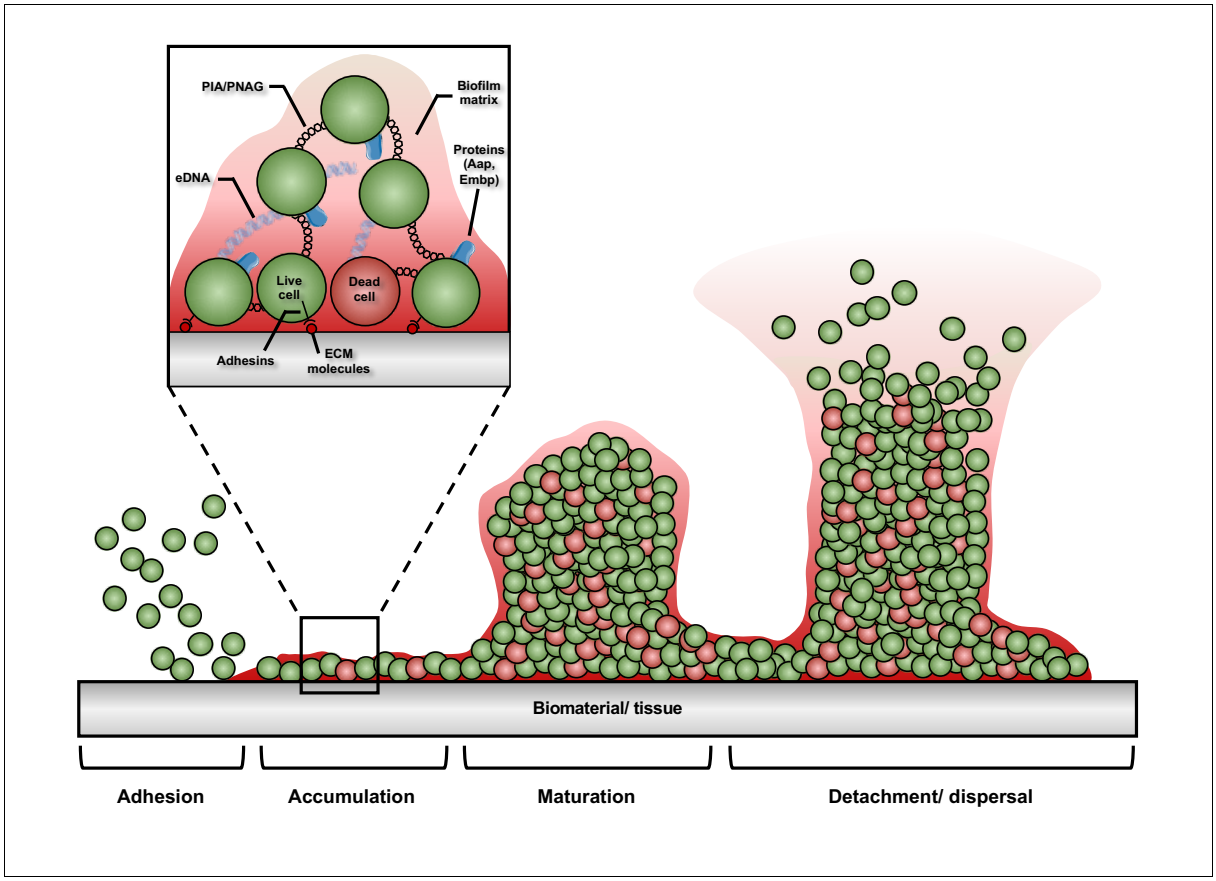

Figure 2.2. Stages of *S. epidermidis* biofilm formation and major molecules involved in this process. Aap, accumulation-associated protein; ECM, extracellular matrix; eDNA, extracellular DNA; Embp, extracellular matrix-binding protein; PIA/PNAG, polysaccharide intercellular adhesin/ poly-N-acetylglucosamine. Adpted from Arciola et al. (62).

2.1.3.2. Accumulation

Once attachment is successfully established, bacteria start multiplying and accumulating as multilayers of cells, leading to the formation of structures called microcolonies. This stage requires intercellular adhesion, which is mainly achieved by the production of extracellular polymeric substance (commonly referred to as biofilm matrix). This matrix is mostly composed by polysaccharides, proteins and nucleic acids, and functions essentially as a scaffold for the biofilm build up process (63).

Polysaccharide intercellular adhesin (also known as poly-N-acetylglucosamine; PIA/PNAG) is a partially de-acetylated β-1-6-linked N-acetylglucosamine (GlcNAc) homopolymer and was one of the first molecules found to be implicated in *S. epidermidis* biofilm accumulation (64–66). PIA/PNAG biosynthesis is mediated by the products of the *ica* (intercellular adhesion) operon (67,68). The membrane-located GlcNAc transferase IcaA and the accessory IcaD membrane protein are responsible for the synthesis of PIA/PNAG chains from activated GlcNAc monomers. The transmembrane protein IcaC is predicted to participate in the externalization and elongation of the growing polysaccharide chain (68). After this step, the cell surface-located enzyme IcaB partially de-acetylates the GlcNAc residues, introducing positive charge into the otherwise neutral polymer that is essential for the binding of PIA/PNAG to the bacterial cell surface (69).

Although the *ica* operon is frequently found in both commensal and clinically significant *S. epidermidis* isolates, some studies have demonstrated that strains that do not produce PIA/PNAG are also able to form biofilms (70–72). Since then, other factors mediating intercellular adhesion and biofilm accumulation have been identified such as the accumulation-associated protein (Aap) (73), the extracellular matrix-binding protein (Embp) (74), or the small basic protein (Sbp) (75).

Aap is a cell wall-anchored protein encoded by the *aap* gene and comprises two major domains, A and B. Aap is known to interact with PIA/PNAG, forming a protein-polysaccharide biofilm network (76), although it is able to promote biofilm formation in a PIA/PNAG-independent manner (73). Embp is a large protein (1 MDa) that combines intercellular adhesive and extracellular matrix binding properties and mediates biofilm accumulation in *ica*-negative and *aap*-negative *S. epidermidis* (74). Sbp is a recently described molecule (75) and was found to promote assembly of *S. epidermidis* cell aggregates and establishment of multilayered biofilms by influencing PIA/PNAG- and Aap-mediated intercellular adhesion.

2.1.3.3. Maturation

This stage is characterized by a balanced production of adhesive (discussed above) and disruptive factors, leading to the characteristic three-dimensional shape of biofilms. At this point, the production of disruptive factors is of extremely importance, so that channels can be created, and water, ions, and nutrients can be delivered to the deepest cell layers (77). Different kinds of molecules have been proposed to play a role during this process, namely proteases (78), nucleases (79–81), and PSMs (44,82). PSMs are peptides with known surfactant properties, and their role as facilitators of staphylococcal biofilm maturation is now well established. β-class PSMs in particular are produced at high amounts when cells adopt a biofilm mode of growth and have been shown to contribute for biofilm structuring and dissemination (83). Their expression is directly under the regulation of the cell density-dependent accessory gene regulator (Agr) quorum-sensing system, which renders it a key player in biofilm maturation (84).

2.1.3.4. Detachment/ dispersal

Once a biofilm reaches a given cell density, the Agr system orchestrates the downregulation of genes no longer needed (e.g. cell adhesion-related genes), and upregulation of genes encoding disruptive factors, as is the case of those encoding PSMs (85). This imbalance between adhesive and disruptive determinants in favor of the latter ultimately leads to the detachment of single bacterial cells or large cell clusters from the biofilm (86). Besides molecular effectors, environmental conditions such as temperature, pH, nutrients availability or shear forces may mediate release of cells from the biofilm (87). In a biofilm-associated infection scenario, this is particularly problematic since it leads to bacterial dissemination and biofilm formation elsewhere in the body (88). For instance, infections like endocarditis (89) or sepsis (90) are often the result of this kind of event. Although *in vitro* studies have implicated different *S. epidermidis* disruptive molecules in this stage, only PSMs have been shown to have *in vivo* relevance so far (82).

2.1.4. Impact of biofilms on infectious diseases

Even though the occurrence of biofilm formation in infectious diseases is not extensively well documented, the National Institutes of Health (NIH) estimates that 80% of all human microbial infections are associated with biofilms (77). This is a huge problem, especially when a biofilm grows on the surface of a medical device since its removal or replacement is often required (91). This implies high morbidity rates, with serious economic burden for the health system (92). At a lesser extent, microorganisms can also adhere

to biotic surfaces (e.g. human tissues), form a biofilm, and lead to a wide range of infections, such as cystic fibrosis (93), otitis media (94), infective endocarditis (89), dental caries and periodontitis (95), bacterial vaginosis (96), among others.

Biofilm-associated infections are hard to eradicate or frequently relapsing, which is partly explained by the fact that the biofilm matrix impedes the penetration of antimicrobial molecules (97,98), phagocytic cells (99,100), reactive oxygen species (ROS) (101,102), among others. Nevertheless, the understanding that the biofilm matrix acts solely as a physical barrier has been challenged over the years. In a study published by Singh et al. (103), it was demonstrated that the ability of different classes of antibiotics to kill biofilm cells are independent of penetration.

Another important issue about biofilm-associated infections is that biofilm cells employ different mechanisms to evade the host immune response. In *S. epidermidis*, it has been demonstrated that the diffusion of antibodies is not hindered by the biofilm matrix itself, but instead the biofilm biomass leads to dilution of antibodies, interfering with processes like opsonophagocytosis (41). In *S. aureus*, extracellular proteins found in the biofilm matrix were found to induce a protective immune response against infection (104). Inactivation of AMPs and complement proteins has also been observed in bacterial biofilms (105,106). Another issue related with biofilms is the fact that cells adopting this mode of growth exhibit a decreased growth rate, which leads to lower efficiency of antibiotics whose action is dependent on actively growing cells (107).

2.1.5. Innate immune response to S. epidermidis *infection*

When compared to *S. aureus*, the information on the host response to *S. epidermidis* infections is very limited. The first line of defense against *S. epidermidis* infections is provided by an innate immune response that comprises: (i) its recognition by phagocytic cells, particularly neutrophils (also referred to as polymorphonuclear leukocytes, PMNs) and macrophages; (ii) secretion of cytokines and chemokines. The latter leads to the recruitment of higher amounts of phagocytic cells to the site of infection (104). The role of the adaptive immune response in *S. epidermidis* infections is poorly understood. Nonetheless, it has been accepted that the adaptive response does not play a significant role in this context (42). This is supported by the fact that an immunoglobulin derived from donors with high titers of antistaphylococcal antibodies failed to reduce the incidence of sepsis in premature infants (109,110).

2.1.5.1. Recognition and killing by phagocytic cells

Phagocytes use pattern recognition receptors, such as Toll-like receptors (TLRs), that recognize conserved structures on the surface of pathogens, the so-called pathogen-associated molecular patterns (PAMPs) (111). In Gram-positive bacteria, lipoproteins and lipoteichoic acids (LTAs) are the most commonly recognized PAMPs (6). When PAMPs bind to TLRs, a cascade of protein activation takes place and results in the activation of the nuclear factor NF-κB and activator protein 1, transcriptional factors that promote cytokine production (112).

There is significant evidence reporting an immune response triggered by *S. epidermidis* via TLR2, which usually forms heterodimers with TLR1 and TLR6 (**Figure 2.3**) (113). These receptors recognize different staphylococci cell wall-associated molecules, such as lipoproteins, LTA and peptidoglycan (114). Nevertheless, activation of TLR2 by LTA in staphylococci is still a matter of debate (115,116). As purification of LTA is extremely difficult, the hypothesis that such activation is simply the result of TLR-stimulating contaminants has not been ruled out yet (117). PSMs secreted by *S. epidermidis* seem to be recognized by TLR2/TLR6 heterodimers (118), as well by formyl peptide receptor 2 (FPR2/ALX) expressed in neutrophils (119). PIA/PNAG was also reported to stimulate TLR2 (113,120,121). As for LTA, the TLR2-stimulating ability of both PSMs and PIA/PNAG still lacks confirmatory studies using gene deletion mutants. Finally, the role of this receptor in the response to *S. epidermidis* infections has also been confirmed through *in vivo* studies with TLR2 knock-out mice in bacteremia models (113,122).

Once a pathogen is recognized, the ultimate function of phagocytes is to ingest and destroy it, which is facilitated by host protective antibodies and the complement system (108). After being ingested by phagocytic cells, pathogens are internalized into membrane-bound vacuoles called phagosomes (123). These vesicles undergo a maturation process into highly microbicidal organelles known as phagolysosomes (124). The microbicidal activity of these organelles is mostly attributed to their acidic pH (~5.4 or less) due to proton translocation across the phagolysosome membrane mediated by a vacuolar-type ATPase (125). Another microbicidal mechanisms employed by phagocytes include production of ROS, as well as oxygen-independent processes involving AMPs (126). Neutrophils use an additional microbicidal mechanism to eliminate pathogens, known as neutrophil extracellular traps (NETs), that involves the release of extracellular nucleic acids capable of entrapping bacteria (127). Although the importance of this process in the clearance of *S. epidermidis* infections has not been confirmed, it has recently been shown that *S. epidermidis* biofilms elicit the generation of NETs (128). Macrophages have

also been demonstrated to phagocytose and eliminate *S. epidermidis* cells (129). Besides their phagocytic functions, macrophages are professional antigen-presenting cells (APCs), hence they have the ability to process pathogen's antigens, break them into peptides and present them in conjunction with class II major histocompatibility complex (MHC) molecules to T cells, acting as a bridge between innate and adaptive immunity (130).

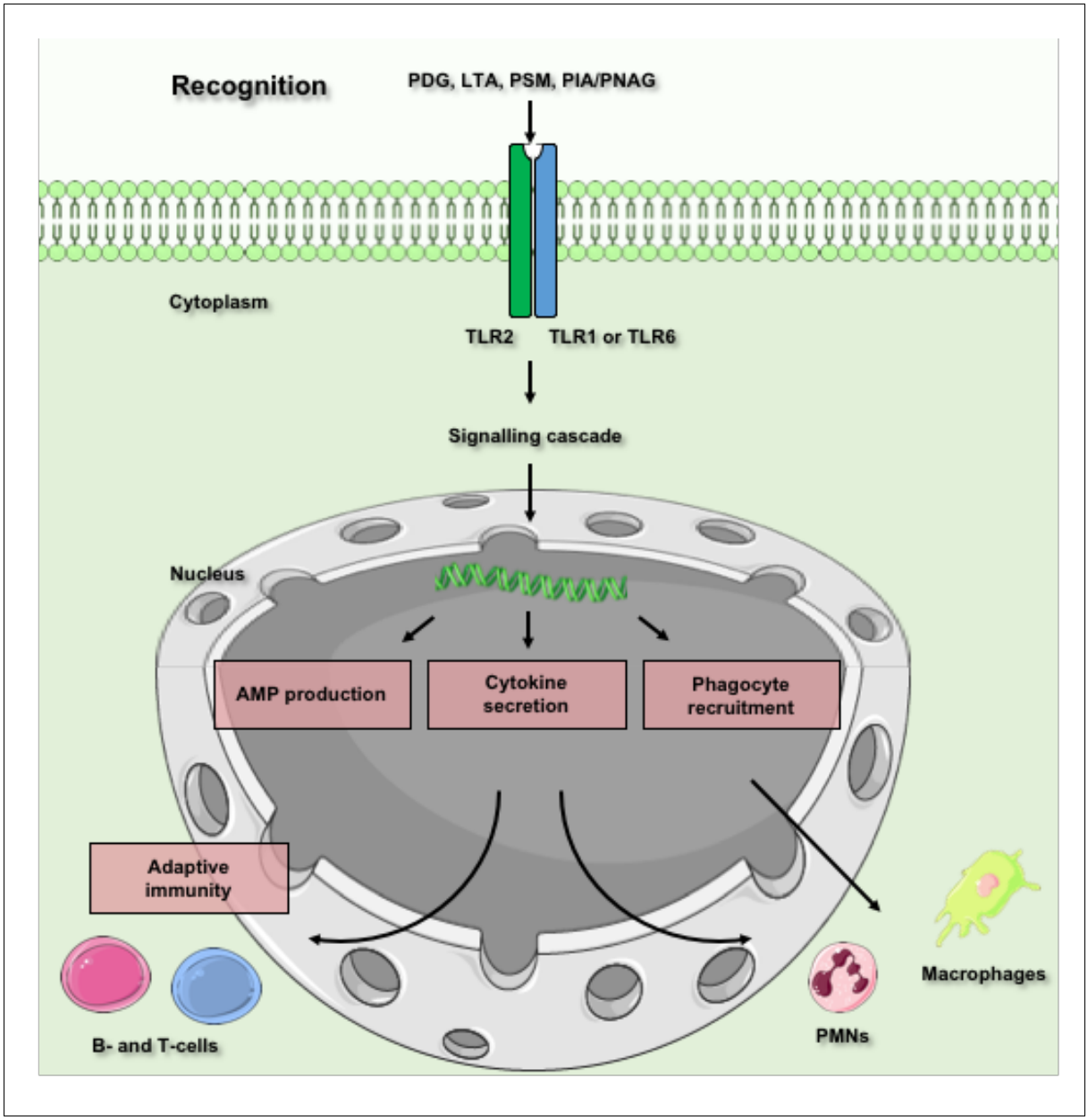

Figure 2.3. Simplified representation of *S. epidermidis* recognition by the host innate immune system. AMP, antimicrobial peptides; LTA, lipoteichoic acid; PDG, peptidoglycan; PIA/PNAG, polysaccharide intercellular adhesin/poly-N-acetylglucosamine; PSM, phenol-soluble modulin; TLR, Toll-like receptor. Adapted from Bescró et al. (131).

2.1.5.2. Secretion of cytokines

Cytokines represent a growing group of small cell-signaling proteins that play a complex regulatory role in the context of inflammation and immunity, such as cell recruitment, differentiation and activation (132). Cytokines are produced and released by a wide range of cells, particularly those of the immune system, such as macrophages and lymphocytes (133). Given their primary function in the regulation of inflammation, cytokines are commonly classified into pro- and anti-inflammatory. Among well-characterized pro-inflammatory cytokines are interleukin-1β (IL-1β), IL-6, IL-12, tumor necrosis factor-alpha (TNF-α), and interferon gamma (IFN-γ), whereas IL-4, IL-10, IL-13, and transforming growth factor-beta (TGF-β) are well-known cytokines with anti-inflammatory activity (134).

From a general point of view, cytokines perform their functions by binding to a specific receptor on the surface of the target cell, which triggers a signaling cascade that leads to alteration of cell function. This alteration usually encompasses positive or negative regulation of several genes and their transcription factors, which ultimately result in production of other cytokines, increased expression of surface receptors for other molecules or eventually the suppression of the cytokine's own effect (135). A wide variety of factors are known to stimulate cells to produce cytokines, such as infectious agents and internal stimuli, like cytokines themselves (132), or even complement activation (136).

During the past few years, host inflammatory responses to *S. epidermidis* infections have received some attention. *In vitro* induction of cytokine production by different staphylococcal species in peripheral blood mononuclear cells (PBMCs) revealed secretion of high amounts of proinflammatory cytokines, namely IL-1β and IL-6, although the levels induced by *S. epidermidis* were significantly lower than those induced by *S. aureus* (137). Similarly, stimulation of cord blood cells and PBMCs with *S. epidermidis* also resulted in expression of IL-1β, IL-6 and TNF-α (138). Similar experiments with monocyte-derived dendritic cells demonstrated that *S. epidermidis* induced the release of the anti-inflammatory cytokine IL-10 (139). Spiliopoulou et al. (140) reported that stimulation of monocyte-derived macrophages with *S. epidermidis* biofilm cells resulted in lower amounts of proinflammatory cytokines, such as IFN-γ, TNF-α and IL-12, and higher amounts of IL-13, as compared to stimulation with planktonic cells. Schommer et al. (141) compared biofilm-positive and isogenic biofilm-negative strains and also observed that biofilm-producing strains induced reduced inflammatory response in J774A.1 macrophages characterized by lower production of IL-1β. When compared to other bacterial pathogens, *S. epidermidis* induced

significantly lower levels of TNF-α, IL-1β, IL-6 and IL-8 than *Escherichia coli* and group B streptococci in cord blood (142).

Data derived from *in vivo* studies have confirmed the results obtained *in vitro*. Using a murine model of catheter-associated *S. epidermidis* biofilm infection, IL-10 was pointed out as an important molecule in the control of the inflammatory response but not of the bacterial burden (143). In an intradermal infection model, *S. epidermidis* induced higher levels of IL-10 and lower levels of IL-12 and TNF-α than *Propionibacterium acnes* (144). Ferreirinha et al. (145) challenged mice intraperitoneally with a PIA/PNAG-producing strain and its isogenic PIA/PNAG-defective mutant, which resulted in elevated IL-6 and IL-10 levels, while no increase in TNF-α and IL-12 was detected. Furthermore, production of IL-6 and IL-10 was higher in mice infected with the PIA/PNAG-producing strain. Following a different approach, França et al. (146) used a murine model of hematogenously disseminated infection to assess the inflammatory response induced by three bacterial cell populations (planktonic, biofilm, and biofilm-released cells). 2 h after the bacterial challenge, it was observed that infection with biofilm and biofilm-released cells induced higher production of TNF-α than infection with planktonic cells. Conversely, 6 h after infection, levels of TNF-α and IL-6 detected in biofilm-infected mice were significantly lower than those detected in mice infected with planktonic and biofilm-released cells.

Collectively, and excluding slight variations, possibly attributable to strains and experimental conditions used, it has been demonstrated over the years that *S. epidermidis* elicits lower production of pro-inflammatory cytokines, while triggering the production of anti-inflammatory cytokines. This phenomenon is particularly evident for biofilm cells and is thought to contribute to the persistent character of *S. epidermidis* infections (131).

2.1.5.3. Complement activation

Another relevant process in the innate immune response is the activation of the complement system. Complement refers to a family of proteins that opsonizes pathogens and act as proinflammatory chemoattractant molecules, so that phagocytic cells are recruited to the infection site to destroy invading pathogens (147). Most of these proteins are normally inactive, and the recognition of PAMPs triggers their activation. This process involves a cascade of proteolytic cleavages, in which the activation of one protein enzymatically cleaves and activates the next protein in the cascade (148).

The activation of the complement system can follow three different pathways: (i) classical, (ii) lectin, and (iii) alternative pathways (147). The classical pathway requires either direct recognition of bacterial surface structures or binding to surface-bound antibodies (149). The lectin pathway is activated by the binding of mannose-binding lectin or ficolins to mannose residues on the pathogen's surface (150). The alternative pathway is continuously and spontaneously activated by the hydrolysis of the thioester bond present in a molecule called C3 (151).

The major purpose of complement activation is opsonization, a process that enhances phagocytosis. Phagocytic cells migrate to the site of infection following the production of chemoattractant molecules, such as the small peptide fragments C3a and C5a, and release of formylated peptides by the pathogen itself. This leads to deposition of C3b on the bacterial surface, promoting phagocytic uptake (152). Unlike the alternative pathway, the classical and lectin pathways seem to play a major role in host defense against *S. epidermidis* infections (106). While complement activation seems to have an important role in the neutrophil-mediated killing of planktonic *S. epidermidis* cells, biofilm formation protects *S. epidermidis* from IgG and complement opsonization, as well as neutrophil-mediated killing (106).

2.2. Iron and its biological importance

2.2.1. General chemical properties

Iron belongs to the subfamily of transition elements and is one of the most abundant metals on Earth (154). It is a key nutrient for almost all living organisms, including bacteria, with very few exceptions (155,156), since it participates in essential biochemical processes, such as electron transfer and catalysis (157). In nature, most iron exists under the form of two oxidative states: ferrous (Fe^{2+}) and ferric (Fe^{3+}) iron. Under aqueous, aerobic environments, Fe^{2+} is spontaneously oxidized to Fe^{3+}, leading to the formation of ferric hydroxide. Additionally, the solubility of ferric hydroxide under neutral pH conditions usually found in the human body is extremely low (158). To overcome this low solubility issue, superior organisms are able to produce proteins (e.g. transferrin and ferritin) that are able to bind Fe^{3+} and maintain it stable while making it simultaneously available for biochemical processes (159). The binding of most iron to proteins along with its low solubility is also part of a strategy to control the proliferation of undesirable bacteria and other microorganisms, a process commonly referred to as nutritional immunity (160).

2.2.2. Iron reservoirs in the human body

The adult human body contains approximately 3-5 g of iron (161). Even though this represents a large quantity, the levels of free available iron in the body are kept to a minimum (162). Therefore, most of iron is complexed as Fe^{2+} in several proteins, such as metalloproteins. In these proteins, iron is mostly found in the form of heme prosthetic groups (163). Hemoglobin, a well-known metalloprotein present in erythroid precursors and mature erythrocytes, represents the major iron reservoir (~65%). The remaining iron is stored in hepatocytes, bound to ferritin, and within macrophages (164). A small proportion can be found in muscles within myoglobin, or as part of other cellular iron-containing proteins (165). Another fraction of the iron is present in the so-called labile iron pool, which consists of redox-active iron ions (both Fe^{2+} and Fe^{3+}) bound to a variety of low affinity ligands (166).

2.2.3. Iron-binding proteins

2.2.3.1. Heme proteins: hemoglobin

Heme is a common prosthetic group of many proteins, composed of a large heterocyclic ring, called protoporphyrin IX, and an iron atom in its ferrous state. Porphyrins are an important class of chelating agents that can coordinate to a metal through their four nitrogen atoms as electron-pair donors (167). After the insertion of Fe^{2+} into protoporphyrin IX, which takes place in the mitochondria, heme is further exported to the cytoplasmic space for its incorporation into proteins (168). According to the protein to which it is attached, heme can play different functions.

In mammals, heme is mostly found within hemoglobin in erythrocytes, and its function is to deliver oxygen to living tissues (169). Hemoglobin contains four heme groups and most of the iron in the human body is found in this molecule. Release of heme upon lysis of erythrocytes would be problematic as it participates in the generation of toxic hydroxyl radicals when not bound to proteins (170). Macrophages are responsible for counteracting this phenomenon by efficiently uptake and dispose heme. Besides avoiding toxicity, this process is extremely important in the recycling of iron, as well as in reducing the free iron pool available to pathogens (171).

2.2.3.2. Transferrin

Dietary iron absorption takes place mostly at the duodenum and the upper portions of the jejunum. After uptake and storage inside enterocytes, iron is eventually exported into circulation. At this stage, iron is bound to transferrin delivered to sites of usage and storage (172). Transferrin is a glycoprotein produced

by the liver, and a potent, reversible iron chelator. Its affinity for Fe^{3+} ions is high, with equilibrium constants around 10^{19}- 10^{20} M^{-1} at physiological pH, while affinity for Fe^{2+} ions is negligible (173). In healthy adult individuals, normal serum transferrin levels range from 2.0 to 3.0 g/L (25.0 to 37.5 μM) (174). Nevertheless, only 30% is iron saturated, which ensures that a large transferrin proportion is still capable of accommodating an increase in the serum iron levels (175). Transferrin-bound iron is mostly delivered to erythroid, hepatic, and immune cells through a receptor-mediated (transferrin receptors 1 and 2, TfR1 and TfR2) endocytosis process (176).

2.2.3.3. Lactoferrin

Lactoferrin is another glycoprotein with great affinity for iron. It shares sequence and structure similarities with transferrin and is primarily found in human secretions. Even though lactoferrin is not involved in iron transport, it is thought to play an important role in limiting bacterial growth through reduction of the amount of circulating free iron. During infection, lactoferrin is released by PMNs during degranulation so that localized sequestration of iron is achieved (177). However, most recent studies have suggested that the antimicrobial properties of lactoferrin might be iron-independent (178,179).

2.2.4. Bacterial iron acquisition systems

With very few exceptions (155,156), most bacteria rely on their ability to scavenge several biologically essential metals, and iron in particular, for their survival both *in vitro* and *in vivo* (180–183). As previously stated, most of iron in mammals is found intracellularly, which renders it very difficult to access by extracellular pathogens. In addition, the tiny amount of iron residing extracellularly is mostly bound by high affinity iron-binding proteins. This ensures that the amount of free iron in solution is approximately 10^{-24} M (183). This is an extremely low level to support bacterial proliferation, as microorganisms typically require iron concentrations of approximately 10^{-6} M for growth (184). To overcome this situation, bacteria have developed specialized mechanisms to acquire iron and use it in their favor for their own cellular functions (185).

Mutagenesis studies in different bacterial pathogens have demonstrated that specific inactivation of iron acquisition-related genes leads to measurable loss in virulence (50,186–190), leading to a perception of the bacterial iron acquisition systems as virulence factors.

2.2.4.1. ABC transporter-mediated iron uptake

One common strategy that bacteria employ to meet their iron requirements is to express specific surface receptors coupled to specialized transport systems so that they are able to translocate iron across their cytoplasmic membrane (191). Most of iron transport systems belongs to the class of ATP-binding cassette (ABC) transporters, which mediates the import of iron either in its ionic form or coupled to host-synthesized, iron-binding proteins, heme or siderophores.

Classically, an ABC transporter (**Figure 2.4**) comprises three distinct domains: (i) a high affinity substrate binding protein (in Gram-positive bacteria it is anchored to the cytoplasmic membrane as a lipoprotein); (ii) a homodimeric or heterodimeric transmembrane domain (permease) for transport of the substrate across the cytoplasmic membrane; and (iii) an ATPase located in the cytoplasmic compartment that provide energy for the transport system (192).

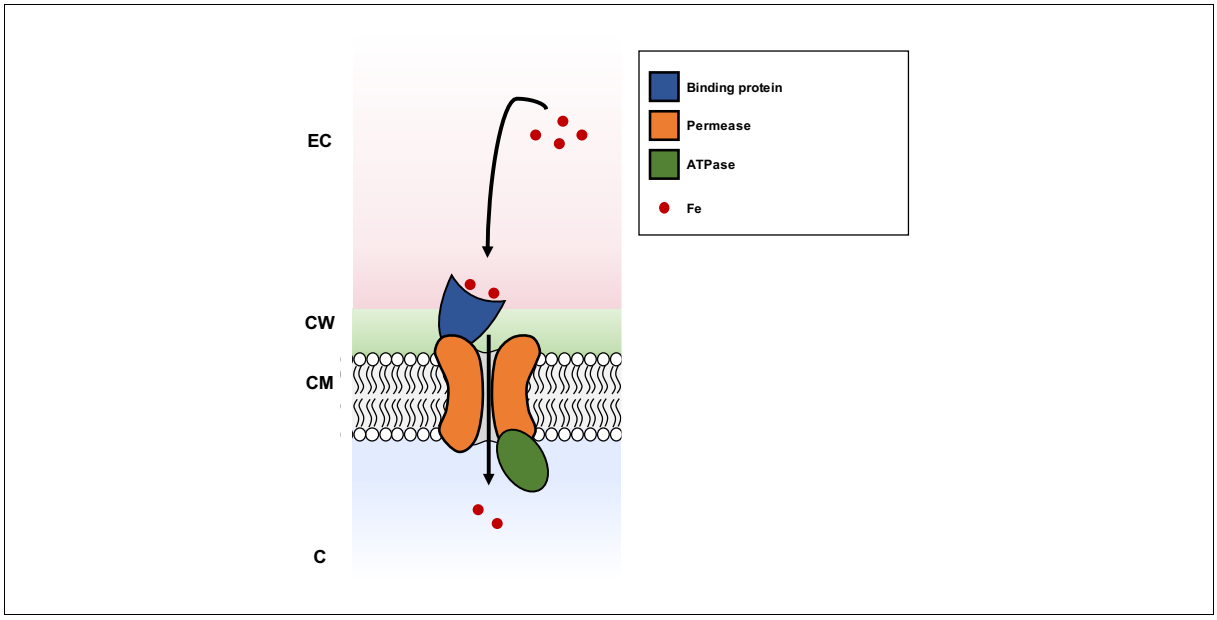

Figure 2.4. Schematic representation of an ABC transporter in Gram-positive bacteria. Iron is captured by the binding protein and translocated through permeases. The energy required for the process comes from ATPase-mediated ATP hydrolysis. C, cytoplasm; CM, cell membrane; CW, cell wall; EC, extracellular space. Adapted from Davidson et al. (193).

2.2.4.2. Siderophore-mediated iron uptake

Siderophore-mediated iron uptake is a widely spread strategy among bacteria to survive in iron-restricted environments. Siderophores are a class of small (usually less than 1 kDa), potent iron-chelating organic molecules with high affinity for Fe^{3+} (194). Siderophores comprise an impressive diversity of molecules and can be classified according to the functional groups constituting the iron-coordinating ligands as

catecholates, hydroxamates, carboxylates, and mixed ligands (**Figure 2.5**). Siderophores generally form hexadentate, octahedral, complexes with a ferric ion in a 1:1 ratio of siderophore to iron (195). Owing to their high affinity for iron (pM[§] values in the range of 20-30 (196)), siderophores can compete for this element against host iron-binding proteins, such as transferrin or ferritin. Siderophores are synthesized intracellularly and secreted into the environment as iron-free compounds (195). Once Fe^{3+}-siderophore complexes are formed, their transport across the bacterial cell membrane to the cytoplasm takes place through a myriad of uptake systems, ABC transporters in particular (197). The subsequent release of iron from high affinity siderophores may follow two different mechanisms: (i) enzymatic reduction of siderophore-bound Fe^{3+} to Fe^{2+} (198,199) or (ii) enzyme-catalyzed siderophore hydrolysis (200). By the time bacterial iron requirements are met, the transcription of genes encoding iron transport systems is downregulated through the action of a repressor protein called Fur (Ferric uptake regulator; discussed in section **2.2.5**) (201).

2.2.4.3. Siderophore biosynthesis

There are two major pathways for siderophore biosynthesis: the non-ribosomal peptide synthetase (NRPS) and the NRPS-independent synthetase (NIS) pathways (202).

Siderophores synthesized through NRPS are composed by a peptide scaffold assembled in the absence of a ribosome, which usually incorporates proteinogenic and non-proteinogenic amino acids that may suffer some modifications, namely methylation, glycosylation, hydroxylation, among others (203). Several siderophores are synthesized via this pathway, such as enterobactin (*E. coli* (204)), yersiniabactin (*Yersinia pestis* (205)), or mycobactin (*Mycobacterium tuberculosis* (206)).

Conversely, the assembly of siderophores through NIS is far less understood. The assembly of siderophores via this pathway involves the condensation of a carboxylic acid (usually citric or succinic acid) with an amine or alcohol group. All NIS enzymes characterized so far possess a conserved N-terminal iron uptake chelate (Iuc) A/IucC domain and have a C- terminal domain related to iron transport or metabolism (196). Among known siderophores synthesized via NIS pathway are aerobactin (*E. coli* (207)), vibrioferrin (*Vibrio parahaemolyticus* (208)), alcaligin (*Bordetella pertussis* (209)), or staphyloferrins A (182,210) and B (211) (*S. aureus*).

[§] The pM value expresses the concentration of free iron in solution under particular sets of experimental conditions (typically at a total iron chelator concentration of 10^{-5} M and a total iron concentration of 10^{-6} M, in a solution at pH 7.4).

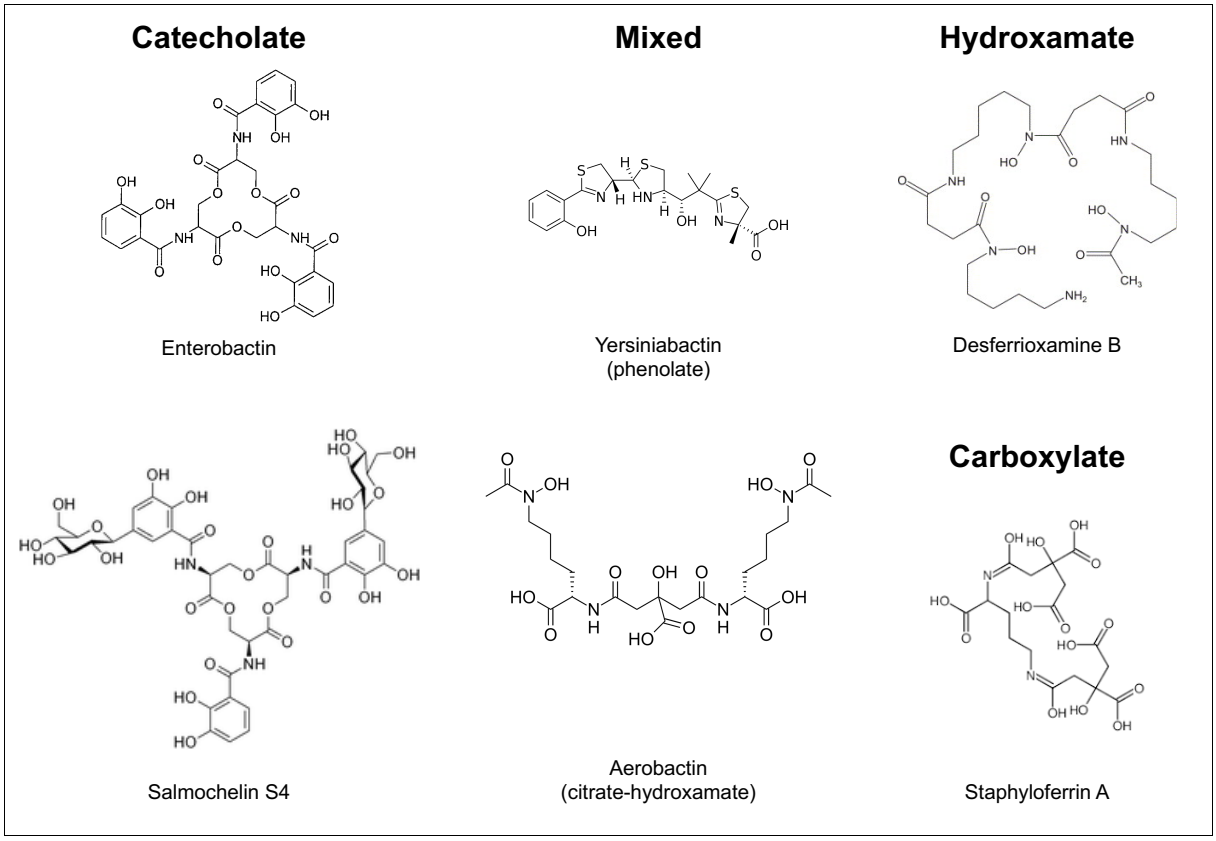

Figure 2.5. Different structural families of siderophores and representative members. Adapted from Holden et al. (212).

2.2.4.4. Siderophore-mediated iron acquisition in staphylococci

Most of the knowledge on siderophore-mediated iron acquisition in staphylococci is derived from studies in *S. aureus*, while studies of this process in *S. epidermidis* are totally absent. To date, two siderophores belonging to the carboxylate family and synthesized via the NIS pathway have been characterized: staphyloferrin A and staphyloferrin B (213).

Staphyloferrin A is composed of D-ornithine and two molecules of citrate, and its biosynthesis requires the activity of enzymes encoded by the *sfaABCD* operon (182,210). Synthesis of an intermediate molecule, δ-citryl-d-ornithine, and its further condensation to another molecule of citrate are carried out by synthetases SfaD and SfaB, respectively (210). SfaC is a putative ornithine racemase and is presumably involved in the generation of D-ornithine. SfaA shares homology with transporters form the Major Facilitator Superfamily (MFS) and is likely involved in the transport of the assembled siderophore to the extracellular milieu. After sequestering iron, the iron-siderophores complexes are then internalized through the ABC transporter HtsABC (182).

Biosynthesis of staphyloferrin B is mediated by the products encoded by the *sbnA–I* operon (211). There are four different molecules in its composition: L-2,3-diaminopropionic acid, citrate, 1,2-diaminoethane, and α-ketoglutarate. The condensation of these molecules is predicted to require the activity of three NIS synthetases, SbnC, SbnE and SbnF (214,215).

S. aureus is also able to uptake xenosiderophores (siderophores secreted by other species) of the iron(III)-hydroxymate type through its ferric hydroxamate uptake (Fhu) transport system encoded by five genes (216). *fhuC*, *fhuB*, and *fhuG* are located in an operon that encodes an ATPase and two membrane permeases, respectively (217). *fhuD1* and *fhuD2* are genetically unlinked to the *fhuCBG* operon and encode iron(III)-hydroxamate-binding lipoproteins (218).

2.2.4.5. Role of siderophores during infection

During infection, pathogenic bacteria face very harsh conditions, particularly iron restriction (219). When iron becomes a limiting nutrient, pathogens upregulate siderophore biosynthesis and secretion, so that they outcompete host iron-binding proteins and deliver it back to the bacterial cytoplasm (194). A wide range of relevant pathogens rely on siderophore-mediated iron acquisition to establish an infection, such as *E. coli* (49), *Pseudomonas aeruginosa* (50) or *M. tuberculosis* (48). Despite being of paramount importance in the sequestration of iron from the host, recent literature suggests that siderophores play several other roles that go beyond iron acquisition (212).

Pyoverdin, produced by *P. aeruginosa,* was shown to induce mitochondrial fragmentation in *Caenorhabditis elegans,* generating a hypoxic response and cell death (220). A similar process was observed for different *Enterobacteriaceae*, in which siderophores generate a hypoxic response in host cells by activating the host transcription factor HIF-1 (hypoxia-inducible factor 1), a key transcriptional regulator during adaptation to hypoxia (221,222). Yersiniabactin, aerobactin, and deferoxamine are capable of inhibiting ROS production by different innate immune cells as a consequence of reduced iron availability (223). Enterobactin inhibits macrophages antimicrobial responses against intracellular infection by *Salmonella enterica* serovar Typhimurium through chelation of the intracellular labile iron pool, and modulation of the expression of essential iron-regulatory proteins, such as divalent metal transporter 1, ferroportin, and hepcidin (224).

2.2.5. Bacterial regulation of iron acquisition systems

The expression of different bacterial virulence factors, particularly those associated with iron acquisition, is triggered by a decreased intracellular iron content (225). The regulatory protein Fur is a conserved mechanism across bacteria responsible for the regulation of transcriptional responses to iron deprivation, and is now recognized as the canonical global iron-responsive regulator in bacteria (201). In general, when the intracellular iron content surpasses the level required for proper cellular function, there is an association of one Fe^{2+} ion with two Fur monomers. In its dimeric form, Fur is able to bind a conserved 19-bp DNA motif within the operator region of target genes, called the Fur box, which blocks RNA polymerase and ultimately leads to repression of gene transcription (226). Once the intracellular iron levels become depleted, the Fe^{2+} ion dissociates from the Fur dimer, the Fur box becomes unoccupied, and transcription of target genes is resumed (226). In *S. aureus*, Fur has been shown to regulate the transcription of iron acquisition- (182,227,228) and other virulence-related genes (229), and it seems to be involved in biofilm formation (230). Current knowledge about the involvement of iron and Fur as transcription regulators in *S. epidermidis* is limited and hence this issue is addressed in the following chapter.

2.3. References

1. Euzéby JP. List of bacterial names with standing in nomenclature: a folder available on the internet. Int J Syst Evol Microbiol. 1997;47(2):590–2.
2. Murray PR, Rosenthal KS, Pfaller MA. Medical microbiology. In: Medical microbiology. 8th ed. Elsevier Health Sciences; 2015.
3. Grice EA, Kong HH, Conlan S, Deming CB, Davis J, Young AC, et al. Topographical and temporal diversity of the human skin microbiome. Science. 2009;324(5931):1190–2.
4. Cogen AL, Yamasaki K, Sanchez KM, Dorschner RA, Lai Y, MacLeod DT, et al. Selective antimicrobial action is provided by phenol-soluble modulins derived from *Staphylococcus epidermidis*, a normal resident of the skin. J Invest Dermatol. 2010;130(1):192–200.
5. Cogen AL, Yamasaki K, Muto J, Sanchez KM, Crotty Alexander L, Tanios J, et al. *Staphylococcus epidermidis* antimicrobial delta-toxin (phenol-soluble modulin-gamma) cooperates with host antimicrobial peptides to kill group A *Streptococcus*. PLoS One. 2010;5(5):e8557.
6. Otto M. *Staphylococcus epidermidis* - the 'accidental' pathogen. Nat Rev Microbiol. 2009;7(8):555–67.
7. Marchant EA, Boyce GK, Sadarangani M, Lavoie PM. Neonatal sepsis due to coagulase-negative staphylococci. Clin Dev Immunol. 2013;2013:586076.
8. Lim MS, Elenitoba-Johnson KSJ. The molecular pathology of primary immunodeficiencies. J Mol Diagnostics. 2004;6(2):59–83.
9. Roberts RL, Stiehm ER. Immunodeficiency. In: Encyclopedia of life sciences. 2007. p.1–8.

10. Ilyas M, Maganty N, Ginsberg Z, Sharma A. Skin infections due to bacteria in solid organ transplant recipients: a review. Dermatology. 2018;233(5):358–65.

11. Klastersky J, Aoun M. Opportunistic infections in patients with cancer. Ann Oncol. 2004;15(4):iv329–iv335.

12. McCann MT, Gilmore BF, Gorman SP. *Staphylococcus epidermidis* device-related infections: pathogenesis and clinical management. J Pharm Pharmacol. 2008;60(12):1551–71.

13. Hogan S, Stevens NT, Humphreys H, Gara JPO, Neill EO. Current and future approaches to the prevention and treatment of staphylococcal medical device-related infections. Curr Pharm Des. 2015;21(1):100–13.

14. Becker K, Heilmann C, Peters G. Coagulase-negative staphylococci. Clin Microbiol Rev. 2014;27(4):870–926.

15. Ross AA, Müller KM, Weese JS, Neufeld JD. Comprehensive skin microbiome analysis reveals the uniqueness of human skin and evidence for phylosymbiosis within the class Mammalia. Proc Natl Acad Sci. 2018;115(25):E5786–95.

16. Norberg A, Christopher NC, Ramundo ML, Bower JR, Berman SA. Contamination rates of blood cultures obtained by dedicated phlebotomy vs intravenous catheter. J Am Med Assoc. 2003;289(6):726–9.

17. Schifman RB, Strand CL, Meier FA, Howanitz PJ. Blood culture contamination: a College of American Pathologist Q-Probes study involving 640 institutions and 497134 specimens from adult patients. Arch Pathol Lab Med. 1998;122(3):216–21.

18. Hall KK, Lyman JA. Updated review of blood culture contamination. Clin Microbiol Rev. 2006;19(4):788–802.

19. Widerström M. Significance of *Staphylococcus epidermidis* in health care-associated infections, from contaminant to clinically relevant pathogen: this is a wake-up call! J Clin Microbiol. 2016;54(7):1679–81.

20. Haque M, Sartelli M, McKimm J, Bakar MA. Health care-associated infections - an overview. Infect Drug Resist. 2018;11:2321–33.

21. Klevens RM, Edwards JR, Richards CL, Horan TC, Gaynes RP, Pollock DA, et al. Estimating health care-associated infections and deaths in U.S. Hospitals, 2002. Public Health Rep. 2007;122(2):160–6.

22. European Centre for Disease Prevention and Control. Annual epidemiological report for 2016: healthcare-associated infections in intensive care units. Available from: https://ecdc.europa.eu/sites/portal/files/documents/AER_for_2016-HAI_0.pdf [Accessed 4th July 2019]

23. Allegranzi B, Nejad SB, Combescure C, Graafmans W, Attar H, Donaldson L, et al. Report on the burden of endemic health care-associated infection worldwide. WHO Library Cataloguing-in-Publication Data. 2011.

24. Pittet D, Allegranzi B, Storr J, Nejad SB, Dziekan G, Leotsakos A, et al. Infection control as a major World Health Organization priority for developing countries. J Hosp Infect. 2008;68(4):285–92.

25. Rodrigues M do R, Lebre AI, Alves A, Félix AM, Tavares D, Noriega E, et al. Infeções e resistências aos antimicrobianos: relatório anual do programa prioritário 2018. Direção Geral da Saúde. 2018.

26. Chambers ST. Diagnosis and management of staphylococcal infections of vascular grafts and stents. Intern Med J. 2005;35(Suppl 2):S72-8.

27. Otto M. *Staphylococcus epidermidis*: a major player in bacterial sepsis? Future Microbiol. 2017;12:1031–3.

28. Rosenthal VD, Maki DG, Mehta Y, Leblebicioglu H, Memish ZA, Al-Mousa HH, et al. International Nosocomial Infection Control Consortiu (INICC) report, data summary of 43 countries for 2007-2012. Device-associated module. Am J Infect Control. 2014;42(9):942–56.

29. Baddour LM, Wilson WR, Bayer AS, Fowler VG, Tleyjeh IM, Rybak MJ, et al. Infective endocarditis in adults: diagnosis, antimicrobial therapy, and management of complications - a scientific statement for healthcare professionals from the American Heart Association. Circulation. 2015;132(15):1435–86.

30. Benito N, Miro JM, De Lazzari E, Cabell CH, Del Rio A, Altclas J, et al. Health care-associated native valve endocarditis: importance of non-nosocomial acquisition. Ann Intern Med. 2009;150(9):586–94.

31. Rohde H, Burandt EC, Siemssen N, Frommelt L, Burdelski C, Wurster S, et al. Polysaccharide intercellular adhesin or protein factors in biofilm accumulation of *Staphylococcus epidermidis* and *Staphylococcus aureus* isolated from prosthetic hip and knee joint infections. Biomaterials. 2007;28(9):1711–20.

32. Tornero E, García-Oltra E, García-Ramiro S, Martínez-Pastor JC, Bosch J, Climent C, et al. Prosthetic joint infections due to *Staphylococcus aureus* and coagulase-negative staphylococci. Int J Artif Organs. 2012;35(10):884–92.

33. Mack D, Davies AP, Harris LG, Knobloch JKM, Rohde H. *Staphylococcus epidermidis* biofilms:Functional molecules, relation to virulence, and vaccine potential. Top Curr Chem. 2009;288:157–82.

34. Büttner H, Mack D, Rohde H. Structural basis of *Staphylococcus epidermidis* biofilm formation: mechanisms and molecular interactions. Front Cell Infect Microbiol. 2015;5(2235-2988 (Electronic)):14.

35. Van Epps JS, Younger JG. Implantable device-related infection. Shock. 2016;46(6):597–608.

36. M. O. Methicillin-resistant *Staphylococcus aureus* infection is associated with increased mortality. Future Microbiol. 2012;7(2):189–91.

37. Blum-Menezes D, Bratfich OJ, Padoveze MC, Moretti ML. Hospital strain colonization by *Staphylococcus epidermidis*. Brazilian J Med Biol Res. 2009;42(3):294–8.

38. Widerström M, Monsen T, Karlsson C, Wiström J. Molecular epidemiology of meticillin-resistant coagulase-negative staphylococci in a Swedish county hospital: evidence of intra- and interhospital clonal spread. J Hosp Infect. 2006;64(2):177–83.

39. James H, Ghannoum M, Jurevic R. The story of biofilms. J Invasive Fungal Infect. 2011;5(2):37–42.

40. Otto M. *Staphylococcus epidermidis* pathogenesis. In: Fey PD. (ed.) *Staphylococcus epidermidis* Methods in Molecular Biology (Methods and Protocols). Totowa: Humana Press; 2014. p.17–31.

41. Cerca N, Jefferson KK, Oliveira R, Pier GB, Azeredo J. Comparative antibody-mediated phagocytosis of *Staphylococcus epidermidis* cells grown in a biofilm or in the planktonic state. Infect Immun. 2006;74(8):4849–55.

42. Nguyen TH, Park MD, Otto M. Host Response to *Staphylococcus epidermidis* Colonization and Infections. Front Cell Infect Microbiol. 2017;7:90.

43. Lai Y, Villaruz AE, Li M, Cha DJ, Sturdevant DE, Otto M. The human anionic antimicrobial peptide dermcidin induces proteolytic defence mechanisms in staphylococci. Mol Microbiol. 2007;63(2):497–506.

44. Periasamy S, Chatterjee SS, Cheung GYC, Otto M. Phenol-soluble modulins in staphylococci: What are they originally for? Commun Integr Biol. 2012;5(3):275–7.

45. Vuong C, Kidder JB, Jacobson ER, Otto M, Proctor RA, Somerville GA. *Staphylococcus epidermidis* Polysaccharide Intercellular Adhesin Production Significantly Increases during Tricarboxylic Acid Cycle Stress. Society. 2005;187(9):2967–73.

46. Wang R, Braughton KR, Kretschmer D, Bach THL, Queck SY, Li M, et al. Identification of novel cytolytic peptides as key virulence determinants for community-associated MRSA. Nat Med. 2007;13(12):1510–4.

47. Vadyvaloo V, Otto M. Molecular genetics of *Staphylococcus epidermidis* biofilms on indwelling medical devices. Int J Artif Organs. 2005;28(11):1069–78.

48. Madigan CA, Martinot AJ, Wei JR, Madduri A, Cheng TY, Young DC, et al. Lipidomic Analysis Links Mycobactin Synthase K to Iron Uptake and Virulence in *M. tuberculosis*. PLoS Pathog. 2015;11(3):e1004792.

49. Caza M, Lépine F, Dozois CM. Secretion, but not overall synthesis, of catecholate siderophores contributes to virulence of extraintestinal pathogenic *Escherichia coli*. Mol Microbiol. 2011;80(1):266–82.

50. Meyer JM, Neely A, Stintzi A, Georges C, Holder IA. Pyoverdin is essential for virulence of *Pseudomonas aeruginosa*. Infect Immun. 1996;64(2):518–23.

51. Vert, M.; Doi, Y.; Hellwich, K.; Hess, M.; Hodge, P.; Kubisa, P.; Rinaudo, M.; Schue F. Terminology for biorelated polymers and applications (IUPAC Recommendations 2012). Pure Appl Chem. 2012;84(2):377–410.

52. Brandwein M, Steinberg D, Meshner S. Microbial biofilms and the human skin microbiome. npj Biofilms Microbiomes. 2016;2:3.

53. De Vos WM. Microbial biofilms and the human intestinal microbiome. npj Biofilms Microbiomes. 2015;1:15005.

54. Flemming HC, Wingender J, Szewzyk U, Steinberg P, Rice SA, Kjelleberg S. Biofilms: An emergent form of bacterial life. Nat Rev Microbiol. 2016;14(9):563–75.

55. Fey PD, Olson ME. Current concepts in biofilm formation of *Staphylococcus epidermidis*. Future Microbiol. 2010;5(6):917–33.

56. Bos R, Van Der Mei HC, Busscher HJ. Physico-chemistry of initial microbial adhesive interactions - Its mechanisms and methods for study. FEMS Microbiol Rev. 1999;23(2):179–230.

57. Heilmann C, Hussain M, Peters G, Götz F. Evidence for autolysin-mediated primary attachment of *Staphylococcus epidermidis* to a polystyrene surface. Mol Microbiol. 1997;24(5):1013–24.

58. Heilmann C, Thumm G, Chhatwal GS, Hartleib J, Uekötter A, Peters G. Identification and characterization of a novel autolysin (Aae) with adhesive properties from *Staphylococcus epidermidis*. Microbiology. 2003;149(Pt 10):2769–78.

59. Nilsson M, Frykberg L, Flock JI, Pei L, Lindberg M, Guss B. A fibrinogen-binding protein of *Staphylococcus epidermidis*. Infect Immun. 1998;66(6):2666–73.

60. Williams RJ, Henderson B, Sharp LJ, Nair SP. Identification of a fibronectin-binding protein from *Staphylococcus epidermidis*. Infect Immun. 2002;70(12):6805–10.

61. Arrecubieta C, Lee MH, Macey A, Foster TJ, Lowy FD. SdrF, a *Staphylococcus epidermidis* surface protein, binds type I collagen. J Biol Chem. 2007;282(26):18767–76.

62. Arciola CR, Campoccia D, Montanaro L. Implant infections: Adhesion, biofilm formation and immune evasion. Nat Rev Microbiol. 2018;16(7):397–409.

63. Flemming HC. The perfect slime. Colloids Surfaces B Biointerfaces. 2011;86(2):251–9.

64. Rohde H, Burandt EC, Siemssen N, Frommelt L, Burdelski C, Wurster S, et al. Polysaccharide intercellular adhesin or protein factors in biofilm accumulation of *Staphylococcus epidermidis* and *Staphylococcus aureus* isolated from prosthetic hip and knee joint infections. Biomaterials. 2007;28(9):1711–20.

65. Maira-Litrán T, Kropec A, Abeygunawardana C, Joyce J, Mark G, Goldmann DA, et al. Immunochemical properties of the staphylococcal poly-N-acetylglucosamine surface polysaccharide. Infect Immun. 2002;70(8):4433–40.

66. Ziebuhr W, Heilmann C, Götz F, Meyer P, Wilms K, Straube E, et al. Detection of the intercellular adhesion gene cluster (*ica*) and phase variation in *Staphylococcus epidermidis* blood culture strains and mucosal isolates. Infect Immun. 1997;65(3):890–6.

67. Heilmann C, Schweitzer O, Gerke C, Vanittanakom N, Mack D, Götz F. Molecular basis of intercellular adhesion in the biofilm-forming *Staphylococcus epidermidis*. Mol Microbiol. 1996;20(5):1083–91.

68. Gerke C, Kraft A, Süßmuth R, Schweitzer O, Götz F. Characterization of the N-Acetylglucosaminyltransferase activity involved in the biosynthesis of the *Staphylococcus epidermidis* polysaccharide intercellular adhesin. J Biol Chem. 1998;273(29):18586–93.

69. Vuong C, Voyich JM, Fischer ER, Braughton KR, Whitney AR, DeLeo FR, et al. Polysaccharide intercellular adhesin (PIA) protects *Staphylococcus epidermidis* against major components of the human innate immune system. Cell Microbiol. 2004;6(3):269–75.

70. Dice B, Stoodley P, Buchinsky F, Metha N, Ehrlich GD, Hu FZ. Biofilm formation by *ica*-positive and *ica*-negative strains of *Staphylococcus epidermidis in vitro*. Biofouling. 2009;25(4):367–75.

71. Esteban J, Molina-Manso D, Spiliopoulou I, Cordero-Ampuero J, Fernndez-Roblas R, Foka A, et al. Biofilm development by clinical isolates of *Staphylococcus* spp. from retrieved orthopedic prostheses. Acta Orthop. 2010;81(6):674–9.

72. Yu S, Wei Q, Zhao T, Guo Y, Ma LZ. A survival strategy for *Pseudomonas aeruginosa* that uses exopolysaccharides to sequester and store iron to stimulate psl-dependent biofilm formation. Appl Environ Microbiol. 2016;82(21):6403–13.

73. Rohde H, Burdelski C, Bartscht K, Hussain M, Buck F, Horstkotte MA, et al. Induction of *Staphylococcus epidermidis* biofilm formation via proteolytic processing of the accumulation-associated protein by staphylococcal and host proteases. Mol Microbiol. 2005;55(6):1883–95.

74. Christner M, Franke GC, Schommer NN, Wendt U, Wegert K, Pehle P, et al. The giant extracellular matrix-binding protein of *Staphylococcus epidermidis* mediates biofilm accumulation and attachment to fibronectin. Mol Microbiol. 2010;75(1):187–207.

75. Decker R, Burdelski C, Zobiak M, Büttner H, Franke G, Christner M, et al. An 18 kDa Scaffold Protein Is Critical for *Staphylococcus epidermidis* Biofilm Formation. PLoS Pathog. 2015;11(3):1–32.

76. Bateman A, Holden MTG, Yeats C. The G5 domain: A potential N-acetylglucosamine recognition domain involved in biofilm formation. Bioinformatics. 2005;21(8):1301–3.

77. Joo HS, Otto M. Molecular basis of in vivo biofilm formation by bacterial pathogens. Chem Biol. 2012;19(12):1503–13.

78. Boles BR, Horswill AR. Agr-mediated dispersal of *Staphylococcus aureus* biofilms. PLoS Pathog. 2008;4(4):e1000052.

79. Mann EE, Rice KC, Boles BR, Endres JL, Ranjit D, Chandramohan L, et al. Modulation of eDNA release and degradation affects *Staphylococcus aureus* biofilm maturation. PLoS One. 2009;4(6):e5822.

80. Beenken KE, Spencer H, Griffin LM, Smeltzer MS. Impact of extracellular nuclease production on the biofilm phenotype of *Staphylococcus aureus* under *in vitro* and *in vivo* conditions. Infect Immun. 2012;80(5):1634–8.

81. Kiedrowski MR, Kavanaugh JS, Malone CL, Mootz JM, Voyich JM, Smeltzer MS, et al. Nuclease modulates biofilm formation in community-associated methicillin-resistant *Staphylococcus aureus*. PLoS One. 2011;6(11):e26714.

82. Wang R, Khan BA, Cheung GYC, Bach THL, Jameson-Lee M, Kong KF, et al. *Staphylococcus epidermidis* surfactant peptides promote biofilm maturation and dissemination of biofilm-associated infection in mice. J Clin Invest. 2011;121(1):238–48.

83. Otto M. Staphylococcal Infections: Mechanisms of Biofilm Maturation and Detachment as Critical Determinants of Pathogenicity. Annu Rev Med. 2012;64:175–88.

84. Xu T, Wang XY, Cui P, Zhang YM, Zhang WH, Zhang Y. The Agr quorum sensing system represses persister formation through regulation of phenol-soluble modulins in *Staphylococcus aureus*. Front Microbiol. 2017;8:2189.

85. Le KY, Dastgheyb S, Ho T V., Otto M. Molecular determinants of staphylococcal biofilm dispersal and structuring. Front Cell Infect Microbiol. 2014;4:167.

86. Schoenfelder SMK, Lange C, Eckart M, Hennig S, Kozytska S, Ziebuhr W. Success through diversity - How *Staphylococcus epidermidis* establishes as a nosocomial pathogen. Int J Med Microbiol. 2010;300(6):380–6.

87. Boles BR, Horswill AR. Staphylococcal biofilm disassembly. Trends Microbiol. 2011;19(9):449–55.

88. Guilhen C, Forestier C, Balestrino D. Biofilm dispersal: multiple elaborate strategies for dissemination of bacteria with unique properties. Mol Microbiol. 2017;105(2):188–210.

89. Elgharably H, Hussain ST, Shrestha NK, Blackstone EH, Pettersson GB. Current hypotheses in cardiac surgery: biofilm in infective endocarditis. Semin Thorac Cardiovasc Surg. 2016;28(1):56–9.

90. Fleming D, Rumbaugh K. The consequences of biofilm dispersal on the host. Sci Rep. 2018;8(1):10738.

91. Percival SL, Suleman L, Vuotto C, Donelli G. Healthcare-associated infections, medical devices and biofilms: risk, tolerance and control. J Med Microbiol. 2015;64(Pt 4):323–34.

92. Donlan RM, Costerton JW. Biofilms: survival mechanisms of clinically relevant microorganisms. Clin Microbiol Rev. 2002;15(2):167–93.

93. Høiby N, Bjarnsholt T, Moser C, Jensen PØ, Kolpen M, Qvist T, et al. Diagnosis of biofilm infections in cystic fibrosis patients. APMIS. 2017;125(4):339–43.

94. Gu X. b, Keyoumu Y., Long L., Zhang H. Detection of bacterial biofilms in different types of chronic otitis media. Eur Arch Oto-Rhino-Laryngology. 2013;271(11):2877–83.

95. Sanz M, Beighton D, Curtis MA, Cury JA, Dige I, Dommisch H, et al. Role of microbial biofilms in the maintenance of oral health and in the development of dental caries and periodontal diseases. Consensus report of group 1 of the Joint EFP/ORCA workshop on the boundaries between caries and periodontal disease. J Clin Periodontol. 2017;44(Supplement 18):S5–11.

96. Machado D, Castro J, Palmeira-de-Oliveira A, Martinez-de-Oliveira J, Cerca N. Bacterial vaginosis biofilms: challenges to current therapies and emerging solutions. Front Microbiol. 2016;6:1528.

97. Anderson GG, O'Toole GA. Innate and induced resistance mechanisms of bacterial biofilms. Curr Top Microbiol Immunol. 2008;322:85–105.

98. Goltermann L, Tolker-Nielsen T. Importance of the exopolysaccharide matrix in antimicrobial tolerance of *Pseudomonas aeruginosa* aggregates. Antimicrob Agents Chemother. 2017;61(4):e02696.

99. Leid JG, Willson CJ, Shirtliff ME, Hassett DJ, Parsek MR, Jeffers AK. The exopolysaccharide alginate protects *Pseudomonas aeruginosa* biofilm bacteria from IFN-gamma-mediated macrophage killing. J Immunol. 2005;175(11):7512–8.

100. Thurlow LR, Hanke ML, Fritz T, Angle A, Aldrich A, Williams SH, et al. *Staphylococcus aureus* biofilms prevent macrophage phagocytosis and attenuate inflammation *in vivo*. J Immunol. 2011;186(11):6585–96.

101. Hay ID, Wang Y, Moradali MF, Rehman ZU, Rehm BHA. Genetics and regulation of bacterial alginate production. Environ Microbiol. 2014;16(10):2997–3011.

102. Ryder VJ, Chopra I, O'Neill AJ. Increased mutability of staphylococci in biofilms as a consequence of oxidative stress. PLoS One. 2012;7(10):e47695.

103. Singh R, Sahore S, Kaur P, Rani A, Ray P. Penetration barrier contributes to bacterial biofilm-associated resistance against only select antibiotics, and exhibits genus-, strain- and antibiotic-specific differences. Pathog Dis. 2016;74(6):ftw056.

104. Gil C, Solano C, Burgui S, Latasa C, García B, Toledo-Arana A, et al. Biofilm matrix exoproteins induce a protective immune response against *Staphylococcus aureus* biofilm infection. Infect Immun. 2014;82(3):1017–29.

105. Domenech M, Ramos-Sevillano E, García E, Moscoso M, Yuste J. Biofilm formation avoids complement immunity and phagocytosis of *Streptococcus pneumoniae*. Infect Immun. 2013;81(7):2606–15.

106. Kristian SA, Birkenstock TA, Sauder U, Mack D, Götz F, Landmann R. Biofilm formation induces C3a release and protects *Staphylococcus epidermidis* from IgG and complement deposition and from neutrophil-dependent killing. J Infect Dis. 2008;197(7):1028–35.

107. Lewis K. Riddle of biofilm resistance. Antimicrob Agents Chemother. 2001;45(4):999–1007.

108. Foster TJ. Immune evasion by staphylococci. Nat Rev Microbiol. 2005;3(12):948–58.

109. Bloom B, Schelonka R, Kueser T, Walker W, Jung E, Kaufman D, et al. Multicenter study to assess safety and efficacy of INH-A21, a donor-selected human staphylococcal immunoglobulin, for prevention of nosocomial infections in very low birth weight infants. Pediatr Infect Dis J. 2005;24(10):858–66.

110. DeJonge M, Burchfield D, Bloom B, Duenas M, Walker W, Polak M, et al. Clinical trial of safety and efficacy of IHN-A21 for the prevention of nosocomial staphylococcal bloodstream infection in premature infants. J Pediatr. 2007;151(3):260–5.

111. Akira S, Hemmi H. Recognition of pathogen-associated molecular patterns by TLR family. Immunol Lett. 2003;85(2):85–95.

112. Takeda K, Akira S. TLR signaling pathways. Semin Immunol. 2004;16(1):3–9.

113. Strunk T, Coombs MRP, Currie AJ, Richmond P, Golenbock DT, Stoler-Barak L, et al. TLR2 mediates recognition of live *Staphylococcus epidermidis* and clearance of bacteremia. PLoS One. 2010;5(4):e10111.

114. Fournier B. The function of TLR2 during staphylococcal diseases. Front Cell Infect Microbiol. 2013;2:167.

115. Götz Kariya F, Kiyohara A, Suda Y, Krikae F, Masahito Hashimoto T, Tawaratsumida K. Not Lipoteichoic Acid but Lipoproteins Appear to Be the Dominant Immunobiologically Active Compounds in *Staphylococcus aureus*. J Immunol. 2006;177(5):3162–9.

116. von Aulock S, Hartung T, Hermann C. Comment on "Not lipoteichoic acid but lipoproteins appear to be the dominant immunobiologically active compounds in *Staphylococcus aureus*." J Immunol. 2007;178(5):2610.

117. Hashimoto M, Tawaratsumida K, Kariya H, Aoyama K, Tamura T, Suda Y. Lipoprotein is a predominant Toll-like receptor 2 ligand in *Staphylococcus aureus* cell wall components. Int Immunol. 2006;18(2):355–62.

118. Hajjar AM, O'Mahony DS, Ozinsky A, Underhill DM, Aderem A, Klebanoff SJ, et al. Cutting edge: functional interactions between Toll-like receptor (TLR) 2 and TLR1 or TLR6 in response to phenol-soluble modulin. J Immunol. 2001;166(1):15–9.

119. Rautenberg M, Joo H-S, Otto M, Peschel A. Neutrophil responses to staphylococcal pathogens and commensals via the formyl peptide receptor 2 relates to phenol-soluble modulin release and virulence. FASEB J. 2010;25(4):1254–63.

120. Stevens NT, Sadovskaya I, Jabbouri S, Sattar T, O'gara JP, Humphreys H, et al. *Staphylococcus epidermidis* polysaccharide intercellular adhesin induces IL-8 expression in human astrocytes via a mechanism involving TLR2. Cell Microbiol. 2009;11(3):421–32.

121. Lai Y, Cogen AL, Radek KA, Park HJ, MacLeod DT, Leichtle A, et al. Activation of TLR2 by a small molecule produced by *Staphylococcus epidermidis* increases antimicrobial defense against bacterial skin infections. J Invest Dermatol. 2010;130(9):2211–21.

122. Bi D, Qiao L, Bergelson I, Ek CJ, Duan L, Zhang X, et al. *Staphylococcus epidermidis* bacteremia induces brain injury in neonatal mice via toll-like receptor 2-dependent and -independent pathways. J Infect Dis. 2015;212(9):1480–90.

123. Flannagan RS, Jaumouillé V, Grinstein S. The Cell Biology of Phagocytosis. Annu Rev Pathol Mech Dis. 2011;7:61–98.

124. Fairn GD, Grinstein S. How nascent phagosomes mature to become phagolysosomes. Trends Immunol. 2012;33(8):397–405.

125. Lukacs GL, Rotstein OD, Grinstein S. Phagosomal acidification is mediated by a vacuolar-type H^+-ATPase in murine macrophages. J Biol Chem. 1990;265(34):21099–107.

126. Nauseef WM. How human neutrophils kill and degrade microbes: an integrated view. Immunol Rev. 2007;219:88–102.

127. Yipp BG, Kubes P. NETosis: how vital is it? Blood. 2013;122(16):2784–94.

128. Dapunt U, Gaida MM, Meyle E, Prior B, Hänsch GM. Activation of phagocytic cells by *Staphylococcus epidermidis* biofilms: effects of extracellular matrix proteins and the bacterial stress protein GroEL on netosis and MRP-14 release. Pathog Dis. 2016;74(5):ftw035.

129. Riool M, De Boer L, Jaspers V, Van Der Loos CM, Van Wamel WJB, Wu G, et al. *Staphylococcus epidermidis* originating from titanium implants infects surrounding tissue and immune cells. Acta Biomater. 2014;10(12):5202–12.

130. Davis MM, Boniface JJ, Reich Z, Lyons D, Hampl J, Arden B, et al. Ligand recognition by alpha beta T cell receptors. Annu Rev Immunol. 1998;16:523–44.

131. Brescó MS, Harris LG, Thompson K, Stanic B, Morgenstern M, O'Mahony L, et al. Pathogenic mechanisms and host interactions in *Staphylococcus epidermidis* device-related infection. Front Microbiol. 2017;8:1401.

132. Malik STA, Balkwill FR. Cytokines. In: The nude mouse in oncology research. 2018.

133. Duque GA, Descoteaux A. Macrophage cytokines: involvement in immunity and infectious diseases. Front Immunol. 2014;5:491.

134. Cavaillon JM. Pro- versus anti-inflammatory cytokines: myth or reality. Cell Mol Biol. 2001;47(4):695–702.

135. Corwin EJ. Understanding cytokines. Part I: Physiology and mechanism of action. Biol Res Nurs. 2000;2(1):30–40.

136. de Boer JP, Wolbink GJ, Thijs LG, Baars JW, Wagstaff J, Hack CE. Interplay of complement and cytokines in the pathogenesis of septic shock. Immunopharmacology. 1992;24(2):135–48.

137. Megyeri K, Mándi Y, Degré M, Rosztóczy I. Induction of cytokine production by different staphylococcal strains. Cytokine. 2002;19(4):206–12.

138. Strunk T, Prosser A, Levy O, Philbin V, Simmer K, Doherty D, et al. Responsiveness of human monocytes to the commensal bacterium *Staphylococcus epidermidis* develops late in gestation. Pediatr Res. 2012;72(1):10–8.

139. Laborel-Préneron E, Bianchi P, Boralevi F, Lehours P, Fraysse F, Morice-Picard F, et al. Effects of the *Staphylococcus aureus* and *Staphylococcus epidermidis* secretomes isolated from the skin microbiota of atopic children on $CD4^+$ T cell activation. PLoS One. 2015;10(10):e0141067.

140. Spiliopoulou AI, Kolonitsiou F, Krevvata MI, Leontsinidis M, Wilkinson TS, Mack D, et al. Bacterial adhesion, intracellular survival and cytokine induction upon stimulation of mononuclear cells with planktonic or biofilm phase *Staphylococcus epidermidis*. FEMS Microbiol Lett. 2012;330(1):56–65.

141. Schommer NN, Christner M, Hentschke M, Ruckdeschel K, Aepfelbacher M, Rohde H. *Staphylococcus epidermidis* uses distinct mechanisms of biofilm formation to interfere with phagocytosis and activation of mouse macrophage-like cells J774A.1. Infect Immun. 2011;79(6):2267–76.

142. Mohamed MA, Cunningham-Rundles S, Dean CR, Hammad TA, Nesin M. Levels of pro-inflammatory cytokines produced from cord blood in-*vitro* are pathogen dependent and increased in comparison to adult controls. Cytokine. 2007;39(3):171–7.

143. Gutierrez-Murgas YM, Skar G, Ramirez D, Beaver M, Snowden JN. IL-10 plays an important role in the control of inflammation but not in the bacterial burden in *S. epidermidis* CNS catheter infection. J Neuroinflammation. 2016;13:271.

144. Bialecka A, Mak M, Biedron R. Different pro-inflammatory and immunogenic potentials of *Propionibacterium acnes* and *Staphylococcus epidermidis*: implications for chronic inflammatory acne. Arch Immunol Ther Exp. 2005;53(1):79–85.

145. Ferreirinha P, Pérez-Cabezas B, Correia A, Miyazawa B, França A, Carvalhais V, et al. Poly-N-acetylglucosamine production by *Staphylococcus epidermidis* cells increases their *in vivo* proinflammatory effect. Infect Immun. 2016;84(10):2933–43.

146. França A, Pérez-Cabezas B, Correia A, Pier GB, Cerca N, Vilanova M. *Staphylococcus epidermidis* biofilm-released cells induce a prompt and more marked in vivo inflammatory-type response than planktonic or biofilm cells. Front Microbiol. 2016;7:1530.

147. Rus H, Cudrici C, Niculescu F. The role of the complement system in innate immunity. Immunol Res. 2005;33(2):103–12.

148. Mayilyan KR, Kang YH, Dodds AW, Sim RB. The complement system in innate immunity. In: Heine H. (ed.) Innate immunity of plants, animals, and humans nucleic acids and molecular biology. Berlin: Springer; 2007. p.219–36.

149. Sim RB. Complement, classical pathway. In: Delves PJ. (ed.) Encyclopedia of immunology. 2nd ed. London: Academic Press; 1998. p.604–12.

150. Fujita T, Matsushita M, Endo Y. The lectin-complement pathway - Its role in innate immunity and evolution. Immunol Rev. 2004;198(185–202).

151. Harboe M, Mollnes TE. The alternative complement pathway revisited. J Cell Mol Med. 2008;12(4):1074–84.

152. Bajic G, Degn SE, Thiel S, Andersen GR. Complement activation, regulation, and molecular basis for complement-related diseases. EMBO J. 2015;34(22):2735–57.

153. Aarag Fredheim EG, Granslo HN, Flægstad T, Figenschau Y, Rohde H, Sadovskaya I, et al. *Staphylococcus epidermidis* polysaccharide intercellular adhesin activates complement. FEMS Immunol Med Microbiol. 2011;63(2):269–80.

154. Frey PA, Reed GH. The ubiquity of iron. ACS Chem Biol. 2012;7(9):1477–81.

155. Troxell B, Xu H, Yang XF. *Borrelia burgdorferi*, a pathogen that lacks iron, encodes manganese-dependent superoxide dismutase essential for resistance to streptonigrin. J Biol Chem. 2012;287(23):19284–93.

156. Archibald F. *Lactobacillus plantarum*, an organism not requiring iron. FEMS Microbiol Lett. 1983;19(1):29–32.

157. Hudson JM, Heffron K, Kotlyar V, Sher Y, Maklashina E, Cecchini G, et al. Electron transfer and catalytic control by the iron-sulfur clusters in a respiratory enzyme, *E. coli* fumarate reductase. J Am Chem Soc. 2005;127(19):6977–89.

158. Schwertmann U. Solubility and dissolution of iron oxides. In: Plant and Soil. 1991. p. 1–25.

159. Brock JH. Iron-binding proteins. Acta Paediatr Scand Suppl. 1989;361:31–43.

160. Skaar EP. The battle for iron between bacterial pathogens and their vertebrate hosts. PLoS Pathog. 2010;6(8):e1000949.

161. Zhang AS, Enns CA. Iron homeostasis: Recently identified proteins provide insight into novel control mechanisms. J Biol Chem. 2009;284(2):711–5.

162. Waldvogel-Abramowski S, Waeber G, Gassner C, Buser A, Frey BM, Favrat B, et al. Physiology of iron metabolism. Transfus Med Hemotherapy. 2014;41(3):213–221.

163. Liu J, Chakraborty S, Hosseinzadeh P, Yu Y, Tian S, Petrik I, et al. Metalloproteins containing cytochrome, iron–sulfur, or copper redox centers. Chem Rev. 2014;114(8):4366–469.

164. Meynard D, Babitt JL, Lin HY. The liver: Conductor of systemic iron balance. Blood. 2014;123(2):168–76.

165. Soares MP, Hamza I. Macrophages and iron metabolism. Immunity. 2016;44(3):492–504.

166. Kakhlon O, Cabantchik ZI. The labile iron pool: characterization, measurement, and participation in cellular processes. Free Radic Biol Med. 2002;33(8):1037–46.

167. Walker FA, Simonis U. Iron porphyrin chemistry. In: King RB. (ed.) Encyclopedia of inorganic and bioinorganic chemistry. 10th ed. John Wiley & Sons, Ltd; 2011.

168. Martinez-Guzman O, Dietz J V, Bohovych I, Medlock AW, Khalimonchuk O, Reddi AR. Mitochondrial-nuclear heme trafficking is regulated by GTPases that control mitochondrial dynamics. bioRxiv. 2019;

169. Mairbäurl H, Weber RE. Oxygen transport by hemoglobin. Compr Physiol. 2012;2(2):1463–89.

170. Emerit J, Beaumont C, Trivin F. Iron metabolism, free radicals, and oxidative injury. Biomed Pharmacother. 2001;55(6):333–9.

171. Alam MZ, Devalaraja S, Haldar M. The heme connection: Linking erythrocytes and macrophage biology. Front Immunol. 2017;8:33.

172. Gulec S, Anderson GJ, Collins JF. Mechanistic and regulatory aspects of intestinal iron absorption. Am J Physiol Liver Physiol. 2014;307(4):G397-409.

173. Gkouvatsos K, Papanikolaou G, Pantopoulos K. Regulation of iron transport and the role of transferrin. Biochim Biophys Acta - Gen Subj. 2012;1820(3):188–202.

174. Kelly AU, McSorley ST, Patel P, Talwar D. Interpreting iron studies. BMJ. 2017;357:j2513.

175. European Association for the Study of the Liver. EASL clinical practice guidelines for HFE hemochromatosis. J Hepatol. 2010;53(1):3–22.

176. Cao H, Schroeder B, Chen J, Schott MB, McNiven MA. The endocytic fate of the transferrin receptor is regulated by c-Abl kinase. J Biol Chem. 2016;291(32):16424–37.

177. Mayeur S, Spahis S, Pouliot Y, Levy E. Lactoferrin, a pleiotropic protein in health and disease. antioxid redox signal. 2016;24(14):813–36.

178. Farnaud S, Evans RW. Lactoferrin - a multifunctional protein with antimicrobial properties. Mol Immunol. 2003;40(7):395–405.

179. Arnold RR, Russell JE, Champion WJ, Brewer M, Gauthier JJ. Bactericidal activity of human lactoferrin: Differentiation from the stasis of iron deprivation. Infect Immun. 1982;35(3):792–9.

180. Dale SE, Doherty-Kirby A, Lajoie G, Heinrichs DE. Role of siderophore biosynthesis in virulence of *Staphylococcus aureus*: identification and characterization of genes involved in production of a siderophore. Infect Immun. 2004;72(1):29–37.

181. Takase H, Nitanai H, Hoshino K, Otani T. Impact of siderophore production on *Pseudomonas aeruginosa* infections in immunosuppressed mice. Infect Immun. 2000;68(4):1834–9.

182. Beasley FC, Vinés ED, Grigg JC, Zheng Q, Liu S, Lajoie GA, et al. Characterization of staphyloferrin A biosynthetic and transport mutants in *Staphylococcus aureus*. Mol Microbiol. 2009;72(4):947–63.

183. Raymond KN, Dertz EA, Kim SS. Enterobactin: An archetype for microbial iron transport. Proc Natl Acad Sci. 2003;100(7):3584–8.

184. Miethke M. Molecular strategies of microbial iron assimilation: from high-affinity complexes to cofactor assembly systems. Metallomics. 2013;5(1):15–28.

185. Andrews SC, Robinson AK, Rodríguez-Quiñones F. Bacterial iron homeostasis. FEMS Microbiol Rev. 2003;27(2–3):215–37.

186. Beasley FC, Marolda CL, Cheung J, Buac S, Heinrichs DE. *Staphylococcus aureus* transporters Hts, Sir, and Sst capture iron liberated from human transferrin by staphyloferrin A, staphyloferrin B, and catecholamine stress hormones, respectively, and contribute to virulence. Infect Immun. 2011;79(6):2345–55.

187. Rabsch W, Methner U, Voigt W, Tschäpe H, Reissbrodt R, Williams PH. Role of receptor proteins for enterobactin and 2,3-dihydroxybenzoylserine in virulence of *Salmonella enterica*. Infect Immun. 2003;71(12):6953–6.

188. Reddy PV, Puri RV, Chauhan P, Kar R, Rohilla A, Khera A, et al. Disruption of mycobactin biosynthesis leads to attenuation of *Mycobacterium tuberculosis* for growth and virulence. J Infect Dis. 2013;208(8):1255–65.

189. Montañez GE, Neely MN, Eichenbaum Z. The streptococcal iron uptake (Siu) transporter is required for iron uptake and virulence in a zebrafish infection model. Microbiology. 2005;151(Pt 11):3749–57.

190. Runci F, Gentile V, Frangipani E, Rampioni G, Leoni L, Lucidi M, et al. Contribution of active iron uptake to *Acinetobacter baumannii* pathogenicity. Infect Immun. 2019;87(4):e00755.

191. Köster W. ABC transporter-mediated uptake of iron, siderophores, heme and vitamin B12. Res Microbiol. 2001;152(3–4):291–301.

192. Wilkens S. Structure and mechanism of ABC transporters. F1000Prime Rep. 2015;7:14.

193. Davidson AL, Dassa E, Orelle C, Chen J. Structure, function, and evolution of bacterial ATP-binding cassette systems. Microbiol Mol Biol Rev. 2008;72(2):317–64.

194. Wilson BR, Bogdan AR, Miyazawa M, Hashimoto K, Tsuji Y. Siderophores in iron metabolism: from mechanism to therapy potential. Trends Mol Med. 2016;22(12):1077–90.

195. Hider RC, Kong X. Chemistry and biology of siderophores. Nat Prod Rep. 2010;27(5):637–57.

196. Carroll CS, Moore MM. Ironing out siderophore biosynthesis: a review of non-ribosomal peptide synthetase (NRPS)-independent siderophore synthetases. Crit Rev Biochem Mol Biol. 2018;53(4):356–81.

197. Chu BC, Garcia-Herrero A, Johanson TH, Krewulak KD, Lau CK, Peacock RS, et al. Siderophore uptake in bacteria and the battle for iron with the host; a bird's eye view. BioMetals. 2010;23(4):601–11.

198. Ganne G, Brillet K, Basta B, Roche B, Hoegy F, Gasser V, et al. Iron release from the siderophore pyoverdine in *Pseudomonas aeruginosa* involves three new actors: FpvC, FpvG, and FpvH. ACS Chem Biol. 2017;12(4):1056–65.

199. Matzanke BF, Anemüller S, Schünemann V, Trautwein AX, Hantke K. FhuF, Part of a siderophore-reductase system. Biochemistry. 2004;43(5):1386–92.

200. Lin H, Fischbach MA, Liu DR, Walsh CT. *In vitro* characterization of salmochelin and enterobactin trilactone hydrolases IroD, IroE, and Fes. J Am Chem Soc. 2005;127(31):11075–84.

201. Troxell B, Hassan HM. Transcriptional regulation by Ferric Uptake Regulator (Fur) in pathogenic bacteria. Front Cell Infect Microbiol. 2013;3:59.

202. Barry SM, Challis GL. Recent advances in siderophore biosynthesis. Curr Opin Chem Biol. 2009;13(2):205–15.

203. Süssmuth RD, Mainz A. Nonribosomal Peptide Synthesis - Principles and Prospects. Angew Chemie - Int Ed. 2017;56(14):3770–821.

204. Gehring AM, Mori I, Walsh CT. Reconstitution and characterization of the *Escherichia coli* enterobactin synthetase from EntB, EntE, and EntF. Biochemistry. 1998;37(8):2648–59.

205. Gehring AM, Mori I, Perry RD, Walsh CT. The nonribosomal peptide synthetase HMWP2 forms a thiazoline ring during biogenesis of yersiniabactin, an iron-chelating virulence factor of *Yersinia pestis*. Biochemistry. 1998;7(33):11637–50.

206. Quadri LEN, Sello J, Keating TA, Weinreb PH, Walsh CT. Identification of a *Mycobacterium tuberculosis* gene cluster encoding the biosynthetic enzymes for assembly of the virulence-conferring siderophore mycobactin. Chem Biol. 1998;5(11):631–45.

207. Neilands JB. Mechanism and regulation of synthesis of aerobactin in *Escherichia coli* K12 (pColV-K30). Can J Microbiol. 2010;38(7):728–33.

208. Tanabe T, Funahashi T, Nakao H, Miyoshi SI, Shinoda S, Yamamoto S. Identification and characterization of genes required for biosynthesis and transport of the siderophore vibrioferrin in *Vibrio parahaemolyticus*. J Bacteriol. 2003;185(23):6938–49.

209. Bergeron RJ, McManis JS, Perumal PT, Algee SE. The Total Synthesis of Alcaligin. J Org Chem. 1991;190(11):3940–7.

210. Cotton JL, Tao J, Balibar CJ. Identification and characterization of the *Staphylococcus aureus* gene cluster coding for staphyloferrin A. Biochemistry. 2009;48(5):1025–35.

211. Cheung J, Beasley FC, Liu S, Lajoie GA, Heinrichs DE. Molecular characterization of staphyloferrin B biosynthesis in *Staphylococcus aureus*. Mol Microbiol. 2009;74(3):594–608.

212. Holden VI, Bachman MA. Diverging roles of bacterial siderophores during infection. Metallomics. 2015;7(6):986–95.

213. Beasley FC, Heinrichs DE. Siderophore-mediated iron acquisition in the staphylococci. J Inorg Biochem. 2010;104(3):282–8.

214. Kobylarz MJ, Grigg JC, Liu Y, Lee MSF, Heinrichs DE, Murphy MEP. Deciphering the substrate specificity of SbnA, the enzyme catalyzing the first step in staphyloferrin B biosynthesis. Biochemistry. 2016;55(6):927–39.

215. Kobylarz MJ, Grigg JC, Takayama SIJ, Rai DK, Heinrichs DE, Murphy MEP. Synthesis of L-2,3-diaminopropionic acid, a siderophore and antibiotic precursor. Chem Biol. 2014;21(3):379–88.

216. Speziali CD, Dale SE, Henderson JA, Vinés ED, Heinrichs DE. Requirement of *Staphylococcus aureus* ATP-binding cassette-ATPase FhuC for iron-restricted growth and evidence that it functions with more than one iron transporter. J Bacteriol. 2006;188(6):2048–55.

217. Sebulsky MT, Hohnstein D, Hunter MD, Heinrichs DE. Identification and characterization of a membrane permease involved in iron-hydroxamate transport in *Staphylococcus aureus*. J Bacteriol. 2000;182(16):4394–400.

218. Sebulsky MT, Heinrichs DE. Identification and characterization of *fhuD1* and *fhuD2*, two genes involved in iron-hydroxamate uptake in *Staphylococcus aureus*. J Bacteriol. 2001;183(17):4994–5000.

219. Cassat JE, Skaar EP. Iron in infection and immunity. Cell Host Microbe. 2013;13(5):509–19.

220. Kirienko N V., Kirienko DR, Larkins-Ford J, Wählby C, Ruvkun G, Ausubel FM. *Pseudomonas aeruginosa* disrupts *Caenorhabditis elegans* iron homeostasis, causing a hypoxic response and death. Cell Host Microbe. 2013;13(4):406–16.

221. Hartmann H, Eltzschig HK, Wurz H, Hantke K, Rakin A, Yazdi AS, et al. Hypoxia-independent activation of HIF-1 by Enterobacteriaceae and their siderophores. Gastroenterology. 2008;134(3):756–67.

222. Holden VI, Lenio S, Kuick R, Ramakrishnan SK, Shah YM, Bachman MA. Bacterial siderophores that evade or overwhelm lipocalin 2 induce hypoxia inducible factor 1α and proinflammatory cytokine secretion in cultured respiratory epithelial cells. Infect Immun. 2014;82(9):3826–36.

223. Paauw A, Leverstein-van Hall MA, van Kessel KPM, Verhoef J, Fluit AC. Yersiniabactin reduces the respiratory oxidative stress response of innate immune cells. PLoS One. 2009;4(12):e8240.

224. Saha P, Xiao X, Yeoh BS, Chen Q, Katkere B, Kirimanjeswara GS, et al. The bacterial siderophore enterobactin confers survival advantage to *Salmonella* in macrophages. Gut Microbes. 2018;10(3):412–23.

225. Porcheron G, Dozois CM. Interplay between iron homeostasis and virulence: Fur and RyhB as major regulators of bacterial pathogenicity. Vet Microbiol. 2015;179(1–2):2–14.

226. Fillat MF. The FUR (ferric uptake regulator) superfamily: diversity and versatility of key transcriptional regulators. Arch Biochem Biophys. 2014;546:41–52.

227. Hazmanian SK, Skaar EP, Gaspar AH, Humayun M, Gornicki P, Jelenska J, et al. Passage of heme-iron across the envelope of *Staphylococcus aureus*. Science. 2003;299(5608):906–9.

228. Torres VJ, Pishchany G, Humayun M, Schneewind O, Skaar EP. *Staphylococcus aureus* IsdB is a hemoglobin receptor required for heme iron utilization. J Bacteriol. 2006;188(24):8421–9.

229. Torres VJ, Attia AS, Mason WJ, Hood MI, Corbin BD, Beasley FC, et al. *Staphylococcus aureus fur* regulates the expression of virulence factors that contribute to the pathogenesis of pneumonia. Infect Immun. 2010;78(4):1618–28.

230. Johnson M, Cockayne A, Williams PH, Morrissey JA. Iron-responsive regulation of biofilm formation in *Staphylococcus aureus* involves Fur-dependent and Fur-independent mechanisms. J Bacteriol. 2005;187(23):8211–5.

231. Horan TC, Andrus M, Dudeck MA. CDC/NHSN surveillance definition of health care–associated infection and criteria for specific types of infections in the acute care setting. Am J Infect Control. 2008;36(5):309–32.

CHAPTER 3

General effect of iron availability on *S. epidermidis* biofilm formation

Summary

The molecular mechanisms behind biofilm formation in *S. epidermidis* are nowadays fairly well understood. Nevertheless, and regardless of their importance, a large proportion of this knowledge comes from studies performed under experimental conditions that do not resemble the ones that *S. epidermidis* usually experiences *in vivo*. While causing infection in humans, *S. epidermidis* faces long periods of iron starvation. Surprisingly, pretty much nothing is known regarding how *S. epidermidis* acquire iron, even though it is able to survive and eventually form biofilms in an iron-deprived environment as is the case of the human body. In order to uncover that, biofilms of three *S. epidermidis* strains were grown under iron-enriched and iron-deficient conditions and several physiologic and transcriptomic changes were assessed. Data revealed that while physiologic iron levels do not compromise biofilm formation, iron excess or iron deficiency is detrimental for this process. Besides, biofilm cells were not affected in the same way when grown planktonically. By studying biofilm cells in detail, it was found that their viability and cultivability were seriously compromised by iron deficiency. A temporal analysis of biofilm formation revealed that iron excess or iron deficiency: i) impaired biomass accumulation from 6 h onwards, and ii) induced changes in the biofilm structure, indicating that iron availability plays a pivotal role from an early biofilm development stage. Lastly, the transcription of putative iron acquisition systems was assessed and found to be modulated by iron availability. In this chapter, not only a range of evidence that iron plays a pivotal role in *S. epidermidis* biofilm formation is provided, but also its iron acquisition mechanisms are explored.

Part of the work described in this chapter was published in 2017, in International Journal of Medical Microbiology, 307(8):552–563.

3.1 Brief introduction

The emergence of *S. epidermidis* as one of the most important nosocomial pathogens, as well as its remarkable ability to from biofilms have been discussed thoroughly **in Chapter 2**. If successful at crossing the host protective barriers (skin and mucous membranes), *S. epidermidis* has to cope with a plethora of adverse conditions, which encompasses a dramatic decrease of iron concentration in extracellular fluid and plasma that takes place a few hours after infection begins (1). It has previously been demonstrated that *S. epidermidis* biofilm cells cultured in human blood upregulate the transcription of genes putatively involved in iron acquisition (2). While the function of these genes has never been experimentally confirmed, this finding suggests that iron acquisition is an important process for *S. epidermidis* to survive within the host.

Even though the importance of iron for different pathogens has been confirmed, studies have been mostly performed with bacterial cells grown planktonically (3–5). This raises some issues, as the iron requirements for planktonic and biofilm growth are thought to be different (6). Concerning staphylococci, the number of studies showing modulation of biofilm formation by iron has been scarce and limited to *S. aureus* (7–9). In this chapter, it was aimed to assess whether iron plays an important role in *S. epidermidis* biofilm formation.

3.2 Materials and methods

3.2.1 Strains, culture media, and chemicals

S. epidermidis RP62A (ATCC® 35984™) is a culture collection strain well-known for its remarkable biofilm-producing ability and was used as a control strain. *S. epidermidis* PT11006 and PT12003 are clinical isolates obtained after patient informed consent under approval from the Ethics Committee Board of Hospital Geral de Santo António, Porto, Portugal (015/09: 014-DEFI/014-CES). All strains have been confirmed to be *ica*-positive (10). For each experiment, isolated colonies were picked from Tryptic Soy Agar (TSA, Liofilchem, Teramo, Italy) plates, inoculated into Tryptic Soy Broth (TSB) (Liofilchem), and incubated overnight (~16 h) at 37°C with shaking at 120 rpm (ES-20 Shaker-Incubator, BioSan, Riga, Latvia). Iron (III) chloride ($FeCl_3$) was purchased from Sigma-Aldrich (St. Louis, MO, USA). 2,2′-bipyridine (Bip) was purchased from VWR (Carnaxide, Portugal). Bip was dissolved in absolute ethanol (50 mM stock) and stored at −20 °C until further use.

3.2.2 Biofilm formation assays

Biofilms were grown either in 96- (for biofilm biomass quantification) or in 24-well (for gene expression analysis) microplates made of polystyrene plastic (Thermo Fisher Scientific Inc., Waltham, MA, USA). For confocal microscopy analysis, biofilms were grown in Lab-Tek® Chamber Slide™ System 8 Well Permanox® Slides (Thermo Fisher Scientific Inc.). For PIA/PNAG extraction and quantification, biofilms were grown on Nunclon™Δ 9 cm Petri dishes (Thermo Fisher Scientific Inc.). Briefly, overnight cultures were adjusted with TSB to an optical density at 640 nm (OD_{640}) equivalent to ~2×10^8 CFU/mL and diluted 1:100 in TSB supplemented with 0.4% (w/v) glucose (TSB_G, Thermo Fisher Scientific Inc.), iron-enriched TSB_G (TSB_G containing different $FeCl_3$ concentrations) and iron-depleted TSB_G (TSB_G containing different Bip concentrations). pH measurements of the different culture media tested were performed with Model 15 pH meter (Denver Instrument, NY USA). Bip was added to the medium and allowed to stand for at least 30 min prior inoculation for fully iron chelation. Subsequently, the diluted bacterial suspension was placed into the plates and incubated at 37°C with shaking at 120 rpm (ES-20 Shaker-Incubator) for the appropriate period (from 6 to 24 h).

3.2.3 Quantification of biofilm biomass

After incubation, the bacterial cells in suspension were carefully removed, biofilms were washed twice with 200 µL of 0.9% sodium chloride (NaCl), and then stained by crystal violet technique, as previously described (11). Briefly, biofilms were fixed with methanol (Thermo Fisher Scientific Inc.) for 20 min and stained with 1% (v/v) crystal violet (Merck Millipore, Darmstadt, Germany) for 15 min. Excess stain was rinsed off with tap water and the stain bound to the biofilm was resolubilized with 33% (v/v) glacial acetic acid (Thermo Fisher Scientific Inc.). Absorbance was measured at 570 nm (A_{570}) using a microplate reader (Synergy HT, BioTek Instruments, VT, USA). Experiments were run at least in triplicate with technical triplicates for each condition tested.

3.2.4 Planktonic growth curves

Planktonic growth was assessed at 37°C in TSB containing a range of concentrations of $FeCl_3$ or Bip. Overnight-grown bacteria were diluted in a conical flask to an OD_{640} ~0.1 and then incubated at 37°C, 120 rpm (ES-20 Shaker-Incubator). OD_{640} was measured hourly up to 10 h of incubation (when appropriate, concentrated samples were diluted in TSB for accurate measurement). Three independent experiments were performed for each condition tested. OD data were transformed into ln(OD) and plotted versus time (h) to identify the exponential phase (linear portion of the graph). Growth rates (µ, h^{-1}) were

given by the slope of that portion, which was determined through linear regression. Doubling times (t_d, min) were calculated according to Eq. (1).

(1) $$t_d = \frac{ln2}{\mu} \times 60$$

3.2.5 Cell cultivability and viability assessment

24 h-old biofilms were grown as mentioned above. Suspended and biofilm cells were collected, centrifuged at 5000*g* for 10 min, resuspended in 1 mL of 0.9% NaCl and then sonicated for 10 s at 30% amplitude, using a 13 mm probe tip (Cole-Parmer 750-W Ultrasonic Homogenizer 230 VAC, IL, USA). By following this process, cell clusters were disrupted without compromising cell viability (12). Cultivability of both suspended and biofilm cells was assessed by CFU counting. Biofilm cells were further studied for viability through flow cytometry using SYBR Green and propidium iodide (PI) staining as optimized before (13), with minor modifications. In brief, 20 μL of cell suspension were mixed with 180 μL of phosphate buffered saline (PBS) containing 1:80000 of SYBR Green (Invitrogen, CA, USA) and 20 μg/mL of PI (Sigma-Aldrich), and the number of cells assessed using an EC800™ flow cytometer (Sony Biotech, CA, USA). A total of 65000 events were acquired with a sample flow rate of 10 μL/min. Data analysis was performed using EC800™1.3.6 analysis software (Sony Biotech). Two to three biological replicates were performed for this analysis.

3.2.6 Confocal laser scanning microscopy (CLSM) analysis

Biofilms were formed on the chamber slide system as described above, and then stained with (i) 4',6-diamidine-2'-phenylindole dihydrochloride (DAPI) nucleic acid stain (Sigma-Aldrich) for visualization of cells, and (ii) wheat germ agglutinin (WGA) conjugated with Texas Red (Thermo Fisher Scientific, Inc.) for staining of GlcNAc residues. All staining procedures were performed according to the manufacturer's instructions. Stained biofilms were examined under CLSM using an Olympus FluoView FV1000 (Olympus, Lisboa, Portugal) with a 40× water-immersion objective (40×/ 1.15 W), and images of different regions of each surface were acquired with 640 × 640 resolution. Two independent biological experiments were performed, and representative images were selected. Images were reconstructed from average intensity projection through confocal image Z-stacks series using ImageJ (14).

3.2.7 Dot blot detection of PIA/PNAG

Preparation of bacterial cell wall extracts for PIA/PNAG detection was performed as previously described (15). Bacterial biofilms were thoroughly washed as described above, scraped from the plate, and

resuspended in 1× PBS. Cells were centrifuged at 5000*g* for 10 min at 4°C, the supernatant was discarded, and washed once with 1× PBS. Cells were then sonicated for 30 s at 30% amplitude, using a Branson Ultrasonic Corp 250 DIG Sonifier (13 mm probe tip, Thermo Fisher Scientific, Inc.). The process was repeated 4 times with a resting period on ice of 30s between sonication cycles. OD_{600} was measured and all samples were adjusted to the same OD. Samples were centrifuged at 5000*g* for 10 min at 4°C and supernatants were collected. For PIA/PNAG detection, a polyvinylidene difluoride (PVDF) membrane (Millipore, Bedford, MA) cut to the appropriate dimensions was sequentially equilibrated with methanol and 1× PBS. The membrane was carefully placed onto a filter paper pre-soaked in 1× PBS in order to avoid formation of air bubbles. For PIA/PNAG titration, 2-fold dilution series (from 1:2 to 1:256) were performed and each dilution was applied to the membrane in 5-µL volumes. The membrane was then blocked overnight with shaking at 4°C with a 3% (w/v) bovine serum albumin (BSA)/ PBS solution. After incubation, the membrane was transferred to a PBS-T solution (1× PBS, 0.05% (v/v) Tween 20) and incubated for 15 min with shaking at room temperature (RT). WGA lectin peroxidase-conjugated diluted 1:10000 in PBS-T was applied to the membrane for 60 min with shaking at RT. After washing three times for 15 min in PBS-T, the membrane was developed according to instructions given by the manufacturer, using Amersham ECL Western Blotting Detection Reagent (GE Life Sciences, Freiburg, Germany). After 1 min the membrane was covered with plastic wrap and exposed to Universalfilm Super RX-N (Fujifilm, Tokyo, Japan) during 15 s for detection.

3.2.8 Gene expression analysis

3.2.8.1 RNA extraction

RNA extraction from *S. epidermidis* biofilm cells was based on a previously optimized protocol (16). This method combines mechanical (glass beads) lysis of bacterial cells along with silica membrane-based RNA isolation (ExtractMe RNA Bacteria & Yeast Kit, Blirt S.A., Poland). Bacterial biofilms were thoroughly washed as described before, scraped from the plate, pooled in 0.9% NaCl, and immediately placed on ice. Biofilm cells were centrifuged at 16000*g* for 10 min at 4°C and the supernatant was discarded. Then, the bacterial pellet was thoroughly suspended in 600 µL of RYBL Buffer (provided with the kit). The resulting suspension was transferred into 2 mL safe lock tubes containing 0.5 g of acid-washed 150–212 mm silica beads (Sigma-Aldrich). The tubes were then placed into a cell disruptor (FastPrep®-24, MP Biomedicals, CA, USA) and run for 35 s at 6.5 m/s. The samples were immediately placed on ice for 5 min and the beat-beading step was repeated thrice. Afterwards, samples were centrifuged at 16000*g* for 1.5 min at 4°C, the supernatants transferred into 2 mL DNase/RNase-free tubes and mixed with an

equal volume of 70% (v/v) ethanol. The samples (including any remaining precipitate) were transferred to the silica-membrane columns and centrifuged at 15000*g* for 1 min at RT. The following steps were performed according to the manufacturer's instructions.

3.2.8.2 DNase treatment

To degrade genomic DNA, each RNA sample was digested with 2 μL of DNase I plus 4 μL of 10× DNase I Reaction Buffer and incubated at 37°C for 30 min. Then, to inactivate the DNase I activity, 4 μL of 25 mM ethylenediaminetetraacetic acid (EDTA, pH 8.0) were added to the mixture and incubated at 65°C for 10 min. All reagents were purchased from Thermo Fisher Scientific Inc.

3.2.8.3 RNA quality determination

The concentration and purity of the total RNA was spectrophotometrically determined using a NanoDrop 1000 (Thermo Fisher Scientific Inc.). A_{260}/A_{280} and A_{260}/A_{230} ratios were used as indicators of protein and polysaccharide/ phenol/ chaotropic salts contamination, respectively. RNA integrity was assessed by visualization of the 23S/16S rRNA band pattern. RNA samples were analyzed in a 1% (w/v) agarose gel. Non-denaturing electrophoresis was carried-out at 80 V for 60 min. The gel was stained with Midori Green DNA staining (Nippon Genetics Europe GmbH, Germany) in Tris–acetate–EDTA (TAE) buffer and visualized using ChemiDoc™ XRS+ (Bio-Rad, CA, USA). RNA was stored at −80°C until further use.

3.2.8.4 cDNA synthesis

cDNA synthesis was performed using the RevertAid First Strand cDNA Synthesis Kit (Thermo Fisher Scientific, Inc.) following the manufacturer's instructions. The same amount of total RNA (300 ng) from each sample was reverse transcribed in a 10 μL reaction volume using random hexamer primers as priming strategy. To determine the possibility of genomic DNA carry-over, control reactions were performed under the same conditions but lacking the reverse transcriptase enzyme (NRT control). All RNA samples extracted were absent of significant genomic DNA, as determined by an average quantification cycle (Cq) difference of 18.16 ± 3.89.

3.2.8.5 Gene expression quantification

Biofilm cells gene expression was determined by quantitative (real-time) PCR (qPCR). qPCR analysis was performed using Xpert iFast SYBR Mastermix (GRiSP, Lda., Porto, Portugal) in a 10 μL reaction volume. Each PCR reaction contained 2 μL of 1:200 diluted cDNA or NRT control, 5 μL of master mix, 1 μL of primer mixture (in the final reaction, each primer was at 0.3 μM), and 2 μL of nuclease-free water. qPCR

runs were performed on a CFX 96 (BioRad, Hercules, CA, USA) with the following cycle parameters: 95°C for 3 min, and 40 cycles of 95°C for 5 s, 60°C for 25 s. Melt analysis was performed at the end to ensure the absence of unspecific products and primer dimers. All genes were quantified in duplicate for biological triplicates. The expression of the genes tested was normalized to the expression of the reference gene 16S rRNA using the Pfaffl method (17), and considering TSB_G as the control condition. Data were log transformed (Log_2) before statistical analysis was performed. Information about the primers used in this study is listed in **Table 3.1**. Primers were designed with the aid of Primer3 (18) using *S. epidermidis* RP62A genome sequence (NCBI accession no. NC_002976) as template. mFold was used for prediction of secondary structures (19). No secondary structures were found for the operating temperatures used. Gene specificity of all primers was confirmed using Primer-BLAST (20). PCR amplification efficiency (E) for each gene was determined from the slope of a standard curve (generated with a 10-fold dilution series of cDNA), according to Eq. (2).

(2) $$E = 10^{\left(\frac{-1}{slope}\right)}$$

Table 3.1. List of primers used in qPCR experiments, respective product size and amplification efficiencies

Target gene	Forward sequence (5'-3')	Reverse sequence (5'-3')	Product size (bp)	Efficiency (%)*
16S rRNA	GGGCTACACACGTGCTACAA	GTACAAGACCGGGAACGTA	176	89.7
SERP1775	CTGCTGCTAAACTTGCCCCT	TCTGGCTCGGTGATACAAGG	88	97.5
SERP1776	GGAAGCACCTGCATTCACAC	GGCGCTTTAGCAATTGCAGG	93	85.6
SERP1778	GTTTATCCCCTGCGACACAT	GGCGAATGTTCGTGTCAAT	119	87.4
SERP1779	GCACTTTTTCGCGCTACTTT	TCGAACGATTAACGCAATGA	129	96.8
SERP0306	GTGGTGGACAAAGACAACGC	GCAACCTTCTTCTTCGTTGAGC	152	90.2
SERP0400	AGGGGTGAGTCAGCTCTCTT	GCCCACTCCATAGTACCAGC	198	92.1
SERP0401	ACTGGTCGTTATGGCAATTTGT	ACGGACGTTCCTATCGATGC	141	100.2
SERP0402	TCAGACGACATCATTGCGCT	ACGTTGTCCCCTTATCTCCTC	132	96.4
SERP0403	CAACGTTTGGACCAGGAGGA	TTTGACCATGCGGGCTTTTG	99	90.0
SERP0949	ACATCATCGTGGTGAAACGA	GCATTTCCTTGACCTTTTGC	150	88.5
SERP1951	CCTCTTGAGCACGACTAGCA	TGCTTTCAGGTGGACAACAA	117	94.0
SERP1953	TCACAAGTGGAGAAGCATCAT	CAGTCCCACTTAGAAATGCACG	195	92.1

*Amplification efficiency was calculated as described in Materials and Methods.

3.2.9 In silico *analysis*

Sequences of different putative iron-related proteins were retrieved from *S. epidermidis* RP62A (NCBI accession no. NC_002976) and queried against *S. aureus* strain Newman (NCBI accession no. NC_009641) to search for homologous proteins. Analysis was performed with BLASTp tool (21), using the default parameters. Identification of putative Fur boxes in *S. epidermidis* RP62A genome were

performed with FIMO tool (22), using the default parameters and the 19 bp Fur box consensus sequence 5' GATAATGATAATCATTATC 3' (23) as the input motif.

3.2.10 Iron quantification

Iron concentration in TSB culture medium was assessed by a ferrozine-based method, adapted from Mladěnka et al. (24). Briefly, 100 μL of ammonium iron (II) sulfate standards (containing 0.1 - 10 nmol iron (II)) or culture medium samples were initially mixed with 50 μL of 1.4 M hydroxylamine aqueous solution to prevent iron (II) oxidation and/ or to reduce any iron (III) present in the samples. After 30 min, 50 μL of 5 mM ferrozine solution (in 5 M ammonium acetate buffer, pH 9.5) was added to the mixture. All reagents were purchased from VWR. Formation of the iron-ferrozine complex was then determined at 562 nm. All experiments were performed in 96-well microplates. Absorbance was measured at 562 nm (A_{562}) using a microplate reader (Synergy HT). Two independent experiments with technical duplicates were performed for each standard or sample.

3.2.11 Statistical analysis

Data transformation, linear regressions and statistical analysis were performed with GraphPad Prism version 7.0a (La Jolla, CA, USA). For comparisons among different groups, two-away ANOVA with multiple comparisons test was used. A $p < 0.05$ was considered statistically significant.

3.3 Results

3.3.1 S. epidermidis *biofilm formation is highly modulated by iron availability*

Biofilm formation in TSB_G alone (total iron content of 6.30 ± 0.47 μM, as determined by the ferrozine-based method) or supplemented with iron concentrations up to 0.10 mM $FeCl_3$, which covers the physiologic serum iron concentrations usually found in humans (0.01 - 0.04 mM) (25), was similar (**Figure 3.1A**). However, a supraphysiologic iron concentration in the order of 1.00 mM had a detrimental effect on biofilm accumulation. Biofilm formation ability was also evaluated under iron-limiting conditions, which were attained by the use of the synthetic iron chelator Bip. This compound has been widely employed for iron depletion in different culture media (8,26,27). All strains exhibited significant decrease in biofilm formation under this condition, especially when Bip concentrations reached very high levels (from 0.50 to 1.00 mM) (**Figure 3.1B**)**.** To rule out the hypothesis that this observation was instead the result of the ethanol present in Bip stock solution, biofilm formation in TSB_G supplemented with 2% (v/v) ethanol (concentration present in the highest Bip concentration tested) was also assessed. Although ethanol has been reported to modulate biofilm formation in *S. epidermidis* (28), ethanol at such

concentration did not affect biofilm formation for the strains tested here (**Figure 3.1C**). Moreover, supplementation with $FeCl_3$ or Bip did not change the pH of the culture medium (**Figure 3.1D**), thus pH effects were also ruled out.

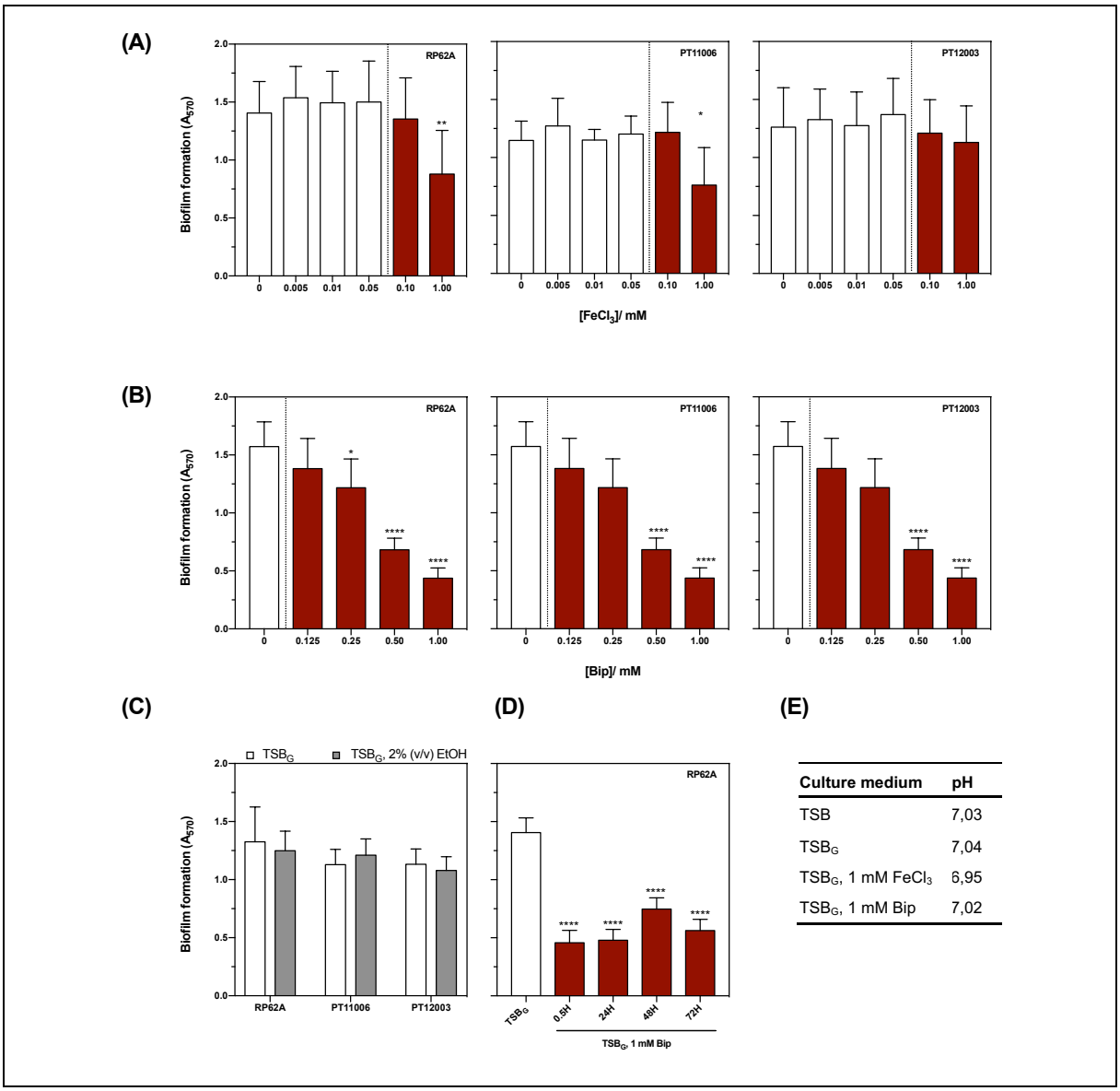

Figure 3.1. General effect of iron availability on biofilm formation. Biofilms of three different *S. epidermidis* strains were allowed to grow on 96-well microtiter plates for 24 h at 37°C in TSB_6 containing increasing concentrations of **(A)** $FeCl_3$ and **(B)** Bip. Experimental conditions with iron concentrations out of the physiologic range are represented by red bars. **(C)** Effects of ethanol were ruled out by growing biofilms in TSB_6 supplemented with 2% (v/v) ethanol. **(D)** Effect of the iron chelation period on biofilm formation. Biofilms were stained with crystal violet and quantified at A_{570}. Data are represented as mean ± standard deviation of at least three independent assays. Significant differences are depicted with: * $p < 0.05$; ** $p < 0.01$; **** $p < 0.0001$. **(D)** pH measurements of the different culture media used.

An important issue when using an iron chelator is that it might chelate other important trace elements (e.g. calcium or magnesium) at some degree. To confirm that the effect observed was actually due to the sequestration of iron, biofilm formation was screened in iron-depleted medium (TSB_6, 1.00 mM Bip) complemented with a range of increasing $FeCl_3$ concentrations (up to 1.00 mM). The impaired biofilm

formation was fully reversed by co-addition of iron in a dose-dependent manner up to 0.2 mM $FeCl_3$ (**Figure 3.2A**). As previously observed, higher concentrations had a detrimental effect. Similar experiments were performed with co-addition of calcium and magnesium ions (in the form of calcium and magnesium chloride, respectively), but in this case the effect was not reversed (**Figure 3.2B** and **C**). Collectively, these results strongly suggest that the effects observed are solely attributable to iron sequestration.

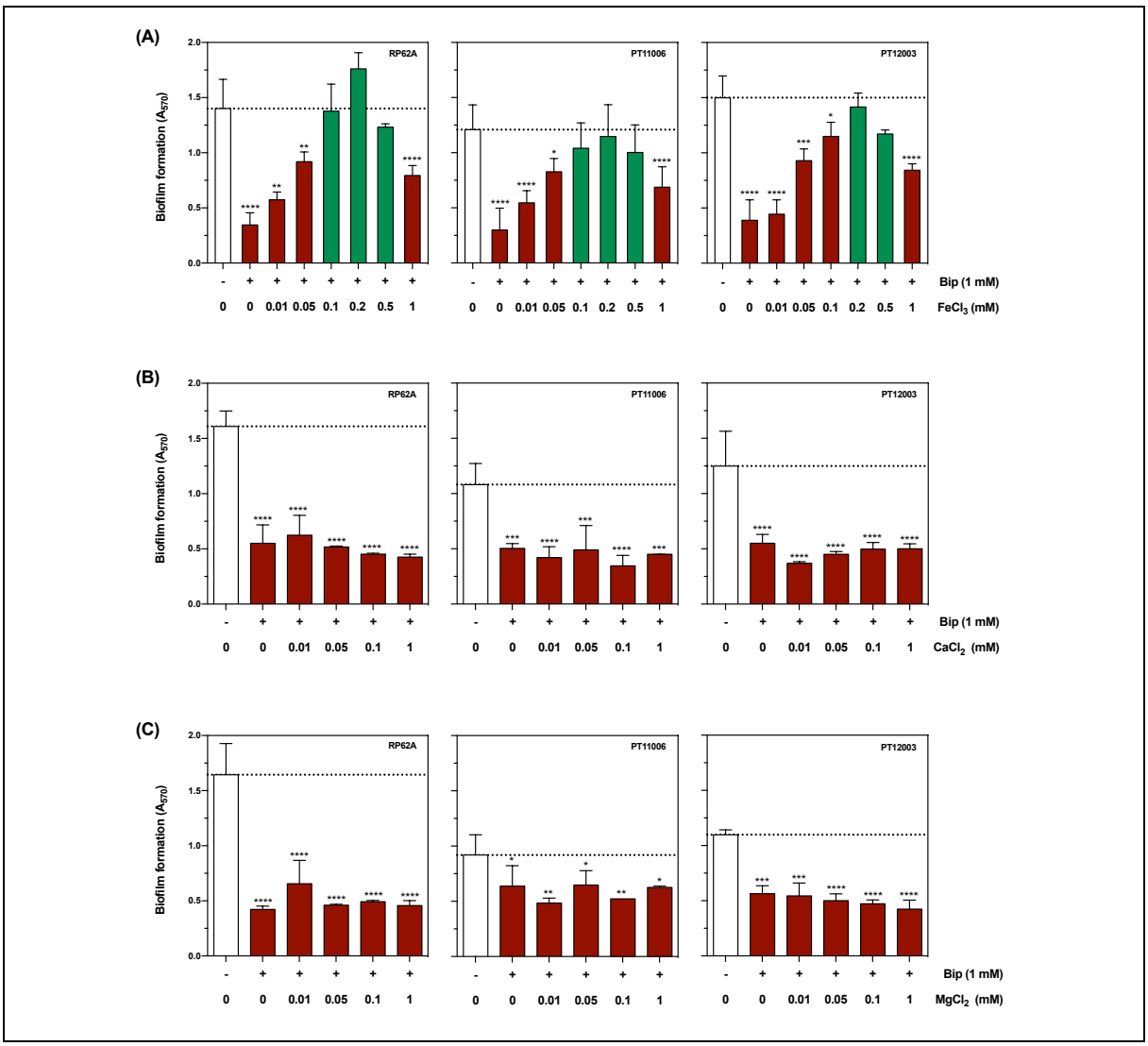

Figure 3.2. Supplementation of iron-depleted medium with iron but not calcium or magnesium restores biofilm formation. Biofilms of three different *S. epidermidis* strains were allowed to grow on 96-well microtiter plates for 24 h at 37°C in iron-depleted medium (TSB_6, 1 mM Bip) supplemented with increasing concentrations of **(A)** $FeCl_3$, **(B)** $CaCl_2$, and **(C)** $MgCl_2$. Biofilms were stained with crystal violet and quantified at A_{570}. Data are represented as mean ± standard deviation of three independent assays. Significant differences are depicted with: * $p < 0.05$; ** $p < 0.01$; *** $p < 0.001$; **** $p < 0.0001$.

3.3.2 S. epidermidis *withstands higher variations in iron availability when grown planktonically*

Given the pivotal role of iron on a myriad of basic physiologic processes, it was hypothesized that effects observed on biofilm formation could be attributable to an impaired cell growth rate. To assess this, planktonic cells were grown under the exact same conditions (**Figure 3.3**; **Table 3.2).** Not surprisingly, iron concentrations up to 0.10 mM were not detrimental for planktonic growth. Furthermore, and in opposition to biofilms, supplementation with 1.00 mM $FeCl_3$ had no significant ($p > 0.05$) effect on the planktonic growth rate. On the other hand, when iron in the culture medium was depleted, cell growth was partly affected in a dose-dependent manner, with a significant increase ($p < 0.05$) in the doubling time when Bip reached a concentration of 1 mM (**Table 3.2**). Additionally, a lower cell density after 10 h of incubation was also noticed.

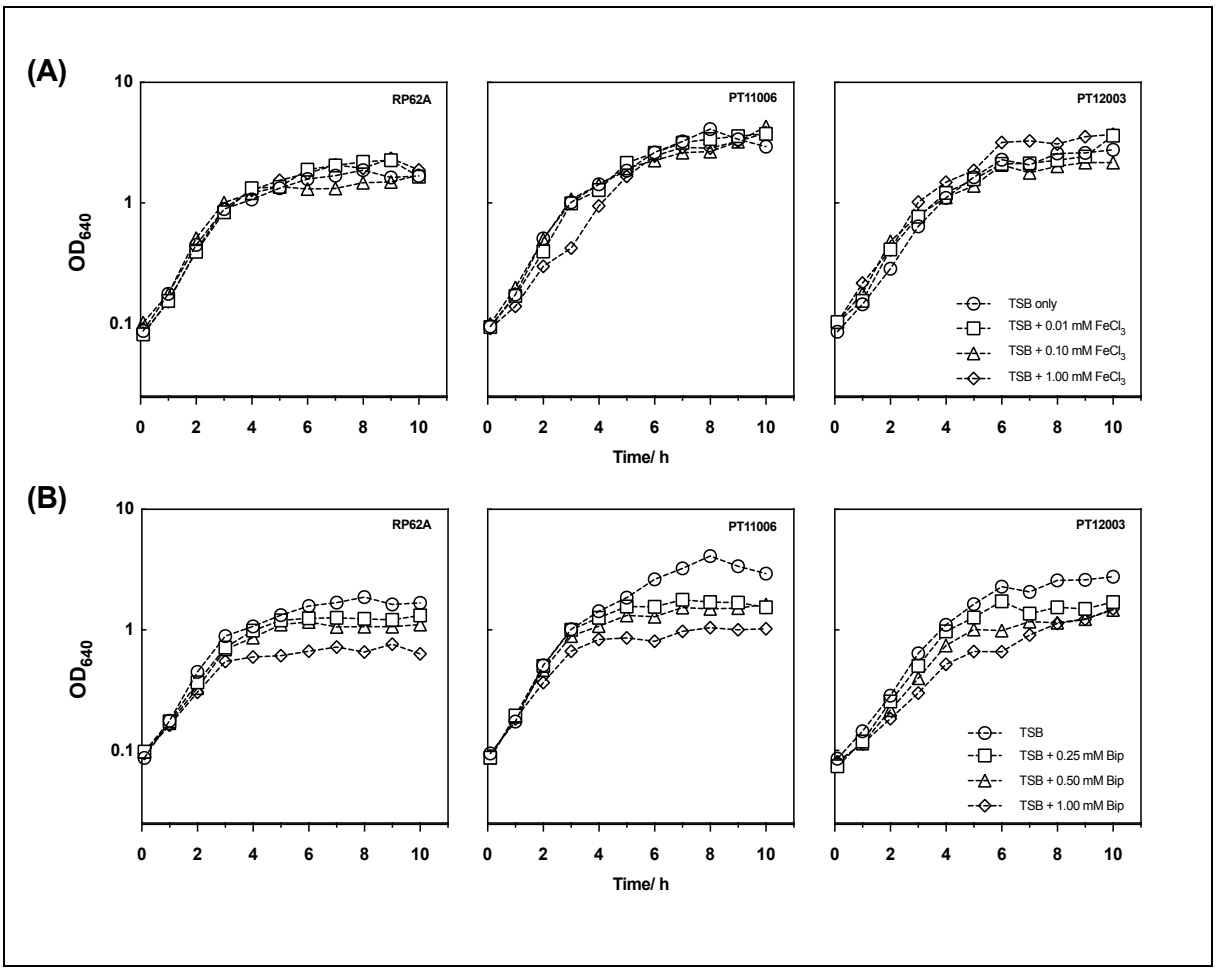

Figure 3.3. Effect of iron availability on planktonic growth. Three different *S. epidermidis* strains were allowed to grow planktonically in conical flasks at 37°C in TSB containing increasing concentrations of **(A)** $FeCl_3$ and **(B)** Bip. OD_{640} was measured hourly up to 10 h of incubation. Data are represented as mean ± standard deviation of at least two independent experiments.

Table 3.2. Doubling times (t_d, in min) of *S.* epidermidis grown in TSB containing increasing concentrations of $FeCl_3$ and Bip. ** $p < 0.01$; **** $p < 0.0001$

Condition	RP62A	PT11006	PT12003
TSB	54.0 ± 7.4	50.5 ± 3.2	59.1 ± 4.6
TSB + 0.01 mM $FeCl_3$	52.3 ± 11.9	52.2 ± 11.6	69.5 ± 10.3
TSB + 0.10 mM $FeCl_3$	49.7 ± 14.4	50.4 ± 8.9	53.2 ± 2.5
TSB + 1.00 mM $FeCl_3$	49.6 ± 11.2	62.5 ± 17.7	54.7 ± 5.1
TSB + 0.25 mM Bip	58.7 ± 4.6	50.9 ± 2.8	58.9 ± 7.2
TSB + 0.50 mM Bip	59.0 ± 6.5	54.1 ± 1.4	67.3 ± 5.3
TSB + 1.00 mM Bip	**68.1 ± 6.2****	**64.7 ± 5.4****	**80.4 ± 2.9 ******

3.3.3 Cultivability and viability of S. epidermidis *biofilm cells are compromised by iron deficiency but not by its excess*

To further understand the physiologic changes induced by iron availability, the cultivability and viability of biofilm cells were assessed. Cultivability was reduced in most cases when cells were cultured under iron-limiting conditions despite not being compromised by excessive amounts of iron (**Table 3.3**). Interestingly, by analyzing the proportion of biofilm/ suspended cells, it was noted that biofilm cells represented a higher percentage when shifts in the iron concentration were introduced (except for strain PT12003 when cultured in TSB_6, 1 mM Bip). This observation rules out the hypothesis that significant changes in iron availability induced cells to detach from the biofilm.

Similarly, flow cytometry experiments showed that total biofilm cell counts were significantly reduced under iron deficiency (up to 1-Log), but not under iron excess (**Figure 3.4A**). Additionally, double staining with SYBR Green and PI has confirmed the results on cultivability, highlighting a greater proportion of dead and damaged cells under iron deficiency (**Figure 3.4B**). Significant increments in the cell size were also observed for both conditions in all strains (**Figure 3.4C**).

Table 3.3. Cultivability of biofilm (B) and suspended (S) cells grown under different iron availability conditions

Condition	RP62A			PT11006			PT12003		
	Log_{10} CFU/mL		B:S*	Log_{10} CFU/mL		B:S*	Log_{10} CFU/mL		B:S*
	Biofilm cells	Suspended cells		Biofilm cells	Suspended cells		Biofilm cells	Suspended cells	
TSB_6 + 1.00 mM Bip	7,29 ± 0,42	6,46 ± 0,40	87:13	7,26 ± 0,42	6,04 ± 0,59	94:6	6,29 ± 0,40	6,80 ± 0,26	24:76
TSB_6 + 0.50 mM Bip	7,84 ± 0,41	6,59 ± 0,41	95:5	7,47 ± 0,49	6,01 ± 0,50	97:3	8,30 ± 0,17	7,77 ± 0,27	77:23
TSB_6	8,43 ± 0,14	8,42 ± 0,17	50:50	8,39 ± 0,12	7,98 ± 0,26	72:28	8,63 ± 0,17	8,60 ± 0,15	50:50
TSB_6 + 0.10 mM $FeCl_3$	8,31 ± 0,35	8,17 ± 0,45	58:42	8,57 ± 0,39	8,12 ± 0,30	73:27	8,73 ± 0,50	8,59 ± 0,33	58:42
TSB_6 + 1.00 mM $FeCl_3$	8,42 ± 0,31	7,71 ± 0,72	83:17	8,65 ± 0,47	7,69 ± 0,46	90:10	8,90 ± 0,47	8,10 ± 0,46	86:14

Biofilms of three different *S. epidermidis* strains were allowed to grow on 96-well microtiter plates for 24 h at 37°C in TSB_6 containing increasing concentrations of $FeCl_3$ or Bip. Data are represented as mean ± standard deviation of three independent experiments. *****Proportion of biofilm/ suspended cells (B:S) is represented as percentages.

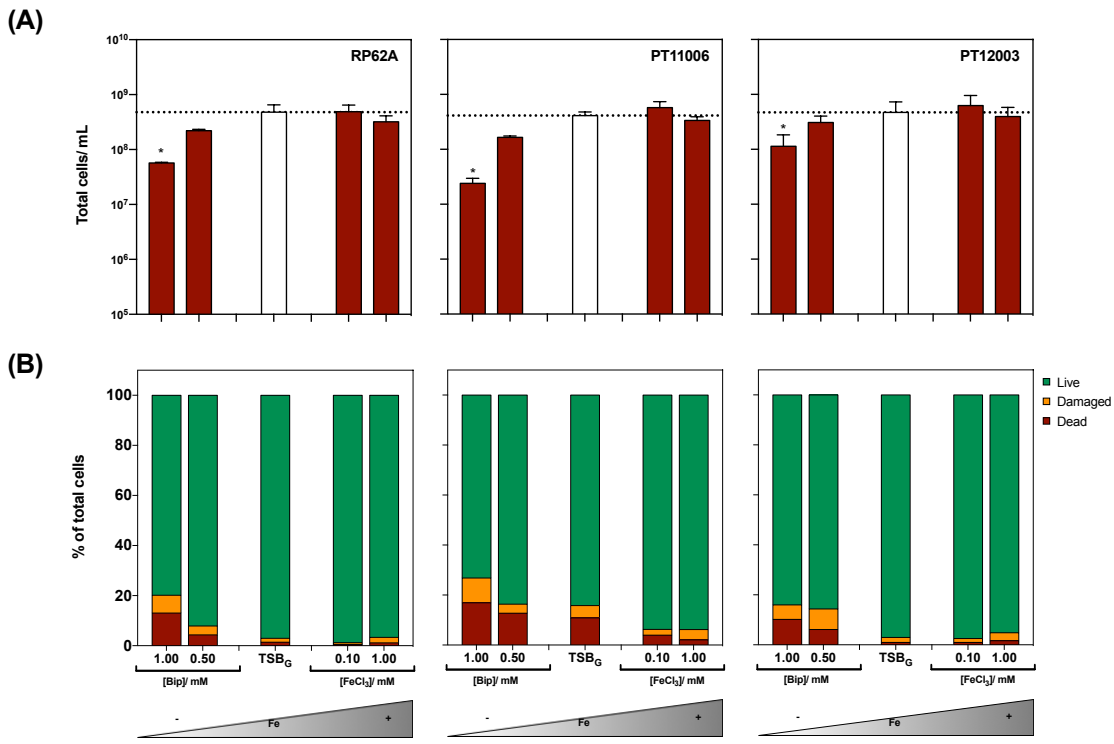

(C)

Condition	RP62A	PT11006	PT12003
TSB_G	47,06 ± 2,24	39,75 ± 0,30	36,89 ± 0,06
TSB_G, 0.10 mM $FeCl_3$	51,90 ± 1,03	42,67 ± 2,18	38,36 ± 0,06
TSB_G, 1.00 mM $FeCl_3$	88,60 ± 5,28****	82,06 ± 1,29****	66,07 ± 9,67***
TSB_G, 0.50 mM Bip	61,33 ± 4,38*	126,88 ±13,89****	78,08 ± 4,96****
TSB_G, 1.00 mM Bip	72,60 ± 7,84***	48,11 ± 13,89	80,52 ± 9,59****

Figure 3.4. Viability of biofilm cells grown under iron restriction and excess. Biofilms of three different *S. epidermidis* strains were allowed to grow on 96-well microtiter plates for 24 h at 37°C in TSB_G containing increasing concentrations of $FeCl_3$ or Bip. Biofilm cells were studied by flow cytometry for **(A)** total cell counting, and **(B)** proportion of live, damaged, and dead cells. **(C)** Relative cell size according to Forward Scatter (FSC) measurements by flow cytometry. Data are represented as mean ± standard deviation of two independent experiments. Significant differences are depicted with: * $p < 0.05$; ** $p < 0.01$; *** $p < 0.001$; **** $p < 0.0001$. Fe-, iron deficiency; Fe+, iron excess.

3.3.4 Iron deficiency impacts biofilm development from an early development stage and leads to reduced PIA/PNAG production

A temporal analysis of biofilm formation (**Figure 3.5A**) indicated that iron availability plays a major role right from an early development stage (6 h). Even though further biomass accumulation is noticeable across all conditions, this process is clearly hampered by shifts in iron availability, especially under low-iron conditions.

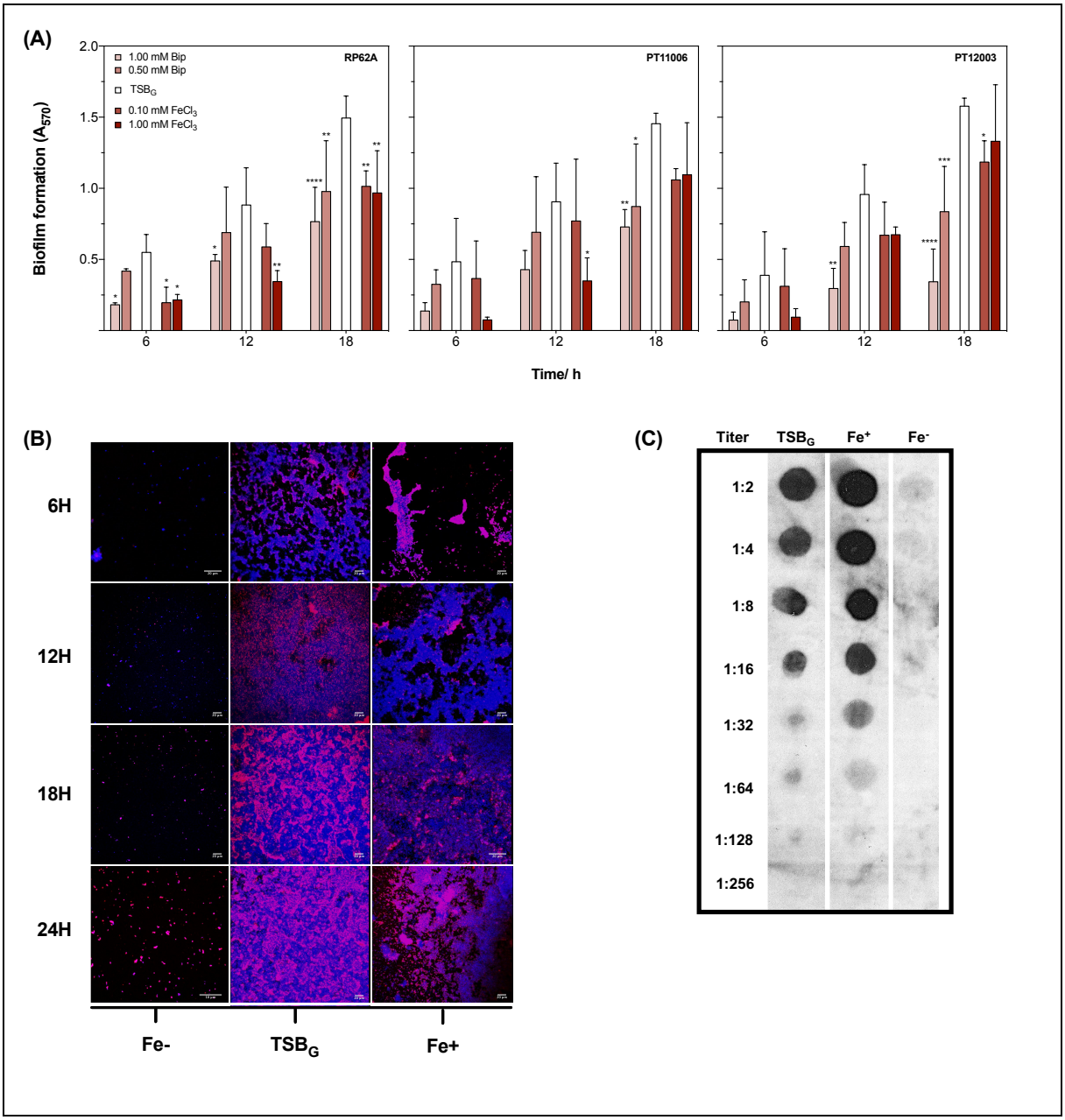

Figure 3.5. Temporal analysis of biofilm formation and interconnection between iron availability and PIA/PNAG production. Biofilms of three different *S. epidermidis* strains were allowed to grow at 37°C in TSB_G containing increasing concentrations of $FeCl_3$ and Bip. **(A)** Biomass accumulation on 96-well microtiter plates was evaluated from 6 to 18 h using crystal violet staining. Data are represented as mean ± standard deviation of three independent assays. Significant differences are depicted with: * $p < 0.05$; ** $p < 0.01$; *** $p < 0.001$; **** $p < 0.0001$. **(B)** Biofilms were also grown on an 8-well chamber slide system and examined under CLSM for structure analysis and PIA/PNAG production after appropriate staining with DAPI (depicted in blue) and WGA-Texas Red (depicted in red). Representative images of each condition tested for strain PT12003 are shown. **(C)** Quantification of PIA/PNAG production in *S. epidermidis* RP62A biofilms by dot blot analysis. Serial dilutions of cell wall extracts were spotted onto PVDF membranes which were then incubated with WGA coupled to peroxidase. Bound WGA was then visualized by chemiluminescence. Fe-, iron deficiency; Fe+, iron excess.

A similar set of experiments was carried out in a chamber slide system and biofilms were examined through CLSM for biofilm structure and PIA/PNAG production (**Figure 3.5B**). PIA/PNAG has long been known as a major component of the staphylococcal biofilm matrix, and a key molecule for intercellular

adhesion during biofilm accumulation (29). When strains were grown in TSB_G, a classical staphylococcal biofilm structure was observed with cells being evenly distributed across the surface and embedded by a prominent PIA/PNAG mesh. Conversely, iron excess seems to have a detrimental effect on biofilm accumulation during the first 12 h, with cells being assembled mainly as clusters. This seems to be an initial adaption period after which cells are able to accumulate and achieve a wider distribution (18 h). However, an apparent decrease in biofilm formation from 18 to 24 h was observed. Although this observation may suggest a biofilm disruption event, we have evidence that this might simply be an artifact. In fact, 24 h-old biofilms formed in the chamber slide system under iron excess proved to be very unstable, especially for strain RP62A, and slightly disrupted by the washing steps employed to remove loosely attached cells, an unpreventable phenomenon that usually occurs when using fed-batch systems (30). This has led us to hypothesize that the extracellular biofilm matrix is somehow affected by excess iron. Staining with WGA showed that PIA/PNAG production was not affected at this point. Also, a dot blot analysis of cell wall extracts from RP62A biofilms revealed that iron excess does not have any effect on the production of PIA/PNAG (**Figure 3.5C**). Therefore, the effect observed is likely the result of another unknown mechanism. Lastly, biofilms formed under iron-depleted conditions (Fe-) exhibited a reduced number of cells throughout the period in analysis. Cells were found to be distributed across the surface mostly as microcolonies, being those structures surrounded with small amounts of PIA/PNAG. Immuno-dot blot analysis confirmed that production of PIA/PNAG is almost abrogated under these conditions (**Figure 3.5C**).

3.3.5 Bioinformatics analysis of putative iron-related genes

A recent study performed by França et al. (2) highlighted a group of genes in *S. epidermidis* with putative function in iron uptake/ homeostasis that were found to be differentially expressed after incubation of biofilm cells with human blood. To find out whether the proteins encoded by these genes share homology with proteins with known function in *S. aureus*, which is far better characterized at the level of iron acquisition mechanisms, a bioinformatics analysis was carried out (**Table 3.4**). Products of the *SERP1778-1781* locus (**Figure 3.6**) share homology with the *sfaABCD*-encoded enzymes, which have been demonstrated to be involved in the biosynthesis of a siderophore called staphyloferrin A (31). Siderophores are low-molecular weight, high-affinity iron chelators capable of compete for iron with other host's iron-binding proteins, and are one of the most common iron acquisition systems among bacteria (32). Siderophore production in *S. epidermidis* has been reported before (33), although genetic information underlying siderophore biosynthesis in this species remains to be elucidated.

Immediately upstream is the *SERP1775-1777* locus whose products share homology with components of the ABC transporter HtsABC, which has been shown to be the transporter of iron-staphyloferrin A complexes (31). Interestingly, and similarly to *S. aureus*, this locus lacks a gene encoding the ATP-binding protein of a classical ABC-type transporter. In *S. aureus*, it has been demonstrated that the ATP-binding protein required for the internalization of both staphyloferrin A (31) and B (34) is FhuC. In *S. epidermidis*, and according to previous results on *S. aureus*, the *SERP0306* locus seems to encode the protein that plays that role, since it was found to be up-regulated when biofilm cells were cultured in human blood (2), and it shares homology with the *S. aureus* ATP-binding protein FhuA.

Table 3.4. BLAST closest matches of *S. epidermidis* RP62A putative iron-related proteins in *S. aureus* strain Newman

***S. epidermidis* RP62A**	***S. aureus* strain Newman protein**			
Protein	**Protein**	**Function**	**Identity (%)**	**Similarity (%)**
SERP1775	NWMN_2076 (HtsC)	Siderophore ABC transporter, permease	75	90
SERP1776	NWMN_2077 (HtsB)	Siderophore ABC transporter, permease	72	89
SERP1777	NWMN_2078 (HtsA)	Siderophore ABC transporter, lipoprotein	72	84
SERP1778	NWMN_2079 (SfaC)	Alanine racemase	63	81
SERP1779	NWMN_2080 (SfaB)	Siderophore synthetase	64	78
SERP1780	NWMN_2081 (SfaA)	MFS transporter	75	90
SERP1781	NWMN_2082 (SfaD)	IucA/IucC family siderophore biosynthesis protein	60	75
SERP0306	NWMN_0616 (FhuA)	Ferrichrome transport, ATP-binding protein	84	92
SERP0400	NWMN_0702 (SstA)	Siderophore ABC transporter, permease	80	94
SERP0401	NWMN_0703 (SstB)	Siderophore ABC transporter, permease	72	89
SERP0402	NWMN_0704 (SstC)	Siderophore ABC transporter, ATP-binding protein	73	88
SERP0403	NWMN_0705 (SstD)	Siderophore ABC transporter, lipoprotein	41	63
SERP0949	NWMN_0705 (SstD)	Siderophore ABC transporter, lipoprotein	70	85
SERP1951	NWMN_2261 (HrtA)	Heme ABC transporter, ATP-binding protein	69	83
SERP1952	NWMN_2262 (HrtB)	Heme ABC transporter, permease	53	76
SERP1953	NWMN_2263 (HssR)	Heme response regulator, DNA-binding protein	71	87
SERP1954	NWMN_2264 (HssS)	Sensor histidine kinase	65	80

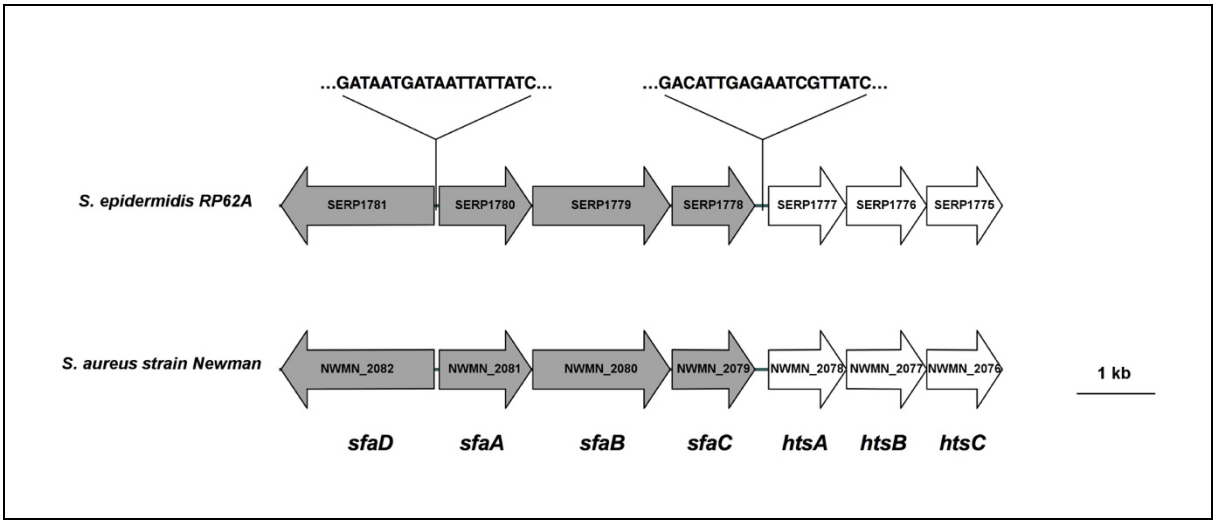

Figure 3.6. Genetic map of the *SERP1775-1781* locus in *S. epidermidis* RP62A. The genetic organization of this locus is identical to NWMN_2076-2082 locus in *S. aureus* strain Newman, which encodes the biosynthetic machinery for the siderophore staphyloferrin A and its transporter HtsABC. Open reading frames are indicated by arrows, which show the direction of transcription. Putative Fur boxes were identified in the intergenic regions.

The products of the *SERP0400-0402* locus are homologs of the *S. aureus* Sst system, described as a putative siderophore transporter (35), even though its substrate specificity is yet to be determined. In most bacterial species, and like the *sfa-hts* locus, genes encoding for siderophore transporters are usually found in the vicinity of the biosynthetic genes (36). However, products of the genes immediately up- or downstream this locus do not share homology with siderophore-related proteins from other species. Besides staphyloferrin A, another siderophore called staphyloferrin B has been identified and characterized in *S. aureus*, which is synthesized by the products of the *sbn* loci (37), and internalized by the SirABC transporter (38,39). However, Sbn homologs have not been found in *S. epidermidis*, and the only proteins that share homology with SirABC are those encoded by the *SERP1775-1777* locus.

The products of *SERP0949* and *SERP0403* genes have been annotated as transferrin-binding proteins. However, bioinformatics analysis has shown that SERP0403, and SERP0949 at a lower degree, shares homology with *S. aureus* SstD, which is the substrate-binding protein of the previously discussed Sst transporter.

SERP1951 and SERP1953 are homologs of *S. aureus* HrtA and HssR, respectively. Together with HrtB (SERP1952), HrtA forms the efflux pump HrtAB that plays a significant function in intracellular heme homeostasis and control of heme-associated toxicity. HrtAB is in turn activated by the two-component regulatory system HssRS (SERP1953-1954) in response to heme exposure (40,41).

Identification of putative Fur boxes up- or downstream these loci was also performed. Fur protein regulates the expression of genes in response to intracellular iron levels, exerting their action by binding with high affinity to a 19-bp inverted repeat sequence known as the Fur box (42). In general, the presence of a Fur box consensus sequence overlapping or upstream a given gene is predictive that its transcription is iron-regulated via Fur activity (43). Bioinformatics analysis led to the identification of putative Fur box sequences up- or downstream every single locus tested, suggesting that their expression is regulated not only by iron levels but also in a Fur-dependent manner.

3.3.6 S. epidermidis *uses distinct mechanisms to acquire iron and maintain iron homeostasis*

To experimentally confirm the involvement of the aforementioned genes in iron acquisition/ homeostasis processes, biofilms of different strains were grown under iron-enriched (Fe+) or iron-deficient (Fe-) culture conditions (TSB_6, supplemented with 1 mM $FeCl_3$ or 1 mM Bip, respectively), and the transcription of those genes was evaluated through qPCR. Remarkably, transcription of genes putatively encoding components of a siderophore transporter (*SERP0400-0402*, *SERP1775-1776*, and *SERP0306*) and siderophore biosynthesis-related proteins (*SERP1778-1779*) were found to be up-regulated under Fe- conditions (**Table 3.5A-B**). This suggests that *S. epidermidis* relies on a siderophore-mediated strategy to overcome iron limitation. Interestingly, *SERP1775-1776* and *SERP1778-1779* transcripts were also found to be slightly increased under Fe+ conditions, while *SERP0306* was clearly downregulated for this condition. Whether siderophore production also takes place when iron is readily available should be the aim of future research.

Transcription of *SERP0949* and *SERP0403* was also found to be significantly up-regulated under Fe- conditions (except in strain PT11006) (**Table 3.5B**). The most likely hypothesis is that these putative siderophore-binding proteins may have affinity either for iron-siderophore or iron-Bip complexes. Further experimental confirmation should be achieved through characterization of these proteins for substrate specificity.

Lastly, *SERP1951* transcript levels (**Table 3.5C**) were significantly higher under Fe+. This supports the role of SERP1951 as part of an efflux pump which controls iron-associated toxicity. Under Fe- conditions, its transcription remained either unchanged or downregulated, indicating that cells were attempting to hold as much intracellular iron as possible.

Table 3.5. Effect of iron availability on the transcription of putative iron-related genes

Process	Gene	Putative function	RP62A			PT11006			PT12003		
			Fe+	Fe-	*p* value*	Fe+	Fe-	*p* value*	Fe+	Fe-	*p* value*
A) Siderophore biosynthesis	*SERP1778*	Amino-acid racemase	1,856	2,509	0,5853	0,701	2,982	0,0838	2,268	3,259	0,4949
	SERP1779	Siderophore synthetase	2,283	2,866	0,6262	1,468	4,036	0,0526	1,793	3,252	0,3166
B) Siderophore uptake (ABC transporter)	*SERP1775*	Permease	0,494	2,279	0,1398	1,355	2,649	0,3216	1,959	3,088	0,4372
	SERP1776	Permease	0,019	1,938	0,1131	1,114	3,569	0,0634	2,059	3,761	0,2434
	SERP0306	ATP-binding protein	-1,349	2,928	**0,0008**	-2,252	0,007	0,0867	-0,785	3,795	**0,0026**
	SERP0400	Permease	-0,306	2,837	**0,0110**	0,052	1,604	0,4193	1,055	4,893	**0,0105**
	SERP0401	Permease	-0,290	3,399	**0,0032**	1,425	2,117	0,5950	1,559	5,070	**0,0186**
	SERP0402	ATP-binding protein	-0,269	2,699	**0,0160**	1,661	1,966	0,8148	1,660	4,924	**0,0281**
	SERP0403	Siderophore-binding protein	-0,435	2,666	**0,0121**	1,699	1,800	0,9375	1,808	4,495	**0,0685**
	SERP0949	Siderophore-binding protein	-0,252	4,091	**0,0006**	2,053	-1,172	**0,0160**	0,881	4,612	**0,0127**
C) Heme-regulated transport	*SERP1951*	ATP-binding protein	1,471	-3,775	**<0,0001**	7,602	-0,480	**<0,0001**	4,698	0,279	**0,0036**
D) Heme sensing syste	*SERP1953*	DNA-binding response regulator	-0,114	0,414	0,6586	0,643	0,126	0,6905	1,686	1,980	0,8559

Biofilms of three different *S. epidermidis* strains were allowed to grow on 24-well microtiter plates for 24 h at 37°C in TSB_6 (control condition) or TSB_6 containing 1 mM $FeCl_3$ (Fe+) or 1 mM Bip (Fe-). Biofilms were scrapped off, RNA was extracted, and cDNA synthesis was carried out for gene transcription analysis by quantitative PCR (qPCR). Genes in study are putatively involved in **(A and B)** siderophore biosynthesis and transport and **(C and D)** heme-sensing/ -export. Fold change data were calculated according to Pfaffl method and log-transformed (Log_2). Average data from three independent RNA extractions are represented. Values above and below 0 indicate up- and down-regulation of transcription, respectively, in comparison to the control condition (TSB_6); *****Two-away ANOVA with multiple comparisons test was used to detect differences in transcription between Fe+ and Fe- conditions. $p < 0.05$ was considered statistically significant (significant differences depicted in bold).

On the other hand, *SERP1953* (*hssR*) was found to be equally expressed between the two conditions (**Table 3.5D**). In comparison with the control condition (TSB_G only), its expression did not suffer any change, except for strain PT12003. Taking into account its putative role as part of a two-component heme regulatory system, one would expect an altered expression in response to a disruption in iron availability, which would in turn activate/ deactivate the expression of the efflux pump HrtAB. Also, a putative Fur box was identified upstream its coding sequence, hence suggesting an iron-regulated transcription. Nevertheless, and although this study does not elucidate the role of HssR, it seems that unlike *S. aureus* the activation/repression of HrtAB in *S. epidermidis* does not rely on the HssRS system.

Based on both bioinformatics analysis and transcription data, a model portraying the different mechanisms that *S. epidermidis* employs to acquire iron and maintain its homeostasis is proposed in **Figure 3.7**.

3.4 Discussion

It has been well established that virtually all microorganisms rely on iron to proliferate whereupon this dependence has been explored as a potential therapeutic target (32). Regarding staphylococci, relevant research on this topic has been published. However, not only these studies have mostly been performed on planktonic growth, but also a strong focus on *S. aureus* is noticeable (31,44–46). As a major cause of bloodstream infections (47), *S. epidermidis* is thought to have efficient mechanisms to overcome severe iron restriction found in an environment like blood. This study sheds light into how disruptions in iron homeostasis severely impact *S. epidermidis* biofilm formation, especially when iron becomes a limiting nutrient.

Firstly, it is important to take into account that this bacterial species is primarily a major commensal inhabitant of the human skin, which is regarded as an iron-replete environment (48). As a result, it is not surprising that biofilm formation was not hampered by a wide range of iron concentrations, even those out of the physiologic range (up to 0.10 mM) (**Figure 3.1**). Nonetheless, and despite iron being indispensable for life, it is known that its excess leads to abnormal production of ROS, which in turn leads to cellular damage (49). A scenario of iron excess was simulated by adding 1 mM $FeCl_3$ to the culture medium routinely used, and a compromised biofilm formation was in fact detected for this condition. Surprisingly, such observation was not accompanied neither by an impaired planktonic growth rate (**Figure 3.3A**) nor by a significant decrease in cell viability (**Figure 3.4B**) and cultivability (**Table 3.3**).

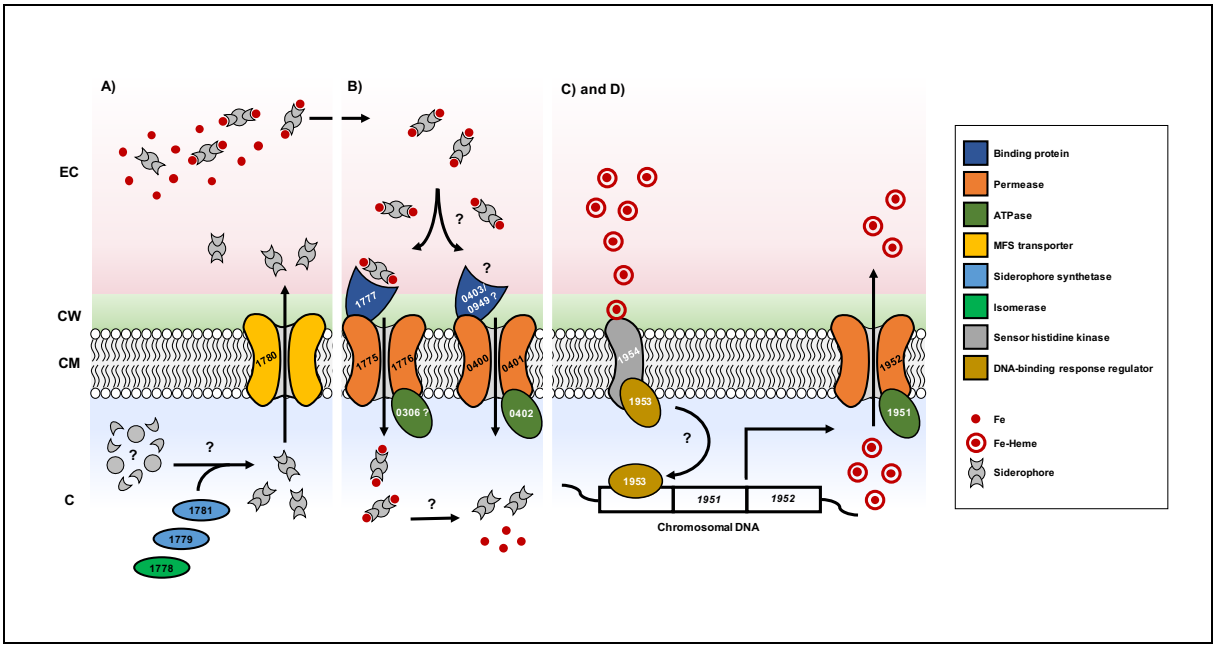

Figure 3.7. Model for the distinct mechanisms that *S. epidermidis* uses to acquire iron and maintain its homeostasis. **(A)** The biosynthetic genes for siderophore production encode three different enzymes required for siderophore synthesis (SERP1778, SERP1779 and SERP1781), and a transporter (SERP1780) for its export to the extracellular medium. **(B)** Once outside the cell, the exported siderophores then bind to available iron (Fe^{3+}) molecules and are imported back to the cell through an ABC transporter composed by the products of the locus *SERP1775-77*, and possibly of the gene *SERP0306*. The locus *SERP0400-0403* and *SERP0949* also encodes an ABC transporter whose substrate specificity is currently not known. **(C and D)** Iron acquisition from heme sources is likely to occur through the machinery encoded by the locus *SERP1951-1954*, which is also responsible for the control of intracellular heme homeostasis and heme-associated toxicity (for detailed information about this process in *S. aureus* please refer to (40,41).

Taking into account such high iron concentration did negatively affect biofilm but not planktonic growth, it was hypothesized that extreme iron concentrations somehow trigger cells to adopt a planktonic, free-floating lifestyle. Surprisingly, it was observed quite the opposite: the higher the iron concentration is, the lower the proportion of suspended cells in the whole cultivable population (**Table 3.3**). This, in turn, suggested that cells were not being dispersed/detached from the biofilm. A temporal analysis of biofilm formation showed that the reduced biofilm formation initially observed is essentially the result of a reduced cell attachment and further accumulation, ruling out the hypothesis that cells are being detached from the biofilm. Impaired production of extracellular matrix might also contribute for this phenotype, even though it is not related with decreased PIA/PNAG production. Studies on *P. aeruginosa*, a microorganism for which iron-related research is more developed, have shown that elevated iron concentrations also have an inhibitory effect on biofilm formation (50), which seems to be related with decreased release of extracellular DNA (51). Whether a similar mechanism takes place in *S. epidermidis* was not assessed and deserves further investigation.

In contrast to iron excess, iron-limiting conditions proved to be severely deleterious for biofilm formation (**Figure 3.1**), which is partly explained by a reduced growth rate (**Figure 3.3**; **Table 3.2**), but also by reduced cell viability (**Figure 3.4B**) and cultivability (**Table 3.3**), and consequent decreased PIA/PNAG production (**Figure 3.5B-C**). Studies carried out on *S. aureus* report contradictory outcomes. Similarly to what we have found, Lin et al. (8) demonstrated that iron depletion has a detrimental effect on biofilm formation, which is mainly related with decreased cell adherence and PIA/PNAG production. However, Johnson et al. (52) showed that biofilm formation was induced under low-iron growth conditions. Of note, these studies used different strains and culture media, hence it is conceivable that the observed differences were the result of strain-to-strain variation, as found in other studies (53,54), or due to differences in the experiment design itself. To account for this kind of variation, three different strains were used across the experiments here described. Taken together, data shows that a reduced biofilm formation under low-iron conditions is the combined result of changes in cell growth rate and viability and a significant reduction in the production of PIA/PNAG. Interestingly, it seems clear that most *S. epidermidis* cells are induced to grow as a biofilm either by iron excess or deficiency, even though the latter condition caused a reduction in the total number of cells. It has long been hypothesized that cells growing under certain conditions, namely nutrient limitation or presence of toxic compounds, are induced to adopt a biofilm lifestyle (55), which is in accordance to the observations reported in this chapter.

Another aim of this study was to explore the molecular mechanisms that *S. epidermidis* employs to acquire iron and maintain its homeostasis, which remains unknown to date. Beasley et al. (31) reported that the *sfa-hts* locus, known to encode proteins involved in siderophore biosynthesis and its import, is conserved in the CoNS for which genomic sequences are available.

Here, it is provided both *in silico* and experimental evidence that such cluster of genes is also iron-regulated in *S. epidermidis*, supporting the role of this locus in siderophore biosynthesis and transport, as well as opening the door for further in-depth characterization of siderophore production in this species. Besides, other genetic loci putatively encoding siderophore transporters were identified, the transcription of which has also been shown to be triggered by iron-limiting conditions. Therefore, data described in this chapter strongly suggest that *S. epidermidis* relies on siderophore production as a means to acquire iron. However, unlike *S. aureus*, *S. epidermidis* seems to have the necessary machinery for the production of one single siderophore, yet it has different transporters for its internalization. Whether such transporters

are specific or may function as alternative uptake systems for siderophores produced by other bacterial species should be the target of future research.

Also, *S. epidermidis* is equipped with a homolog of *S. aureus* HrtA. HrtA is part of an efflux pump system in *S. aureus* that allows cells to cope with heme-associated toxicity (41). However, the mechanism behind its activation/ repression seems to be different in both species. When *S. epidermidis* cells were cultured under iron excess, it was observed a conflicting result. According to the transcriptional studies, cells exhibited increased *hrtA* transcription (indicative of excess iron being exported out of the cell), and simultaneously increased transcription of siderophore biosynthetic genes (indicative of active siderophore production). Even though results suggest that iron-siderophore complexes were not being internalized under this condition, this is worth further investigation.

Collectively, the results reported in this study support the hypothesis that targeting iron metabolism may be an attractive strategy to prevent biofilm development by this species. This may be accomplished either by reducing the iron availability in the surrounding medium, or by interfering with its acquisition. Meanwhile, a better comprehension about the molecular mechanisms behind this process must be accomplished in a near future.

3.5 References

1. Ganz T. Iron in innate immunity: starve the invaders. Curr Opin Immunol. 2009;21(1):63–7.
2. França A, Carvalhais V, Maira-Litrán T, Vilanova M, Cerca N, Pier G. Alterations in the *Staphylococcus epidermidis* biofilm transcriptome following interaction with whole human blood. Pathog Dis. 2014;70(3):444–8.
3. Torres VJ, Pishchany G, Humayun M, Schneewind O, Skaar EP. *Staphylococcus aureus* IsdB is a hemoglobin receptor required for heme iron utilization. J Bacteriol. 2006;188(24):8421–9.
4. Gi M, Lee KM, Kim SC, Yoon JH, Yoon SS, Choi JY. A novel siderophore system is essential for the growth of *Pseudomonas aeruginosa* in airway mucus. Sci Rep. 2015;5:14644.
5. Folsom JP, Parker AE, Carlson RP. Physiological and proteomic analysis of *Escherichia coli* iron-limited chemostat growth. J Bacteriol. 2014;196(15):2748–61.
6. Weinberg ED. Suppression of bacterial biofilm formation by iron limitation. Med Hypotheses. 2004;63(5):863–5.
7. Johnson M, Cockayne A, Morrissey JA. Iron-regulated biofilm formation in *Staphylococcus aureus* Newman requires *ica* and the secreted protein Emp. Infect Immun. 2008;76(4):1756–65.
8. Lin MH, Shu JC, Huang HY, Cheng YC. Involvement of iron in biofilm formation by *Staphylococcus aureus*. PLoS One. 2012;7(3):e34388.

9. Johnson M, Cockayne A, Williams PH, Morrissey JA. Iron-responsive regulation of biofilm formation in *Staphylococcus aureus* involves *fur*-dependent and *fur*-independent mechanisms. J Bacteriol. 2005;187(23):8211–5.

10. Freitas AI, Lopes N, Oliveira F, Brás S, França Â, Vasconcelos C, et al. Comparative analysis between biofilm formation and gene expression in *Staphylococcus epidermidis* isolates. Future Microbiol. 2018;13:415–27.

11. Stepanovic S, Vukovic D, Hola V, Di Bonaventura G, Djukic S, Cirkovi I, et al. Quantification of biofilm in microtiter plates: overview of testing conditions and practical recommendations for assessment of biofilm production by staphylococci. APMIS. 2007;115(8):891–9.

12. Freitas AI, Vasconcelos C, Vilanova M, Cerca N. Optimization of an automatic counting system for the quantification of *Staphylococcus epidermidis* cells in biofilms. J Basic Microbiol. 2014;54(7):750–7.

13. Cerca F, Trigo G, Correia A, Cerca N, Azeredo J, Vilanova M. SYBR green as a fluorescent probe to evaluate the biofilm physiological state of *Staphylococcus epidermidis*, using flow cytometry. Can J Microbiol. 2011;57(10):850–6.

14. Schindelin J, Arganda-Carreras I, Frise E, Kaynig V, Longair M, Pietzsch T, et al. Fiji: an open-source platform for biological-image analysis. Nat Methods. 2012;9(7):676–82.

15. Jefferson KK, Cerca N. Bacterial-Bacterial Cell Interactions in Biofilms: Detection of polysaccharide intercellular adhesins by blotting and confocal microscopy. In: Colgan SP. (ed.) Cell-cell interactions methods in molecular biology. Humana Press; 2006. p.119–26.

16. França A, Freitas AI, Henriques AF, Cerca N. Optimizing a qPCR gene expression quantification assay for *S. epidermidis* biofilms: A comparison between commercial kits and a customized protocol. PLoS One. 2012;7(5):e37480.

17. Pfaffl MW, Pfaffl MW. A new mathematical model for relative quantification in real-time RT-PCR. Nucleic Acids Res. 2001;29(9):e45.

18. Untergasser A, Cutcutache I, Koressaar T, Ye J, Faircloth BC, Remm M, et al. Primer3 - new capabilities and interfaces. Nucleic Acids Res. 2012;40(15).

19. Zuker M. Mfold web server for nucleic acid folding and hybridization prediction. Nucleic Acids Res. 2003;31(13):3406–15.

20. Ye J, Coulouris G, Zaretskaya I, Cutcutache I, Rozen S, Madden TL. Primer-BLAST: a tool to design target-specific primers for polymerase chain reaction. BMC Bioinformatics. 2012;13(1):134.

21. Altschul SF, Gish W, Miller W, Myers EW, Lipman DJ. Basic local alignment search tool. J Mol Biol. 1990;215(3):403–10.

22. Grant CE, Bailey TL, Noble WS. FIMO: Scanning for occurrences of a given motif. Bioinformatics. 2011;27(7):1017–8.

23. De Lorenzo V, Wee S, Herrero M, Neilands JB. Operator sequences of the aerobactin operon of plasmid ColV-K30 binding the ferric uptake regulation (*fur*) repressor. J Bacteriol. 1987;169(6):2624–30.

24. Mladěnka P, Macáková K, Zatloukalová L, Řeháková Z, Singh BK, Prasad AK, et al. *In vitro* interactions of coumarins with iron. Biochimie. 2010;92(9):1108–14.

25. Worwood M. Disorders of iron metabolism. In: Williams DL, Marks V. (eds.) Scientific foundations of biochemistry in clinical practice. 2nd ed. Oxford, UK: Butterworth-Heinemann; 2014. p. 446–52.

26. Hayrapetyan H, Siezen R, Abee T, Groot MN. Comparative genomics of iron-transporting systems in *Bacillus cereus* strains and impact of iron sources on growth and biofilm formation. Front Microbiol. 2016;7(JUN):1–13.

27. Reid DW, O'May C, Kirov SM, Roddam L, Lamont IL, Sanderson K. Iron chelation directed against biofilms as an adjunct to conventional antibiotics. AJP Lung Cell Mol Physiol. 2009;296(5):L857–8.

28. Knobloch JK-M, Horstkotte M a, Rohde H, Kaulfers P-M, Mack D. Alcoholic ingredients in skin disinfectants increase biofilm expression of *Staphylococcus epidermidis*. J Antimicrob Chemother. 2002;49(4):683–7.

29. Jabbouri S, Sadovskaya I. Characteristics of the biofilm matrix and its role as a possible target for the detection and eradication of *Staphylococcus epidermidis* associated with medical implant infections. FEMS Immunol Med Microbiol. 2010;59(3):280–91.

30. França A, Carvalhais V, Vilanova M, Pier GB, Cerca N. Characterization of an *in vitro* fed-batch model to obtain cells released from *S. epidermidis* biofilms. AMB Express. 2016;6(1):23.

31. Beasley FC, Vinés ED, Grigg JC, Zheng Q, Liu S, Lajoie GA, et al. Characterization of staphyloferrin A biosynthetic and transport mutants in *Staphylococcus aureus*. Mol Microbiol. 2009;72(4):947–63.

32. Miethke M, Marahiel MA. Siderophore-based iron acquisition and pathogen control. Microbiol Mol Biol Rev. 2007;71(3):413–51.

33. Lindsay JA, Riley T V., Mee BJ. Production of siderophore by coagulase-negative staphylococci and its relation to virulence. Eur J Clin Microbiol Infect Dis. 1994;13(12):1063–6.

34. Speziali CD, Dale SE, Henderson JA, Vinés ED, Heinrichs DE. Requirement of *Staphylococcus aureus* ATP-binding cassette-ATPase FhuC for iron-restricted growth and evidence that it functions with more than one iron transporter. J Bacteriol. 2006;188(6):2048–55.

35. Morrissey J a., Cockayne A, Hill PJ, Williams P. Molecular cloning and analysis of a putative siderophore ABC transporter from *Staphylococcus aureus*. Infect Immun. 2000;68(11):6281–8.

36. Crosa JH, Walsh CT. Genetics and assembly line enzymology of siderophore biosynthesis in bacteria. Microbiol Mol Biol Rev. 2002;66(2):223–49.

37. Hammer ND, Skaar EP. Molecular mechanisms of *Staphylococcus aureus* iron acquisition. Annu Rev Microbiol. 2011;65(1545-3251 (Electronic)):129–47.

38. Beasley FC, Marolda CL, Cheung J, Buac S, Heinrichs DE. *Staphylococcus aureus* transporters Hts, Sir, and Sst capture iron liberated from human transferrin by staphyloferrin A, staphyloferrin B, and catecholamine stress hormones, respectively, and contribute to virulence. Infect Immun. 2011;79(6):2345–55.

39. Beasley FC, Heinrichs DE. Siderophore-Mediated iron acquisition in the staphylococci. J Inorg Biochem. 2010;104(3):282–8.

40. Friedman DB, Stauff DL, Pishchany G, Whitwell CW, Torres VJ, Skaar EP. *Staphylococcus aureus* redirects central metabolism to increase iron availability. PLoS Pathog. 2006;2(8):0777–89.

41. Torres VJ, Stauff DL, Pishchany G, Bezbradica JS, Gordy LE, Iturregui J, et al. A *Staphylococcus aureus* regulatory system that responds to host heme and modulates virulence. Cell Host Microbe. 2007;1(2):109–19.

42. Baichoo N, Helmann JD. Recognition of DNA by Fur: a reinterpretation of the Fur box consensus sequence. J Bacteriol. 2002;184(21):5826–32.

43. Lee J-W, Helmann JD. Functional specialization within the Fur family of metalloregulators. BioMetals. 2007;20(3–4):485–99.

44. Brozyna JR, Sheldon JR, Heinrichs DE. Growth promotion of the opportunistic human pathogen, *Staphylococcus lugdunensis*, by heme, hemoglobin, and coculture with *Staphylococcus aureus*. Microbiologyopen. 2014;3(2):182–95.

45. Cornelis P, Dingemans J. *Pseudomonas aeruginosa* adapts its iron uptake strategies in function of the type of infections. Front Cell Infect Microbiol. 2013;3(November):75.

46. Dale SE, Doherty-Kirby A, Lajoie G, Heinrichs DE. Role of siderophore biosynthesis in virulence of *Staphylococcus aureus*: identification and characterization of genes involved in production of a siderophore. Infect Immun. 2004;72(1):29–37.

47. Widerström M, Wiström J, Sjöstedt A, Monsen T. Coagulase-negative staphylococci: update on the molecular epidemiology and clinical presentation, with a focus on *Staphylococcus epidermidis* and *Staphylococcus saprophyticus*. Eur J Clin Microbiol Infect Dis. 2012;31(1):7–20.

48. Ledala N, Zhang B, Seravalli J, Powers R, Somerville GA. Influence of iron and aeration on *Staphylococcus aureus* growth, metabolism, and transcription. J Bacteriol. 2014;196(12):2178–89.

49. Oliveira F, Rocha S, Fernandes R. Iron metabolism: from health to disease. J Clin Lab Anal. 2014;28(3):210–8.

50. Musk DJ, Banko DA, Hergenrother PJ. Iron salts perturb biofilm formation and disrupt existing biofilms of *Pseudomonas aeruginosa*. Chem Biol. 2005;12(7):789–96.

51. Yang L, Barken KB, Skindersoe ME, Christensen AB, Givskov M, Tolker-Nielsen T. Effects of iron on DNA release and biofilm development by *Pseudomonas aeruginosa*. Microbiology. 2007;153(5):1318–28.

52. Johnson M, Cockayne A, Williams PH, Morrissey JA. Iron-responsive regulation of biofilm formation in *Staphylococcus aureus* involves Fur-dependent and Fur-independent mechanisms. J Bacteriol. 2005;187(23):8211–5.

53. França A, Vilanova M, Cerca N, Pier GB. Monoclonal antibody raised against PNAG has variable effects on static *S. epidermidis* biofilm accumulation in vitro. Int J Biol Sci. 2013;9(5):518–20.

54. Oliveira F, Lima CA, Brass S, França A, Cerca N. Evidence for inter- and intraspecies biofilm formation variability among a small group of coagulase-negative staphylococci. FEMS Microbiol Lett. 2015;362(20):fnv175.

55. Donlan RM, Costerton JW. Biofilms: Survival mechanisms of clinically relevant microorganisms. Clin Microbiol Rev. 2002;15(2):167–93.

CHAPTER 4

S. epidermidis iron acquisition systems and their individual role in biofilm formation

Summary

According to the genetic and mRNA expression analysis shown in **Chapter 3**, *S. epidermidis* has a single locus putatively involved in the production of a siderophore, as well as two different ABC-like transporters for uptake of iron-siderophore complexes and/ or iron bound to other molecules. In order to experimentally confirm the function of these genes and assess their individual role in *S. epidermidis* growth under iron restriction, several deletion mutants were constructed, following an allelic replacement approach. Deletion mutants were characterized at different levels, with special focus on their biofilm formation ability. Most importantly, it was possible to demonstrate that the *SERP1778-1781* (*sfaABCD*) locus is involved in siderophore biosynthesis and its expression is important in maintaining the iron cell content. Deletion of *sfaABCD*, *SERP1775-1777* (*htsABC*) and *SERP0306* (*fhuA*) loci showed a mild negative effect on growth under iron restriction, whereas it was absolutely deleterious for biofilm formation under iron restriction. These data support previous findings that *S. epidermidis* biofilm formation requires a high availability of iron, which is mainly provided by siderophore biosynthesis and its uptake.

Part of the work described in this chapter was presented at the 18th International Symposium on Staphylococci and Staphylococcal Infections (ISSSI2018, Copenhagen, Denmark, 23 - 26 August 2018).

4.1. Brief introduction

A major hurdle in the study of *S. epidermidis* physiology and pathogenicity has been the inability to genetically manipulate a large proportion of clinical isolates (1). Different approaches have been devised to overcome this issue with more or less success (2,3). Nevertheless, studies have relied on a small subset of transformable strains, which include the reference biofilm-positive strains RP62A and 1457 (4,5). Strain 1457 has been largely used for biofilm-related research over the years (6–11) and presents some important advantages over RP62A, namely: (i) susceptibility to a wider range of antibiotic classes, allowing the use of multiple antibiotic resistance markers in genetic manipulation (5), (ii) higher amenability to genetic manipulation (3,12,13).

Due to these advantages, it was decided to perform a range of allelic replacement experiments in strain 1457 in an attempt to experimentally validate the function of different putative iron acquisition genes that were studied in **Chapter 3**, and that were confirmed to be iron-regulated. As a result, *SERP1778-81* (*sfaABCD*), *SERP1775-77* (*htsABC*), *SERP0400-3* (*sstABCD*), and *SERP0306* (*fhuA*) loci were deleted and resultant mutant strains were studied.

4.2. Materials and methods

4.2.1. Strains, plasmids, antibiotics, and culture media

Bacterial strains and plasmids used in this study are described in **Table 4.1**. Unless otherwise noted, strains were cultured at 37°C. For genetic manipulations, *E. coli* was grown in Lysogeny Broth (LB: 10 g/L tryptone, 5 g/L yeast extract, 10 g/L NaCl). Staphylococci were grown in TSB (BD Diagnostic Systems, Heidelberg, Germany). Solid media were prepared by adding 1.5% (w/v) agar (BD) to the culture medium. For selection of plasmids and recombinant alleles, antibiotics (Sigma-Aldrich) were added to the medium at the following concentrations: ampicillin (100 µg/mL) for *E. coli* selection and plasmid maintenance; trimethoprim (30 µg/mL), spectinomycin (150 µg/mL), erythromycin (10 µg/mL), and tetracycline (10 µg/mL) for staphylococci selection; and chloramphenicol (10 µg/mL) for staphylococcal plasmids maintenance. Iron restriction was achieved by slightly modifying a chemically defined medium (CDM) recipe (14), in which its original iron source (ammonium iron (II) sulfate) was omitted. This culture medium is henceforward referred to as CDM_{Fe-}. Iron-enriched conditions were achieved either by using TSB or by supplementing CDM_{Fe-} with 10 µM $FeCl_3$ (CDM_{Fe+}). All solutions and media were made with water purified through a Milli-Q water purification system (Millipore, MA, USA).

Table 4.1. Bacterial strains, plasmids and phages used in this chapter

Strain, plasmid or phage	Description*	Reference
***E. coli* strains**		
DH5α	Chemically competent cells for cloning purposes	New England Biolabs (NEB)
TOP10	Chemically competent cells for cloning purposes	Thermo Fisher Scientific, Inc
***S. aureus* strains**		
RN4220	Derived from NCTC8325-4; r_K m_{K^+}; accepts foreign DNA	(15)
PS187 Δ*hsdR* Δ*sauPSI*	*S. aureus* PS187 strain deficient in type IV and type I restriction systems	(13)
***S. epidermidis* strains**		
RP62A	Wild-type (WT) clinical isolate from a catheter sepsis; *icaADBC*+. *aap*+, *embp*+, strong biofilm formation	ATCC® 35984™
1457	WT clinical isolate from a central venous catheter infection; *icaADBC*+, *aap*+, *embp*+, strong biofilm formation	(16)
1457Δ*agr*::*spcR*	Mutant carrying a deletion of the accessory gene regulator (*agr*) system; Spt^R	(17)
1457-M12	*icaA*::Tn*917* insertion mutant, PIA/PNAG, biofilm-negative	(9)
1457Δ*hts*::*dhfr*	Mutant carrying a deletion of *htsABC* (*hts* = *SERP1775-17777*); Tmp^R	This study
1457Δ*sfa*::*spcR*	Mutant carrying a deletion of *sfaABCD* (*sfa* = *SERP1778-1781*); Spt^R	This study
1457Δ*fhuA*::*ermC*	Mutant carrying a deletion of *fhuA* (*fhuA* = *SERP0306*); Ery^R	This study
1457Δ*sst*::*tetM*	Mutant carrying a deletion of *sstABCD* (*sst* = *SERP0400-0403*)#	This study
1457Δ*hts* p*hts*	Complemented mutant 1457Δ*hts*; *in trans* expression of *hts* from its natural promoter; Tmp^R, Cm^R	This study
1457Δ*sfa* p*sfa*	Complemented mutant 1457Δ*sfa*; *in trans* expression of *sfa* from its natural promoter; Spt^R, Cm^R	This study
1457Δ*fhuA* p*fhuA*	Complemented mutant 1457Δf*huA*; *in trans* expression of *fhuA* from its natural promoter; Ery^R, Cm^R	This study
1457Δ*sst* p*sst*	Complemented mutant 1457Δ*sst*; *in trans* expression of *sst* from its natural promoter; Cm^R	This study
Plasmids		
pBASE6	Temperature-sensitive suicide mutagenesis vector; Amp^R, Cm^R	(18)
pB-*hts*	pBASE6 derivative containing *hts*::*dhfr;* Cm^R, Tmp^R	This study
pB-*sfa*	pBASE6 derivative containing *sfa*::*spcR*; Cm^R, Spt^R	This study
pB-*fhuA*	pBASE6 derivative containing *fhuA*::*ermC*; Cm^R, Ery^R	This study
pB-*sst*	pBASE6 derivative containing *sst*::*tetM*; Cm^R, Tet^R	This study
pRB473	Shuttle vector for cloning in *E. coli* and staphylococci; constitutive gene expression in staphylococci via *vegII* promoter	(19)
p*hts*	pRB473 derivative containing *htsABC* and its natural promoter	This study
p*sfa*	pRB473 derivative containing *sfaABCD* and its natural promoter	This study
p*fhu*	pRB473 derivative containing *fhuA* and its natural promoter	This study
p*sst*	pRB473 derivative containing *sstABCD* and its natural promoter	This study
Phages		
ϕ187	*S. aureus* phage; WT	(20)
A6C	*S. epidermidis*; WT	(6)

*Abbreviations: Amp^R, Cm^R, Ery^R, Spt^R, Tet^R, Tmp^R, resistance to ampicillin, chloramphenicol, erythromycin, spectinomycin, tetracycline and trimethoprim respectively. #*tetM* resistance cassette is not working properly.

4.2.2. Gene expression analysis

Gene expression analysis was performed essentially as described in section **3.2.8**, with some minor modifications. RNA was extracted using the RNeasy Mini Kit (QIAGEN, Hilden, Germany) according to the manufacturer's instructions. cDNA synthesis was performed using the iScript™ cDNA Synthesis Kit

(BioRad) following the manufacturer's instructions. qPCR analysis was performed using Applied Biosystems™ SYBR™ Select Master Mix (Thermo Fisher Scientific, Inc).

4.2.3. Genetic manipulations

Standard DNA manipulations were performed essentially as described by Sambrook et al. (21). Restriction endonucleases were purchased from New England Biolabs, Inc. (Frankfurt, Germany) or Thermo Scientific Inc. Phusion High-Fidelity DNA Polymerase and DyNAzyme II DNA Polymerase were purchased from Thermo Scientific Inc. Plasmid DNA was purified using the QIAprep Spin Miniprep Kit (QIAGEN) according to the manufacturer's instructions. For plasmid purification from staphylococci, the resuspension buffer provided with the plasmid isolation kit was supplemented with 25 U of lysostaphin (Sigma-Aldrich), and the cell suspension was incubated for 30 min at 37°C. Oligonucleotides and DNA sequencing services were purchased from Eurofins Genomics (Ebersberg, Germany).

4.2.4. Construction of mutant strains

An allelic replacement strategy was used for the construction of four deletion mutants in *S. epidermidis* 1457 strain (**Figure 4.1**). The list of primers used is shown in **Table 4.2**. For each mutant, two ~1kb fragments flanking regions up-stream and down-stream the coding region to be deleted and an antibiotic resistance cassette were amplified using Phusion High-Fidelity DNA Polymerase (Thermo Fisher Scientific Inc.). Amplicons were ligated and cloned into plasmid pBASE6 (18) using (i) Gibson Assembly® Cloning Kit (New England Biolabs, Inc.), according to the manufacturer's instructions, or (ii) circular polymerase extension cloning (CPEC), as described by Quan and Tian (22). Resulting plasmids were introduced by electroporation, first into *S. aureus* RN4220 and then into *S. epidermidis* 1457Δ*agr* or 1457-M12. Next, using phage A6C, plasmids were introduced into *S. epidermidis* 1457. Selection of mutants was performed essentially as described (23). Correctness of the chromosomal mutations was verified using PCR with primers that bind to genetic regions not involved in the mutagenesis process, and afterwards respective amplicons were sequenced. For complementation, DNA fragments containing the deleted coding sequences and their anticipated natural promoters were amplified and cloned into plasmid pRB473, as described above. Plasmids were introduced by electroporation first into *S. aureus* PS187ΔΔ and then into *S. epidermidis* 1457 mutant strains using phage Φ187, following a previously published protocol (24).

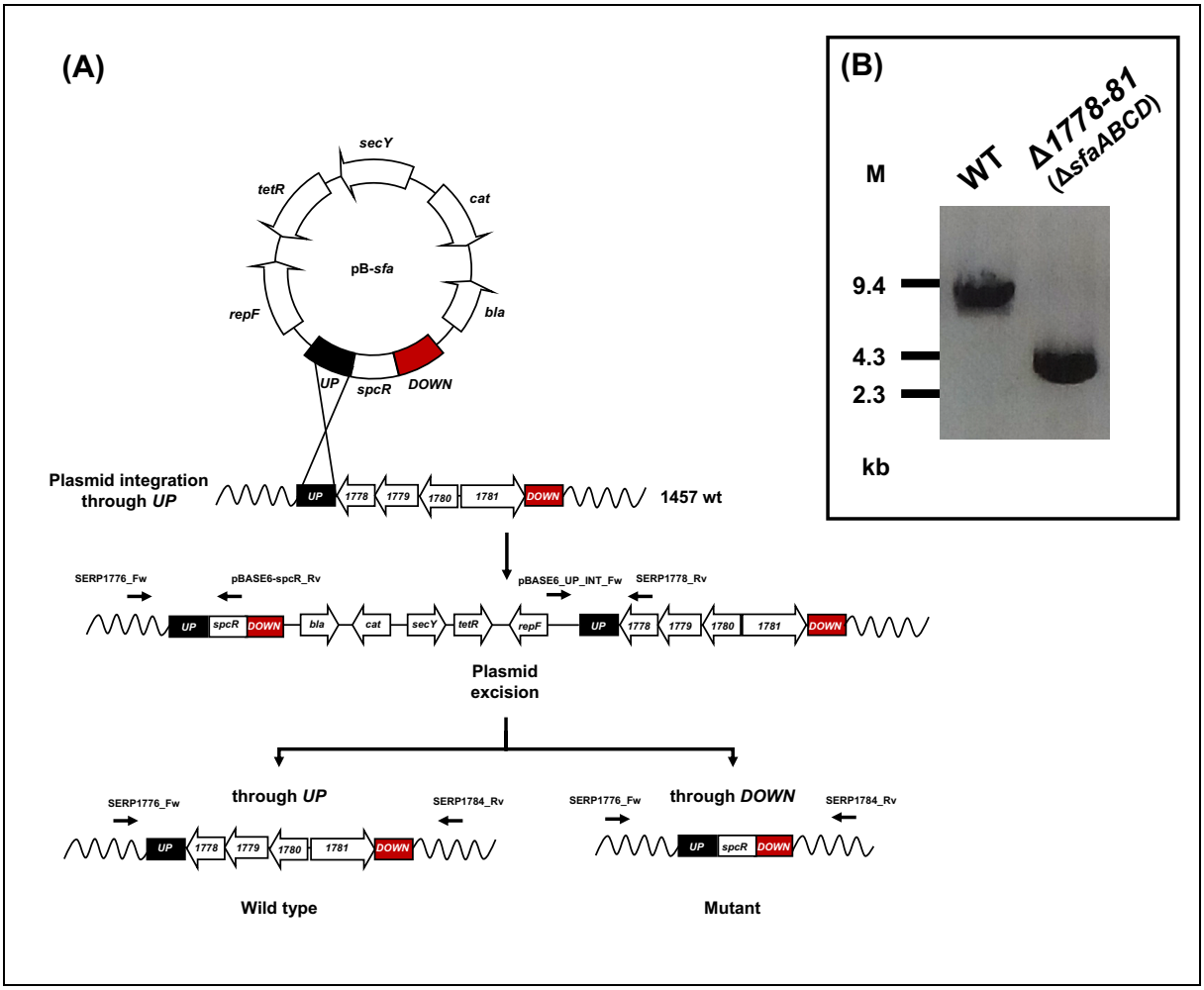

Figure 4.1. Allelic replacement strategy to generate deletion mutants in *S. epidermidis* 1457. **(A)** Schematic representation of the allelic replacement strategy used (all deletion mutants were obtained following this strategy; the construction of the *SERP1778-81* (*sfaABCD*) deletion mutant is shown for illustrative purposes only). **(B)** By performing a PCR analysis using an appropriate primer pair (SERP1776_Fw and SERP1784_Rv) the success of the mutagenesis protocol could be confirmed by a clear shift in band size (8826 bp for 1457 wild-type (WT); 3947 bp for 1457Δ*sfa*).

Table 4.2. Sequences of oligonucleotides used in this chapter

Designation	Purpose	Sequence (5' - 3')*
Δ*htsABC*		
SERP1775_UP_Fw	Amplification of fragments for construction of plasmid pB-*hts*	cccgccctgccactcatcgcagtgcagcgg**aattc**GCAATGACAATAGCGAAC (*Eco*RI)
SERP1775_UP_Rv		tattgataatgtcatTAAATTTGATAGTTTCAATATCGTATTTTTTAG
dhfR_Fw		aaactatcaaatttaATGACATTATCAATAATTGTCG
dhfR_Rv		tatacatattaaggaCTATTTCCCTTTTCTACGC
SERP1777_DOWN_Fw		agaaaagggaaatagTCCTTAATATGTATATGCTTACATTATTAG
SERP1777_DOWN_Rv		ctgcgcgctagcccgggtaccgagctccgg**aattc**GATGATTTCAAGAGTAGAAATGAG (*Eco*RI)
SERP1774_Fw ¥	Screening of plasmid integration through upstream region (5')	CTGTTTTGCCTTCTGGTAGCTG
pBASE6-dhfR_Rv		AGTGTATTCCCAGTGGTCAGT
pBASE6-dhfR_Fw	Screening of plasmid integration through upstream region (3')	TCTTTCGACTGAGCCTTTCG
SERP1775_Rv		TCTGGCTCGGTGATACAAGG
SERP1777_Fw	Screening of plasmid integration through downstream region (5')	GCTTACGTGTTCCTACAGAAG
pBASE6_DOWN_INT_Rv		CCTCGCAGCACGATATAAAG
dhfR_Fw	Screening of plasmid integration through downstream region (3')	AAACTATCAAATTTAATGACATTATCAATAATTGTCG
SERP1778_Rv ¥		GGCGAATGTTCGTGTCAAT
pRB1775-77_Fw	Amplification of fragments for construction of plasmid p*hts*	gcggaattcgagctcggtacccggg**gatcc**CTACATCTTACGTAATAAAAATAAGAAATAAG (*Bam*HI)
pRB1775-77_Rv		gaatccaagcttgcatgcctgcagg**tcgac**TAGTTCTTATTTACCTTTAACTCAAC (*Sal*I)

¥ These oligonucleotides were used for confirmation of deletion

***** Restriction sites are underlined and in bold

Table 4.2. (continued)

Designation	Purpose	Sequence (5' - 3')*
Δ*sfaABC*		
SERP1778_UP_Fw	Amplification of fragments for construction of plasmid pB-*sfa*	cactcatcgcagtgcagcgg**aattc**CTTTGTTTGTCATTATGAACATAC (*Eco*RI)
SERP1778_UP_Rv		tagagtcgacTAGTTCTTATTTACCTTTAACTCAAC
spcR_Fw		ataagaactaGTCGACTCTAGAGGATCGATC
spcR_Rv		ctttttgattGCATGCAAATGTCACTAATATTAATAAAC
SERP1781_DOWN_Fw		atttgcatgcAATCAAAAAGCACTTGAGC
SERP1781_DOWN_Rv		gcccgggtaccgagctccgg**aattc**GAGAGTATCCGTGCTGATATC (*Eco*RI)
SERP1776_Fw ¥	Screening of plasmid integration through upstream region (5')	GGAAGCACCTGCATTCACAC
pBASE6-spcR_Rv		ACTGTTCAATAAAGCTGACCGT
pBASE6_UP_INT_Fw	Screening of plasmid integration through upstream region (3')	AGCTAGAGAGTCATTACCCCAG
SERP1778_Rv		GGCGAATGTTCGTGTCAAT
SERP1781_Fw	Screening of plasmid integration through downstream region (5')	TGGACCACTAGTGACGCAAA
pBASE6_DOWN_INT_Rv		CCTCGCAGCACGATATAAAG
spcR_2_Fw	Screening of plasmid integration through downstream region (3')	AAGATGTCGCTGCAGAATGG
SERP1784_Rv ¥		AAACCTACGCATCGCAAACC
SERP1778-81_Fw	Amplification of fragments for construction of plasmid p*sfa*	cccgccctgccactcatcgcagtgcagcgg**aattc**TTAGCACTGGGAATATATAGG (*Eco*RI)
SERP1778-81_Rv		actctagaggatccccgggtaccgagctcg**aattc**TCAATCTCTTGATGTATACCA (*Eco*RI)

¥ These oligonucleotides were used for confirmation of deletion

***** Restriction sites are underlined and in bold

Table 4.2. (continued)

Designation	Purpose	Sequence (5′ - 3′)*
Δ*fhuA*		
SERP0306_UP_Fw	Amplification of fragments for construction of plasmid pB-*fhuA*	cctgccactcatcgcagtgcagcgg**aattc**GTGGGTTATAAATATTTGAGTAAAC (*Eco*RI)
SERP0306_UP_Rv		gtctcattcaattAATAATTCCCCTACTTTCATTC
ermC_Fw		taggggaattattAATTGAATGAGACATGCTAC
ermC_Rv		taagatgttgcatGAAAACTGGTTTAAGCCG
SERP0306_DOWN_Fw		taaaccagttttcATGCAACATCTTATAAAAAAACATG
SERP0306_DOWN_Rv		cgctagcccgggtaccgagctccgg**aattc**AAGACAAGAATATAATCAAAAACTTTAC (*Eco*RI)
SERP0305_Fw ¥	Screening of plasmid integration through upstream region (5′)	CTCTGCAGGTATCAATGCA
ermC_Rv		taagatgttgcatGAAAACTGGTTTAAGCCG
pBASE6_UP_INT_Fw	Screening of plasmid integration through upstream region (3′)	AGCTAGAGAGTCATTACCCCAG
SERP0306_Rv		GCAACCTTCTTCTTCGTTGAGC
SERP0306_Fw	Screening of plasmid integration through downstream region (5′)	GTGGTGGACAAAGACAACGC
pBASE6_DOWN_INT_Rv		CCTCGCAGCACGATATAAAG
ermC_Fw	Screening of plasmid integration through downstream region (3′)	taggggaattattAATTGAATGAGACATGCTAC
SERP0308_Rv ¥		ACTGTCATGATTAATGCG
pRB0306_Fw	Amplification of fragments for construction of plasmid p*fhuA*	gtgcagcggaattcgagctcggtacccggg**gatcc**AATATCAATATATTATAAAGTTAAAAAGTTG (*Bam*HI)
pRB0306_Rv		ggtgagaatccaagcttgcatgcctgcagg**tcgac**GGCAATGTCCTCCTATTG (*Sal*HI)

¥ These oligonucleotides were used for confirmation of deletion

***** Restriction sites are underlined and in bold

Table 4.2. (continued)

Designation	Purpose	Sequence (5' - 3')*
Δ*sstABC*		
SERP0400_UP_Fw	Amplification of fragments for construction of plasmid pB-*sst*	cctgccactcatcgcagtgcagcgg**aattc**CATACTACTGATTTAAGAAAGAAAGC (*Eco*RI)
SERP0400_UP_Rv		aagagcatatttgTAGTTAATCTCCTTGCTAAATATTAAAG
tetM_Fw		aggagattaactaCAAATATGCTCTTACGTGCTATTATT
tetM_Rv		tcttattataagaAAATATTGAAGGCTAGTCAGTAAAATTC
SERP0403_DOWN_Fw		gccttcaatatttTCTTATAATAAGAGAAAATCAACCG
SERP0403_DOWN_Rv		cgctagcccgggtaccgagctccgg**aattc**ATTCATGAATGCTGGTGC (*Eco*RI)
SERP0398_Fw ¥	Screening of plasmid integration through upstream region (5')	AAATGTGGGTGGAAACAG
tetM_INT_Rv		ATTATTTGTTCCCGCTATC
pBASE6_UP_INT_Fw	Screening of plasmid integration through upstream region (3')	AGCTAGAGAGTCATTACCCCAG
SERP0400_Rv		GCCCACTCCATAGTACCAGC
SERP0403_Fw	Screening of plasmid integration through downstream region (5')	CAACGTTTGGACCAGGAGGA
pBASE6_DOWN_INT_Rv		CCTCGCAGCACGATATAAAG
tetM_INT_Fw	Screening of plasmid integration through downstream region (3')	TAACAATCAAAGAGCCAGAC
SERP0405_Rv ¥		ACTTATTTAGGAAATGGGTC
pRB0400-3_Fw	Amplification of fragments for construction of plasmid p*sst*	gtgcagcggaattcgagctcggtacccggg**gatcc**TATAGTACTTTTAAAGAGATTTCTATTAAAATT (*Bam*HI)
pRB0400-3_Rv		ggtgagaatccaagcttgcatgcctgcagg**tcgac**TTATTTTTCAACTTTCTCTACTACTTC (*Sal*HI)

¥ These oligonucleotides were used for confirmation of deletion

***** Restriction sites are underlined and in bold

4.2.5. Quantification of bacterial iron content

2 mL of cultures grown overnight in TSB (BD) were harvested by centrifugation at 5000*g*, for 10 min at 4°C. Cells were washed twice in ultrapure water and diluted into CDM_{Fe-} to an OD_{640} of 0.025 (~10^7 CFU/mL) in disposable plastic tubes. Chloramphenicol was added to the growth medium of the plasmid-bearing strains for plasmid maintenance. Cultures were incubated at 37°C, 120 rpm (ES-20 Shaker-Incubator) for 24 h. Afterwards, cultures were harvested by centrifugation at 5000*g*, for 10 min at 4°C and the pellet washed thrice with metal-free ultrapure water to remove salts.

Samples were then assayed for intracellular iron content by the scientific staff at Departamento de Engenharia Química - Instituto Superior de Engenharia do Porto (DEQ-ISEP, Polytechnic of Porto, Portugal). Bacterial samples were homogenized and dispersed in ultrapure water were placed in previously weighed Teflon vessels (MS105, Mettler Toledo, Switzerland), and then dried in an oven at 90°C (P Selecta, Barcelona, Spain) until three reproducible weight values were obtained. Microwave-assisted digestion of samples was performed by adding 10 mL of Suprapur® nitric acid 65% (v/v) (Merck) to each vessel containing the dried and accurately weighed samples. The microwave-assisted digestion proceeded accordingly with the steps described in **Table 4.3**, using a Mars-X 1500 W (Microwave Accelerated Reaction System for digestion and extraction, CEM Mathews, NC, USA), configured with a 14-position carousel and equipped with pressure and temperature sensors. After digestion, and cooling to approximately 30°C, samples were kept frozen in polycarbonate containers at -20°C until analysis.

Table 4.3. Microwave conditions for the digestion of bacterial samples

Ramp/ min	Pressure/ Psi	Temperature/ ºC	Hold/ min
5:00	150	50	10:00
10:00	200	100	10:00
10:00	200	140	15:00

Iron quantification was carried out using an Analytik Jena ContrAA 700 High-Resolution Continuum Source Flame Atomic Absorption Spectrometer (Analytik Jena, Jena, Germany) equipped with a xenon short-arc lamp XBO 301 (GLE, Berlin, Germany) with a nominal power of 300 W operating in a hot-spot mode as a continuum radiation source. Iron was analyzed at 248.3270 nm by using the Graphite Furnace module equipped with an MPE60 autosampler (Analytik Jena) and argon 5.0 purity grade (Linde, München, Germany) as the inert gas. Transversal and pyrolytically coated graphite tubes with integrated

platforms were used. In order to obtain maximum absorbance and minimum background values, operational parameters were optimized and are presented in **Table 4.4**.

Table 4.4 Optimized operational parameters for the graphite furnace analysis of iron

Step	Name	Temperature/ ºC	Ramp/ ºC/s	Hold/ s	Time/ s
1	Drying	80	6	20	26.7
2	Drying	90	3	20	23.3
3	Drying	110	5	10	14.0
4	Pyrolysis	350	50	20	24.8
5	Pyrolysis	1100	300	10	12.5
6	Gas adaptation	1100	0	5	5.0
7	Atomize	2000	1500	4	4.6
8	Clean	2450	500	4	4.9

External calibration curves were daily constructed based on, at least, six standard solutions of iron prepared from 1000 mg/L stock solutions (Panreac Quimica SA, Barcelona, Spain). Magnesium nitrate hexahydrate (traceable to SRM from NIST; Merck) was used as a matrix modifier at 0.1% (w/v). All glassware and plastic material were soaked in nitric acid (50% v/v), thoroughly rinsed with ultrapure water and dried before use. The instrument performance was checked using analytical blanks and standards analyzed daily and regularly along with samples. All measurements were performed, at least, in triplicate. Results were normalized to the cell dry weight.

4.2.6. Transmission electron microscopy (TEM)

TEM experiments were performed by the "Histology and Electron Microscopy" scientific staff at Instituto de Investigação e Inovação em Saúde (I3S, University of Porto, Portugal). Cell pellets were prepared as described in section **4.2.5**. Samples were then fixed overnight with 2.5% (w/v) glutaraldehyde/ 2% (w/v) paraformaldehyde in cacodylate buffer 0.1 M (pH 7.4). Samples were washed in 0.1 M sodium cacodylate buffer and fixed in 2% (w/v) osmium tetroxide in the 0.1 M sodium cacodylate buffer overnight, followed by new fixation in 1% (w/v) uranyl acetate overnight. Dehydration was performed in gradient series of ethanol solutions and propylene oxide and included in EPON™ resin by immersion of samples in increasing series of propylene oxide to EPON™ (till 0:1 ratio) for 60 min each. Sample inclusion in EPON™ resin was performed in a silicon mold. Sections with 60 nm thickness were prepared on a RMC Ultramicrotome (PowerTome, USA) using a diamond knife and recovered to 200 mesh Formvar Ni-grids, followed by 2% (w/v) uranyl acetate and saturated lead citrate solution. Visualization was performed at 80 kV in a JEM

1400 microscope (JEOL, Japan) and digital images were acquired using a CCD digital camera Orious 1100 W (Tokyo, Japan).

4.2.7. Detection of siderophore production

Bacterial cultures were prepared as described in section **4.2.5**, except that the incubation period in CDM_{Fe-} was 72 h. Afterwards, cultures were harvested by centrifugation at 5000*g*, for 10 min at 4°C. Culture supernatants were collected and filter-sterilized (pore size 0.2 µm) for analysis of siderophore production using a modified Chrome Azurol S (CAS) agar diffusion assay as described previously (25). CAS agar plates were prepared as follows: firstly, 60.5 mg CAS (Sigma-Aldrich) were dissolved in 50 mL of ultrapure water, and mixed with 10 ml iron (III) solution (1 mM mM $FeCl_3.6H_2O$, 10 mM HCl); this solution was slowly mixed under stirring with 72.9 mg hexadecyltrimethylammonium (HDTMA) dissolved in 40 mL ultrapure water, resulting in a dark blue solution; this solution was autoclaved and mixed with an autoclaved mixture of 900 mL ultrapure water, 15 g of agar, 30.24 g of piperazine-N,N′-bis(2-ethanesulfonic acid) (PIPES), and 12 g of a solution of 50% (v/v) NaOH to raise the pH to the pKa of PIPES (6.8); lastly, the mixture was poured onto Petri dishes and stored in a refrigerator until further use. For detection of siderophore production, holes were created in CAS agar plates by using a 1 mL micropipette tip. Each hole was filled with 200 µL of culture supernatant. CDM_{Fe-} was used as negative control. After incubation of the plate at 37°C for 24 h, the formation of an orange halo around each hole was indicative of siderophore presence in the supernatant.

4.2.8. Planktonic growth curves

1457 WT and mutant strains were tested for the ability to grow in iron-deficient conditions using CDM_{Fe-} as culture medium. To that end, 2 mL of cultures grown overnight in TSB (BD) were harvested by centrifugation at 5000*g*, for 10 min at 4°C. Cells were washed twice in Millipore-filtered water and diluted into CDM_{Fe-} to an OD_{640} of 0.025 (~10^7 CFU/mL) in a conical glass flask. Chloramphenicol was added to the growth medium of the plasmid-bearing strains for plasmid maintenance. Flasks were incubated at 37°C, 120 rpm (ES-20 Shaker-Incubator). OD_{640} was measured hourly up to 8 h and at 24 h of incubation (when appropriate, concentrated samples were diluted in CDM_{Fe-} for accurate measurement). At least three independent experiments were performed for each condition tested.

4.2.9. Biofilm formation assays

Biofilms were grown either on 96-well microplates made of polystyrene plastic (Orange Scientific, Braine-l'Alleud, Belgium) for quantification of biofilm biomass, or on Lab-Tek® Chamber Slide™System 8 Well Permanox® Slides (Thermo Fisher Scientific Inc.) for confocal microscopy analysis. Cultures were prepared as described above, diluted into CDM_{Fe-} to an OD_{640} of 0.25 (~10^8 CFU/mL) and further diluted 1:100 into (i) CDM_{Fe-}; (ii) CDM_{Fe+}; or (iii) TSB. Afterwards, diluted bacterial suspensions were placed into the microplates/ chamber slides and incubated for 24 h at 37°C under static conditions.

4.2.10. Quantification of biofilm biomass

Performed as described in section **3.2.3.**

4.2.11. CLSM analysis

Performed as described in section **3.2.6.**

4.2.12. Sequence analysis

Sequences of the putative iron-related genes (previously studied in Chapter 3) were retrieved from *S. epidermidis* RP62A (NCBI accession no. NC_002976) and queried against *S. epidermidis* 1457 (NCBI accession no. CP020463) to search for homologous genes using BLASTn tool (26). Alignments of the respective amino acid sequences and putative Fur boxes were performed with ClustalX version 2.1 (27).

4.2.13. Statistical analysis

Statistical analysis was performed with GraphPad Prism version 7.0a (La Jolla, CA, USA). For comparisons among different groups, two-away ANOVA with multiple comparisons test was used. A $p < 0.05$ was considered statistically significant.

4.3. Results

4.3.1. *Homology and transcriptional analysis*

Prior to genetic manipulations, a homology analysis was performed to ensure that the iron acquisition genes identified in RP62A are present in 1457 and follow the same organization (**Figure 4.2**). Putative Fur boxes were also identified in 1457 genome in the same locations previously demonstrated in RP62A. For simplification purposes, all genes in study were provisionally named after their respective homologs in *S. aureus* (**Table 4.5**).

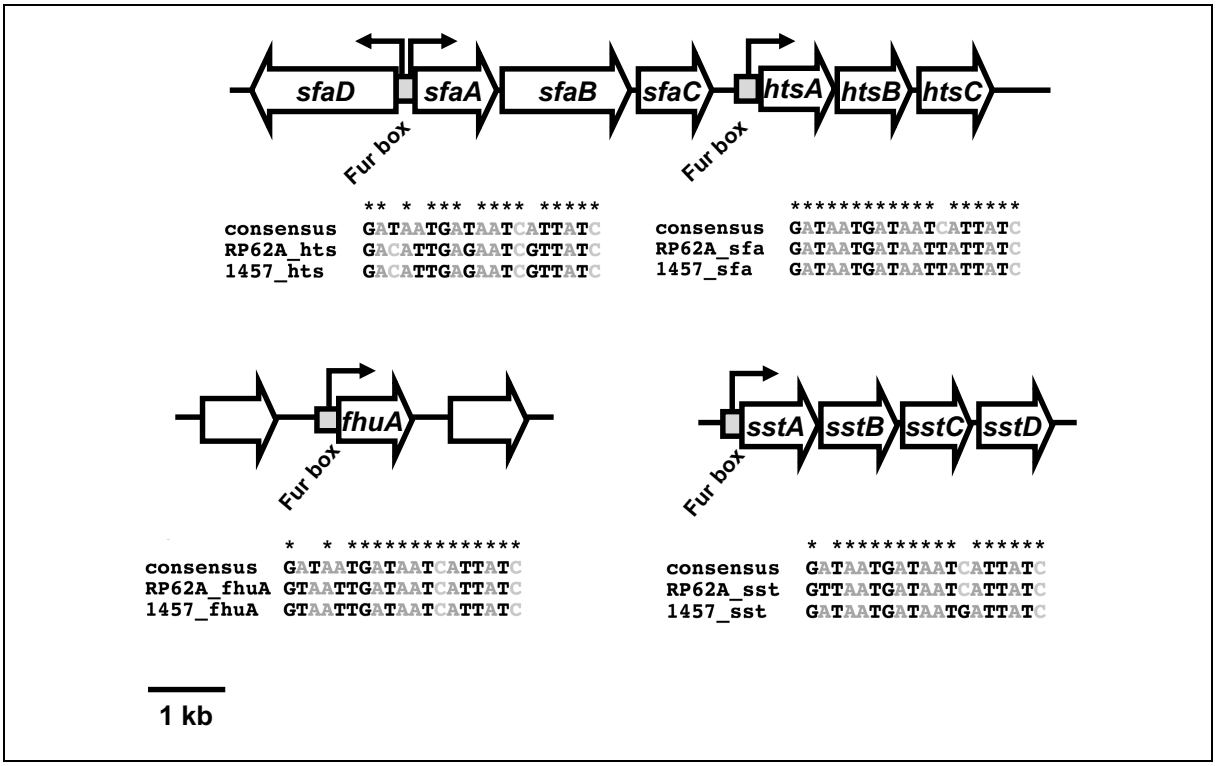

Figure 4.2. Genomic organization of different iron acquisition genes within *S. epidermidis*. Assignments are based on the annotated genomes of *S. epidermidis* RP62A (NC_002976) and 1457 (CP020463) strains. Open reading frames are indicated by arrows, which show the direction of transcription. Predicted transcriptional start sites are indicated by bent arrows. Putative Fur boxes are shown as grey boxes and alignments of their nucleotide sequences are provided below.

Table 4.5. Nomenclature adopted for the genes studied in this chapter

Locus tag in RP62A	Locus tag in 1457	Gene name
SERP1775	*B4U56_03575*	*htsC*
SERP1776	*B4U56_03570*	*htsB*
SERP1777	*B4U56_03565*	*htsA*
SERP1778	*B4U56_03560*	*sfaC*
SERP1779	*B4U56_03555*	*sfaB*
SERP1780	*B4U56_03550*	*sfaA*
SERP1781	*B4U56_03545*	*sfaD*
SERP0306	*B4U56_10485*	*fhuA*
SERP0400	*B4U56_10035*	*sstA*
SERP0401	*B4U56_10030*	*sstB*
SERP0402	*B4U56_10025*	*sstC*
SERP0403	*B4U56_10020*	*sstD*

Alignment of the respective amino acid sequences showed that all proteins are highly conserved between both strains (**Figure 4.3**). Additionally, transcription of selected genes (*htsC* and *sfaC*) in 1457 was studied and confirmed to be iron-regulated, as observed for RP62A (**Table 4.6**).

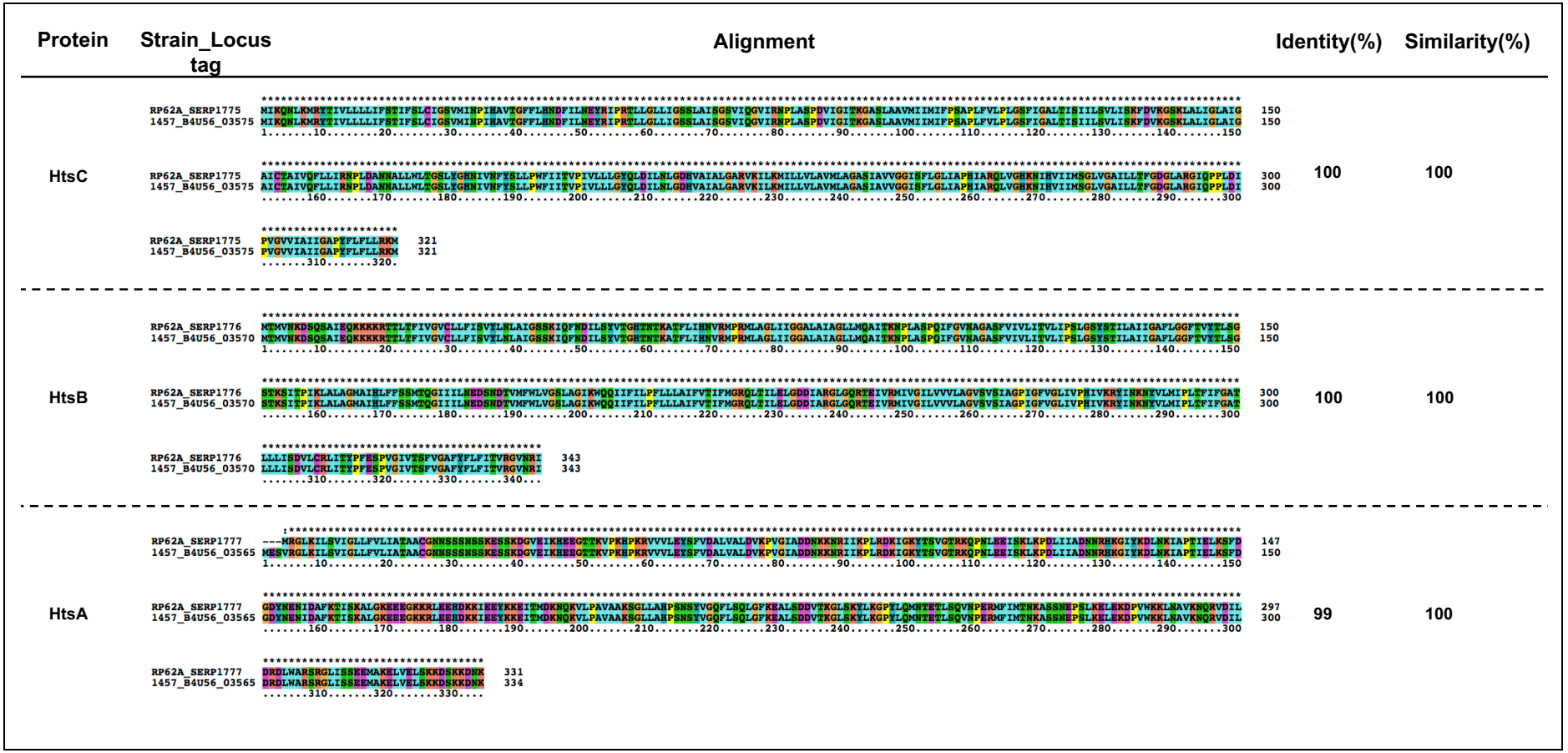

Figure 4.3. Sequence alignment of putative iron-related proteins from RP62A and homologous proteins in 1457.

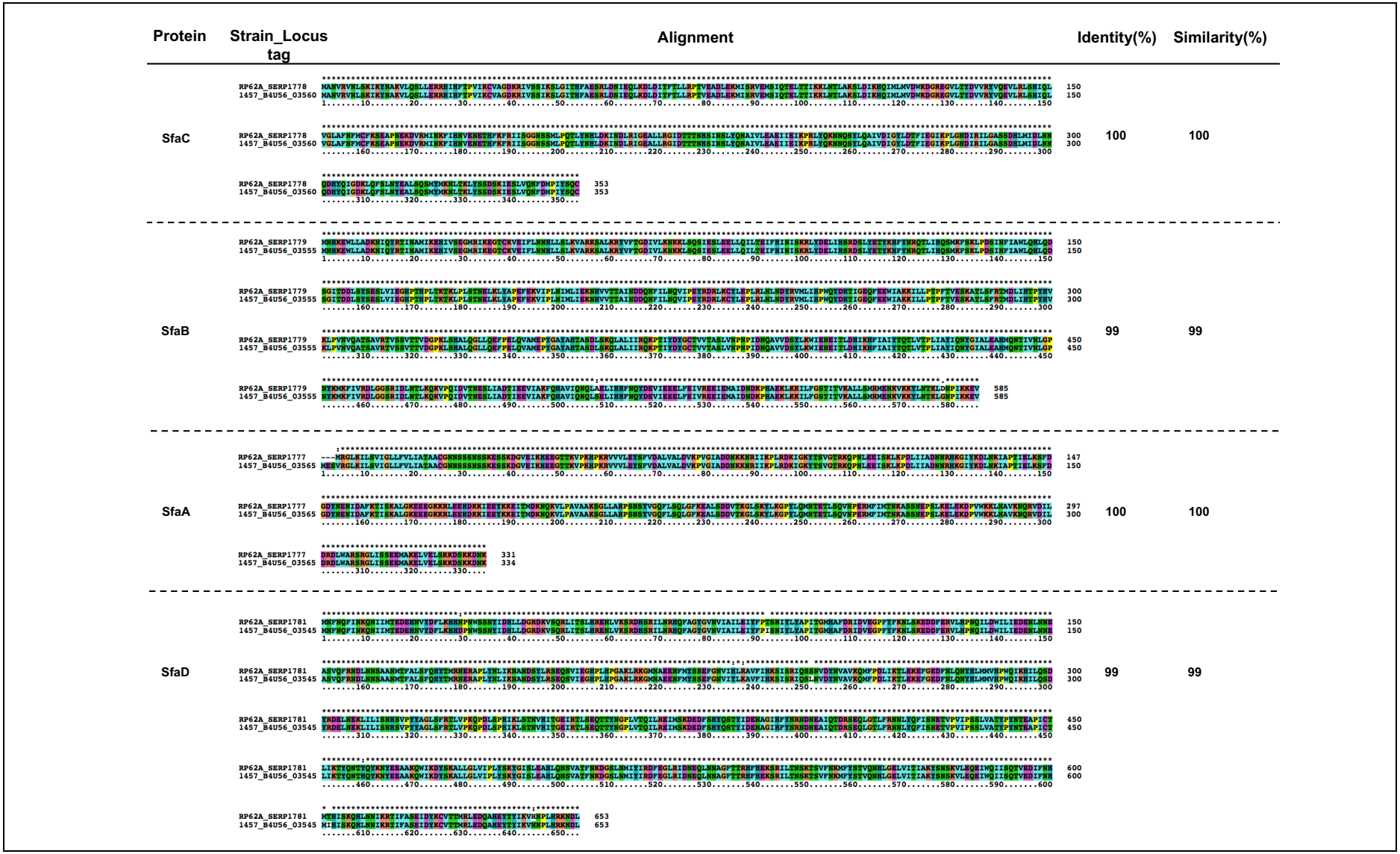

Figure 4.3. (continued).

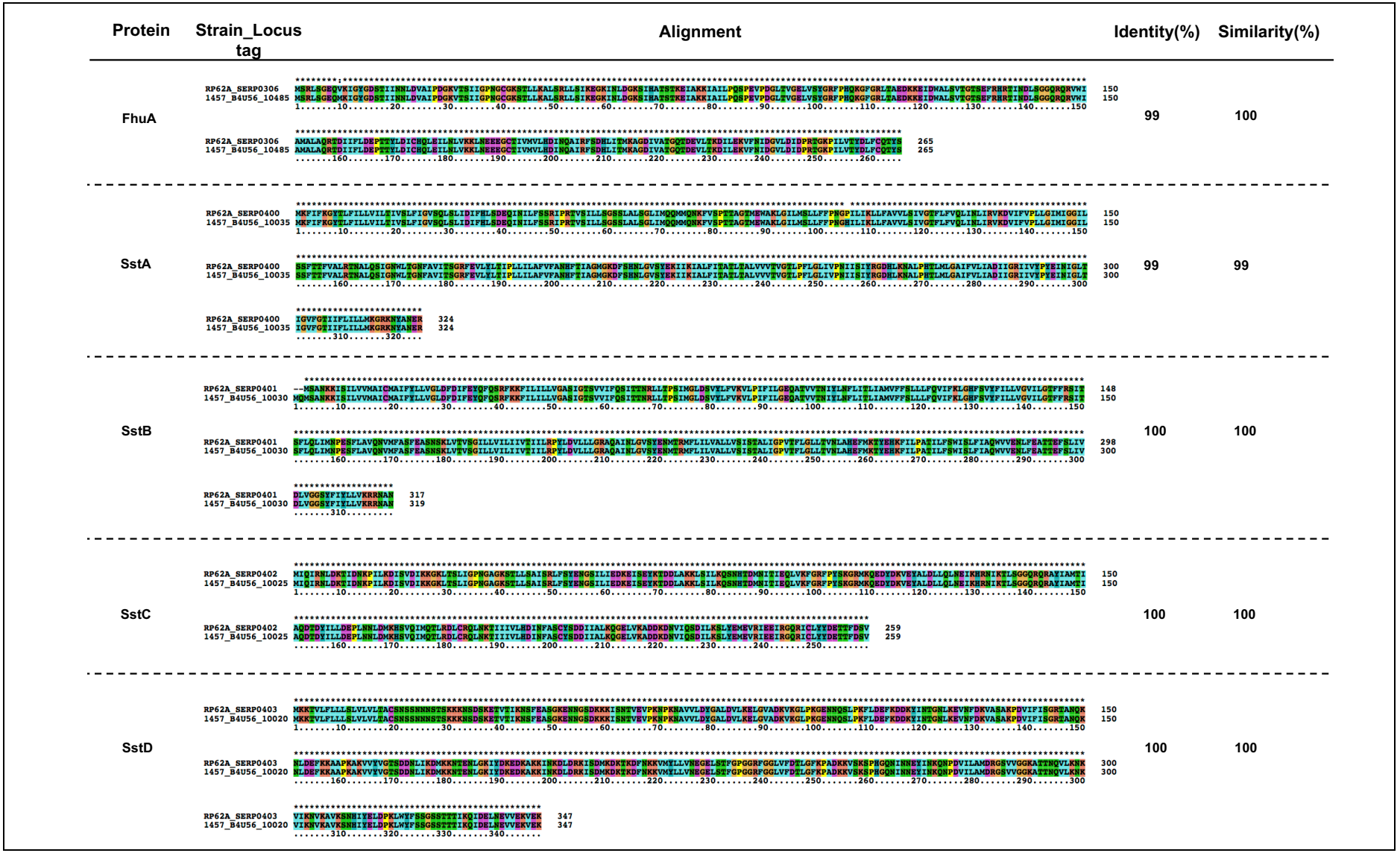

Figure 4.3. (continued).

Table 4.6. Effect of iron availability on the transcription of putative iron-related genes in strains RP62A and 1457

Process	Gene	Putative function	RP62A			1457		
			Fe+	Fe-	*p* value*	Fe+	Fe-	*p* value*
Siderophore uptake (ABC transporter)	*htsC*	Permease	0,366	1,588	**0,00003**	4,254	4,396	0,35950
Siderophore biosynthesis	*sfaC*	Amino-acid racemase	0,867	1,705	**0,00043**	3,234	4,810	**0,00001**

Biofilms were allowed to grow in TSB_6 (control condition) or TSB_6 containing 1 mM $FeCl_3$ (Fe+) or 1 mM Bip (Fe-) for transcription analysis by quantitative PCR (qPCR). Data are represented as average fold changes from two independent RNA extractions. Values above and below 0 indicate up- and down-regulation of transcription, respectively, in comparison to the control condition (TSB_6);

*Two-away ANOVA with multiple comparisons test was used to detect differences in transcription between Fe+ and Fe- conditions. $p < 0.05$ was considered statistically significant (significant differences depicted in bold).

4.3.2. Biofilm formation by strain 1457 is modulated by iron availability

An important factor to bear in mind when studying bacteria is the intra-species genomic and physiological variability (28,29), something that has been acknowledged for *S. epidermidis* and other CoNS species (30). To confirm that iron availability modulates biofilm formation in strain 1457 in the same manner as observed with other isolates (**Chapter 3**, section **3.3.1**), biofilm formation experiments were performed under iron-enriched and iron-deficient conditions. As shown in **Figure 4.4**, a similar effect was observed for strain 1457, suggesting that the effect of iron availability over biofilm formation is conserved across different *S. epidermidis* strains.

After these confirmatory experiments, deletion mutant strains were obtained by following an allelic replacement strategy using 1457 as the parental strain (**Figure 4.5**).

4.3.3. The **sfaABCD** *locus mediates siderophore biosynthesis and is important for growth under iron restriction*

As demonstrated in **Chapter 3**, *sfaABCD* genes are transcribed under iron-restricted conditions and encode products that share homology with siderophore biosynthesis-related proteins. Therefore, the hypothesis was tested that the *sfa* locus is involved in siderophore biosynthesis.

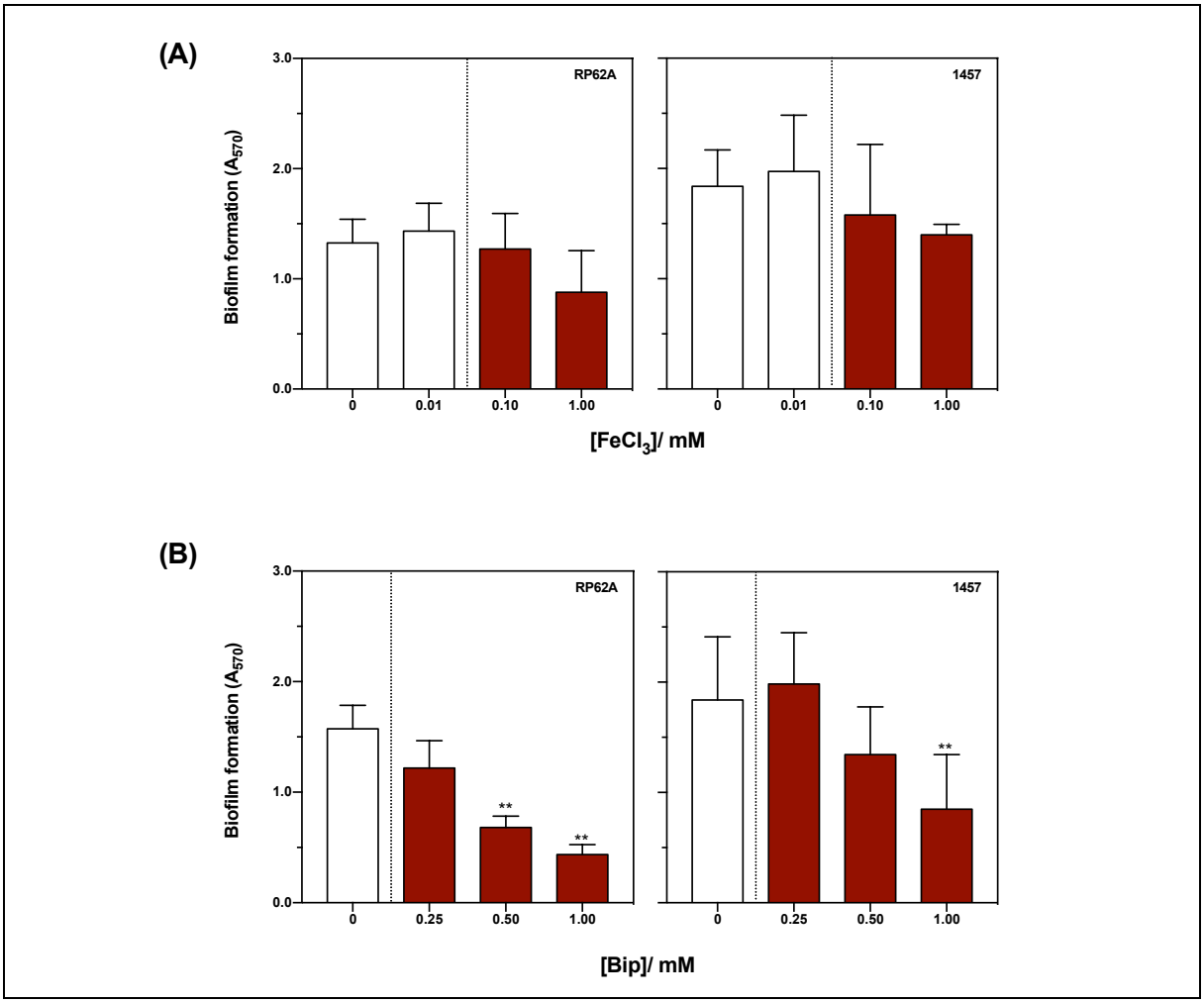

Figure 4.4. General effect of iron availability on biofilm formation in *S. epidermidis* strain 1457. Biofilms of *S. epidermidis* strains RP62A and 1457 were allowed to grow on 96-well microtiter plates for 24 h at 37°C in TSB_6 containing increasing concentrations of **(A)** $FeCl_3$ and **(B)** Bip. Experimental conditions with iron concentrations out of the physiologic range are represented by red bars. Biofilms were stained with crystal violet and quantified at A_{570}. Data are represented as mean ± standard deviation of three independent assays. Significant differences are depicted with: ** $p < 0.01$.

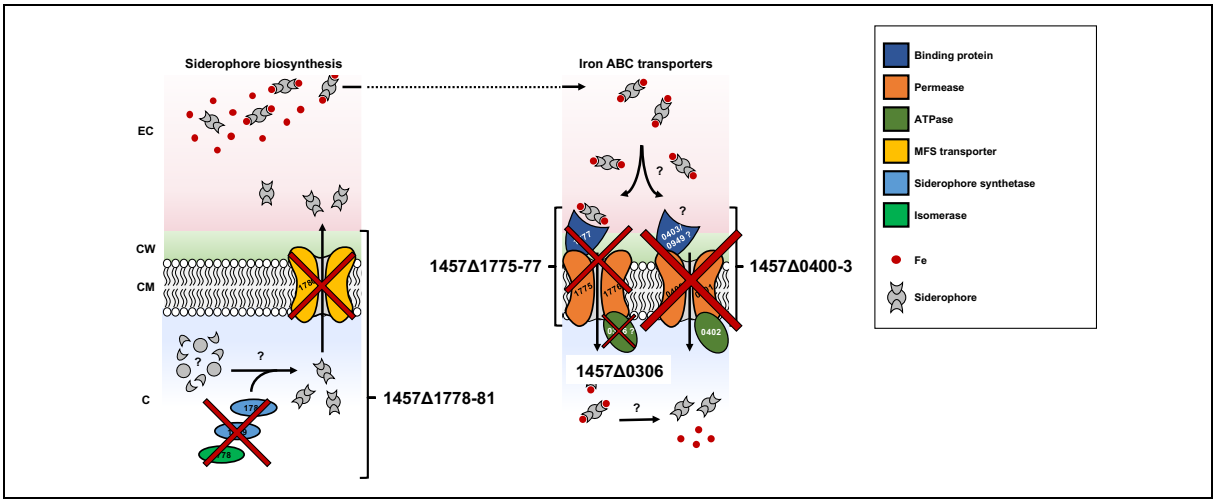

Figure 4.5. Model depicting the iron acquisition systems that were deleted through allelic replacement in *S. epidermidis* 1457. C, cytoplasm; CM, cell membrane; CW, cell wall; EC, extracellular space; MFS, Multiple Facilitator Superfamily.

Strains WT, Δ*sfa* and Δ*sfa* p*sfa* were cultured under iron-deficient conditions (CDM_{Fe-}) to induce siderophore production, and culture supernatants were assayed for the presence of siderophore (**Figure 4.6A**). Unlike the WT, Δ*sfa* was completely unable to secrete siderophore to the culture supernatant. This phenotype was fully reversed by complemented expression of *sfa* (Δ*sfa* p*sfa*). Of note, the slight yellow hallo observed for Δ*sfa* was also observed for the negative control (CDM_{Fe-}), which might have been the result of some medium components known to chelate iron, such as phosphates (31).

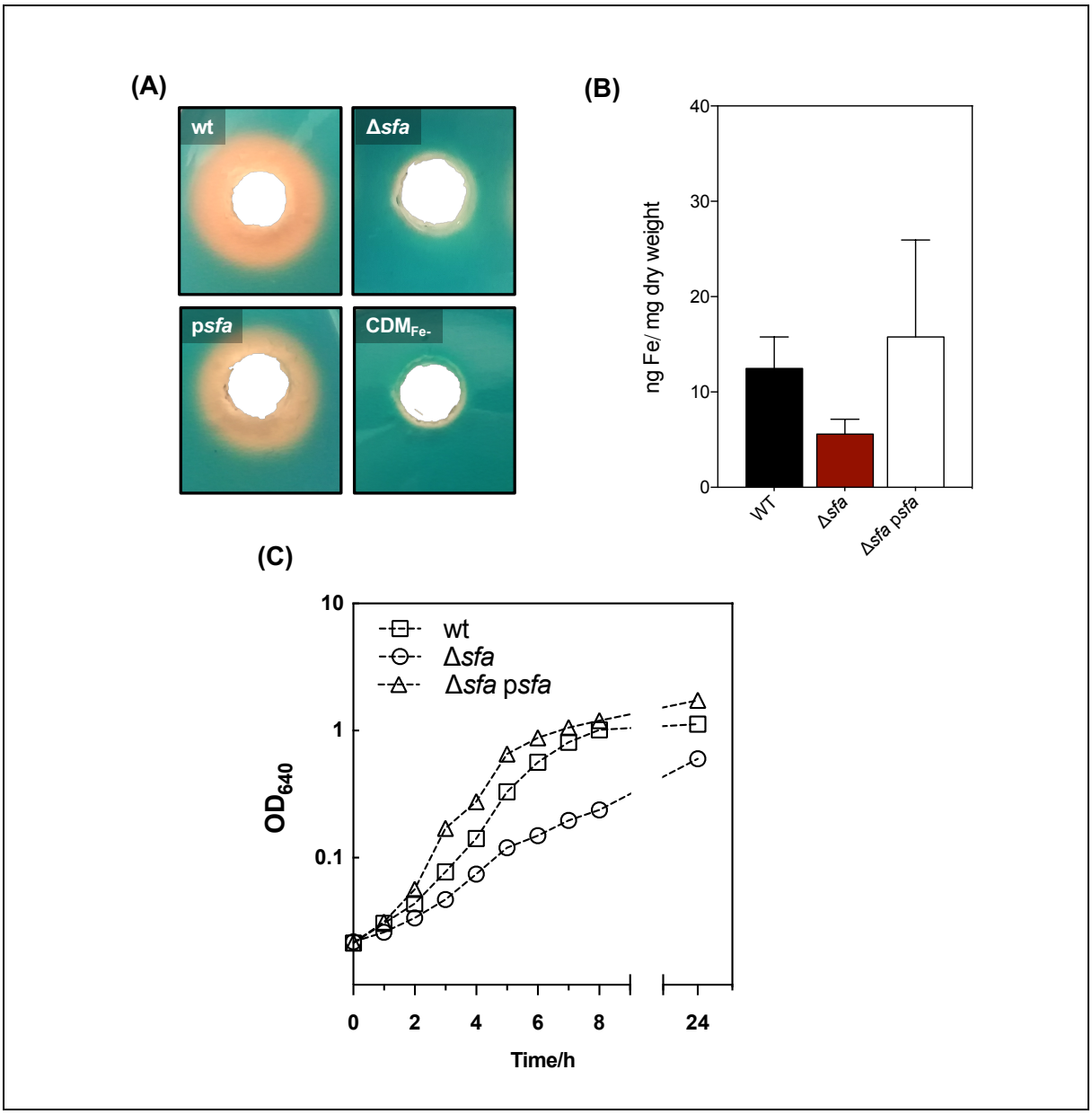

Figure 4.6. Effect of deletion of the *sfaABCD* locus on siderophore production, iron uptake and growth under iron-deficient conditions. **(A)** 1457 WT, deletion mutant Δ*sfa* and complemented strain Δ*sfa* p*sfa* were grown in CDM_{Fe-} for 72 h at 37°C and the culture supernatants were tested for siderophore production using a modified CAS agar diffusion assay. The formation of an orange halo around each hole was indicative of siderophore presence in the supernatant. **(B)** Iron contents in wt, Δ*sfa* and Δ*sfa* p*sfa* as analyzed by atomic absorption spectroscopy. **(C)** Strains were allowed to grow for 24 h at 37°C, 120 rpm in CDM_{Fe-}. Data are representative of three independent assays.

Since deletion of *sfa* had a dramatic effect on siderophore production, it would be expected that the total iron content for the mutant strain was also affected. Compared with the WT strain, Δ*sfa* revealed a lower iron content, although not statistically significant. *in trans* gene complementation (Δ*sfa* p*sfa*) resulted in the reestablishment of the cell iron content (**Figure 4.6B**).

Lastly, growth assays on iron-restricted medium demonstrated that deletion of *sfa* locus impaired growth rate, particularly during the first 8 h of growth (**Figure 4.6C**). Conversely, the complemented expression of *sfa* (Δ*sfa* p*sfa*) restored and even enhanced bacterial growth when compared to WT.

4.3.4. Deletion of different putative iron ABC transporter genes has different outcomes on S. epidermidis *growth under iron-deficient conditions*

The *htsABC* locus is predicted to encode components (substrate binding and permease proteins) of a siderophore ABC transporter, which is supported by its close proximity to the *sfa* siderophore biosynthetic genes, as well as experimental studies on its *S. aureus* homolog (32). *S. epidermidis* mutant strain carrying a deletion of the *htsABC* genes exhibited a slower growth rate under iron-restricted conditions during the first 8 h, but eventually achieved a cell density similar to WT strain after 24 h (**Figure 4.7A**).

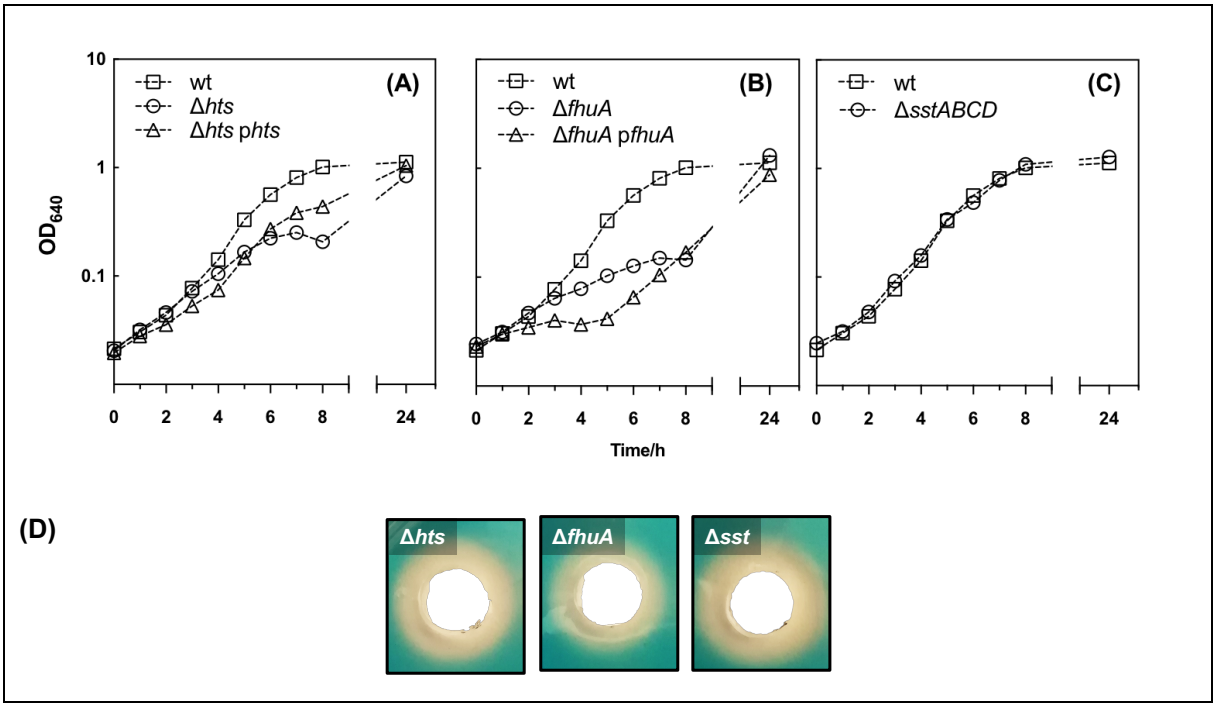

Figure 4.7. Effect of deletion of different iron ABC transporter components on the growth of *S. epidermidis* under iron-restricted conditions. WT, mutants, and complemented strains (**A**, *htsABC*; **B**, *fhuA*; **C**, *sstABCD*) were allowed to grow for 24 h at 37°C, 120 rpm in CDM_{Fe-}. Data are representative of three independent assays. **(D)** The presence of siderophore in the culture supernatants of the mutant strains was assayed by the modified CAS method described above**.**

Deletion of *fhuA*, which is predicted to encode the missing ATP-binding protein of the HtsABC transporter, had a similar effect (**Figure 4.7B**). On the other hand, deletion of the *sstABCD* locus, whose *S. aureus* homolog has been described as a putative siderophore transporter (33), had no detectable effect on *S. epidermidis* growth under iron-restricted conditions (**Figure 4.7C**). The complemented expression of *hts* (Δ*hts* p*hts*) and *fhuA* (Δ*fhuA* p*fhuA*) partly restored the bacterial growth defect exhibited by the respective mutants. At the time these experiments were performed, Δ*sst* complemented strain (Δ*sst* p*sst*) had not yet been constructed. The strain was obtained later and will be tested in a near future. None of the mutations had any effect in the production of siderophore (**Figure 4.7D**). Quantification of iron content for these mutants is an ongoing work.

4.3.5. Different iron uptake systems are pivotal for S. epidermidis *biofilm formation under iron restriction conditions*

In **Chapter 3** it was demonstrated that iron restriction is detrimental for biofilm formation by *S. epidermidis*, even though it is still capable to grow planktonically. To dissect the individual contribution of each iron acquisition system on biofilm formation, strains were tested for biofilm formation under different iron availability conditions (**Figure 4.8**).

When bacteria were grown in TSB, an iron-rich culture medium, Δ*sfa,* Δ*hts* and Δ*fhuA* were able to form as much biofilm as the WT strain. Conversely, biofilm formation by these strains was markedly lower when an iron-deficient medium (CDM_{Fe-}) was used, especially by the siderophore-deficient strain Δ*sfa*. This effect was partially or fully reversed either by *in trans* gene complementation or by supplementing CDM_{Fe-} with 10 μM $FeCl_3$ (CDM_{Fe+}). Surprisingly, biofilm formation by Δ*sst* mutant strain was not affected under iron-restricted conditions, but was somewhat impaired under iron-enriched conditions, especially when cultured on TSB. As for the growth experiments, the Δ*sst* complemented strain (Δ*sst* p*sst*) was not available at the time biofilm experiments were performed and will be tested in a near future.

Biofilms formed by these strains under iron-restricted conditions were further examined through CLSM for the assessment of biofilm organization and the PIA/PNAG content in the biofilm matrix (**Figure 4.9**). While WT and Δ*sst* formed thick biofilms containing a high density of cells widespread across the surface and high amounts of PIA/PNAG, Δ*sfa,* Δ*hts* and Δ*fhuA* formed sparse biofilms mostly composed of cell clusters embedded in small amounts of PIA/PNAG. Gene complementation reversed the biofilm phenotype of all mutant strains.

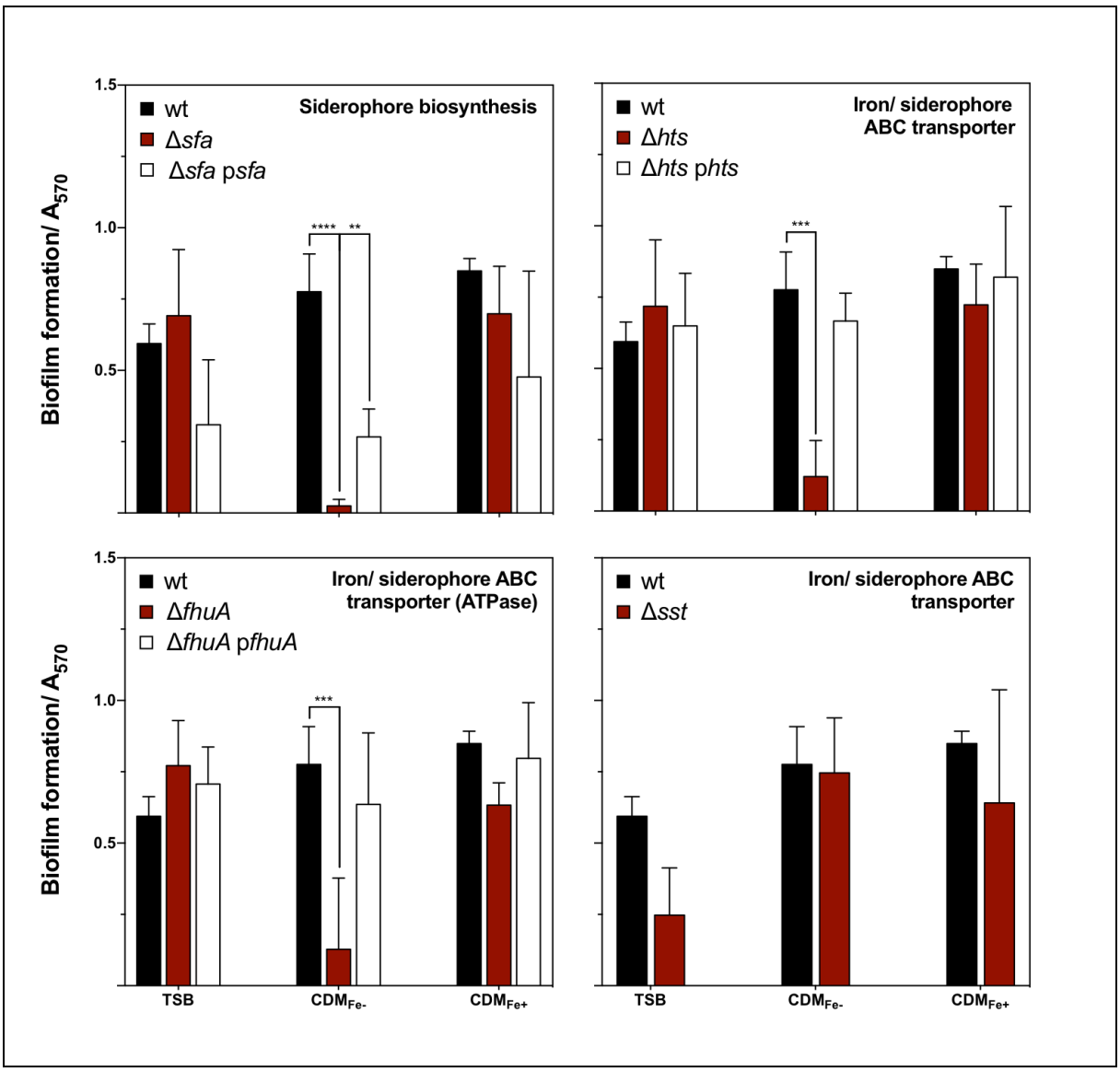

Figure 4.8. Effect of the deletion of different iron acquisition systems on *S. epidermidis* biofilm formation. Strains were allowed to grow statically for 24 h at 37°C on 96-well microplates. Biofilm quantification was performed through crystal violet staining. Data are represented as mean ± standard deviation of three independent assays. TSB, Tryptic Soy Broth; CDM_{Fe-}, Chemically Defined Medium without added iron; CDM_{Fe+}, Chemically Defined Medium supplemented with 10 µM $FeCl_3$. Putative function of each gene/ locus is indicated above the corresponding graph. Significant differences are depicted with: ** $p < 0.01$; *** $p < 0.001$; **** $p < 0.0001$.

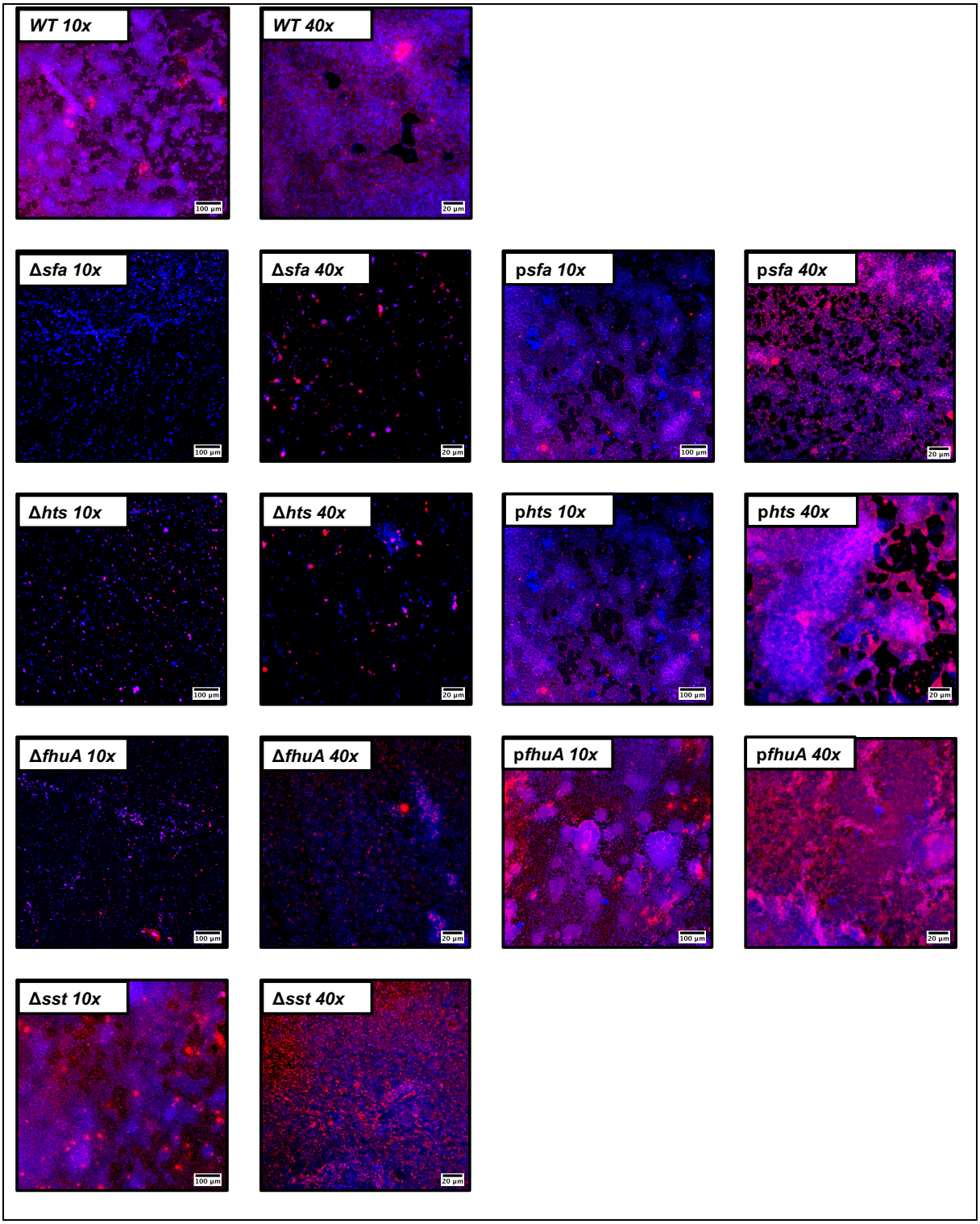

Figure 4.9. CLSM analysis of biofilms formed by different iron acquisition deletion mutants under iron-restricted conditions. Biofilms were allowed to grow on an 8-well chamber slide system in CDM_{Fe-} at 37°C for 24 h. CLSM was used for biofilm structure analysis and PIA/PNAG production after appropriate staining with DAPI (depicted in blue) and WGA-Texas Red (depicted in red). Representative images of Z-stack projections from two independent experiments are shown (scale bars, 100 μm for 10×; 20 μm for 40×).

4.3.6. Deletion of iron acquisition systems induces alterations in the cell wall thickness and ultrastructure

Investigation of WT and mutant strains grown under iron-restricted conditions using TEM demonstrated some interesting features (**Figure 4.10**). WT and Δ*sst* exhibited a cytoplasm with an uneven electron density, a cytoplasm membrane tightly adhered to the cell wall, and a uniform cell wall thickness. Δ*sfa* displayed a wrinkled cytoplasm and an apparent loss of cellular material, although no significant increase in the cell wall thickness was observed. Regarding Δ*hts* and Δ*fhuA,* the most prominent changes were a higher number of dividing cells and also a significant increase in the cell wall thickness ($p < 0.001$) (**Figure 4.11**).

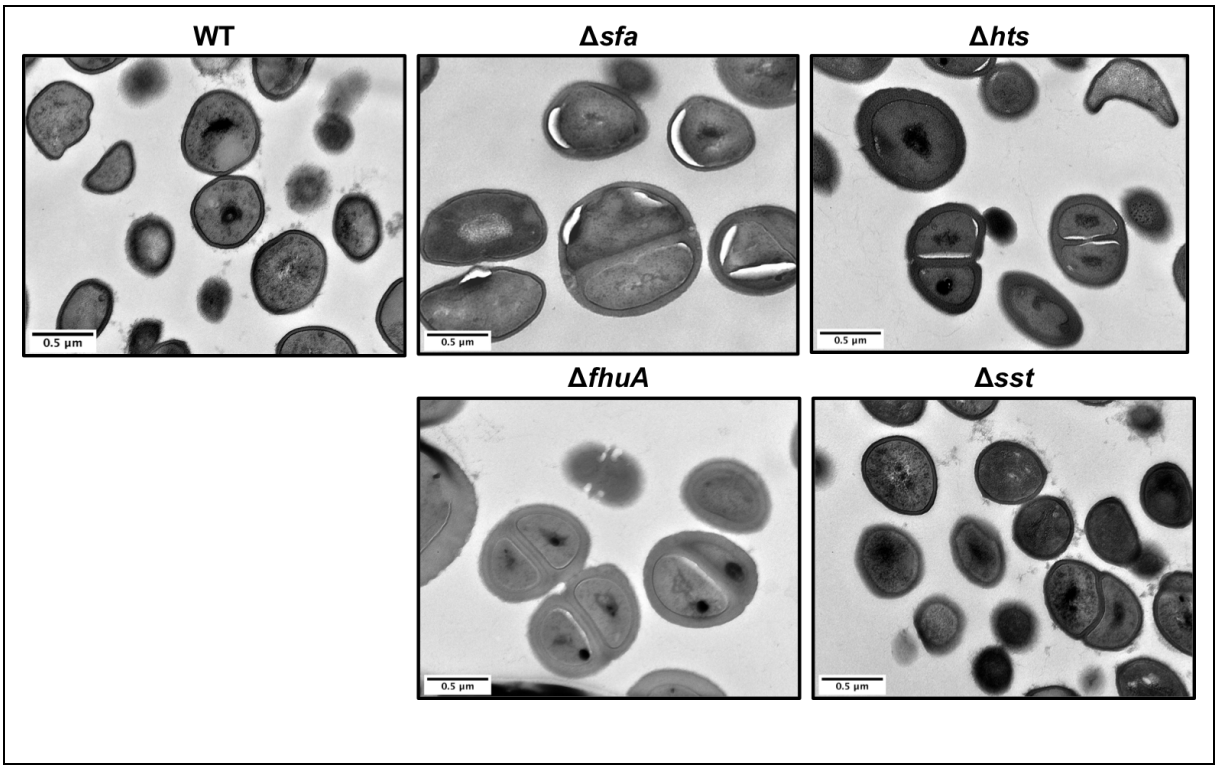

Figure 4.10. Representative TEM images of WT and deletion mutants grown under iron-restricted conditions (scale bar, 0.5 µm).

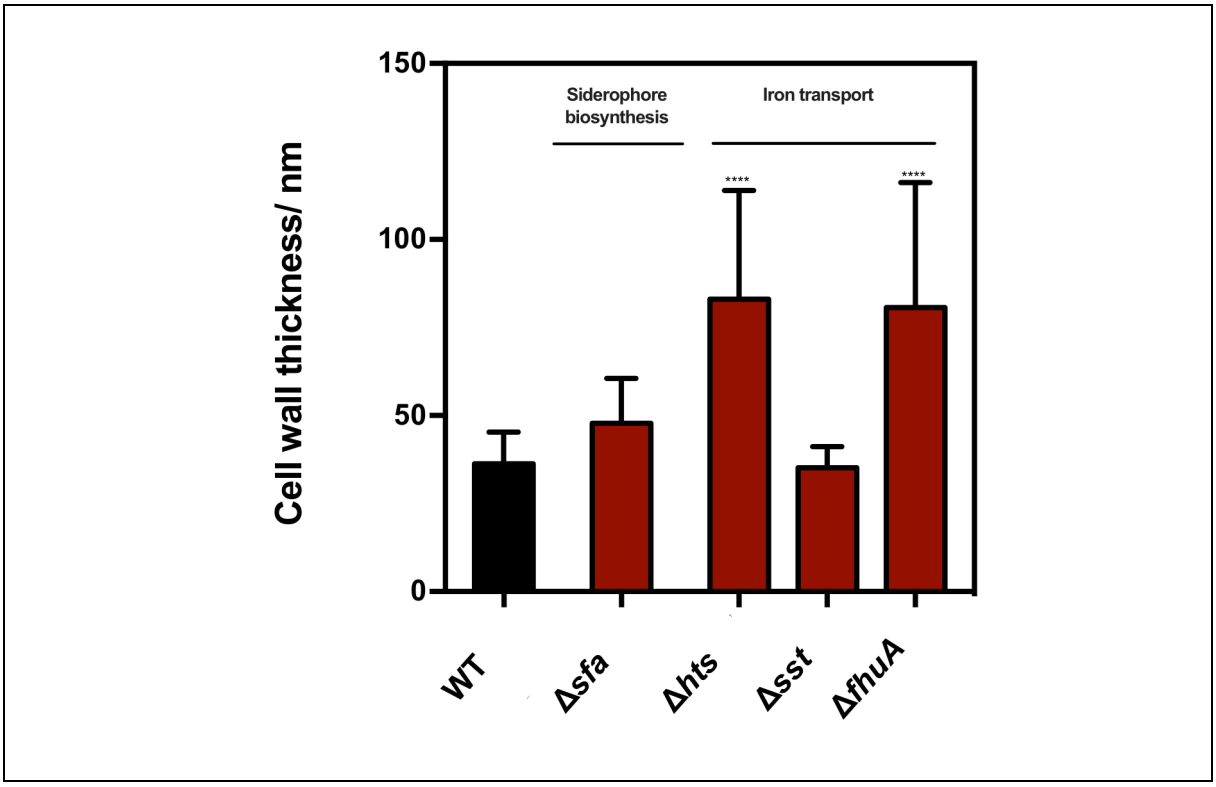

Figure 4.11. Effect of the deletion of different iron acquisition systems on the cell wall thickness. Data are represented as mean ± standard deviation of 50 measurements per cell, $N = 20$ cells. Significant differences in comparison with the WT strain are depicted with: **** $p < 0.0001$.

4.4. Discussion

The importance of iron acquisition systems for bacteria, especially those involving siderophores, has been extensively reviewed in **Chapter 2**. **Chapter 3** describes the identification of a group of four loci in *S. epidermidis* genome putatively involved in iron acquisition processes and demonstrated that their transcription is iron-regulated. In the present chapter it was attempted to dissect the individual role of these loci in the adaptation of *S. epidermidis* to iron restriction by following an allele replacement approach in *S. epidermidis* 1457 strain. It is assumed that this is the first study reporting the construction and characterization of specific iron acquisition deletion mutants in *S. epidermidis*. Additionally, and maybe most importantly, a clear link between a genetic region (locus *SERP1778-1781*, named after its homologous region in *S. aureus* as *sfaABCD*) and siderophore production is shown for the first time, in *S. epidermidis*. According to available genomic information, the *sfa* locus is widespread across *S. epidermidis* and other CoNS, demonstrating the importance of siderophore production for these species. Meiwes et al. (34) reported the isolation of a compound with siderophore activity from iron starved cultures of different staphylococcal species, including *S. epidermidis*, that they called staphyloferrin A. By deleting the entire *sfa* locus, a complete absence of siderophores in iron starved cultures was registered, an effect that was not observed for the other mutant strains, as well as a decreased iron content of the

cells. These findings support the predicted function of the *sfaABCD* locus in the biosynthesis of staphyloferrin A in *S. epidermidis*, which has been confirmed before for *S. aureus* (32,35). However, and unlike in *S. aureus* (32), *sfa* deletion is detrimental for *S. epidermidis* growth under iron restriction, in particular when accounting for biofilm formation. While two distinct siderophore biosynthetic regions have been described in *S. aureus* (involved in the synthesis of staphyloferrin A (32) and staphyloferrin B [38]), the *S. epidermidis* genome lacks additional putative siderophore biosynthetic regions. In agreement, experimental data described here support the hypothesis that *S. epidermidis* is able to produce a single siderophore (staphyloferrin A) that is fundamental for this species to survive and establish biofilms under low-iron conditions. On the other hand, it is interesting to note that more virulent species, *S. aureus* included, but also *E. coli* (37,38), *P. aeruginosa* (39,40) or *Bacillus anthracis* (41) produce more than one siderophore. This certainly provide these species with an adaptive advantage in iron-restricted environments and might explain why they exhibit a higher pathogenicity when compared to *S. epidermidis*.

Even though the lack of siderophore production resulted in delayed growth under iron restriction, the Δ*sfa* mutant strain was still able to replicate. This led to the hypothesis that siderophore-independent mechanisms were providing the cells with the required amount of iron for replication. According to previous data, it is likely that those mechanisms involve the action of the HtsABC and SstABCD transporters, as well as the FhuA ATPase. To test that hypothesis, each one of these putative iron acquisition systems has been deleted from the *S. epidermidis* 1457 chromosome to generate strains 1457Δ*htsABC,* 1457Δ*sstABCD* and 1457Δ*fhuA*. Based on experiments performed in *S. aureus*, HtsABC has been primarily implicated in heme acquisition (42), a function that is reflected in its name (heme transport system). This idea was lately challenged by Beasley et al. (32) who demonstrated that a *hts* deletion strain was still able to grow in a medium with heme as a sole iron source. Instead, they demonstrated that HtsABC, along with FhuA (also referred to as FhuC (43)) are involved in the uptake of staphyloferrin A. In the present study, the phenotypes exhibited by Δ*hts* and Δ*fhuA* were very similar. Under iron restriction, both strains demonstrated: (i) a delayed growth rate (but achieving cell densities comparable to the WT after 24 h of growth); (ii) a significant impaired biofilm formation ability; and (iii) increased cell wall thickness. Although experiments did not allow the establishment of a direct relationship between HtsABC/ FhuA and siderophore uptake, they provided a clear demonstration that these molecules play an important role in the survival of *S. epidermidis* in low-iron environments. Further study of the *hts* and *fhuA* single mutants, as well as the construction of a *hts fhuA* double mutant will be required for a definitive confirmation of the function of HtsABC and FhuA.

Conversely, deletion of the *sstABCD* locus did not induce major differences when compared to the WT. In *S. aureus*, SstABCD was described as a putative siderophore transporter (33) and found to mediate the uptake of iron-catecholamine hormones complexes (44), which suggests its involvement in the uptake of iron bound to catecholate siderophores. According to current knowledge, neither *S. aureus* (44) nor *S. epidermidis* have the ability to synthesize catecholate-type siderophores, thus Sst seems to be a complementary route that staphylococci employ to acquire iron from xenosiderophores. As a result, the effect of the *sst* locus deletion was likely overshadowed by the production of staphyloferrin A. In the future, the construction of a Δ*sfa* Δ*sst* double mutant should help to elucidate the role of Sst in *S. epidermidis*. Still, this mutant displayed an intriguing result, as loss of Sst led to decreased, yet not significant, biofilm formation in TSB medium. Although this phenomenon has not been further explored, it is tempting to advance one possible hypothesis: as a complex medium, TSB might have in its composition iron-binding compounds (e.g., catechol compounds) that are acquired through this transporter and acts as a major source of iron for the cells. Detailed analysis of TSB chemical composition would help to elucidate this question.

Taken together, the fact that deletions of *sfa*, *hts* and *fhuA* loci did not completely inhibit growth under low-iron conditions supports redundancy of *S. epidermidis* iron acquisition mechanisms. This is not entirely unexpected, as expression of different molecules for the same purpose suggests redundancy, something that have been demonstrated in other pathogens (45–47). However, and when it comes to biofilm formation, a whole different scenario was observed. Individual deletion of *sfa*, *hts* or *fhuA* loci proved to be deleterious for biofilm formation and redundancy in this case was apparently insufficient to meet the bacterial iron demands. Comparative transcriptomic analyses performed in different microorganisms have demonstrated that a wide range of molecules are differentially expressed under planktonic and biofilm growth (48–51). Accordingly, it is likely that processes upregulated during biofilm formation demand higher iron availability. Higher iron requirements during biofilm formation has been reported for different bacterial species, such as *P. aeruginosa* [54, 55] and *Mycobacterium* spp. (54,55). Regarding *S. epidermidis*, the findings described in **Chapter 3**, along with the consistent observation that biofilm cells display an upregulated transcription of both *sfa* and *hts* clusters even under iron-enriched conditions[§], support the hypothesis that this species has a higher iron demand during biofilm formation.

[§]This phenomenon is demonstrated throughout this thesis in four different *S. epidermidis* strains.

The findings described throughout this chapter demonstrate that *S. epidermidis* possesses a genetic locus, *sfaABCD*, encoding the necessary machinery for siderophore biosynthesis. Inactivation of either siderophore biosynthesis or HtsABC/ FhuA transport system has a markedly negative impact on biofilm formation under iron-restricted conditions, which renders their inhibition a promising approach in preventing *S. epidermidis* biofilm formation.

4.5. References

1. Monk IR. Genetic manipulation of staphylococci - breaking through the barrier. Front Cell Infect Microbiol. 2012;2:49.
2. Costa SK, Donegan NP, Corvaglia A-R, François P, Cheung AL. Bypassing the restriction system to improve transformation of *Staphylococcus epidermidis*. J Bacteriol. 2017;199(16):e00271-17.
3. Winstel V, Kühner P, Krismer B, Peschel A, Rohde H. Transfer of plasmid DNA to clinical coagulase-negative staphylococcal pathogens by using a unique bacteriophage. Appl Environ Microbiol. 2015;81(7):2481–8.
4. Sadovskaya I, Vinogradov E, Li J, Jabbouri S. Structural elucidation of the extracellular and cell-wall teichoic acids of *Staphylococcus epidermidis* RP62A, a reference biofilm-positive strain. Carbohydr Res. 2004;339(8):1467–73.
5. Galac MR, Stam J, Maybank R, Hinkle M, Mack D, Rohde H, et al. Complete genome sequence of *Staphylococcus epidermidis* 1457. Genome Announc. 2017;5(22):e00450-17.
6. Rohde H, Burdelski C, Bartscht K, Hussain M, Buck F, Horstkotte MA, et al. Induction of *Staphylococcus epidermidis* biofilm formation via proteolytic processing of the accumulation-associated protein by staphylococcal and host proteases. Mol Microbiol. 2005;55(6):1883–95.
7. Decker R, Burdelski C, Zobiak M, Büttner H, Franke G, Christner M, et al. An 18 kDa scaffold protein is critical for *Staphylococcus epidermidis* biofilm formation. PLoS Pathog. 2015;11(3):e1004735.
8. Cogen AL, Yamasaki K, Muto J, Sanchez KM, Crotty Alexander L, Tanios J, et al. *Staphylococcus epidermidis* antimicrobial delta-toxin (phenol-soluble modulin-gamma) cooperates with host antimicrobial peptides to kill group A *Streptococcus*. PLoS One. 2010;5(5):e8557.
9. Mack D, Rohde H, Dobinsky S, Riedewald J, Nedelmann M, Knobloch JKM, et al. Identification of three essential regulatory gene loci governing expression of *Staphylococcus epidermidis* polysaccharide intercellular adhesin and biofilm formation. Infect Immun. 2000;68(7):3799–807.
10. Wang R, Khan BA, Cheung GYC, Bach THL, Jameson-Lee M, Kong KF, et al. *Staphylococcus epidermidis* surfactant peptides promote biofilm maturation and dissemination of biofilm-associated infection in mice. J Clin Invest. 2011;121(1):238–48.
11. Schommer NN, Christner M, Hentschke M, Ruckdeschel K, Aepfelbacher M, Rohde H. *Staphylococcus epidermidis* uses distinct mechanisms of biofilm formation to interfere with phagocytosis and activation of mouse macrophage-like cells J774A.1. Infect Immun. 2011;79(6):2267–76.

12. Mack D, Bartscht K, Fischer C, Rohde H, De Grahl C, Dobinsky S, et al. Genetic and biochemical analysis of *Staphylococcus epidermidis* biofilm accumulation. Methods Enzymol. 2001;336:215–39.

13. Winstel V, Liang C, Sanchez-Carballo P, Steglich M, Munar M, Broker BM, et al. Wall teichoic acid structure governs horizontal gene transfer between major bacterial pathogens. Nat Commun. 2013;4:2345.

14. Hussain M, Hastings JGM, White PJ. A chemically defined medium for slime production by coagulase-negative staphylococci. J Med Microbiol. 1991;34(3):143–7.

15. Kreiswirth BN, Löfdahl S, Betley MJ, O'reilly M, Schlievert PM, Bergdoll MS, et al. The toxic shock syndrome exotoxin structural gene is not detectably transmitted by a prophage. Nature. 1983;305(5936):709–12.

16. Mack D, Siemssen N, Laufs R. Parallel induction by glucose of adherence and a polysaccharide antigen specific for plastic-adherent *Staphylococcus epidermidis*: evidence for functional relation to intercellular adhesion. Infect Immun. 1992;60(5):2048–57.

17. Vuong C, Gerke C, Somerville GA, Fischer ER, Otto M. Quorum-sensing control of biofilm factors in *Staphylococcus epidermidis*. J Infect Dis. 2003;188(5):706–18.

18. Geiger T, Francois P, Liebeke M, Fraunholz M, Goerke C, Krismer B, et al. The stringent response of *Staphylococcus aureus* and its impact on survival after phagocytosis through the induction of intracellular PSMs expression. PLoS Pathog. 2012;8(11):e1003016.

19. Brückner R. A series of shuttle vectors for *Bacillus subtilis* and *Escherichia coli*. Gene. 1992;122(1):187–92.

20. Pantůček R, Doškař J, Růžičková V, Kašpárek P, Oráčová E, Kvardová V, et al. Identification of bacteriophage types and their carriage in *Staphylococcus aureus*. Arch Virol. 2004;149(9):1689–703.

21. Sambrook J, Fritsch EF, Maniatis T. Molecular cloning: a laboratory manual. Cold Spring Harbor laboratory press. 2nd ed. New York. Cold Spring Harbor, NY: Cold Spring Harbor Laboratory Press; 1989.

22. Quan J, Tian J. Circular polymerase extension cloning for high-throughput cloning of complex and combinatorial DNA libraries. Nat Protoc. 2011;6(2):242–51.

23. Bae T, Schneewind O. Allelic replacement in *Staphylococcus aureus* with inducible counter-selection. Plasmid. 2006;55(1):58–63.

24. Winstel V, Kühner P, Rohde H, Peschel A. Genetic engineering of untransformablecoagulase-negative staphylococcal pathogens. Nat Protoc. 2016;11(5):949–59.

25. Shin SH, Lim Y, Lee SE, Yang NW, Rhee JH. CAS agar diffusion assay for the measurement of siderophores in biological fluids. J Microbiol Methods. 2001;44(1):89–95.

26. Altschul SF, Gish W, Miller W, Myers EW, Lipman DJ. Basic local alignment search tool. J Mol Biol. 1990;215(3):403–10.

27. Thompson JD, Gibson TJ, Plewniak F, Jeanmougin F, Higgins DG. The CLUSTAL X Windows interface: flexible strategies for multiple sequence alignment aided by quality analysis tools. Nucleic Acids Res. 1997;25(24):4876–82.

28. Arnold JW, Simpson JB, Roach J, Kwintkiewicz J, Azcarate-Peril MA. Intra-species genomic and physiological variability impact stress resistance in strains of probiotic potential. Front Microbiol. 2018;9:242.

29. Lan R, Reeves PR. Intraspecies variation in bacterial genomes: the need for a species genome concept. Trends Microbiol. 2000;8(9):396–401.

30. Oliveira F, Lima CA, Bráss S, França A, Cerca N. Evidence for inter- and intraspecies biofilm formation variability among a small group of coagulase-negative staphylococci. FEMS Microbiol Lett. 2015;362(20):fnv175.

31. Rasmussen L, Toftlund H. Phosphate compounds as iron chelators in animal cell cultures. Vitr Cell Dev Biol. 1986;22(4):177–9.

32. Beasley FC, Vinés ED, Grigg JC, Zheng Q, Liu S, Lajoie GA, et al. Characterization of staphyloferrin A biosynthetic and transport mutants in *Staphylococcus aureus*. Mol Microbiol. 2009;72(4):947–63.

33. Morrissey J a., Cockayne A, Hill PJ, Williams P. Molecular cloning and analysis of a putative siderophore ABC transporter from *Staphylococcus aureus*. Infect Immun. 2000;68(11):6281–8.

34. Meiwes J, Fiedler HP, Haag H, Zähner H, Konetschny-Rapp S, Jung G. Isolation and characterization of staphyloferrin A, a compound with siderophore activity from *Staphylococcus hyicus* DSM 20459. FEMS Microbiol Lett. 1990;67(1–2):201–5.

35. Cotton JL, Tao J, Balibar CJ. Identification and characterization of the *Staphylococcus aureus* gene cluster coding for staphyloferrin A. Biochemistry. 2009;48(5):1025–35.

36. Cheung J, Beasley FC, Liu S, Lajoie GA, Heinrichs DE. Molecular characterization of staphyloferrin B biosynthesis in *Staphylococcus aureus*. Mol Microbiol. 2009;74(3):594–608.

37. Neilands JB. Mechanism and regulation of synthesis of aerobactin in *Escherichia coli* K12 (pColV-K30). Can J Microbiol. 2010;38(7):728–33.

38. Gehring AM, Mori I, Walsh CT. Reconstitution and characterization of the *Escherichia coli* enterobactin synthetase from EntB, EntE, and EntF. Biochemistry. 1998;37(8):2648–59.

39. Meyer JM, Neely A, Stintzi A, Georges C, Holder IA. Pyoverdin is essential for virulence of *Pseudomonas aeruginosa*. Infect Immun. 1996;64(2):518–23.

40. Takase H, Nitanai H, Hoshino K, Otani T. Impact of siderophore production on *Pseudomonas aeruginosa* infections in immunosuppressed mice. Infect Immun. 2000;68(4):1834–9.

41. Hayrapetyan H, Siezen R, Abee T, Groot MN. Comparative genomics of iron-transporting systems in *Bacillus cereus* strains and impact of iron sources on growth and biofilm formation. Front Microbiol. 2016;7(JUN):1–13.

42. Skaar EP, Humayun M, Bae T, DeBord KL, Schneewind O. Iron-source preference of *Staphylococcus aureus* infections. Science. 2004;305(5690):1626–8.

43. Hammer ND, Skaar EP. Molecular mechanisms of *Staphylococcus aureus* iron acquisition. Annu Rev Microbiol. 2011;65(1545-3251 (Electronic)):129–47.

44. Beasley FC, Marolda CL, Cheung J, Buac S, Heinrichs DE. *Staphylococcus aureus* transporters Hts, Sir, and Sst capture iron liberated from human transferrin by staphyloferrin A, staphyloferrin B, and catecholamine stress hormones, respectively, and contribute to virulence. Infect Immun. 2011;79(6):2345–55.

45. Dumas Z, Ross-Gillespie A, Kümmerli R. Switching between apparently redundant iron-uptake mechanisms benefits bacteria in changeable environments. Proc R Soc B Biol Sci. 2013;280(1764):20131055.

46. Balderas MA, Nobles CL, Honsa ES, Alicki ER, Maresso AW. Hal is a *Bacillus anthracis* heme acquisition protein. J Bacteriol. 2012;194(20):5513–21.

47. Garcia EC, Brumbaugh AR, Mobley HLT. Redundancy and specificity of *Escherichia coli* iron acquisition systems during urinary tract infection. Infect Immun. 2011;79(3):1225–35.

48. Resch A, Rosenstein R, Nerz C, Götz F. Differential gene expression profiling of *Staphylococcus aureus* cultivated under biofilm and planktonic conditions. Appl Environ Microbiol. 2005;71(5):2663–76.

49. Bayramoglu B, Toubiana D, Gillor O. Genome-wide transcription profiling of aerobic and anaerobic *Escherichia coli* biofilm and planktonic cultures. FEMS Microbiol Lett. 2017;364(3):fnx006.

50. Castro J, França A, Bradwell KR, Serrano MG, Jefferson KK, Cerca N. Comparative transcriptomic analysis of *Gardnerella vaginalis* biofilms vs. planktonic cultures using RNA-seq. npj Biofilms Microbiomes. 2017;3(3):1–7.

51. Yao Y, Sturdevant DE, Otto M. Genomewide analysis of gene expression in *Staphylococcus epidermidis* biofilms: insights into the pathophysiology of *S. epidermidis* biofilms and the role of phenol-soluble modulins in formation of biofilms. J Infect Dis. 2004;191(2):289–98.

52. O'May CY, Sanderson K, Roddam LF, Kirov SM, Reid DW. Iron-binding compounds impair *Pseudomonas aeruginosa* biofilm formation, especially under anaerobic conditions. J Med Microbiol. 2009;58(6):765–73.

53. Frederick JR, Elkins JG, Bollinger N, Hassett DJ, McDermott TR. Factors affecting catalase expression in *Pseudomonas aeruginosa* biofilms and planktonic cells. Appl Environ Microbiol. 2001;67(3):1375–9.

54. Ojha A, Anand M, Bhatt A, Kremer L, Jacobs WR, Hatfull GF. GroEL1: A dedicated chaperone involved in mycolic acid biosynthesis during biofilm formation in mycobacteria. Cell. 2005;123(5):861–73.

55. Ojha A, Hatfull GF. The role of iron in *Mycobacterium smegmatis* biofilm formation: The exochelin siderophore is essential in limiting iron conditions for biofilm formation but not for planktonic growth. Mol Microbiol. 2007;66(2):468–83.

CHAPTER 5

The importance of iron acquisition to the interaction between *S. epidermidis* and the host innate immune system

Summary

In contrast to other pathogens, the interaction of *S. epidermidis* with the host innate immune system has been poorly explored. In order to investigate whether bacterial iron acquisition systems can modulate the interaction of *S. epidermidis* with host cells mediating innate immunity, murine RAW 264.7 cells and human monocyte-derived macrophages (hMDMs) were infected with *S. epidermidis* 1457 WT strain and its isogenic mutants defective in iron acquisition. Bacterial cell growth and phagocyte cells activation were assessed in the infected cultures. The ability of *S. epidermidis* to modulate the production of ROS by human neutrophils as well as its susceptibility to hydrogen peroxide (H_2O_2)-mediated killing was also investigated. The type of macrophage cells had a significant impact on the infection outcome. While RAW 264.7 cells failed to control intracellular replication of the bacteria, hMDMs exhibited a pronounced bactericidal effect. The bacterial fate within hMDMs was also dependent on the induced *in vitro* macrophage polarization: while M1-like macrophages did not allow intracellular replication, M2-like macrophages failed to control bacterial replication during early time points of infection (from 0 to 2 h). Moreover, the lack of siderophore production was associated with lower to null replication within macrophages, inhibition of ROS generation by neutrophils, and higher susceptibility to H_2O_2. Together, results show that different iron acquisition systems affect the interaction between *S. epidermidis* and host macrophages and indicate that lack of siderophore production is detrimental for bacterial survival in the harsh environment found within the phagocytic cells.

5.1 Brief introduction

As professional phagocytic cells, macrophages play a pivotal role in the host innate immune defense against invading pathogens (1). In addition, these cells perform antigen-presenting functions, bridging innate and adaptive immunity (2). Macrophages belong to a family of myeloid cells, sometimes referred to as the mononuclear phagocyte system that also includes monocytes and dendritic cells. Monocytes are derived from myeloid progenitor cells in the bone marrow, where they remain only a very short period of time. These cells are then released into the bloodstream from where they are recruited into tissues throughout the body – in response to inflammatory signals or homeostatic cues – where they mature into different types of resident macrophages (3). Macrophages can be activated in response to specific microenvironmental stimuli and signals and present distinct functional properties, a process called macrophage polarization (4). According to their activation state, monocyte-derived macrophages are commonly referred as "classically activated (M1)" versus "alternatively activated (M2)", or more recently "M1-like" versus "M2-like", and they differ mainly at the level of their cell surface markers, secreted cytokines and biological functions (5). From a simplistic point of view, M1-like macrophages exhibit a proinflammatory, phagocytic profile, while M2-like macrophages are characterized by their anti-inflammatory properties (6).

Both subsets are important in the induction of different branches of the adaptive immune system, which includes activation of T cells (4). T cells mediate antigen-specific responses by recognizing antigens through the T-cell receptor (TCR), that is clonally distributed in the surface of T lymphocytes. The TCR binds to antigen peptides presented by MHC class II molecules on the surface of APCs. Following antigen-recognition, and when co-stimulatory signals are also provided, T cells are activated and promptly proliferate (7). As professional APCs, macrophages provide the two signals required in the activation of a T cell, which are (i) antigen-presentation by MHC molecules and (ii) expression of costimulatory molecules CD80 and CD86, that bind CD28 expressed on the surface of T cells, thus triggering T cell proliferation and differentiation (8,9). Moreover, macrophages present on their surface the activation marker CD83 (10,11), which expression induces the upregulation of CD86 and MHC II, stimulating T-cell activation (12,13).

In this chapter, it was assessed the impact of different iron acquisition systems' expression in the interaction between *S. epidermidis* and different phagocytic cells. A potential role of siderophore production in the modulation of this process is advanced.

5.2 Materials and methods

5.2.1 Strains and growth conditions

Bacterial strains used in this study are described in **Table 5.1**. Strains were cultured overnight at 37°C in TSB (BD). Solid media were prepared by adding 1.5% (w/v) agar (BD) to the culture medium. When appropriate, antibiotics (Sigma-Aldrich) were added to the medium at the following concentrations: chloramphenicol (10 μg/mL), erythromycin (10 μg/mL), spectinomycin (150 μg/mL), tetracycline (10 μg/mL), and trimethoprim (30 μg/mL).

Table 5.1. *S. epidermidis* strains used in this chapter

Strain	Description*	Reference
1457	WT clinical isolate from a central venous catheter infection; *icaADBC*+, *aap*+, *embp*+, strong biofilm formation	(14)
1457-M12 p*gfp*	*icaA*::Tn*917* insertion mutant; constitutive *gfp* expression from plasmid pCN57; Ery^R	Rohde H. unpublished
1457Δ*hts*::*dhfr*	Mutant carrying a deletion of *htsABC* (*hts* = *SERP1775-1777*); Tmp^R	This study
1457Δ*sfa*::*spcR*	Mutant carrying a deletion of *sfaABCD* (*sfa* = *SERP1778-1781*); Spt^R	This study
1457Δ*fhuA*::*ermC*	Mutant carrying a deletion of *fhuA* (*fhuA* = *SERP0306*); Ery^R	This study
1457Δ*sst*::*tetM*	Mutant carrying a deletion of *sstABCD* (*sst* = *SERP0400-0403*)[#]	This study
1457Δ*hts* p*hts*	Complemented mutant 1457Δ*hts*; *in trans* expression of *hts* from its natural promoter; Tmp^R, Cm^R	This study
1457Δ*sfa* p*sfa*	Complemented mutant 1457Δ*sfa*; *in trans* expression of *sfa* from its natural promoter; Spt^R, Cm^R	This study
1457Δ*fhuA* p*fhuA*	Complemented mutant 1457Δ*fhuA*; *in trans* expression of *fhuA* from its natural promoter; Ery^R, Cm^R	This study
1457Δ*sst* p*sst*	Complemented mutant 1457Δ*sst*; *in trans* expression of *sst* from its natural promoter; Cm^R	This study

*Abbreviations: Cm^R, Ery^R, Spt^R, Tmp^R, resistance to chloramphenicol, erythromycin, spectinomycin, and trimethoprim, respectively. [#] *tetM* resistance cassette is not working properly.

5.2.2 Isolation of peripheral blood mononuclear cells

Human samples were obtained in agreement with the principles of the Declaration of Helsinki. PBMCs were isolated from surplus buffy coats, kindly provided by the Immunohemotherapy Department of Centro Hospitalar São João (CHSJ), Porto, Portugal. Procedures were approved by the Hospital Ethical Committee (Protocol 90/19). Informed written consent that the byproducts of their blood collections could be used for research purposes was obtained from the blood donors. Three mL of Histopaque-1077 (Sigma-Aldrich) at RT were added to 15 mL conical centrifuge tubes. Afterwards, 6 mL of blood samples were carefully layered onto Histopaque-1077 containing tubes (1:2 proportion). Tubes were then centrifuged at 400*g*, for 30 min at RT with soft-start and soft-brake functions activated (Heraeus Megafuge® 1.0R, Heraeus, Hanau, Germany). After centrifugation, the following pattern was observed

(from top to bottom): plasma, PBMC's, Histopaque-1077, granulocytes, and red blood cells. PBMCs were carefully transferred into a clean conical centrifuge tube and washed with 1× DPBS (Dulbecco's Phosphate Buffered Saline, without calcium and magnesium, Gibco™, Thermo Fisher Scientific, Inc.). Tubes were centrifuged at 400*g* for 10 min at 4°C and the supernatant was discarded. The cell pellet was resuspended in 5 mL of 1× DPBS and cell count was calculated after staining with Türk's solution (Merck) in a Neubauer chamber.

5.2.3 Monocyte purification by magnetic-activated cell sorting

Monocytes were purified with the CD14 MicroBeads, human (Miltenyi Biotec, Bergisch Gladbach, Germany) according to manufacturer's instructions. PBMCs suspension previously prepared was centrifuged at 300*g* for 10 min, the supernatant was discarded, and cells were resuspended in 80 µL of magnetic-activated cell sorting (MACS) buffer (1× DPBS pH 7.2; 5% (v/v) BSA; 2 mM EDTA) per 10^7 total cells. Then 20 µL of CD14 MicroBeads per 10^7 total cells were added, the cell suspension was carefully mixed and incubated for 15 min in the refrigerator (2-8°C). Afterwards, cells were washed by adding 1 mL of MACS buffer per 10^7 total cells and centrifuged at 300*g* for 10 min. The supernatant was discarded, and cells resuspended in 500 µL MACS buffer up to 10^8 cells.

Magnetic separation was carried out with an MS column (Miltenyi Biotec). The column was placed in a magnetic field of a Mini MACS separator (Miltenyi Biotec) and rinsed with 500 µL of MACS buffer. The cell suspension was added onto the column and washed thrice with 500 µL of MACS buffer to remove unlabeled cell fraction. The column was then removed from the separator and placed on a 15 mL tube. 1 mL of MACS buffer was added onto the column and the magnetically labelled cell fraction were immediately flushed out by using the provided plunger. $CD14^+$ monocytes count was calculated after staining with Türk's solution (Merck) in a Neubauer chamber.

5.2.4 Macrophage differentiation

$CD14^+$ monocytes were plated in either 6-, 24- or 96-well Nunclon™ Delta Surface (Thermo Fisher Scientific Inc, CAT No. 167008) in complete RPMI medium (cRPMI containing RPMI 1640 medium (Gibco), 10 mM HEPES buffer, 2 mM L-glutamine, 5% (v/v) heat-inactivated fetal bovine serum (FBS, Biowest, Riverside, MO, USA) or autologous plasma (where indicated), 100 U/mL penicillin/ streptomycin, 0.05 mM β-mercaptoethanol) in order to differentiate monocytes into macrophages (human monocyte-derived macrophages, hMDMs). Cells were seeded at the desired concentration and

incubated at 37°C in a humidified atmosphere and 5% CO_2. Replacement of culture medium occurred every 3 days up to day 8 of culture. Culture supernatants were partly removed (~50%) and fresh, pre-warmed cRPMI medium was added. To generate human macrophages skewed towards an M1- or M2-like activation state, cRPMI medium was supplemented with either 25 ng/mL of macrophage colony-stimulating factor (M-CSF, R&D Systems, Minneapolis, MN, USA) or 25 ng/mL of granulocyte-macrophage colony-stimulating factor (GM-CSF, PeproTech, Rocky Hill, NJ, USA), respectively. hMDMs experiments were performed with cells prepared from three different donors.

5.2.5 RAW264.7 cell culture

Murine RAW264.7 macrophages (ATCC® TIB-71™) were grown on cRPMI and incubated at 37°C in a humidified atmosphere and 5% CO_2. Cells were passaged for no more than 10 passages. After this point, new cells were revived from frozen stocks.

5.2.6 Stimulation of hMDMs with bacteria

An overnight culture of *S. epidermidis* WT was harvested by centrifugation at 5000*g*, for 10 min at 4°C. Cells were washed twice in 1× DPBS and adjusted in antibiotic-free cRPMI to an OD_{640} of 0.025 (~10^7 CFU/mL). hMDMs cultured in a 96-well plate were washed once with pre-warmed (37°C) antibiotic-free cRPMI and then stimulated with the previously prepared bacterial suspension at different multiplicities of infection (MOIs): 10:1 (1×10^6 CFUs/ 1×10^5 hMDMs), 1:1 (1×10^5 CFUs/ 1×10^5 hMDMs), and 1:10 (1×10^4 CFUs/ 1×10^5 hMDMs). A control with antibiotic-free cRPMI only (no bacteria added) was also tested. The co-cultures were then incubated at 37°C and 5% CO_2 for 8 h. After this period, culture supernatants were discarded, cells washed with 1× DPBS, and 40 µL of 2% (v/v) mouse serum[‡‡] were added to each well. Plates were incubated at 4°C for 15 min and then a mixture of antibodies (acquired from eBioscience, Thermo Fisher Scientific, Inc.: PE/Cy5 mouse anti-human CD86, PE/Cy7 mouse anti-human HLA-DR, FITC mouse anti-human CD83, and PE mouse anti-human CD14 in FACS buffer (2% (v/v) FBS, 1 mM EDTA, 0.1% (v/v) sodium azide in DPBS)) was added. The plate was incubated for ~30 min at 4°C in the dark. Afterwards, cells were washed once with 150 µL of FACS buffer and the plate was centrifuged at 200*g* for 5 min. In order to fix cells, 200 µL of 2% (w/v) paraformaldehyde (in FACS buffer) were added and cells were incubated for 15 min. at RT in the dark. The plate was centrifuged again at 200*g* for 5

[‡‡] Mouse serum was used as a blocking agent. A blocking agent is usually employed to inhibit nonspecific binding of monoclonal antibodies to Fc receptors (highly expressed in macrophages), which contributes significantly to background fluorescence in flow cytometry. The antibodies present in the serum will compete with the test antibodies for the Fc receptors. The origin of the serum should be the same as the origin of the antibodies to be tested (mouse in this case) (53).

min and the supernatant was discarded. 150 µL of FACS buffer were added to each well and cells were detached from the plate by gently pipetting up and down. The cell suspension was then transferred to flow cytometry tubes. Any remaining cells were detached from the plate by adding 150 µL of 5 mM EDTA (in FACS buffer) and left to incubate for 15 min. Single-color compensation controls for flow cytometry analysis were prepared by using OneCompBeads™ Compensation Beads (Thermo Fisher Scientific), as well as an unstained control. Samples were run on a BD FACSCANTO II flow cytometer, and data analyzed using FlowJo software (v.10.5.3).

5.2.7 Bacterial survival within macrophages: gentamicin protection assays

Suspensions of *S. epidermidis* WT and its isogenic mutants were prepared as described above and used to infect previously plated hMDMs (1×10^5 cells) or RAW264.7 (5×10^5 cells) at an MOI of 10:1. To synchronize phagocytosis, plates were centrifuged at 300*g* for 2 min followed by incubation at 37°C in the presence of 5% CO_2. Macrophages were allowed to internalize bacteria for 30 min. Afterwards, culture supernatants were discarded and serum-free cRPMI plus 50 µg/mL gentamicin (AppliChem, Darmstadt, Germany) was added for 60 min to eliminate extracellular bacteria. After this treatment, macrophages were rinsed with 1× DPBS and further incubated in antibiotic-free cRPMI for the desired period of time (0, 2, 6, 12, and 24 h). Release of the gentamicin-protected bacteria (which corresponds to the intracellular fraction) was performed by lysing macrophages with 0.1% (w/v) saponin (Sigma-Aldrich) in 1× PBS for 15 min. In order to eliminate bacterial aggregates, lysates underwent sonication (three cycles of 10 s at 30% amplitude using a Branson W140 Sonifier, Danbury, CT, USA). Lastly, lysates were serially diluted in 1× PBS and plated onto TSA plates for CFU enumeration. Data were obtained from three independent experiments.

5.2.8 Imaging of infected macrophages

RAW264.7 macrophages plated on CellCarrier-96 Ultra Microplates (6055302, PerkinElmer, Waltham, MA, EUA) were infected with *S. epidermidis* WT and its isogenic mutants as described above (section **5.2.7**). At defined time points (0 and 6 h after gentamicin treatment), macrophages were labelled with HCS CellMask™ Deep Red stain (Invitrogen, Thermo Fisher Scientific, Inc.) according to manufacturer's instructions. This stain labels the entire cell and allows delineation of the cell boundary. Intracellular bacteria were stained with 10 µg/mL DAPI (Sigma-Aldrich). Both, DAPI and HCS CellMask™ were added together to cells previously fixed with 4% (w/v) paraformaldehyde and permeabilized with 0.1% (w/v) saponin (Sigma-Aldrich), at RT for 30 min. Plates were then imaged by using an IN Cell Analyzer 2000

microscope (GE Healthcare, Chicago, IL, USA) with a Nikon 40×/0.95 NA Plan Fluor objective (binning 1×1), using a large chip CCD Camera (CoolSNAP K4) with a pixel array of 2048 × 2048 (7.40 μm^2 pixel). The excitation and emission filters used to detect DAPI and HCS CellMask™ were DAPI and Cy5, respectively. Images obtained were analyzed with the IN Cell Investigator Developer Toolbox version 1.9.2 (GE Healthcare).

5.2.9 Live cell imaging of infected macrophages

RAW264.7 macrophages plated on a µ-Dish 35 mm, high (ibidi, Gräfelfing, Germany) were infected with *S. epidermidis* 1457-M12 p*gfp* as described above (section **5.2.7**). After treatment with gentamicin for 1 h, dishes were imaged at the Advanced Light Microscopy scientific platform of I3S using a Leica DMI6000 FFW microscope (Leica Microsystems, Wetzlar, Germany) with a Leica HCX PL FLUOTAR L 40×/0.60 NA CORR PH2 objective, using a Hamamatsu FLASH4.0 camera (Hamamatsu, Japan), under full temperature and CO_2 control. Phase contrast and fluorescence images were taken every 15 min up to 10 h, and analyzed using Image J (15).

5.2.10 Intracellular ROS assay

PMNs were isolated from buffy coats from blood donations (Banco de Sangue, Centro Hospitalar Universitário de São João, Porto, Portugal) following a double gradient technique. Three mL of Histopaque-1077 (Sigma-Aldrich) were carefully layered over 3 mL of Histopaque-1119 (Sigma-Aldrich) in 15 mL conical centrifuge tubes. Afterwards, 6 mL of blood samples were carefully layered onto the upper Histopaque-1077 layer. Tubes were then centrifuged at 700*g*, for 30 min at RT with soft-start and soft-brake functions activated (Heraeus Megafuge® 1.0R, Heraeus, Hanau, Germany). After centrifugation, the following pattern was observed (from top to bottom): plasma, PBMCs, Histopaque-1077, PMNs, Histopaque-1119, and red blood cells. PMNs were carefully transferred into a clean conical centrifuge tube and washed with 1× DPBS. Tubes were centrifuged at 400*g* for 10 min at 4°C and the supernatant was discarded. The cell pellet was resuspended in 5 mL 1× DPBS and cell count was calculated after staining with Türk's solution (Merck) in a Neubauer chamber. Freshly isolated PMNs (5×10^5 cells) were incubated with *S. epidermidis* (5×10^6 CFU/mL) for 60 min and cells stained with ROS-ID® Total ROS/Superoxide detection kit (Enzo Life Sciences, Inc., Farmingdale, NY, USA) according to manufacturer's instructions. PMNs incubated with 50 nM phorbol 12-myristate 13-acetate (PMA, Sigma-Aldrich) were used as positive control for ROS production. Samples were analyzed on a BD FACSCANTO

II flow cytometer, and the data were analyzed using FlowJo software (v.10.5.3). Intracellular ROS was expressed as the fold change in the mean fluorescence intensity (MFI) compared to the WT strain.

5.2.11 Bacterial survival after H_2O_2 challenge

Bacterial suspensions were prepared as described above and adjusted in TSB to an OD_{640} of 0.025 (~10^7 CFU/mL). 1×10^7 CFUs were incubated in TSB plus 0.5 mM H_2O_2 (Sigma-Aldrich) for 60 min at 37°C with shaking at 120 rpm. Bacterial aggregates were eliminated as described above, cells were serially diluted in 1× PBS and plated on TSA plates for CFU enumeration. Data were obtained from three independent experiments.

5.2.12 Statistical analysis

Statistical analysis was performed with GraphPad Prism version 7.0a (La Jolla, CA, USA). For comparisons among different groups, two-away ANOVA with multiple comparisons test was used. A $p < 0.05$ was considered statistically significant.

5.3 Results

5.3.1 Macrophage activation by S. epidermidis

It is known that activated macrophages express specific markers on their surface, such as costimulatory (e.g., CD83, CD86) and antigen-presenting (e.g. HLA-DR) molecules (16). In order to determine the optimal MOI that could elicit activation of macrophages, the expression levels of CD83, CD86 and HLA-DR on the hMDMs surface after exposure to *S. epidermidis* WT strain for 8 h was assessed.

Stimulation with *S. epidermidis* WT at different MOIs resulted in increased expression of the three assessed markers on macrophage cells surface (**Figure 5.1**). When the highest bacterial concentration was tested (MOI of 10:1), it was observed an increment in the expression of CD83 (62.84%), CD86 (29.14%) and HLA-DR (20.45%) when compared to non-stimulated macrophages (cRPMI only). This MOI was thus used throughout the subsequent experiments.

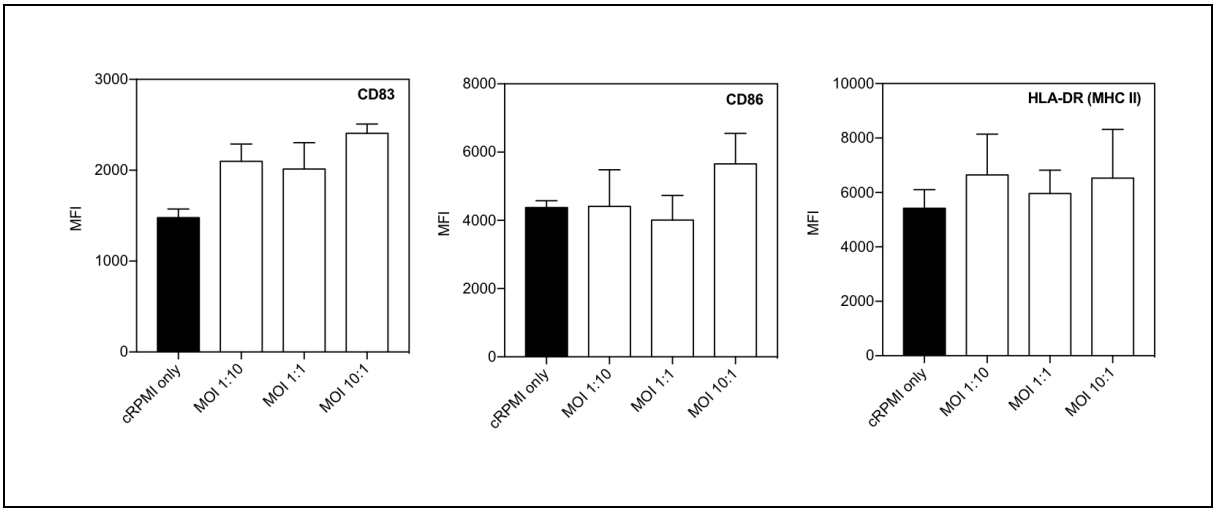

Figure 5.1. Flow cytometry evaluation of the expression of surface markers CD83, CD86 and HLA-DR on hMDMs stimulated with *S. epidermidis* 1457 WT. Basal expression of each marker was assessed incubating hMDMs with medium alone (black bar). Results are represented as mean ± standard deviation of mean fluorescence intensity (MFI) due to staining with respective monoclonal antibodies.

5.3.2 Optimization of gentamicin protection assays

According to the available literature, the ability of *S. epidermidis* to survive inside macrophages was not previously assessed. In order to study this process, it was carried out a gentamicin protection assay using both murine RAW264.7 macrophages and hMDMs. Although gentamicin protection assays have been extensively used over the years (17–21), some control experiments were performed beforehand with the WT strain and its isogenic mutant Δ*sfa* to ensure optimal conditions across these assays.

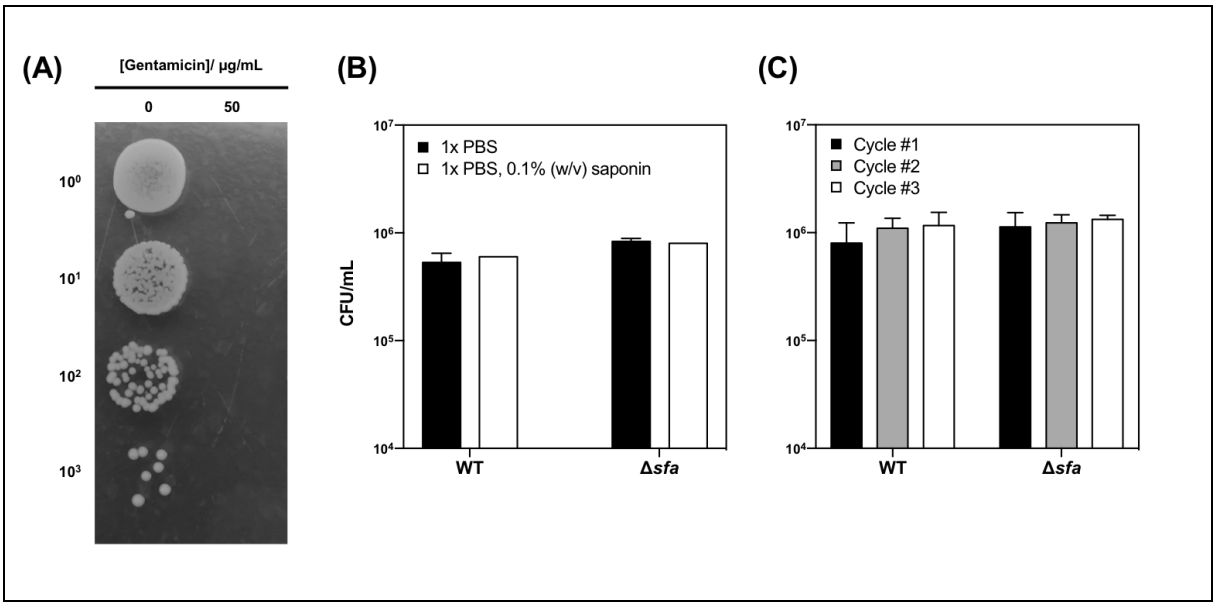

Figure 5.2. Optimization of gentamicin protection assays for *S. epidermidis*. **(A)** Complete inhibition of *S. epidermidis* growth is achieved after exposure to 50 µg/mL of gentamicin for 60 min. Effects of **(B)** saponin and **(C)** sonication in the cultivability of *S. epidermidis*. Cycle #1, 10 s at 30% amplitude; Cycle #2, 2 cycles of 10 s at 30% amplitude); Cycle #3, 3 cycles of 10 s at 30% amplitude.

The first condition to be assayed was the concentration of gentamicin to be used. In this kind of assays, the gentamicin treatment step is crucial since it should completely eliminate all bacteria remaining in the extracellular milieu while not affecting the intracellular bacterial pool. To find out the optimal gentamicin concentration and treatment period, bacteria were suspended in antibiotic-, serum-free cRPMI without or with 50 or 100 μg/mL of gentamicin, for 30 and 60 min. After treatment, bacterial cells were pelleted and washed to remove any trace of antibiotic and CFUs were enumerated. The treatment with 50 μg/mL for 60 min resulted in complete absence of growth (**Figure 5.2A**) and was therefore used throughout all experiments.

Next, it was assessed whether saponin could have a negative impact in the final bacterial counts. Saponin is a detergent often used when permeabilization of cell membranes is required (22). Here, saponin was used to disrupt the cell membrane of macrophages, allowing the release of intracellular bacteria. Treatment with PBS with or without 0.1% saponin (w/v) had no significant effect on the CFU counts (**Figure 5.2B**).

Lastly, the effect of different sonication cycles on cell counts was also assessed[§§]. Aggregation of *S. epidermidis* cells is a very common phenomenon and it is a recurrent source of interference in cell quantification assays (23). If not eliminated, these aggregates can lead to underestimation of bacterial counts. Three different sonication cycles were performed to eliminate bacterial aggregates: cycle #1: 10 s at 30% amplitude; cycle #2: 10 s at 30%, twice; cycle #3: 10 s at 30%, thrice. As shown in **Figure 5.2C**, none of the cycles tested impaired bacterial cultivability. On the contrary, a slight increase in the CFU counts of WT strain was noticed when cycles #2 and #3 were used, suggesting that elimination of cell aggregates occurred. For that reason, cycle #3 of sonication was employed throughout all experiments.

5.3.3 S. epidermidis *is able to survive and proliferate within RAW 264.7 macrophage cells*

After careful optimization of the gentamicin protection assay, the ability of *S. epidermidis* WT and mutant strains to survive and eventually replicate within macrophages was studied. The murine RAW 264.7 macrophage cell line was first used as it has been widely employed in similar experiments with other bacterial species (17,20,24–27).

[§§] CFU counts were performed for cells suspended in a solution of 0.1 % (w/v) saponin.

In order to understand the dynamics of the bacterial cells once inside macrophages, RAW264.7 cells were infected with *S. epidermidis* WT or its isogenic deletion mutants for 30 min, after which a gentamicin treatment was applied to eliminate any bacteria remaining extracellularly. At selected time points after this treatment, cells were either prepared for microscopy analysis or lysed to release intracellular bacteria for CFU enumeration. Imaging allowed the identification of infected macrophages and their semi-qualitative classification according to the number of intracellular bacteria (<5, 5 to 9, or ≥10 intracellular bacteria per macrophage **Figure 5.3**). At 0 h most infected cells contained <5 bacteria (74 to 81%), and a similar scenario was observed at 6 h (68 to 78%). However, the fraction of infected cells containing 5-9 bacteria increased from 0 to 6 h in all cases, except when macrophages were infected with Δ*sfa*.

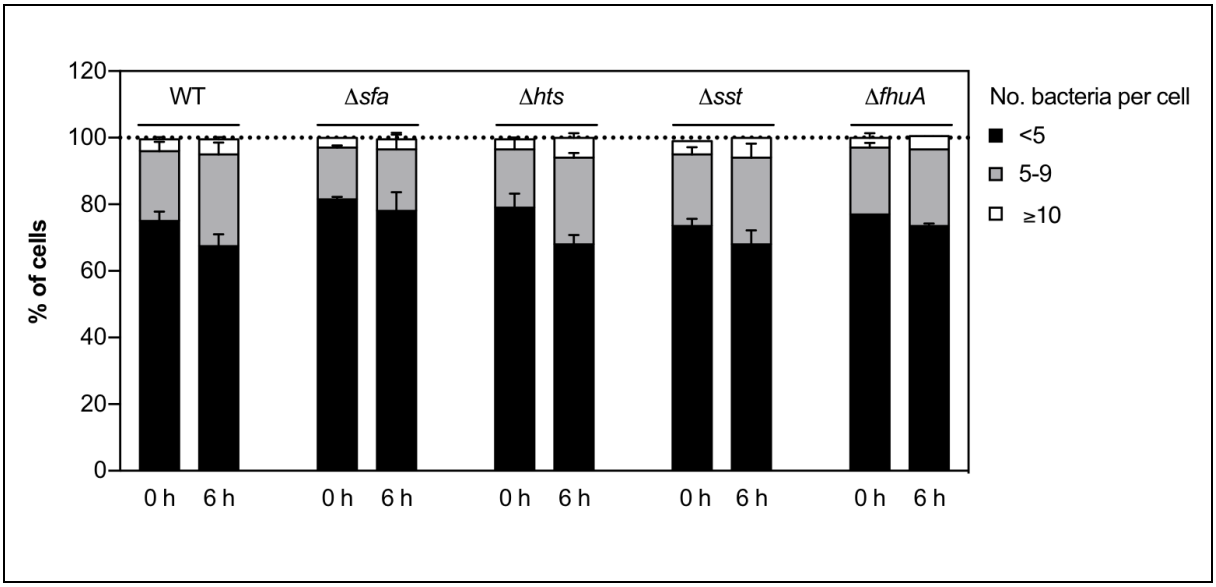

Figure 5.3. Average number of intracellular bacteria per infected macrophage. RAW264.7 were infected with *S. epidermidis* at an MOI of 10, fixed, and stained for imaging at the indicated time points. Infected macrophages were scored as containing <5, 5 to 9, or ≥10 intracellular bacteria. Data are represented as mean ± standard deviation of two independent assays.

Even though the microscopy analysis suggested the occurrence of bacterial proliferation inside macrophages, a clear increment in the number of CFU recovered between 0 and 6 h was detectable for Δ*sst* strain only (not statistically significant, **Figure 5.4A**). A similar phenomenon was reported by Lathrop et al. (18) when studying the replication of *Salmonella enterica* Serovar Typhimurium in hMDMs. Although these authors suggested macrophage death following infection as the source of discrepant results, one must not neglect the fact that different bacterial populations were detected by each experiment. While total cells were detected by the microscopy analysis, irrespective of their viability status, CFU enumeration detected cultivable bacteria only. Therefore, it is likely that intracellular bacterial

proliferation might have occurred, although the macrophages were able to kill a fraction of this bacterial population during this period.

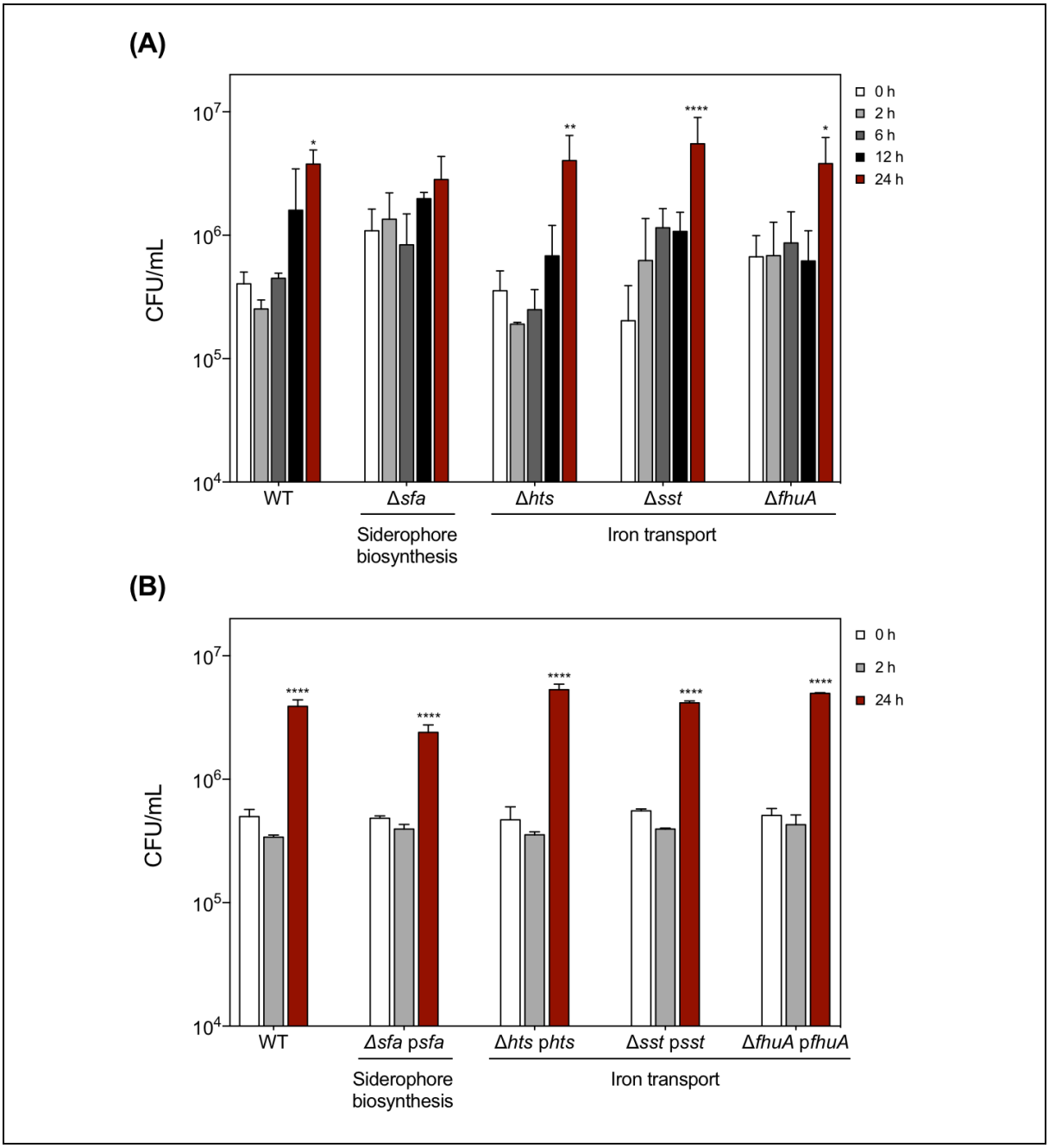

Figure 5.4. *S. epidermidis* is able to survive and replicate within murine RAW 264.7 macrophages. Macrophages were infected with **(A)** WT and its isogenic mutants, or **(B)** complemented strains at an MOI of 10, and the number of gentamicin-protected bacteria was determined at indicated time points after gentamicin treatment. Data are represented as mean ± standard deviations of three independent assays. Significant differences are depicted with: * $p < 0.05$; ** $p < 0.01$; **** $p < 0.0001$.

When the analysis of the recoverable intracellular bacteria was extended up to 24 h of infection, it was observed that all strains were able to survive and proliferate within macrophages (**Figure 5.4A)**.

However, this proliferative trend was apparent from 12 h onwards for most strains, and the extent of proliferation was strain dependent. While WT, Δ*hts*, Δ*sst* and Δ*fhuA* strains exhibited significant replication after 24 h, the extent of replication observed for the siderophore-deficient strain Δ*sfa* was not significant (average fold changes in CFU from 0 to 24 h: WT, 9.36; Δ*hts*, 11.34; Δ*sst,* 27.17; Δ*fhuA*, 5.67; vs Δ*sfa* 2.59). Nevertheless, it must be mentioned that this strain presented the highest cell count at time 0 h. On the one hand, this might be indicative that the lack of siderophore synthesis renders *S. epidermidis* more susceptible to phagocytosis, at least for this macrophage cell line. On the other hand, it may explain the lower extent of replication observed for this strain. Interestingly, according to the findings reported by Flannagan et al. (17) with *S. aureus* and using similar experimental conditions, the number of bacteria recovered 24 h post-infection was similar regardless the initial bacterial input. Therefore, it can be hypothesized that the reduced proliferation was actually the result of the limit of the bacterial load that RAW264.7 macrophages can hold, rather than the bacteria itself. Complemented strains exhibited a phenotype similar to the WT strain (**Figure 5.4B**).

Under the experimental conditions used here, all strains survived and proliferated within RAW 264.7 macrophages. Even though the survival of *S. epidermidis* in macrophages has never been studied before, the observation that this species is able to proliferate within macrophages was somehow surprising, partly due to its lower level of virulence (28). In order to exclude the hypothesis that the intracellular bacterial counts were not influenced by insufficient gentamicin-mediated killing of extracellular bacteria, all culture supernatants were checked for the presence of bacteria and were consistently confirmed to be devoid of bacteria.

Additionally, phase contrast time-lapse live cell imaging was performed with RAW264.7 macrophages infected with an *S. epidermidis* strain that constitutively express *gfp* (1457-M12 p*gfp*) (**Figure 5.5**). Even though few extracellular bacteria can be seen (dashed arrows), they do not exhibit replication over the entire period assayed (10 h). Therefore, this experiment was important to rule out the hypothesis of extracellular proliferation. Nevertheless, and although survival of phagocytosed *S. epidermidis* cells within macrophages was observed (solid arrows), bacterial proliferation was not apparent. This may stem from the fact that (i) images were acquired only for a period of 10 h; and (ii) the strain tested in this experiment is not able to produce PIA/PNAG. Schommer et al. (29) reported that PIA/PNAG-negative strains have higher susceptibility to phagocytosis and trigger a stronger macrophage activation. Likewise, it is conceivable that lack of PIA/PNAG production is also detrimental for intracellular replication. In the future,

live cell imaging with GFP-expressing WT strain over an extended infection period may help to elucidate this question.

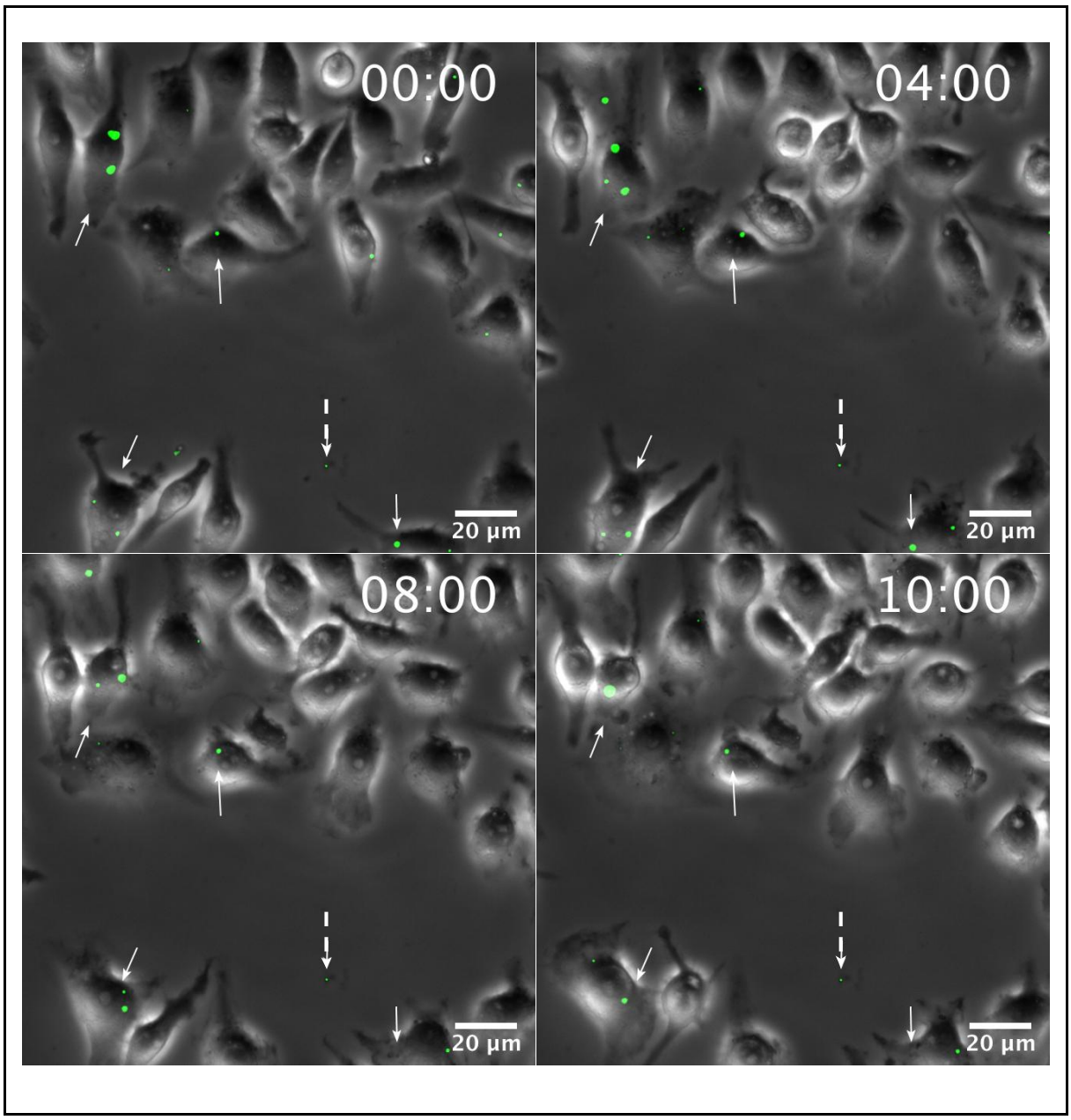

Figure 5.5. Representative images of live cell imaging of RAW264.7 macrophages infected with *S. epidermidis* 1457-M12 p*gfp*. Green, bacteria. Solid arrows indicate infected macrophages. Dashed arrows indicate extracellular bacteria.

5.3.4 The ability of hMDMs to restrict the growth of S. epidermidis *is dependent on their activation state*

After establishing that *S. epidermidis* can proliferate within murine macrophage cells, it was assessed whether the same could be observed using primary human macrophages. Human monocytes were isolated, differentiated into M1- or M2-like macrophages by using GM-CSF or M-CSF, respectively.

Macrophages were then infected with *S. epidermidis* WT or its isogenic deletion mutants and CFU counts were determined at 0, 2 and 24 h after gentamicin treatment (**Figure 5.6**).

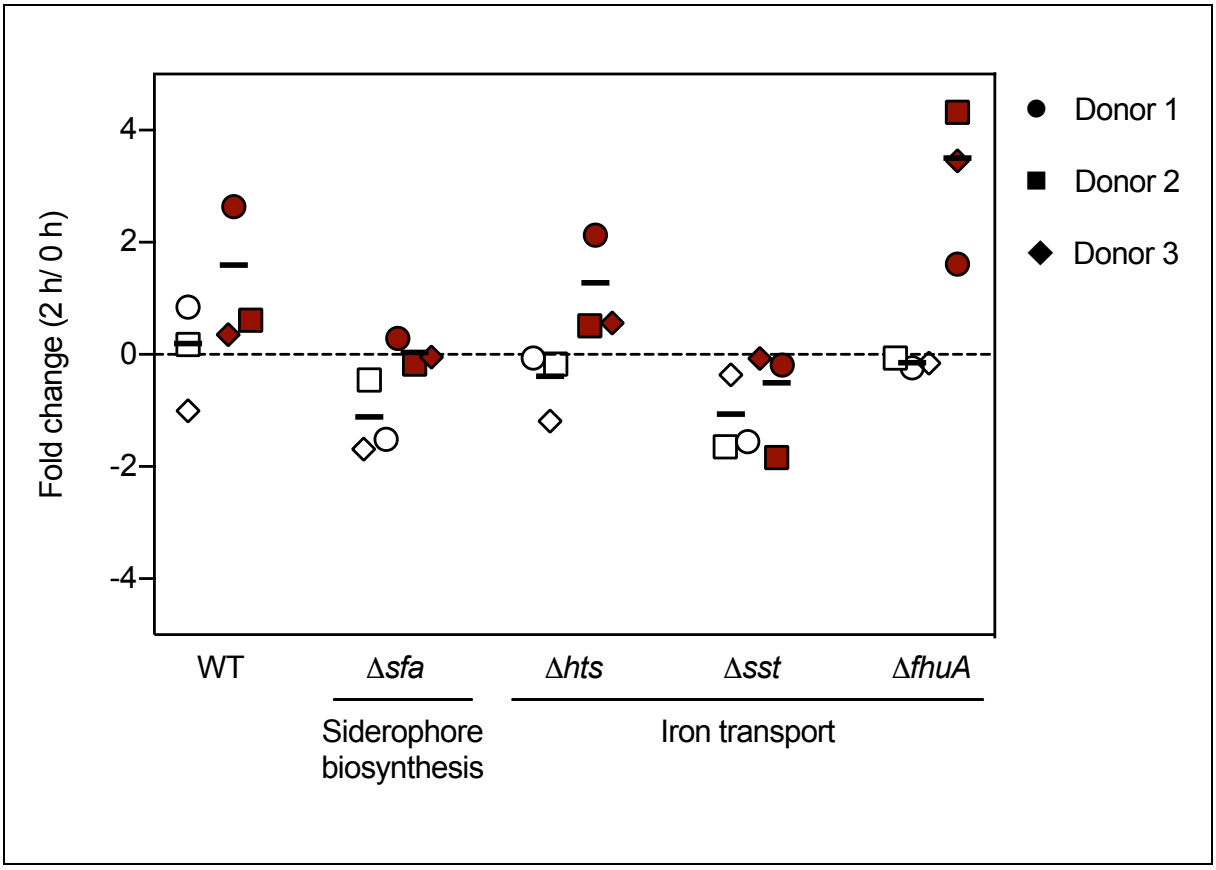

Figure 5.6. hMDMs are able to eliminate phagocytosed *S. epidermidis* cells. M1- (blank symbols) and M2-like (red symbols) hMDMs were infected with *S. epidermidis* at an MOI of 10, and the number of gentamicin-protected bacteria was determined at 0 and 2 h after gentamicin treatment. At 24 h, no intracellular bacteria were recovered. Data are represented in a log scale as average fold changes in CFU (from 0 to 2h) obtained for each donor. Values above and below 0 indicate proliferation and elimination of bacteria, respectively, in comparison to 0 h.

In contrast to what was observed with RAW264.7 macrophages, hMDMs controlled the proliferation of phagocytosed *S. epidermidis* and eventually completely clear bacteria, as no CFU counts could be observed at 24 h. WT, Δ*hts* and Δ*fhuA* were able to survive within M1-like macrophages, and even managed to proliferate within M2-like macrophages from 0 to 2 h. Conversely, there was a detectable decrease in the number of intracellular bacteria within M1-like macrophages infected with both Δ*sfa* and Δ*sst* mutant strains. Moreover, no proliferation of these mutants was observed within M2-like macrophages. Overall, M1-like macrophages showed a higher bactericidal activity than M2-like macrophages. Even though some degree of variation was observed among donors, the overall conclusions remain unchanged.

5.3.5 S. epidermidis *iron acquisition systems modulate neutrophils ROS production and susceptibility to H_2O_2-mediated killing*

Like macrophages, neutrophils are professional phagocytic cells that mediate pathogen clearance during infection (30). One of the main bactericidal mechanisms these cells employ to clear invading pathogens is production of ROS, including the superoxide anion (O_2^-) and hydrogen peroxide (H_2O_2) (31). In order to understand the effects of different *S. epidermidis* iron acquisition systems in the modulation of this neutrophil function, human PMNs were isolated, infected with WT or its isogenic mutants, and production of ROS was assessed through flow cytometry (**Figure 5.7A**).

After 15 min of infection, Δ*hts* triggered the production of significantly higher levels of total ROS, while PMNs responses to infection by the remaining mutant strains and the WT were comparable. After 60 min, increased ROS production initially observed in response to infection by Δ*hts* returned to WT levels. However, a significant drop in ROS production was noticed for Δ*sfa* and Δ*sst*.

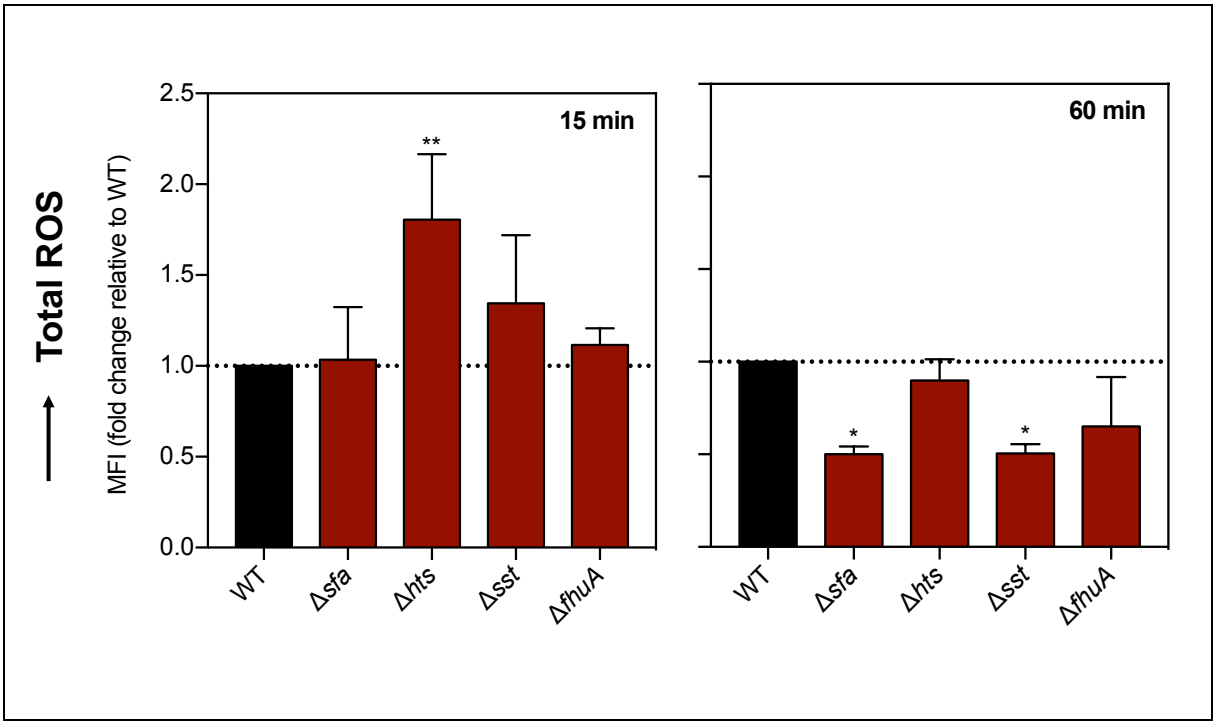

Figure 5.7. *S. epidermidis* iron acquisition systems are important in the modulation of ROS generation by PMNs. Human PMNs were infected with *S. epidermidis* at an MOI of 10 and generation of total ROS was quantified after 15 and 60 min. Data are represented as average fold changes in mean fluorescence intensity (MFI) of two independent assays. Significant differences are depicted with: * $p < 0.05$; ** $p < 0.01$; **** $p < 0.0001$.

Lastly, it was evaluated whether deletions of different iron acquisition systems could have an impact on H_2O_2-mediated killing. Bacterial strains were cultured in a medium containing 0.5 mM H_2O_2 for 60 min, after which CFU counts were enumerated (**Figure 5.8**).

Among all mutant strains, the siderophore-deficient Δ*sfa* was the only one to exhibit significantly lower CFU counts after exposure to H_2O_2. The increased susceptibility displayed by this strain was fully reversed by *in trans* gene complementation (Δ*sfa* p*sfa*). On the other hand, CFU counts for the remaining deletion mutant strains were equal to WT counts.

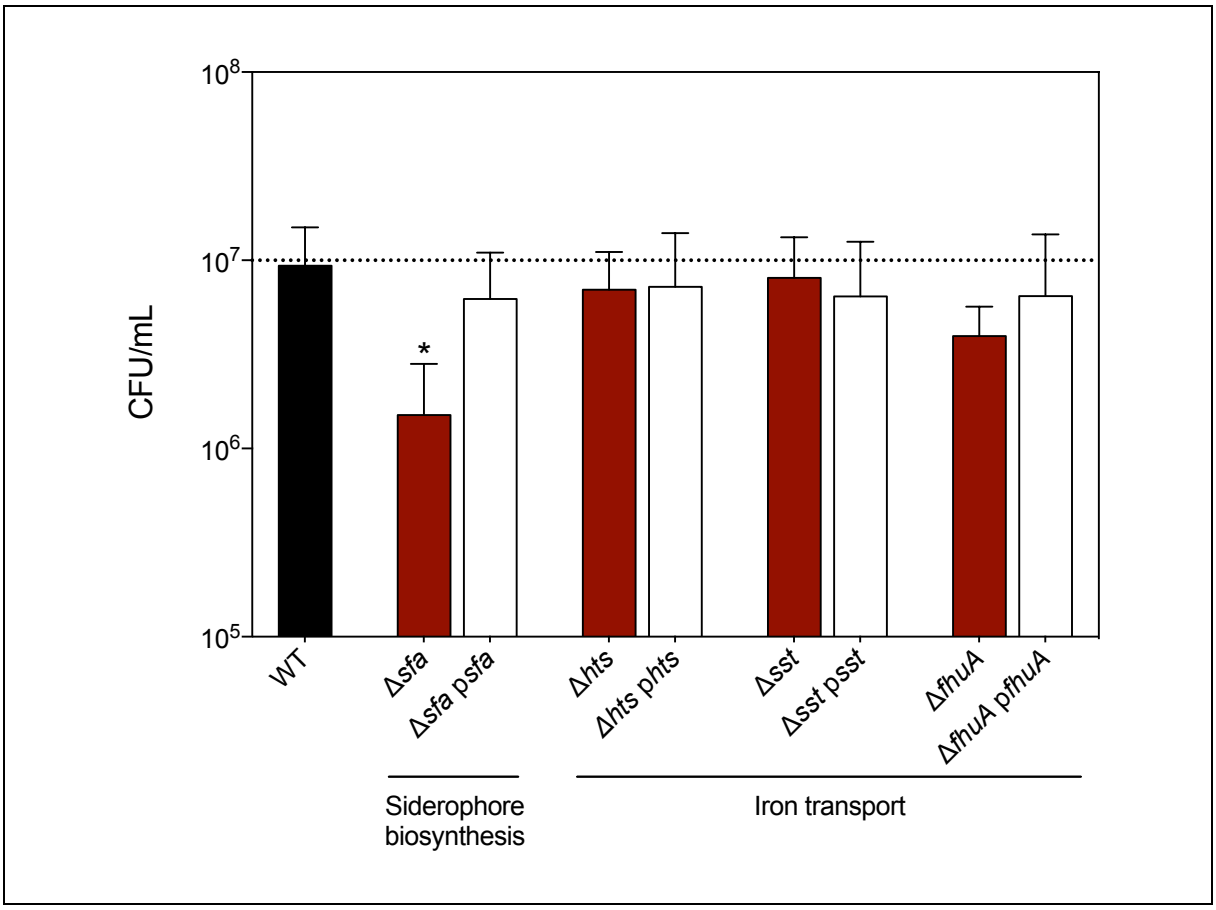

Figure 5.8. Effect of the deletion of different iron acquisition systems on *S. epidermidis* susceptibility to H_2O_2-mediated killing. Data are represented as mean ± standard deviation of four independent assays. Dashed line represents starting bacterial concentration (1×10^7 CFU/mL). Significant differences are depicted with: * $p < 0.05$.

5.4 Discussion

The interaction of *S. epidermidis* with cells of the innate immune system is still a poorly explored field. Given the importance of different iron acquisition systems *S. epidermidis* survival and biofilm formation under iron restriction, it was evaluated whether those systems also play a role in the interaction between this bacterial species and the host innate immune system. Since macrophages play a major role in the

innate immune response, most of experiments described throughout this chapter were focused on these phagocytic cells.

Firstly, it was assessed which MOI would lead to optimal activation of hMDMs in response to infection by *S. epidermidis* WT strain. In the absence of bacterial stimulation, it was observed a basal expression of all markers studied (CD83, CD86 and HLA-DR), as previously shown (10,32–34). When macrophages were stimulated by *S. epidermidis* WT, overall expression of these markers increased, especially when an MOI of 10 (10 bacteria to 1 macrophage) was used.

Afterwards, it was determined the possible impact of the deletion of different iron acquisition systems on the ability of *S. epidermidis* to survive within macrophages. To do this, a murine macrophage cell line, RAW 264.7, was used in the first place, as it offers an unlimited source of cells with phenotypic and functional stability over consecutive passages (24). This is an important technical advantage, as compared with human monocytes, since their differentiation into macrophages is a time-consuming process, and the high variability among blood donors usually makes the interpretation of results more complex (35). The observation that *S. epidermidis* was able to proliferate within these cells was quite surprisingly, as this phenomenon is usually attributable to more pathogenic species, such as *S. aureus* (17), *S. enterica* Serovar Typhimurium (18), *M. tuberculosis* (36). Literature on the interaction between *S. epidermidis* and macrophages is extremely scarce. By using a murine model of biomaterial-associated infection, Boelens et al. (37) and Riool et al. (38) independently demonstrated that *S. epidermidis* can reside intracellularly within macrophages, although proliferation was not reported. *S. epidermidis* was also reported to persist, but not replicate, intracellularly within human fibroblasts and osteoblasts, regarded as nonprofessional phagocytic cells (39).

Despite the aforementioned advantages regarding the use of macrophage cell lines, primary human macrophages are a more physiologically relevant model when studying a human pathogen like *S. epidermidis*, since these macrophages are derived from the pathogen's natural host (40). For that reason, the bacterial survival experiments were repeated using hMDMs. Interestingly, the ability of *S. epidermidis* to persist and replicate intracellularly was not observed when hMDMs were used, as these macrophages managed to completely clear bacterial cells by 24 h. Distinct responses to infection displayed by macrophage cell lines and primary macrophages have recently been reported in *M. tuberculosis* (40). Also, RAW264.7 cells were more susceptible to infection by *S. enterica* than primary macrophages (41).

Interestingly, the fate of *S. epidermidis* within hMDMs during the first two hours of infection was influenced by the type of macrophage polarization. While M1-skewed macrophages did not allow proliferation of any of the strains tested, M2-like macrophages did, something that is in line with findings reported for other species (18,42). This may be explained by the higher bactericidal potential usually observed in M1-like macrophages (6).

When looking at the contribution of different *S. epidermidis* iron acquisition systems to bacterial survival within macrophages, it is possible to conclude from experiments performed with RAW264.7 macrophages that the lack of any of the iron acquisition systems tested was not detrimental for bacterial survival, even though the siderophore-deficient Δ*sfa* strain exhibited lower proliferative potential. In line with this finding, this strain was neither able to persist nor replicate within M1- and M2-like hMDMs. The iron recycling function exhibited by macrophages places these cells in a close relationship with iron homeostasis processes (43), and it is currently known that the polarization status of the macrophages determines their intracellular iron content (44). As part of their strategy to minimize the access to the extracellular iron pool by pathogens, M1-like macrophages upregulate the expression of ferritin and Tfr1 and downregulate the expression of the iron exporter ferroportin, which combined effects lead to iron retention and, ultimately, to a higher microbicidal activity. On the other hand, the reverse was observed in M2-like macrophages, which results in iron release (45). A reduced intracellular iron content of M2-like macrophages may help to explain why the siderophore-deficient Δ*sfa* strain struggled to proliferate intracellularly, since it was demonstrated that siderophore production is an important mechanism used by *S. epidermidis* to grow under iron restriction (as discussed in **Chapter 4**). However, to confirm this assumption, the intracellular iron content of these macrophages should be determined.

Lastly, it was investigated the hypothesis that iron acquisition by *S. epidermidis*, and siderophore production in particular, modulates the production of ROS by phagocytic cells and the bacterial susceptibility to ROS-mediated killing. There is a growing line of evidence that bacterial siderophores play other functions besides iron sequestration, namely modulation of immune responses (46–48). According to the findings described here, deletion of different transport systems seems to have minor effects on the processes indicated above. However, the lack of siderophore production led to a decreased generation of ROS by PMNs, as well as resulted in a higher susceptibility to the action of H_2O_2. The role of different siderophores in protection to H_2O_2 stress has been acknowledged and is attributable to their ability to sequester iron, which makes it unavailable for participating in other reactions that lead to increased ROS

production, such as the Fenton reaction (49–51). Nevertheless, this mechanism has been reported for catecholate siderophores only (49). Similar studies with staphyloferrins (carboxylate siderophores) are apparently absent. Hannauer et al. (52) reported that an *S. aureus* Δ*sfaA* mutant, which is not able to secrete staphyloferrin A (carboxylate siderophore) did not exhibit increased susceptibility to H_2O_2. Nevertheless, as only the efflux transporter was eliminated rather than the entire biosynthetic machinery, this mutant is still able to produce staphyloferrin A that may somehow alleviate the bactericidal effects of H_2O_2. Literature is even scarcer regarding the involvement of siderophores in the modulation of ROS production by phagocytic cells. Saha et al. (47) reported that enterobactin inhibits the generation of ROS in mouse and human PMNs, acting as a defense mechanism against the host bactericidal response. This conclusion is not in line with the observations described here. However, one must bear in mind that: (i) this study used the isolated siderophore molecule instead of a siderophore biosynthetic mutant, and probably most importantly, (ii) enterobactin is a catecholate siderophore, while the siderophore produced by *S. epidermidis* is most likely a carboxylate siderophore.

Collectively, these results suggest that siderophore production contributes to the tolerance of *S. epidermidis* to bactericidal mechanisms employed by phagocytic cells. In the future, an effort should be placed in the isolation and proper identification of this siderophore, so that its antioxidant properties and its involvement in the persistence of *S. epidermidis* within macrophages could be better elucidated. Moreover, results point out that the fate of *S. epidermidis* within macrophages can vary significantly according to their nature (cell line vs primary cells), origin (murine vs human), and polarization (M1- vs M2-like).

5.5 References

1. Gasteiger G, D'osualdo A, Schubert DA, Weber A, Bruscia EM, Hartl D. Cellular innate immunity: an old game with new players. J Innate Immun. 2017;9(2):111–25.
2. Underhill DM, Bassetti M, Rudensky A, Aderem A. Dynamic interactions of macrophages with T Cells during antigen presentation. J Exp Med. 1999;190(12):1909-14.
3. Martinez FO, Gordon S, Locati M, Mantovani A. Transcriptional profiling of the human monocyte-to-macrophage differentiation and polarization: new molecules and patterns of gene expression. J Immunol. 2006;177(10):7303–11.
4. Murray PJ. Macrophage polarization. Annu Rev Physiol. 2017;79:541–66.
5. Jakubzick C V., Randolph GJ, Henson PM. Monocyte differentiation and antigen-presenting functions. Nat Rev Immunol. 2017;17(6):349–62.

6. Atri C, Guerfali FZ, Laouini D. Role of human macrophage polarization in inflammation during infectious diseases. Int J Mol Sci. 2018;19(6):E1801.

7. Punt J. Adaptive Immunity: T cells and cytokines. In: Prendergast GC, Jaffee EM. (eds.) Cancer immunotherapy: immune suppression and tumor growth. 2nd ed. London: Academic Press; 2013. p. 41–53.

8. Bugeon L, Hargreaves REG, Crompton T, Outram S, Rahemtulla A, Porter ACG, et al. Selective silencing of full-length CD80 but not IgV-CD80 leads to impaired clonal deletion of self-reactive T cells and altered regulation of immune responses. Eur J Immunol. 2001;31(1):118–27.

9. Lim W, Gee K, Mishra S, Kumar A. Regulation of B7.1 Costimulatory molecule is mediated by the IFN regulatory factor-7 through the activation of JNK in lipopolysaccharide-stimulated human monocytic cells. J Immunol. 2005;175(9):5690–700.

10. CAO W, LEE SH, LU J. CD83 is preformed inside monocytes, macrophages and dendritic cells, but it is only stably expressed on activated dendritic cells. Biochem J. 2005;385(Pt 1):85–93.

11. Nicod LP, Joudrier S, Isler P, Spiliopoulos A, Pache JC. Upregulation of CD40, CD80, CD83 or CD86 on alveolar macrophages after lung transplantation. J Hear Lung Transplant. 2005;24(8):1067–75.

12. Breloer M, Fleischer B. CD83 regulates lymphocyte maturation, activation and homeostasis. Trends Immunol. 2008;29(4):186–94.

13. Kuwano Y, Prazma CM, Yazawa N, Watanabe R, Ishiura N, Kumanogoh A, et al. CD83 influences cell-surface MHC class II expression on B cells and other antigen-presenting cells. Int Immunol. 2007;19(8):977–92.

14. Mack D, Siemssen N, Laufs R. Parallel induction by glucose of adherence and a polysaccharide antigen specific for plastic-adherent *Staphylococcus epidermidis*: Evidence for functional relation to intercellular adhesion. Infect Immun. 1992;60(5):2048–57.

15. Schindelin J, Arganda-Carreras I, Frise E, Kaynig V, Longair M, Pietzsch T, et al. Fiji: an open-source platform for biological-image analysis. Nat Methods [Internet]. 2012;9(7):676–82. Available from: http://rsbweb.nih.gov/ij/docs/guide/user-guide.pdf

16. Mosser DM, Edwards JP. Exploring the full spectrum of macrophage activation. Nat Rev Immunol. 2008;8(12):958–69.

17. Flannagan RS, Heit B, Heinrichs DE. Intracellular replication of *Staphylococcus aureus* in mature phagolysosomes in macrophages precedes host cell death, and bacterial escape and dissemination. Cell Microbiol. 2016;18(4):514–35.

18. Lathrop SK, Binder KA, Starr T, Cooper KG, Chong A, Carmody AB, et al. Replication of *Salmonella enterica* serovar Typhimurium in human monocyte-derived macrophages. Infect Immun. 2015;83(7):2661–71.

19. VanCleave TT, Pulsifer AR, Connor MG, Warawa JM, Lawrenz MB. Impact of gentamicin concentration and exposure time on intracellular *Yersinia pestis*. Front Cell Infect Microbiol. 2017;7:505.

20. Wu J, Pugh R, Laughlin RC, Andrews-Polymenis H, McClelland M, Bäumler AJ, et al. High-throughput assay to phenotype *Salmonella enterica* Typhimurium association, invasion, and replication in macrophages. J Vis Exp. 2014;11(90):e51759.

21. Amiel E, Lovewell RR, O'Toole GA, Hogan DA, Berwin B. *Pseudomonas aeruginosa* evasion of phagocytosis is mediated by loss of swimming motility and is independent of flagellum expression. Infect Immun. 2010;78(7):2937–45.

22. Jamur MC, Oliver C. Permeabilization of cell membranes. In: Jamur MC, Oliver C. (eds.) Immunocytochemical methods and protocols methods in molecular biology (Methods and Protocols). Humana Press; 2010. p. 63–6.

23. Freitas AI, Vasconcelos C, Vilanova M, Cerca N. Optimization of an automatic counting system for the quantification of *Staphylococcus epidermidis* cells in biofilms. J Basic Microbiol. 2014;54(7):750–7.

24. Taciak B, Białasek M, Braniewska A, Sas Z, Sawicka P, Kiraga Ł, et al. Evaluation of phenotypic and functional stability of RAW 264.7 cell line through serial passages. PLoS One. 2018;13(6):e0198943.

25. Kurosawa M, Oda M, Domon H, Saitoh I, Hayasaki H, Terao Y. *Streptococcus pyogenes* CAMP factor attenuates phagocytic activity of RAW 264.7 cells. Microbes Infect. 2016;18(2):118–27.

26. Yi Z, Gao K, Li R, Fu Y. Changed immune and miRNA response in RAW264.7 cells infected with cell wall deficient mycobacterium tuberculosis. Int J Mol Med. 2018;41(5):2885–92.

27. Teng L, Fu H, Wang M, Deng C, Chen J. Stimulation of RAW264.7 macrophages by sulfated *Escherichia coli* K5 capsular polysaccharide *in vitro*. Mol Med Rep. 2015;12(4):5545–53.

28. Otto M. *Staphylococcus epidermidis* - the 'accidental' pathogen. Nat Rev Microbiol. 2009;7(8):555–67.

29. Schommer NN, Christner M, Hentschke M, Ruckdeschel K, Aepfelbacher M, Rohde H. *Staphylococcus epidermidis* uses distinct mechanisms of biofilm formation to interfere with phagocytosis and activation of mouse macrophage-like cells J774A.1. Infect Immun. 2011;79(6):2267–76.

30. Dupré-Crochet S, Erard M, Nüβe O. ROS production in phagocytes: why, when, and where? J Leukoc Biol. 2013;94(4):657–70.

31. Robinson JM. Reactive oxygen species in phagocytic leukocytes. Histochem Cell Biol. 2008;130(2):281–97.

32. Randolph GJ, Beaulieu S, Lebecque S, Steinman RM, Muller WA. Differentiation of monocytes into dendritic cells in a model of transendothelial trafficking. Science. 1998;16(282(5388)):480–3.

33. Raggi F, Pelassa S, Pierobon D, Penco F, Gattorno M, Novelli F, et al. Regulation of human Macrophage M1-M2 Polarization balance by hypoxia and the triggering receptor expressed on myeloid cells-1. Front Immunol. 2017;8:1097.

34. Ambarus CA, Krausz S, van Eijk M, Hamann J, Radstake TRDJ, Reedquist KA, et al. Systematic validation of specific phenotypic markers for in vitro polarized human macrophages. J Immunol Methods. 2012;375(1–2):196-206.

35. Chanput W, Mes JJ, Wichers HJ. THP-1 cell line: An *in vitro* cell model for immune modulation approach. Int Immunopharmacol. 2014;23(1):37–45.

36. Lerner TR, Borel S, Greenwood DJ, Repnik U, Russell MRG, Herbst S, et al. *Mycobacterium tuberculosis* replicates within necrotic human macrophages. J Cell Biol. 2017;216(3):583–94.

37. Boelens JJ, Dankert J, Murk JL, Weening JJ, van der Poll T, Dingemans KP, et al. Biomaterial-associated persistence of *Staphylococcus epidermidis* in pericatheter macrophages. J Infect Dis. 2002;181(4):1337–49.

38. Riool M, De Boer L, Jaspers V, Van Der Loos CM, Van Wamel WJB, Wu G, et al. *Staphylococcus epidermidis* originating from titanium implants infects surrounding tissue and immune cells. Acta Biomater. 2014;10(12):5202–12.

39. Perez K, Patel R. Survival of *Staphylococcus epidermidis* in fibroblasts and osteoblasts. Infect Immun. 2018;86(10):e00237-18.

40. Andreu N, Phelan J, De Sessions PF, Cliff JM, Clark TG, Hibberd ML. Primary macrophages and J774 cells respond differently to infection with *Mycobacterium tuberculosis*. Sci Rep. 2017;7:42225.

41. Gog JR, Murcia A, Osterman N, Restif O, McKinley TJ, Sheppard M, et al. Dynamics of *Salmonella infection* of macrophages at the single cell level. J R Soc Interface. 2012;9(75):2696–707.

42. Hanke ML, Heim CE, Angle A, Sanderson SD, Kielian T. Correction: Targeting macrophage activation for the prevention and treatment of *Staphylococcus aureus* biofilm infections. J Immunol. 2013;190(5):2159–68.

43. Ganz T. Macrophages and systemic iron homeostasis. J Innate Immun. 2012;4(5–6):446–53.

44. Gaetano C, Massimo L, Alberto M. Control of iron homeostasis as a key component of macrophage polarization. Haematologica. 2010;95(11):1801–3.

45. Corna G, Campana L, Pignatti E, Castiglioni A, Tagliafico E, Bosurgi L, et al. Polarization dictates iron handling by inflammatory and alternatively activated macrophages. Haematologica. 2010;95(11):1814–22.

46. Saha R, Saha N, Donofrio RS, Bestervelt LL. Microbial siderophores: a mini review. J Basic Microbiol. 2013;53(4):303–17.

47. Saha P, Yeoh BS, Olvera RA, Xiao X, Singh V, Awasthi D, et al. Bacterial siderophores hijack neutrophil functions. J Immunol. 2017;198(11):4293–303.

48. Saha P, Xiao X, Yeoh BS, Chen Q, Katkere B, Kirimanjeswara GS, et al. The bacterial siderophore enterobactin confers survival advantage to *Salmonella* in macrophages. Gut Microbes. 2018;10(3):412–23.

49. Achard MES, Chen KW, Sweet MJ, Watts RE, Schroder K, Schembri MA, et al. An antioxidant role for catecholate siderophores in *Salmonella*. Biochem J. 2013;454(3):543–9.

50. Adler C, Corbalán NS, Seyedsayamdost MR, Pomares MF, de Cristóbal RE, Clardy J, et al. Catecholate siderophores protect bacteria from pyochelin toxicity. PLoS One. 2012;7(10):e46754.

51. Peralta DR, Adler C, Corbalán NS, Paz García EC, Pomares MF, Vincent PA. Enterobactin as part of the oxidative stress response repertoire. PLoS One. 2016;11(6):e0157799.

52. Hannauer M, Sheldon JR, Heinrichs DE. Involvement of major facilitator superfamily proteins SfaA and SbnD in staphyloferrin secretion in *Staphylococcus aureus*. FEBS Lett. 2015;589(6):730–7.

53. Andersen MN, Al-Karradi SNH, Kragstrup TW, Hokland M. Elimination of erroneous results in flow cytometry caused by antibody binding to Fc receptors on human monocytes and macrophages. Cytom Part A. 2016;89(11):1001–9.

CHAPTER 6

Major outcomes and future perspectives

Summary

In this chapter are presented the major findings and limitations of this study. Furthermore, research questions are proposed to be addressed in the future.

6.1 Major outcomes and their significance

This study offers the first comprehensive study of the influence of iron availability on *S. epidermidis* growth the molecular determinants involved in iron acquisition. Additionally, it uncovers the involvement of such determinants on processes with major importance for the pathogenesis of this bacterium, such as biofilm formation and interaction with the host innate immune system.

Although significant findings concerning iron acquisition in staphylococci have been achieved during the last decade, they are exclusively derived from studies on *S. aureus*. Here, we have identified important differences at the level of iron acquisition between *S. aureus* and *S. epidermidis* that justify the study of this process to be done independently in both species, namely:

- *S. aureus* is able to produce two different siderophores (Staphyloferrin A and B) and express two transporters fully dedicated to their uptake (HtsABC and SirABC) (1,2). Genomic information, along with experimental data from this thesis, suggest that *S. epidermidis* produces only one siderophore (staphyloferrin A) and its cognate transporter (HtsABC). Therefore, it is reasonable to assume that staphyloferrin A plays a much more important role in *S. epidermidis* than in *S. aureus*;

- *S. aureus* has a system dedicated to heme-bound iron acquisition, called iron-regulated surface determinant (Isd) (3,4). Conversely, and according to the genomic data available to date, the Isd system is absent in *S. epidermidis.*

When compared to *S. aureus*, *S. epidermidis* seems to have a significantly narrower range of options to acquire iron, stressing the importance of siderophore-mediated iron acquisition in *S. epidermidis*.

The findings reported here, provided answers to the three main research questions formulated at the beginning of this thesis.

1. Does iron availability modulate the ability of S. epidermidis *to form a biofilm?*

By employing a range of experimental settings and testing different *S. epidermidis* strains, it was demonstrated that iron availability plays a major role in the process of biofilm formation by this bacterial species. Even though iron restriction produced mild deleterious effects in planktonic bacteria, the severity of this condition became obvious when bacteria were induced to form a biofilm. Slower bacterial growth

rate, reduced cell viability and impaired PIA/PNAG production seem to account for the reduced biofilm formation ability observed under this condition.

2. What are the molecular mechanisms employed by S. epidermidis *to acquire iron and regulate its homeostasis?*

Following previous results from an *ex vivo* model (5), a group of genes was identified putatively involved in different iron acquisition processes and it was demonstrated that their transcription is iron-regulated. Afterwards, the focus was narrowed down on four loci: *SERP1778-1781* (*sfaABCD*); *SERP1775-1777* (*htsABC*); *SERP0306*, (*fhuA*); and *SERP0400-0403* (*sstABCD*). By employing a mutagenesis approach to study putative iron acquisition genes for the first time in *S. epidermidis*, the *sfaABCD* locus was implicated in siderophore biosynthesis. According to the bioinformatics analysis and data obtained in *S. aureus*, the products of the *htsABC and fhuA* loci are predicted to form an ABC transporter responsible for the uptake of iron-siderophore complexes. Although experimental confirmation of this was not provide, deletion of each locus proved to be detrimental for biofilm formation under iron-restricted conditions, suggesting that *S. epidermidis* relies on siderophore-mediated iron acquisition to meet its iron demands and adopt a biofilm mode of growth.

3. Do iron acquisition mechanisms have an impact on S. epidermidis *virulence and its recognition by the host innate immune system?*

Individually, the iron acquisition systems tested do not seem to play a significant role on the ability of *S. epidermidis* to survive and/or proliferate inside macrophages. Nevertheless, the siderophore-deficient strain (Δ*sfa*) was consistently less adapted to the intracellular environment of different macrophage populations (murine cell line, M1- and M2-like hMDMs), inhibited ROS generation by neutrophils, and showed higher susceptibility to H_2O_2-mediated killing. These observations suggest that siderophore production has a role in the interaction between *S. epidermidis* and the host innate immune system, although its *in vivo* relevance must be determined.

6.2 Major limitations

Herein the importance of siderophore-mediated iron acquisition for *S. epidermidis* was highlighted. Nevertheless, one of the major limitations of this study is that information about the ability of this bacterial species to utilize iron from other sources with biological relevance (e.g. human transferrin and hemoglobin) was not provided. Furthermore, and notwithstanding significant efforts to obtain different

deletion mutant strains, an experimental confirmation of the involvement of HtsABC, FhuA and SstABCD on uptake of siderophore-iron complexes is still missing. Lastly, the study on the interaction of *S. epidermidis* with the host innate immunity is mainly focused on macrophages. Besides the fact that some important questions remained to be elucidated regarding the macrophage experiments (e.g. the iron status of M1- and M2-like primary human macrophages), other key players in innate immunity are worth of further research in this context, particularly neutrophils and dendritic cells.

6.3 Future research foci

Although this work provides answers to different relevant aspects about iron acquisition in *S. epidermidis*, many other questions within this framework remain to be elucidated. Some of these questions can be easily addressed in a short term, such as those related with the limitations pointed out above. However, there are other important matters that will require medium to long-term research efforts. Below, a brief discussion on those matters is provided.

6.3.1 How does S. epidermidis *internalize siderophore-bound iron and release iron in the cytoplasm?*

In *S. aureus*, HtsABC and FhuA have been shown to form a transport system that allows iron-siderophore complexes to cross the bacterial membrane into the cytoplasm (2). Although it is likely that such mechanism is conserved among staphylococci, it lacks experimental validation in *S. epidermidis*. Appropriate experiments with the deletion mutants Δ*hts* and Δ*fhuA* will certainly help solving this question. On the other hand, the mechanism by which iron is released from siderophores in the cytoplasm is a far less understood process across Gram-positive bacteria. Recently, Hannauer et al. (6) have suggested that the liberation of iron from staphyoferrin A is mediated by the iron-regulated nitroreductase NtrA in *S. aureus*. Answering this question in *S. epidermidis* will certainly require a further analysis of the genomics and transcriptomics data available. A brief inspection of both RP62A and 1457 genomes for a nitroreductase-encoding gene resulted in the identification of a locus (*SERP0482* and *B4U56_09620*, respectively) with a putative Fur box upstream the coding sequence, making this a good candidate gene for the study of this process in *S. epidermidis*. Additionally, RNA sequencing of cells grown under iron-restricted conditions would certainly be a valuable tool in the identification of candidate genes for this process, as well as novel genes involved in iron acquisition. Ultimately, the complete elucidation of this whole question will increase the diversity of mechanisms that can be targeted for antibacterial purposes.

6.3.2 Is siderophore-mediated iron acquisition an important mechanism during S. epidermidis *infections?*

According to the experimental conditions tested, siderophore production is crucial for biofilm formation and has a mild impact on the interaction with the host innate immune system. Besides, deletion of *htsABC* and *fhuA,* which products form a putative transporter for iron-siderophore complexes, was deleterious for biofilm formation. Therefore, the relevance of siderophore biosynthesis and siderophore-mediated iron acquisition towards the ability of *S. epidermidis* to cause infection is worth further investigation. This can be assessed primarily through an *ex vivo* human whole blood model of infection, and later using *in vivo* infection models, such as the nematode *C. elegans* or mice. Over the last years, *C. elegans* has proven to be an excellent model for studying infectious processes and innate immune responses in human hosts, as well as examining the contribution of specific genes to virulence (7–9). If results are promising, the *in vivo* relevance of this process may be tested in a murine model, for instance using an experimental biomedical device-associated infection model. The construction of double (e.g. Δ*sfa* Δ*hts*) or event triple mutants (e.g. Δ*sfa* Δ*hts* Δ*fhuA*) could be tested in a similar manner.

6.3.3 Do iron-regulated lipoproteins play a role in immune recognition?

For a long time, the predominant staphylococcal PAMP leading to immune recognition via TLR2 was thought to be LTA (10). Lately, it has been raised the hypothesis that TLR2 activation by LTA is rather a result of stimulating contaminants present in LTA preparations, most likely lipoproteins (11). HtsA and SstD are surface-exposed lipoproteins which expression is upregulated under iron restriction, a common condition inside the human body, making them potential PAMPs for recognition by phagocytes. To elucidate this question, a comprehensive approach should be carried out, such as the use of suitable reporter cell lines to assess TLR2 stimulation by *S. epidermidis* Δ*hts* and Δ*sst* mutants.

6.3.4 Does S. epidermidis *rely on siderophore production to modulate the host innate immune response?*

There is an emerging concept that siderophore molecules are involved in other processes besides iron acquisition, particularly modulation of immune responses (12). Results with the siderophore-deficient Δ*sfa* mutant support this notion, as this strain revealed lower adaptation to the macrophage intracellular milieu, affected the generation of ROS by neutrophils, and exhibited higher susceptibility to the action of H_2O_2. Although some technical challenges are envisioned, the isolation and further purification of this siderophore from *S. epidermidis* cultures would allow further testing that could provide an unequivocal

proof of its immunomodulatory role. More specifically, the influence of this molecule on processes like ROS generation, NET formation and degranulation in neutrophils or macrophage activation could be easily assessed.

6.3.5 Will a deeper understand of iron acquisition in S. epidermidis *lead to the development of new therapeutic strategies?*

Thinking long term, once established the *in vivo* relevance of siderophore-mediated iron acquisition in *S. epidermidis* infections, this mechanism may be a suitable target for the development of new therapeutic strategies. A simple approach would be the use of siderophore uptake systems as a gateway for the delivery of the so-called "trojan horse" compounds into the bacterial cytoplasm. This strategy encompasses the use of siderophore-antibiotic conjugates and aims to improve antibiotic uptake by pathogenic bacteria (14). Several siderophore-antibiotic conjugates have proved to be effective against a wide range of multidrug resistant bacteria (15–19), and one of them has successfully completed phase I clinical trials (20). Another "trojan horse" strategy is the use of gallium to outcompete iron for the binding to siderophores, transferrin, and other iron-containing molecules (21). Similarly, this approach has demonstrated antimicrobial activity against several multidrug resistant bacteria (22–27). Although promising, it lacks *in vivo* studies that fully demonstrate its efficacy.

At the same time, several research groups have been dedicated to the development of immunization strategies against *S. epidermidis* infections [25–28], although there is currently no available vaccine for this pathogen. The fact that *S. epidermidis* is primarily a human commensal raises some concerns regarding the development of a vaccine against this species. Nevertheless, experts in the field claim that immunoprophylaxis and immunotherapy of *S. epidermidis* infections would certainly benefit high-risk populations, particularly patients undergoing implantation of permanent biomedical devices, in a cost-effective manner (33,34). Given the recurrent failure of vaccines against *S. epidermidis* novel target candidates are required. Iron acquisition-related molecules might be a good fit for the job as they have a good degree of conservation, and their expression is readily induced during infection in response to iron starvation found in the host (35). Different proteins involved in iron acquisition in *S. aureus* have been or are currently being targeted as vaccine candidates. Perhaps, the most promising vaccine candidate against *S. aureus* was the Merck V710, which was based on IsdB, an iron-regulated protein involved in heme acquisition. Unfortunately, the lack of significant clinical benefit along with increased mortality issues during phase II clinical trials (36), led to the abandonment of its development. Another multivalent

vaccine targeting iron acquisition in *S. aureus* is currently under development by Syntiron/ Sanofi Pasteur consortium (35), although no major details have been made available. Therefore, targeting iron-regulated proteins in *S. epidermidis* may also be a promising approach for the elaboration of a new vaccine against this bacterial species.

6.4 References

1. Cotton JL, Tao J, Balibar CJ. Identification and characterization of the *Staphylococcus aureus* gene cluster coding for staphyloferrin A. Biochemistry. 2009;48(5):1025–35.
2. Beasley FC, Vinés ED, Grigg JC, Zheng Q, Liu S, Lajoie GA, et al. Characterization of staphyloferrin A biosynthetic and transport mutants in *Staphylococcus aureus*. Mol Microbiol. 2009;72(4):947–63.
3. Mazmanian SK, Skaar EP, Gaspar AH, Humayun M, Gornicki P, Jelenska J, et al. Passage of Heme-Iron Across the Envelope of *Staphylococcus aureus*. Science. 2003;299(5608):906–9.
4. Torres VJ, Pishchany G, Humayun M, Schneewind O, Skaar EP. *Staphylococcus aureus* IsdB is a hemoglobin receptor required for heme iron utilization. J Bacteriol. 2006;188(24):8421–9.
5. França A, Carvalhais V, Maira-Litrán T, Vilanova M, Cerca N, Pier G. Alterations in the *Staphylococcus epidermidis* biofilm transcriptome following interaction with whole human blood. Pathog Dis. 2014;70(3):444–8.
6. Hannauer M, Arifin AJ, Heinrichs DE. Involvement of reductases IruO and NtrA in iron acquisition by *Staphylococcus aureus*. Mol Microbiol. 2015;96(6):1192–210.
7. Balla KM, Troemel ER. *Caenorhabditis elegans* as a model for intracellular pathogen infection. Cell Microbiol. 2013;15(8):1313–22.
8. Powell JR, Ausubel FM. Models of *Caenorhabditis elegans* infection by bacterial and fungal pathogens. In: Ewbank J, Vivier E. (eds.) Innate Immunity methods in molecular biology. Humana Press; 2008. p.403–27.
9. Marsh EK, May RC. *Caenorhabditis elegans*, a model organism for investigating immunity. Appl Environ Microbiol. 2012;78(7):2075–81.
10. Morath S, Stadelmaier A, Geyer A, Schmidt RR, Hartung T. Synthetic lipoteichoic acid from *Staphylococcus aureus* is a potent stimulus of cytokine release. J Exp Med. 2002;195(12):1635–40.
11. Hashimoto M, Tawaratsumida K, Kariya H, Aoyama K, Tamura T, Suda Y. Lipoprotein is a predominant Toll-like receptor 2 ligand in *Staphylococcus aureus* cell wall components. Int Immunol. 2006;18(2):355–62.
12. Saha P, Yeoh BS, Olvera RA, Xiao X, Singh V, Awasthi D, et al. Bacterial siderophores hijack neutrophil functions. J Immunol. 2017;198(11):4293–303.
13. Hannauer M, Sheldon JR, Heinrichs DE. Involvement of major facilitator superfamily proteins SfaA and SbnD in staphyloferrin secretion in *Staphylococcus aureus*. FEBS Lett. 2015;589(6):730–7.
14. De Carvalho CCCR, Fernandes P. Siderophores as “Trojan horses”: tackling multidrug resistance? Front Microbiol. 2014;5:290.

15. Page MGP, Dantier C, Desarbre E. *In vitro* properties of BAL30072, a novel siderophore sulfactam with activity against multiresistant gram-negative bacilli. Antimicrob Agents Chemother. 2010;54(6):2291–302.

16. Budzikiewicz H. Siderophore-antibiotic conjugates used as Trojan horses against *Pseudomonas aeruginosa*. Curr Top Med Chem. 2005;1(1):73–82.

17. Wencewicz TA, Long TE, Möllmann U, Miller MJ. Trihydroxamate siderophore-fluoroquinolone conjugates are selective sideromycin antibiotics that target *Staphylococcus aureus*. Bioconjug Chem. 2013;24(3):473–86.

18. Górska A, Sloderbach A, Marszałł MP. Siderophore-drug complexes: potential medicinal applications of the "Trojan horse" strategy. Trends Pharmacol Sci. 2014;35(9):442–9.

19. Page MGP. Siderophore conjugates. Ann N Y Acad Sci. 2013;1277:115–26.

20. Basilea Pharmaceutica AG. Basilea completes BAL30072 antibiotic trial. Pharmaceutical Technology. Available from: https://www.pharmaceutical-technology.com/news/newsbasilea-completes-bal30072-antibiotic-trial/ [Accessed 31 July 2019].

21. Richter K, Van den Driessche F, Coenye T. Innovative approaches to treat *Staphylococcus aureus* biofilm-related infections. Essays Biochem. 2017;61(1):61–70.

22. Arnold CE, Bordin A, Lawhon SD, Libal MC, Bernstein LR, Cohen ND. Antimicrobial activity of gallium maltolate against *Staphylococcus aureus* and methicillin-resistant *S. aureus* and *Staphylococcus pseudintermedius*: An i*n vitro* study. Vet Microbiol. 2012;155(2–4):389–94.

23. Baldoni D, Steinhuber A, Zimmerli W, Trampuz A. *In vitro* activity of gallium maltolate against staphylococci in logarithmic, stationary, and biofilm growth phases: comparison of conventional and calorimetric susceptibility testing methods. Antimicrob Agents Chemother. 2010;54(1):157–63.

24. De Léséleuc L, Harris G, KuoLee R, Chen W. *In vitro* and *in vivo* biological activities of iron chelators and gallium nitrate against *Acinetobacter baumannii*. Antimicrob Agents Chemother. 2012;56(10):5397–400.

25. Huayhuaz JAA, Vitorino HA, Campos OS, Serrano SHP, Kaneko TM, Espósito BP. Desferrioxamine and desferrioxamine-caffeine as carriers of aluminum and gallium to microbes via the Trojan horse effect. J Trace Elem Med Biol. 2017;41:16–22.

26. Kaneko Y, Thoendel M, Olakanmi O, Britigan BE, Singh PK. The transition metal gallium disrupts *Pseudomonas aeruginosa* iron metabolism and has antimicrobial and antibiofilm activity. J Clin Invest. 2007;117(4):877–88.

27. Banin E, Lozinski A, Brady KM, Berenshtein E, Butterfield PW, Moshe M, et al. The potential of desferrioxamine-gallium as an anti-*Pseudomonas* therapeutic agent. Proc Natl Acad Sci. 2008;105(43):16761–6.

28. Shahrooei M, Hira V, Khodaparast L, Khodaparast L, Stijlemans B, Kucharíková S, et al. Vaccination with SesC Decreases *Staphylococcus epidermidis* biofilm formation. Infect Immun. 2012;80(10):3660–8.

29. Maira-Litrán T, Kropec A, Goldmann DA, Pier GB. Comparative opsonic and protective activities of *Staphylococcus aureus* conjugate vaccines containing native or deacetylated staphylococcal poly-N-acetyl-β-(1-6)-glucosamine. Infect Immun. 2005;73(10):6752–62.

30. Sun D, Accavitti MA, Bryers JD. Inhibition of biofilm formation by monoclonal antibodies against *Staphylococcus epidermidis* RP62A accumulation-associated protein. Clin Vaccine Immunol. 2005;12(1):93–100.

31. Hu J, Xu T, Zhu T, Lou Q, Wang X, Wu Y, et al. Monoclonal antibodies against accumulation-associated protein affect EPS biosynthesis and enhance bacterial accumulation of *Staphylococcus epidermidis*. PLoS One. 2011;6(6):e20918.

32. DeJonge M, Burchfield D, Bloom B, Duenas M, Walker W, Polak M, et al. Clinical trial of safety and efficacy of IHN-A21 for the prevention of nosocomial staphylococcal bloodstream infection in premature infants. J Pediatr. 2007;151(3):260–5.

33. Van Mellaert L, Shahrooei M, Hofmans D, Eldere J Van. Immunoprophylaxis and immunotherapy of *Staphylococcus epidermidis* infections: challenges and prospects. Expert Rev Vaccines. 2012;11(3):319–34.

34. Otto M. Novel targeted immunotherapy approaches for staphylococcal infection. Expert Opin Biol Ther. 2010;10(7):1049–59.

35. Sheldon JR, Heinrichs DE. The iron-regulated staphylococcal lipoproteins. Front Cell Infect Microbiol. 2012;2(2235-2988 (Electronic)):41.

36. McNeely TB, Shah NA, Fridman A, Joshi A, Hartzel JS, Keshari RS, et al. Mortality among recipients of the Merck V710 *Staphylococcus aureus* vaccine after postoperative *S. aureus* infections: an analysis of possible contributing host factors. Hum Vaccines Immunother. 2014;10(12):3513–6.